

DEVELOPMENT OF A COASTAL MARGIN OBSERVATION AND ASSESSMENT
SYSTEM (CMOAS) TO CAPTURE THE EPISODIC EVENTS IN A SHALLOW BAY

A Dissertation

by

MOHAMMAD SHAHIDUL ISLAM

Submitted to the Office of Graduate Studies of
Texas A&M University
in partial fulfillment of the requirements for the degree of

DOCTOR OF PHILOSOPHY

May 2009

Major Subject: Civil Engineering

DEVELOPMENT OF A COASTAL MARGIN OBSERVATION AND ASSESSMENT
SYSTEM (CMOAS) TO CAPTURE THE EPISODIC EVENTS IN A SHALLOW BAY

A Dissertation

by

MOHAMMAD SHAHIDUL ISLAM

Submitted to the Office of Graduate Studies of
Texas A&M University
in partial fulfillment of the requirements for the degree of

DOCTOR OF PHILOSOPHY

Approved by:

Chair of Committee,	James S. Bonner
Committee Members,	Billy L. Edge
	Steven F. DiMarco
	Jennifer L. Irish
Head of Department,	David V. Rosowsky

May 2009

Major Subject: Civil Engineering

ABSTRACT

Development of a Coastal Margin Observation and Assessment System (CMOAS) to
Capture the Episodic Events in a Shallow Bay. (May 2009)

Mohammad Shahidul Islam, B.Sc., BUET, Dhaka, Bangladesh;

M.Sc., The University of Tokyo, Japan

Chair of Advisory Committee: Dr. James S. Bonner

Corpus Christi Bay (TX, USA) is a shallow wind-driven bay which is designated as a National Estuary due to its impact on the economy. But this bay experiences periodic hypoxia (dissolved oxygen <2 mg/l) which threatens aerobic aquatic organisms. Development of the Coastal Margin Observation and Assessment System (CMOAS) through integration of real-time observations with numerical modeling helps to understand the processes causing hypoxia in this energetic bay. CMOAS also serves as a template for the implementation of observational systems in other dynamic ecosystems for characterizing and predicting other episodic events such as harmful algal blooms, accidental oil spills, sediment resuspension events, etc.

State-of-the-art sensor technologies are involved in real-time monitoring of hydrodynamic, meteorological and water quality parameters in the bay. Three different platform types used for the installation of sensor systems are: 1) Fixed Robotic, 2) Mobile, and 3) Remote. An automated profiler system, installed on the fixed robotic platform, vertically moves a suite of in-situ sensors within the water column for

continuous measurements. An Integrated Data Acquisition, Communication and Control system has been configured on our mobile platform (research vessel) for the synchronized measurements and real-time visualization of hydrodynamic and water quality parameters at greater spatial resolution. In addition, a high frequency (HF) radar system has been installed on remote platforms to generate surface current maps for Corpus Christi (CC) Bay and its offshore area. This data is made available to stakeholders in real-time through the development of cyberinfrastructure which includes establishment of communication network, software development, web services, database development, etc. Real-time availability of measured datasets assists in implementing an integrated sampling scheme for our monitoring systems installed at different platforms. With our integrated system, we were able to capture evidence of an hypoxic event in Summer 2007.

Data collected from our monitoring systems are used to drive and validate numerical models developed in this study. The analysis of observational datasets and developed 2-D hydrodynamic model output suggests that a depth-integrated model is not able to capture the water current structure of CC Bay. Also, the development of a three-dimensional mechanistic dissolved oxygen model and a particle aggregation transport model (PAT) helps to clarify the critical processes causing hypoxia in the bay. The various numerical models and monitoring systems developed in this study can serve as valuable tools for the understanding and prediction of various episodic events dominant in other dynamic ecosystems.

DEDICATION

To almighty ALLAH, source of all knowledge, love, patience and inspiration,
To my mother, Zobeda Khatun, who sacrifices everything to make me smile in this
world,

To my father, the late Nurul Islam, who prays for me from the heaven,
To my wife, Iffat Zaman (Moon), who illuminates my life in the darkness, and is the
better half of my life.

ACKNOWLEDGEMENTS

I would like to thank my committee chair, Dr. James S. Bonner, for his constant encouragement, invaluable guidance and unyielding patience throughout the course of this research work. He has taught me how to “think globally and act locally” to solve real world problems. I am highly indebted for his academic, financial and moral support to complete this research. I also thank Dr. Billy L. Edge for his counsel on hydrodynamic modeling and his continuous enthusiasm towards my research work. I thank Dr. Steven F. DiMarco and Dr. Jennifer L. Irish for their patience and time commitment as committee members.

Thanks also go to my friends and colleagues and the department faculty and staff for making my time at Texas A&M University a great experience. I also want to thank Dr. Cheryl Page for her encouragement and conscientious manuscript review. Thanks also goes to Dr. Temitope Ojo and the entire staff members at Shoreline Environmental Research Facility (SERF), especially John Perez and Christopher Fuller, for their support in monitoring systems design and conducting field activities in Corpus Christi Bay. I also want to extend my gratitude to the Texas General Land Office (TGLO), the Texas Water Research Institute (TWRI) and the National Science Foundation (NSF) for their financial support.

I would like to acknowledge my elder sister, Najneen Islam, my younger sister, Sharmin Islam, and my brother, Foejul Islam, for their well-wishes and prayers for my success in life.

It would not be possible for me to complete my work without the love, emotional support and patience that my wife, Iffat Zaman, provided throughout the course of this work. She is the cheerleader of my life. I am deeply proud of having her at my side always.

My mother, Zobeda Khatun, does not want anything but my success. Her thoughts, prayer and honesty always encourage me to go forward in life. I am deeply grateful to my mother for all of my achievements. I also want to remember my father, the late Nurul Islam, who is in the heaven watching me and smiling at my success.

Above all, I want to thank all mighty ALLAH, who gives me the strength, patience and support to complete this work.

TABLE OF CONTENTS

	Page
ABSTRACT	iii
DEDICATION	v
ACKNOWLEDGEMENTS	vi
TABLE OF CONTENTS	viii
LIST OF FIGURES.....	xi
LIST OF TABLES	xvii
CHAPTER	
I INTRODUCTION.....	1
Statement of Purpose	1
Background	3
Objectives	13
II A FIXED ROBOTIC PROFILER SYSTEM TO SENSE REAL-TIME EPISODIC PULSES OF THE CONDITION OF CORPUS CHRISTI (CC) BAY	15
Overview	15
Introduction	16
Study Area.....	23
Vertical Robotic Profiling System (with Instrumentation Suite) on Fixed Platforms.....	25
Description of the Developed Cyberinfrastructure.....	30
Results and Discussions.....	34
Conclusions	41
III A MOBILE MONITORING SYSTEM TO UNDERSTAND THE PROCESSES CONTROLLING EPISODIC EVENTS IN CORPUS CHRISTI BAY	43
Overview	43

CHAPTER	Page
Introduction	44
Study Area	50
Mobile Monitoring System	52
Results and Discussions	57
November 29, 2006 Cruise	58
August 07, 2007 Cruise	63
Conclusions	71
IV INTEGRATED REAL TIME MONITORING SYSTEM TO INVESTIGATE THE HYPOXIA IN A SHALLOW WIND-DRIVEN BAY	73
Overview.....	73
Introduction	74
Site Description.....	78
Materials and Methods	80
Descriptions of the Developed Cyberinfrastructure	82
Results and Discussions	85
Investigation of a Hypoxic Event (July 22-25, 2007).....	86
Conclusions	104
V DEVELOPMENT AND INVESTIGATION ON THE RELIABILITY OF A 2-D HYDRODYNAMIC MODEL FOR CORPUS CHRISTI BAY.....	106
Overview	106
Introduction	108
Study Area	114
Numerical Model and Governing Equations	116
Model Development	118
Model Forcing Functions	121
Materials and Methods	122
Results and Discussions.....	124
Model Predicted Tides vs. Observed Tides.....	125
Observed vs. Model Predicted WSE	132
Model-computed Velocities vs. Observed Velocities.....	136
Results from Mobile Platform Cruises.....	140
Conclusions.....	146
VI A MECHANISTIC DISSOLVED OXYGEN MODEL OF CORPUS CHRISTI BAY TO UNDERSTAND CRITICAL PROCESSES CAUSING HYPOXIA	148

CHAPTER	Page
Overview	148
Introduction	149
Study Area.....	152
Materials and Methods	154
Description of the Model Development.....	155
Results and Discussions.....	161
Conclusions.....	169
VII DEVELOPMENT OF A THREE-DIMENSIONAL (3-D) PARTICLE AGGREGATION AND TRANSPORT MODEL TO CHARACTERIZE PARTICLE DYNAMICS IN CORPUS CHRISTI BAY	170
Overview.....	170
Introduction	171
Modeling Background.....	176
Model Development.....	180
Study Area of Interest	183
Data Observation Methods.....	184
Model Error Analysis.....	186
Results and Discussions.....	193
Conclusions.....	202
VIII SUMMARY AND CONCLUSIONS	204
Future Works	207
REFERENCES	209
VITA	223

LIST OF FIGURES

FIGURE	Page
1.1 Schematic diagram of Coastal Margin Observation and Assessment System (CMOAS) for CC Bay	12
2.1 Characteristics of the study area and platform locations.....	24
2.2 Robotic profiler system at one of our fixed robotic platform in the bay.....	26
2.3 Schematic diagram of cyberinfrastructure for fixed robotic profiler system.....	31
2.4 Time gap between in-situ sensor measurements and data availability for various samples collected at platform P2 from January 01-August 31, 2007	35
2.5 Vertical variation of salinity in the water column at platform ‘P3’ during July 23-25, 2007 (■: salinity data points; –: water surface elevation).....	37
2.6 a) Variation of robotic profiler measurement depths and corresponding measurements of b) salinity, c) total particle concentration and d) dissolved oxygen on June 15, 2006, respectively	39
3.1 Characteristics feature of Corpus Christi Bay.....	50
3.2 Schematic diagram of real-time monitoring mobile platform system.....	53
3.3 Snapshot of Graphical User Interface (GUI) generated by our real time data acquisition and visualization software (MPIACS-II) in one of our routine monitoring activities in CC Bay	56
3.4 IDACC transect route (in ship channel in CC Bay) on November 29, 2006 (Note: direction of transect was east-to-west)	58
3.5 Salinity variation along the IDACC route on Nov. 29, 2006 (Note: the colored horizontal lines at the top/bottom of the figure correlate to the transect route as presented in Figure 3.4).....	59
3.6 Variation of wind speed (a) and direction (b) around the platform ‘P2’ on November 28-29, 2006.....	60

FIGURE	Page
3.7 Scatter plot of actual particle concentration variation along the transect route on November 29, 2006 (■: Total Particle concentration ($\mu\text{l/l}$); –: sea-bed profile; Note: the colored horizontal lines at the top/bottom of the figure correlate to the transect route as presented in Figure 3.4)	62
3.8 Average acoustic backscatter intensity variation along the portion of transect route (time= 2100 s~ 4800 s) on November 29, 2006	63
3.9 Vertical DO variation along the transect route on August 07, 2007 (■: DO data points (mg/l); –: sea-bed profile).....	64
3.10 Vertical salinity variation along the transect route on August 07, 2007 (■: Salinity data points (psu); –: sea-bed profile).....	65
3.11 Vertical variation of Richardson number (Ri) along the transect route on August 07, 2007 (■: Ri; –: sea-bed profile).....	68
3.12 Vertical profile of chlorophyll along the transect route on August 07, 2007 (■: Chlorophyll concentration ($\mu\text{g/l}$); –: sea-bed profile).....	70
3.13 Vertical profile of total particle concentration along the transect route on August 07, 2007 (■: total volume of particle concentration ($\mu\text{l/l}$); –: sea-bed profile).....	71
4.1 Features of the study area and platform locations	79
4.2 Schematic diagram of SERF cyberinfrastructure	83
4.3 Vertical variation of salinity at platform ‘P3’ during July 22-25, 2007 (■: salinity data points; –: water surface elevation).....	87
4.4 Vertical salinity variation at platform ‘P2’ during July 22-25, 2007 (■: salinity data points; –: water surface elevation).....	88
4.5 Surface current velocity of CC Bay as captured by our HF-radar system at successive days from July 21 to July 24, 2007 (top left to bottom right). Note: colored- arrow is scaled by color magnitude (cm/s)	90
4.6 Vertical variation of shear at platform P2 during July 22-25, 2007 (■: shear magnitude (1/sec) data points; –: water surface elevation)	91

FIGURE	Page
4.7 Vertical variation of buoyancy frequency at platform ‘P2’ during July 22-25, 2007 (■: buoyancy data points (1/sec); –: water surface elevation)..	92
4.8 Vertical Richardson number (Ri) variation at platform ‘P2’ during July 22-25, 2007 (■: Richardson number; –: water surface elevation)	93
4.9 Vertical dissolved oxygen (DO) variation at platform ‘P2’ during July 22-25, 2007 (■: DO data points (mg/l); –: water surface elevation)	94
4.10 Vertical variation of particle concentration at platform ‘P2’ during July 22-25, 2007 (■: total particle concentration (µl/l); –: water surface elevation)	94
4.11 Scatter plot of actual DO variation along the first transect route on July 24, 2007 (■: DO data points (mg/l); ●: Platform ‘P2’ location; –: sea-bed profile)	96
4.12 Scatter plot of actual salinity variation along the first transect route on July 24, 2007(■: Salinity data points (psu); ●: Platform ‘P2’ location; –: sea-bed profile)	97
4.13 Scatter plot of actual temperature variation along the first transect route on July 24, 2007 (■: Temperature data points (⁰ C); ●: Platform ‘P2’ location; –: sea-bed profile)	98
4.14 Scatter plot of actual chlorophyll (Chl. a) variation along the first transect route on July 24, 2007(■: Chlorophyll (Chl. a) concentration (µg/l); ●: Platform ‘P2’ location; –: sea-bed profile)	99
4.15 Scatter plot of actual particle concentration variation along the first transect route on July 24, 2007 (■: Total Particle concentration (µl/l); ●: Platform ‘P2’ location; –: sea-bed profile)	100
4.16 Scatter plot of actual DO variation along the second transect route on July 24, 2007 (■: DO data points (mg/l); ●: Platform ‘P2’ location; –: sea-bed profile)	102
4.17 Scatter plot of actual salinity variation along the second transect route on July 24, 2007 (■: Salinity data points (psu); ●: Platform ‘P2’ location; –: sea-bed profile)	103
5.1 Site description of study area in Corpus Christi Bay	115

FIGURE	Page
5.2 Schematic diagram of model development	119
5.3 Computational domain of the developed hydrodynamic model	120
5.4 Tidal water surface elevation from ADCIRC model results (blue line) and from NOAA’s published time series (red line) at a) Bob Hall Pier, b) Port Aransas, c) Ingleside and d) Texas State Aquarium stations from May 13, 2007- June 10, 2007	126
5.5 Tidal water surface elevation from ADCIRC model results (blue line) and from NOAA’s published time series (red line) at a) Bob Hall Pier, b) Port Aransas, c) Ingleside and d) Texas State Aquarium stations from July 10~ August 10, 2007	129
5.6 Comparisons of observed (red line) and model predicted (blue line) WSE variation at a) Bob Hall Pier and b) Port Aransas from July 10~ August 10, 2007	133
5.7 Wind speed (blue line) and direction (red line) variation at platform “P3” from July 10~ August 10, 2007	134
5.8 Comparisons of observed (red line) and model predicted (blue line) WSE variation at a) Ingleside and b) Texas State Aquarium stations from May 13~June 10, 2007	136
5.9 Comparison of model-computed velocity magnitude with that of HF-radar measured surface current at mid day of July 12, 2007(a), July 18, 2007 (b), July 24, 2007 (c) and July 30, 2007(d) , respectively	138
5.10 Comparison of model-computed velocity direction with that of HF-radar measured surface current at mid day of July 12, 2007(a), July 18, 2007 (b), July 24, 2007 (c) and July 30, 2007(d) , respectively	139
5.11 Salinity variation along the transect route for the cruise made on July 24, 2007	141
5.12 Salinity variation along the transect route for the cruise made on August 07, 2007	143
5.13 Water current maps along the transect route of the cruise made on August 07, 2007 at successive depths of 1.5m, 1.75m,2.0m,3.0m,3.25m & 3.5m, respectively (from top left to bottom right)	144

FIGURE	Page
5.14 Variation of Richardson (Ri) number along the transect route on August 07, 2007	145
6.1 Characteristic features of Corpus Christi Bay	153
6.2 Salinity variation along the transect route on July 24, 2007. (Note: the colored horizontal lines at the top/bottom of the figure correlate to the transect route as depicted in the inset plot of the figure)	159
6.3 Modeled BOD variation along the black dotted line in Fig. 6.1 after 15 hr of simulation for a) $K_d=0.1/d$ and b) $K_d=0.5/d$. The hydrodynamic conditions and other model parameters held constant.....	162
6.4 Modeled BOD variation along the black dotted line in Fig. 6.1 after 15 hr of simulation for a) $V=10$ cm/s and b) $V=30$ cm/s. $K_d=0.3/d$ and stratification of water column at a depth of 3m is considered.....	163
6.5 Snapshot (15 hr simulation) of DO variation along the black dotted line in Fig. 6.1 under stratified condition with low biological activity conditions ($SOD = 0$ g O_2/m^2 .day, $K_d=0.1/day$)	165
6.6 Snapshot (15 hr simulation) of DO variation along the black dotted line in Fig. 6.1 under stratified condition with normal biological activity conditions ($SOD = 1.5$ g O_2/m^2 .day, $K_d=0.3/day$).....	167
6.7 DO variation along the transect route on July 24, 2007. (Note: the colored horizontal lines at the top/bottom of the figure correlate to the transect route as depicted in the inset plot of the figure)	168
7.1 Map of Corpus Christi Bay and surrounding water bodies. Note: The black rectangle indicates the study area for particle aggregation and transport model development; ●- location of fixed robotic monitoring platforms.....	183
7.2 Initial (t =10 min.) vertical profile of the total particle concentration along the longitudinal and lateral line (shown as dotted line in Figure 7.1), respectively	189
7.3 Vertical profile of model-computed total particle concentration along the longitudinal line (shown in Fig. 7.1) at simulation time of a) 20 min., b) 40 min., and c) 60 min., respectively; Similar profile calculated using analytical solution at d) 20 min., e) 40 min. and f) 60 min., respectively.....	191

FIGURE	Page
7.4 Vertical profile of model-computed total particle concentration along the lateral line (shown in Fig. 7.1) at simulation time of (a) 20 min., (b) 40 min., and (c) 60 min., respectively; Similar profile calculated using analytical solution at (d) 20 min., (e) 40 min. and (f) 60 min., respectively.....	192
7.5 Vertical profile of total particle concentration along the transect route of the July 24, 2007 research cruise; inset plot displays the transect route; (color-coded ■: Total Particle concentration ($\mu\text{l/l}$); ●: Platform ‘P2’ location; –: sea-bed profile).....	194
7.6 Initial vertical profile of total particle concentration along the longitudinal line (shown in Fig. 7.1) for the model simulation.....	195
7.7 Model-computed vertical variation of total particle concentration along the longitudinal line (shown in Fig. 7.1) after a) 20min., b) 40 min., c) 90 min. and d) 180 min. of simulation, respectively; $\alpha=0$	196
7.8 Observed vertical component of fluid velocity at Platform ‘P2’ for 38 hours (starting at 10 am) on July 24, 2007; the wavy solid line denotes the depth of the sea-bed at platform ‘P2’	198
7.9 Model-computed vertical variation of total particle concentration along the longitudinal line (shown in Figure 7.1) after a) 20min., b) 40 min., c) 90 min. and d) 180 min. of simulation, respectively; $\alpha=0.1$	199
7.10 Vertical profile of measured (a) chlorophyll concentration and (b) total particle concentration variation at platform ‘P2’ for 38 hours starting from 10 am on July 24, 2007; the wavy solid line denote the depth of the sea-bed.....	201

LIST OF TABLES

TABLE	Page
6.1 Spatial BOD variation in CC Bay as captured by grab sampling	156
7.1 Basic equations for fractal aggregates under the coalesced fractal sphere assumption (Lee et al. 2000).....	178

CHAPTER I

INTRODUCTION

Statement of Purpose

Coastal areas in the U.S. are the home to a wealth of natural and economic resources. More than half of its population lives within the narrow coastal fringe that makes up 17 percent of the nation's contiguous land area. Texas alone has approximately 2360 miles of shoreline, and two of the nation's top five ports, Houston and Corpus Christi. Estuarine systems associated with the Gulf coast provide economically important habitat for productive marine communities in one of the fastest growing U.S. regions. However, as the human population continues to increase along the coast, it further contributes to the modification of the natural state of these regions through the alteration of the land use pattern, diversion of river water for consumption and many other anthropogenic activities. Many of these coastal water bodies are also used for navigation purposes and therefore, events such as oil spills can deteriorate these ecosystems. In addition of anthropogenic activities, natural perturbations such as precipitation, tropical storms, hurricanes, tsunami etc. can dramatically alter physical, chemical and biological characteristics of these systems. These disturbances are often associated with degradation of ecological integrity at varying scales across space and time.

This dissertation follows the style of *Environmental Monitoring and Assessment*.

These nearshore aquatic environments, often characterized as stochastic pulsed systems, are very dynamic in nature. Therefore, it is not possible to resolve complex multi-scale processes that contribute to various episodic events through discrete sampling. Continuous in-situ monitoring at fixed platforms can aid in resolving the temporal scale of the processes of interest but are limited in characterizing the spatial scale of the processes. On the other hand, sensor systems installed on mobile platforms can measure data at greater spatial but poor temporal resolution. Although sensor systems populated on remote platforms such as shore-based stations, satellite, aircraft etc. can monitor various processes at medium-to-high temporal and spatial resolution but are limited in terms of deployable suitable sensors that can characterize the parameter of interest. If these measured data from various monitoring platforms are available in real-time, it is possible to develop an integrated suitable sampling scheme that will help to capture the extent and frequency of various episodic events occurring in these systems.

The development of suitable cyberinfrastructure to acquire and publish measured data from various monitoring platforms in real time faces significant challenges such as real-time streaming of diverse datasets, data acquisition from heterogeneous instrumentation, data transfer through unreliable communication network, large dataset management etc. In this research, we developed a cyberinfrastructure that is capable of handling these challenges and making data available to stakeholders (i.e., public, scientific community, resource managers and planners, etc.) in near real time. These integrated sensor deployment platforms in conjunction with numerical modeling framework were used to investigate hypoxia which is observed every summer in the

south-east part of Corpus Christi (CC) Bay (Montagna and Kalke 1992). This episodic event occurs when dissolved oxygen levels in the water column dip below 2 mg/l; most aerobic aquatic organisms cannot survive under this condition. CC Bay was selected as the test-bed for the implementation of a sensor-based observation and assessment system in this research.

Background

A scientific paradigm is evolving for the advancement of fundamental understanding and prediction of various episodic events occurring in dynamic natural systems such as coastal and ocean environments. This paradigm involves development of real time environmental observations and assessment systems through integration of sensor-based observational platforms with numerical modeling. The advances in in-situ sensor technologies in recent decades provide an opportunity to measure various physical, chemical and biological parameters in real-time (Agrawal & Pottsmith 2000; Visbeck & Fischer 1995). In addition to these in-situ sensor technologies, rapid progress in infrastructure such as moorings, profiling floats, autonomous underwater vehicles (AUV), gliders, drifters, fiber-optics and electromagnetic cabled platforms, communication technologies, relational database systems and World Wide Web etc. facilitate the implementation of a real-time observatory that can capture high-frequency, episodic, seasonal, interannual, decadal and climate-scale phenomena in the natural systems (Dickey 1991, 2001a; Glenn et al. 2000 a,b; Islam et al. 2006,2007 and Ojo et al. 2007).

State and federal research organizations are spearheading the development of large-scale environmental assessment systems to facilitate the research in oceanic and coastal environments which suffer from various problems due to anthropogenic activities and natural perturbations. The high growth of coastal populations makes these areas more vulnerable. Harmful algal blooms (HAB), accidental oil spills, hypoxia, contaminant movement etc. are a few examples of problems that occur frequently in various coastal regions in the world. A large-scale observation system can help to understand and predict the extent, frequency and duration of these events which are controlled through complex inter-related processes. Among the environmental observation and forecasting systems currently developed in the United States, the Physical Oceanographic Real-Time System (PORTS, http://co-ops.nos.noaa.gov/d_ports.html) maintained by NOAA and CORIE (Baptista et al. 1999) are mentionable. These systems are used for various purposes like navigation safety, tsunami warning, hydropower management, habitat restoration and coastal marine resources protection, etc.

The implementation of environmental observatory is confronted by significant challenges. Continuous in-situ monitoring requires long-term deployment of sensor systems with minimum human intervention and maintenance especially in consideration of costs involved and accessibility of platforms which are often located in harsh environments. Bio-fouling of sensors, especially optical sensors, poses severe restrictions on long-term deployment as data quality quickly deteriorates in highly productive coastal regions. In addition to solving this problem, remote access of sensor systems is required

for troubleshooting of various instruments which will help to lower maintenance costs through reduction of number of non-essential field visits. Establishment of communication links between platforms and the central base station using various data telemetry techniques can facilitate access to sensor systems. Data acquisition from heterogeneous sensors pose a daunting task as each sensor has vendor specific software for collection and processing of raw data, and may not provide much control to the user for data integration with other sensor. Moreover, measured data from various sensors need to be available to stakeholders in real-time for the best use of the data. The management and transfer of diverse data streams such as ASCII, binary, image etc from various instruments also poses a significant challenge for the observatory design.

Sensor systems installed on mobile platforms such as autonomous underwater vehicles (AUV), gliders, research vessels, drifter platforms etc. may help to resolve the spatial scales of interest. The success of these mobile monitoring systems in capturing the phenomena of interest depends on the selection of the optimal sampling frequency and the proper transect route. This demands the development of real-time data acquisition and visualization system which will help to select the sampling scheme “on the fly” depending on the relative intensity of the measured parameters with respect to pre-set peak values of interest. In addition to fixed and mobile monitoring platforms, sensor systems installed on remote platforms such as satellite and shore-based observation stations can characterize the variability of parameters in the upper level of the water column at good spatial and temporal resolution although they are limited in their capability to capture the variability in the lower water depths.

Sensors systems installed on various monitoring platforms are integrated for the development of suitable sampling scheme to capture the events of interest. Also, large datasets collected from these monitoring systems helped to validate and to drive various numerical models which assisted in hypothesis testing and greater understanding of the processes that control various episodic events.

The National Science Foundation (NSF) has provided funding to establish WATER and Environmental Research Systems (WATERS) Network to meet these challenges and to test other aspects of observatory design and operation at different test beds sites of the USA. This network will make available all data collected from various observatories and will help in investigating multiscale environmental phenomena (Montgomery et al 2007). Corpus Christi (TX, USA) Bay has been selected as one of the test bed sites of WATERS network. This bay is home to the nation's seventh largest port and contains numerous petrochemical facilities. Considering its impact on the national economy, CC Bay was designated as a National Estuary in 1992. But water quality in this bay suffers from various problems like accidental oil spills, hypoxia, contaminant movement, existence of high levels of bacteria, sediment resuspension, etc. Among these problems, the occurrence of hypoxia in this shallow bay has drawn national attention. Hypoxic conditions were first reported to occur in the south-east part of the bay in 1988 (Montagna and Kalke 1992) and have been observed every summer thereafter (Ritter and Montagna 1999). The existence of hypoxia in this dynamic system can last on the order of hours to days (Ritter & Montagna 2001). The dynamic processes that control this event can be investigated through real-time measurements of various

hydrodynamic, meteorological and water quality parameters at greater spatial and temporal resolution. The development of a real-time observation and assessment system for CC Bay makes this information available in real time. This can also facilitate capturing the extent, frequency and duration of the event.

The occurrence of hypoxia at the bottom of the bay and the inflow of hypersaline water from two neighboring shallow water bodies (Hodgest et al. 2007) suggest that there exists a significant vertical gradient in water quality and hydrodynamic parameters. The characterization of this gradient is important in understanding hypoxia in the bay. The development of a robotic profiler system on fixed platforms can help in capturing this gradient. This profiler system moves various instruments within water column and collects data at multiple depths. It can also reduce bio-fouling through air drying and sunlight exposure (UV) of the sensor suite between measurement cycles. The control of bio-fouling through this method is more efficient compared to other available methods such as the use of copper-based materials, tributyl tin- (TBT-) based products, slowly dissolving chlorine (trichlorisocyanuric acid), underwater UV-lights and bromine tablets etc. This system is installed at several fixed platforms in the bay for the continuous monitoring of water quality. Measured data at these platforms is made available to stakeholders in real time through the development of various communication infrastructures, relational database system, web services, etc.

Ojo et al. (2007a) developed a portable Integrated Data Acquisition, Communication and Control (IDACC) system that was deployed on a research vessel and could measure variation of water quality parameters ‘synchronously’ over a highly-

resolved spatial regime. This system could acquire and visualize data measured by submersible sensors on an undulating tow-body (Acrobat LTV-50HB, by Sea Sciences Inc.) deployed behind the boat. Although it was able to successfully capture the horizontal variation of various parameters, it had limited success in resolving the vertical gradient of parameters. This system was thus extended and modified in this research to add this feature. Also, the real-time display capability of this system guides transect route selection to sample various parameters in the areas with low-dissolved oxygen conditions. This helps to determine inter-related processes that may induce hypoxia in the bay.

Hydrodynamic information is critical to understand ecosystem health. The surface currents of the bay can be measured at greater spatial and temporal resolution with high frequency (HF) radar systems installed on remote platforms (Barrick et al. 1977; Kelly et al. 2003). Ojo et al. (2007b) measured hourly surface current maps of CC Bay through an HF-radar system installed on two remote platforms. This surface current data together with water quality, meteorological and hydrodynamic measurements at fixed and mobile platforms can provide insight regarding various processes that control the dynamics of the system. Moreover, real-time availability of measured data helps to design an integrated sampling scheme for sensor systems installed on different types of monitoring platforms. This assists in measuring critical parameters at the proper spatial and temporal resolution to understand and to capture the extent, frequency and duration of various episodic events such as hypoxia.

A hydrodynamic model serves as a necessary and complementary tool of the

observation system through its prediction of important hydrodynamic information to decision makers in the case of emergency events like oil spills, storm surges, and contaminant releases (Westerink et al. 2008 & Chen et al. 2007). Various numerical models are available which can be used to develop a hydrodynamic model in the scale of river to ocean. Among them, POM (Blumberg & Mellor 1987), ADCIRC (Luettich et al. 1992), ELCIRC (Zhang et al. 2004 and Baptista et al. 2005), ROMS (Haidvogel et al. 2000), SEOM (Iskandarani et al. 2003) and QUODDY (Lynch et al. 1996) are popular ones. These models vary in their choice of numerical schemes, inclusion of baroclinic terms, turbulence closure schemes, grid structure, representation of boundary conditions and forcing functions, stretched or un-stretched vertical co-ordinate system and level of complexities (2D/3D), etc.. The numerical model, which represents hydrodynamic processes within the domain of interest and involves less computational time and complexity, is a suitable candidate for the choice. Two-dimensional depth-integrated hydrodynamic models have long been used to successfully predict hydrodynamic information such as storm surges and tidal elevations in coastal waters. The key assumption of this simplified version of a hydrodynamic model is that water column needs to be vertically well-mixed. The inflow of hypersaline water from two neighboring water bodies into CC Bay may question the validity of this assumption. HF-radar generated surface current maps and various water quality and hydrodynamic parameters measured at fixed/mobile platforms provide an opportunity to investigate the reliability of a 2D model in capturing the hydrodynamic condition of the bay. This can shed light on the limitation of a 2D model and provide recommendation/criteria for the

development of a suitable numerical model that can capture the detailed hydrodynamic information of the bay.

A three-dimensional mechanistic dissolved oxygen (DO) model can provide greater understanding of the dynamics of DO variation and can help to predict the extent and frequency of hypoxic events in the bay. The main processes that control DO distribution in the bay are surface re-aeration, water column stratification, decomposition of organic matter in the water column and sediment, respiration and photosynthesis, etc. (Thomann and Mueller 1987). The sensitivity analysis of the developed model shed lights on the relative importance of these processes in changing the DO pattern in the bay. This information can then assist in optimizing the available resources in characterizing the key processes causing hypoxia and thereby helps to implement a cost-effective observational system for coastal water quality monitoring.

Biogenic particles can directly contribute to DO dynamics through producing and consuming DO in the water column whereas non-biogenic particles can play a role as carriers. The longer the oxygen-consuming particles remain in the water column, the greater the amount of oxygen they will consume. Schmidt et al. (2002) tried to determine particle residence time in surface waters over the north-western Iberian Margin using natural radionuclide ^{234}Th as a tracer of sinking particle fluxes. As the residence time depends on the hydrodynamic condition of the system, it may change quite frequently in a dynamic system like CC Bay. The development of particle aggregation and transport model helps to characterize the particle dynamics and thereby provide useful information such as particle size distribution, particle concentration,

residence time etc. The basic theory that controls the aggregation characteristics of particles dates back to the work by Smoluchowski (1917). The generation rate of aggregated particles from the collision of particles of varying sizes depends on the collision efficiency and frequency. The collision efficiency factor represents the chemistry involved in coalescence (Sterling, 2003) whereas the collision frequency functions can be described as the contact mechanisms between particles (Gregory, 1989). The aggregation kinetics of particles needs to be determined through fractal theories as aggregate particles in natural systems exhibit fractal characteristics (Jackson et al. 1997). The aggregation model used in this study is based on the proposed fractal theories by Jiang and Logan (1991). The development of the field scale particle aggregation modeling framework presented in this research is an extension of the previous modeling efforts in our group to characterize the particle dynamics in laboratory scale settings (Ernest et al. 1995; Lee et al. 2002 & Sterling et al. 2005).

A comprehensive coastal margin observation and assessment system (CMOAS) for CC Bay is implemented in this research through deployment of previously-mentioned various sensor systems on different types of monitoring platforms and development of numerical models. This system assists in capturing and understanding hypoxic events in CC Bay. The schematic diagram of the developed observation and assessment system is shown in Figure 1.1. Datasets collected from fixed robotic, mobile and remote monitoring platforms are analyzed together to understand various processes causing hypoxia in the bay. The integration of various monitoring systems also helps in developing suitable sampling scheme to capture the extent, frequency and duration of

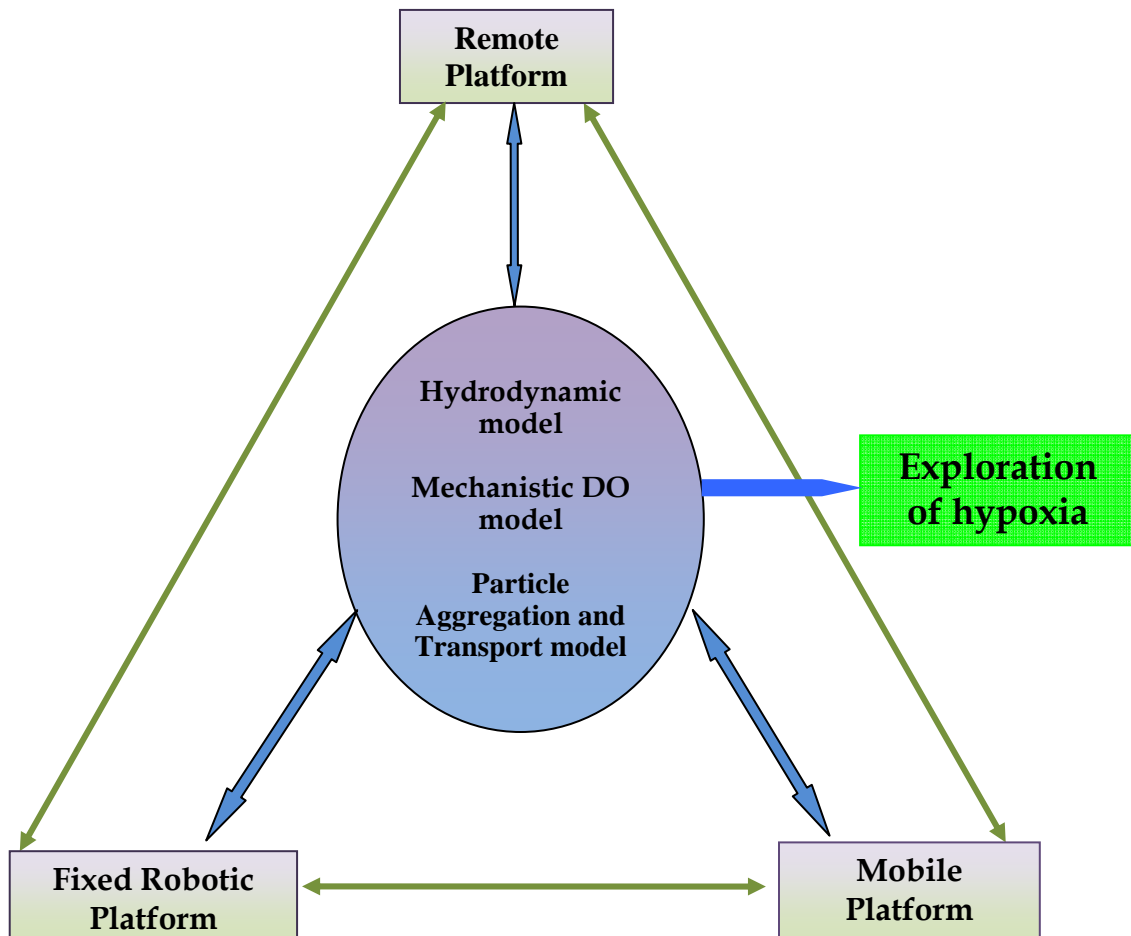


Fig.1.1 Schematic diagram of Coastal Margin Observation and Assessment System (CMOAS) for CC Bay.

hypoxic events. Moreover, observational datasets are used to drive and verify various numerical models developed in this study. The meteorological data collected from fixed robotic platforms are used to drive hydrodynamic model. In addition, hydrodynamic data measured at various platforms are used for the skill assessment of the developed 2-D model. Advection and dispersion coefficients determined from the hydrodynamic model or observational datasets can be used to drive various transport models (Ojo et al.

2007b). These coefficients are used in simulating particle aggregation and transport model and mechanistic DO model. Observational datasets can also be used to initialize and to assign boundary conditions for these two models. Particle dynamics characterized by a particle aggregation and transport model can be linked with the mechanistic DO model through supplying particulate biochemical oxygen demand (BOD) distribution in the computational domain. The output of the mechanistic DO model then help to characterize the key processes causing hypoxia and to predict the extent, frequency and duration of this phenomenon in the bay.

Objectives

The specific objectives represented by field observation and modeling studies, are as follows:

- I. Develop a fixed robotic profiler system to measure vertical variation of water quality parameters at greater temporal resolution. This system reduces bio-fouling of sensors and make measured data available to stakeholders in real time.
- II. Modify and extend an existing mobile monitoring system to capture the vertical gradient of water quality and hydrodynamic parameters in CC Bay. Also, develop software that displays vertical variation of measured parameters and provides guidance in transect route selection to capture the event of interest.
- III. Develop and integrate monitoring systems on different types of platform, and implement the integrated system to capture the extent and timing of an hypoxic

event in CC Bay.

- IV. Develop a two-dimensional depth-integrated hydrodynamic model for CC Bay.

The reliability of this model in capturing hydrodynamic condition of the bay was investigated using measured datasets at various monitoring platforms.

- V. Develop a three-dimensional mechanistic model for dissolved oxygen variation in Corpus Christi Bay based on a finite segment numerical scheme. Also, perform a sensitivity analysis to determine the key processes causing hypoxia in CC Bay, using biochemical oxygen demand (BOD) and dissolved oxygen (DO) as the primary state variables.

- VI. Develop a three-dimensional particle aggregation and transport model to characterize particle dynamics, and use a case study to compare model results against the analytical solution.

CHAPTER II

A FIXED ROBOTIC PROFILER SYSTEM TO SENSE REAL-TIME EPISODIC PULSES OF THE CONDITION OF CORPUS CHRISTI (CC) BAY

Overview

Real time observations of coastal environments can bring significant benefits to the national economy. Various prototype sensor-based observation systems are already being deployed in various coastal regions around the USA. Federal and state agencies are providing support for the planning and implementation of those observation systems. The National Science Foundation (NSF) has established the WATer and Environmental Research Systems (WATERS) Network to test various aspects of observatory design and operation at different test bed sites in the USA. Corpus Christi (CC) Bay was selected as one of the network test beds. This shallow bay is wind-driven and so the dominant processes that control the dynamics of the system can change very rapidly, and real-time availability of the measured data from this system can help in understanding those processes. The implementation of real-time observation system faces several challenges: use of heterogeneous instruments in environmental monitoring, need for reliable data acquisition and delivery, measurement of critical parameters at greater spatial and temporal resolution, data management and reduction of sensor bio-fouling. We have developed and installed a robotic profiler system at several fixed platforms in the bay. This system moves a suite of water quality measuring sensors in the water column periodically and collects data at multiple depths. Our robotic profiler system is designed

to significantly reduce bio-fouling of the sensors, thus increasing the instrument duty cycle. The Cyberinfrastructure (CI) developed as part of this research makes sensor data available to stakeholders in real time. It can process diverse data streams and is robust enough to handle the communication network failure for the reliable delivery of the measured data from the platforms to the user. We have also developed a relational database to store observational datasets from our monitoring platforms. This data will be useful for the exploration of the interrelated processes that control the event of interest and the determination of long-term trends in the variation of those processes. Also, the myriad datasets measured by these systems can be used to drive water quality and hydrodynamic models which will help to predict and understand various episodic events predominant in this energetic system.

Introduction

Coastal environments can be characterized as stochastic pulsed systems (Ojo 2005). The dynamics of these systems are controlled through episodic events and periodic processes. The temporal scale of coastal phenomena can vary from order of seconds to decades. For example, the intensity of wind-generated turbulent motion can fluctuate on the order of seconds whereas sea level rises due to global climate change can occur over decades. Carter (1988) and Steele (1995) have discussed the extent of temporal scale for various important processes that occur in coastal regions. Development of a sensor-based observation system can provide long-term high resolution measurements of critical environmental parameters (Isern and Clark 2003).

This kind of information aids in the understanding the various phenomena that control the dynamics of these systems and will assist in capturing events of interest. The advances in sensor technology in this decade provide an opportunity to collect data at high resolution with reasonable cost. The National Research Council (NRC) therefore recommends the development of a large-scale sensor based observation system to address the grand challenges in environmental science (NRC report, 2001). This observation system can be used to collect data and to investigate questions related to global warming, infectious diseases, invasive species, pollution, land use and other environmental problems. Various prototype observing systems have already been deployed at various parts of USA with the support of federal and state agencies. Among them are the Physical Oceanographic Real-Time System (PORTS 2009), National Ecological Observatory Network (NEON 2009), Global Lake Ecological Observatory Network (GLEON 2009), Coral Reef Environmental Observatory network (CREON 2009) and Ocean Research Interactive Observatory Networks (ORION 2009) mentionable.

The National Science Foundation (NSF) has provided funding to establish WATER and Environmental Research Systems (WATERS) Network to test various aspects of observatory design and operation at different test beds sites of the USA. This network will make available all data collected from various observatories and will help in investigating multiscale environmental phenomena (Montgomery et al. 2007). Corpus Christi (TX, USA) Bay has been selected as one of the test bed sites of WATERS network. This bay is home of the nation's seventh largest port and contains numerous

petrochemical facilities. Considering its impact on the national economy, CC Bay was designated as a National Estuary in 1992. But water quality in this bay suffers from various problems such as accidental oil spill, hypoxia, contaminant movement, harmful algal bloom, existence of high levels of bacteria, sediment resuspension. Among these problems, the occurrence of hypoxia in this shallow bay has drawn national attention. Hypoxic condition was first reported to occur in the south-east part of the bay in 1988, and has been observed every summer thereafter (Ritter and Montagna 1999). Hypoxia can be described as the condition of water column when dissolved oxygen (DO) dips below 2 mg/l and most aerobic aquatic organisms cannot survive under this condition (Rabalais et al. 1996). This shallow bay is not expected to be hypoxic due to the high mixing of aerated surface water with low DO water at the bottom of the bay. However, this condition occurs and can last on the order of hours to days (Ritter and Montagna 2001). Therefore, development of a sensor-based monitoring system will help to measure water quality, hydrodynamic and meteorological parameters at high resolution and thereby assist in understanding hypoxic and other episodic events that control the dynamics of this system. This data also needs to be available in real time so that decision makers can make optimum use of the observed datasets. The benefits of real-time observations in coastal environments are many fold: for example, real-time water level and current information can assist in safe navigation of water vessels; real-time meteorological and hydrodynamic data are assimilated with various forecasting models which are used in warning extreme events such as hurricanes, storm surges . Other applications of real time data are search and rescue (SAR) operations, oil spill trajectory

predictions and clean up operations, prediction of harmful algal blooms (HABs), hypoxic conditions and many other environmental problems that plague coastal regions.

With recent advances in technology, real-time measurements of water quality parameters are possible through the use of submersible in-situ sensors (Agrawal and Pottsmith 2000; Boss et al. 2007; Visbeck & Fischer 1995). The advantage of in-situ sensors is that the parameter of interest can be measured in real time, thereby omitting time gaps between sample collection and data analysis. Also, the progress of communication technology, database management system and computational power provide an opportunity to develop a cyberinfrastructure that will acquire data from various sensors and will make them available to stakeholders in real time. The implementation of cyberinfrastructure (CI) development for environmental observatory faces challenges due to heterogeneous instrumentation in environmental monitoring, complex data stream, unreliable communication network, management of metadata. Different sensor vendors have developed their own software to collect and process the raw data into meaningful units. The accommodation of this broad spectrum of sensors in the observing systems requires the development of user-specified drivers to collect and process raw data. Also, observing systems should have the provision to handle different formats of data such as binary, ASCII, image. Moreover, sensor systems are frequently deployed in remote, harsh environments which contribute to unreliable network connections. Therefore, the observation system should be designed in such a way so that it can store data locally in the case of network failure and will transmit the data to the base station as soon as the communication network is up. Ring Buffer Network Bus

(RBNB) Data turbine (Tilak et al. 2007) and Antelope system from Boulder Real Time Systems (BRTT 2009) are data streaming middleware that can handle diverse sensor systems and can manage or store data reliably in the case of network failure. In those systems, the efficiency of data acquisition from a specific sensor depends on the development of suitable software in collecting data from the instrument data logger. Also, data collected from these systems need to be stored into the relational database system to explore the interrelated processes that contribute to the events of interest. This database system will help to keep the long-term persistent storage of measured dataset.

Long-term deployment of a sensor system on a fixed platform will not help to capture the spatial variation involved in a dynamic system like CC Bay. However, understanding the vertical gradient in hydrodynamic and water quality parameter variation in the bay is very important to characterize episodic events like hypoxia. For example, if the vertical salinity gradient is pronounced and the water column is stratified, oxygen levels at the bottom of the bay will be reduced due to the insufficient mixing with aerated surface water (Turner et al. 1987). Also, long-term deployment of sensors at fixed platforms suffers from bio-fouling which can seriously deteriorate sensor conditions and data-quality. Bio-fouling increases the instrument duty cycle and so raises the cost of maintaining sensor systems in the bay. Therefore, a monitoring system needs to be developed that can measure the vertical variation of parameters at greater temporal resolution and can reduce biofouling of sensors.

Various researchers have been trying to develop an efficient vertical profiling system for the continuous measurements of various parameters in the deep and shallow

waters. Among them Purcell et al. (1997), Honji et al. (1987), Reynolds-Flemin et al. (2002) & Luettich et al. (1993) are mentionable. Purcell et al. (1997) successfully deployed their vertical profilers in the coastal observatory, LEO-15 (Operated by the Rutgers University Institute of Marine and Coastal science) but faced challenges for the long-term deployment of profiler system as sensors are bio-fouled within a week. Also, measured data were not available to stakeholders in real-time due to the lack of proper cyberinfrastructure. Honji's et al. (1987) vertical profiler system can only be used for deep-water applications whereas Luettich et al. (1990) profiler system (PSWIMS) can be applied to the shallow areas of more protected estuarine environments. As water quality parameters always need to be monitored in the harsh unprotected environment, it is necessary to develop a robust ruggedized vertical profiler system for long-term autonomous monitoring of the aquatic system. Reynolds-Fleming et al. (2002) developed a portable autonomous vertical profiler (P-AVP) using off-the-shelf parts with a minimal use of custom components. Their system can be easily transported to a desired deployment site and deployed in relatively unprotected areas. The biggest drawbacks of the system were that sensor packages hit against the platform and are biofouled very quickly. Commercial-off-the-shelf vertical profiler systems such as the system manufactured by YSI, Inc. (YSI 2009) can monitor vertical variation of water quality parameters. But the system can only interface with their sensor products. This seriously limits the use of the profiler system in measuring parameters that were not resolved through their particular sensor products. For example, YSI does not have a particle sizer (e.g. LISST-100X, manufactured by Sequoia Inc.) that can measure particle

concentrations of various particle sizes in the water column, nor a FLOWCAM (Fluid Imaging Technologies, Inc.) that counts, images and analyzes the cells in the water sample. Therefore, in this study a vertical profiler system was developed that can reduce sensor's biofouling, make sensor data available to stakeholders in real time, interface heterogeneous instrumentation from different vendors and is ruggedized and robust enough to be maintained in the harsh environment. The purpose of this paper is to describe the design, construction, test deployment and evaluation of a vertical profiler system that can continuously monitor various hydrodynamic, meteorological and water quality parameters in the bay.

Installation of a sensor system on a fixed platform will not capture the horizontal variation of the parameters of interest. This can be achieved through the installation of in-situ sensors on other platforms such as mobile platforms, bottom tripods, drifters, floats, etc. (Dickey 1991; Dickey et al. 1998). In addition, remote platforms such as satellite, aircraft and shore-based platforms can also be used to deploy various types of sensors. Sensor systems from these various types of platform will then give a good spatial resolution of the parameter of interest. Data collected from various platform types needs to be integrated to understand the event of interest. The integration of various platforms to capture the extent and frequency of hypoxic events in CC Bay is discussed details in Islam et al. (2009c).

The research objective for this chapter was to develop a robotic profiler system that reduces bio-fouling of sensors and measures water quality parameter at multiple depths of the water column at greater temporal resolution. This system was installed on

different fixed platforms in CC Bay. Along with this system, sensors were installed to measure hydrodynamic and meteorological parameters around the fixed platforms. Also, a cyber-infrastructure was developed to collect data from various platforms and to publish data on the web in real-time. This cyberinfrastructure provides the framework to link our local observation network with the other sensor-based observational networks in the USA. Data collected from our fixed robotic platforms test the ability of the system in capturing dynamic processes in CC Bay. The large datasets from our observational network can also be used to drive numerical models which aid in understanding the processes controlling episodic events in the bay.

Study Area

Corpus Christi Bay is located on the Texas coastline and covers an area of approximately 432.9 sq. km (Flint 1985). It is connected to the Gulf of Mexico through a narrow ship channel (15 m depth), which runs from east to west. Freshwater enters the bay via the Nueces River and Nueces Bay, whereas high-saline water enters the bay during summer months from the shallow Upper Laguna Madre and Oso Bay (Figure 2.1). Recently, Packery Channel, located at the southern reaches of the bay, has been opened and it is another source for the water exchange with the Gulf of Mexico. CC Bay is mainly dominated by south-easterly winds although northerly winds occur periodically during the winter months. Figure 2.1 shows characteristic features of the bay. The cross-hatched circles represent locations where hypoxia has been reported (Ritter and Montagna 1999; Hodges and Furnans 2007). The three red solid circles

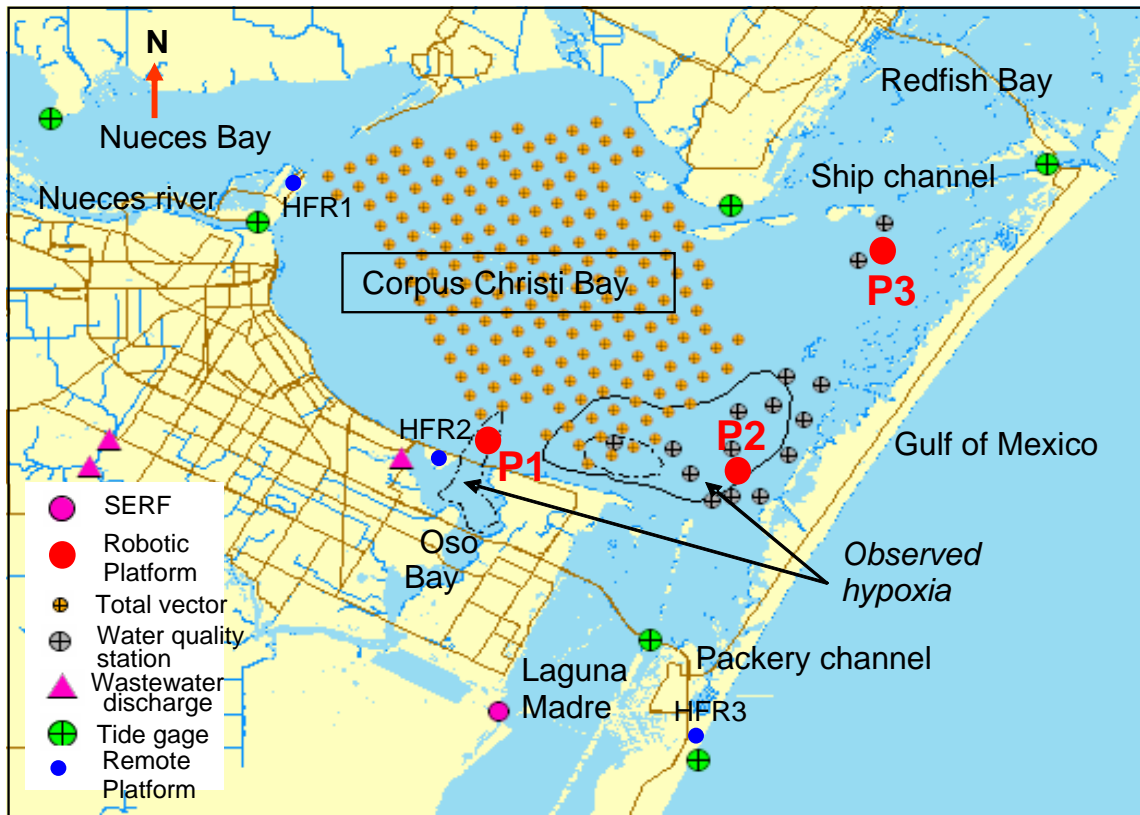


Fig. 2.1 Characteristics of the study area and platform locations.

denote the strategic locations of our fixed robotic platforms. Platform ‘P1’ ($27^{\circ}43.531'N$, $97^{\circ}18.412'W$) is positioned 100m from the mouth of Oso Bay to characterize the effects of Oso Bay inflow, which has been reported to trigger hypoxia in that part of the bay. Platform ‘P2’ ($27^{\circ}43.375' N$, $97^{\circ}11.403'W$) is positioned in the south-east portion of the bay where hypoxia has been documented since 1988 (Ritter and Montagna 1999). Some of the ship channel effects on CC Bay may be captured through our Platform ‘P3’ ($27^{\circ}48.560' N$, $97^{\circ}08.513' W$) in the north-east part of the bay. The data collected from these platforms also provide necessary boundary conditions for the simulation of our

three-dimensional mechanistic model (Islam et al. 2008) to predict the dissolved oxygen (DO) distribution in the bay. The magenta solid circle in the figure shows the location of our research facility (Shorerline Environmental Research Facility, SERF) at Flour Bluff in Corpus Christi. SERF works as a data aggregation point for all data collected from different platforms. The solid blue circles represent the location of our remote platforms where HF-radar systems are installed, and tainted-yellow circles display the locations of total vector in CC Bay generated from our HF-radar system. The wastewater discharge locations (denoted by magenta-colored triangle), tidal gage (represented by solid green circle), and water quality stations (displayed using grey circle) are shown here to indicate the areas of interest for collecting other important information and data, but are not used in this chapter.

Vertical Robotic Profiling System (with Instrumentation Suite) on Fixed Platforms

A robotic profiler system has been designed in this study to measure vertical variation of various water quality parameters at a greater temporal resolution. This profiler system consists of four main parts: a) the payload cage, which houses the instruments; b) the profiler, which raises and lowers the payload; c) the wincube (customized PC/104 computing module); and d) Cyberinfrastructure(CI) which makes measured data available to stakeholders in real time. Fig. 2.2 shows the robotic profiler system at one of our fixed robotic platforms in the bay. The payload is suspended from the profiler by two cables, with a single power/data cable connecting the instruments. This single power/data cable is later diverted into data cable and power cable. The data

cable is then serially linked with the wincube whereas power cable is connected with the

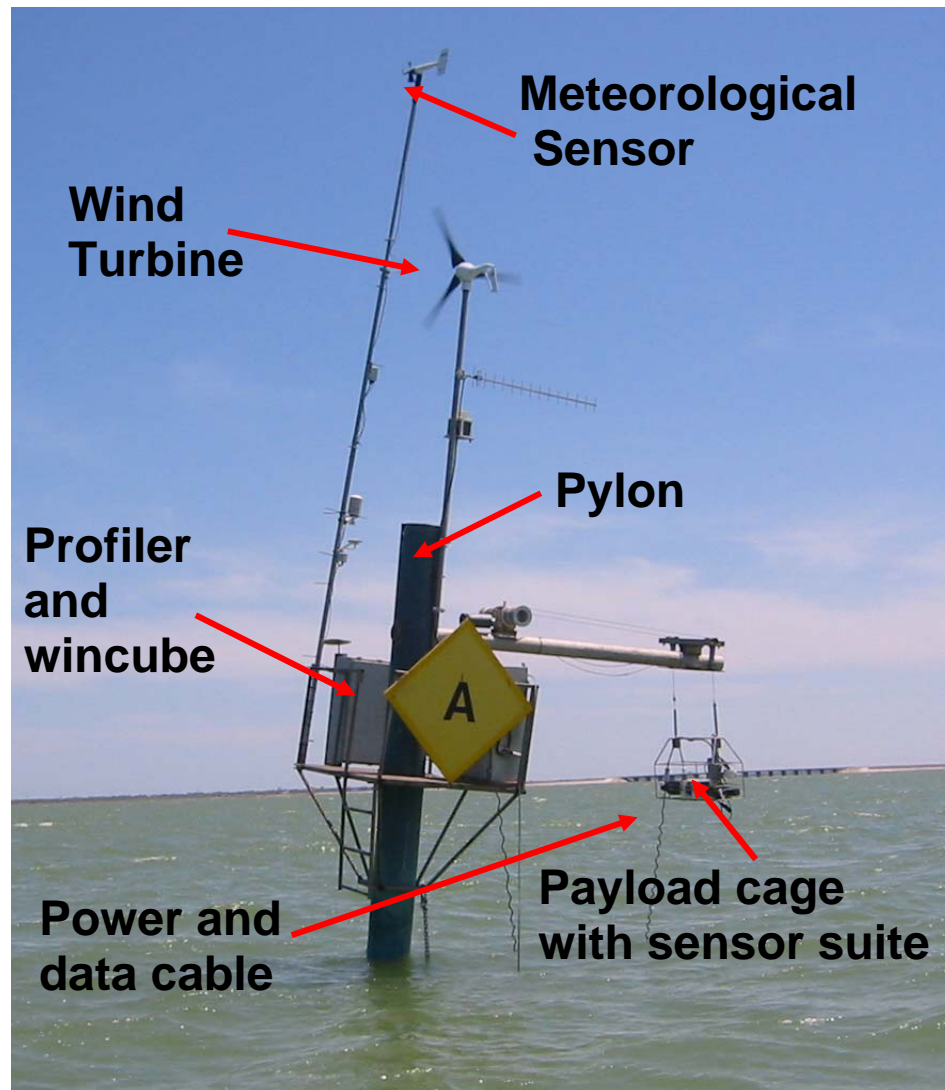


Fig. 2.2 Robotic profiler system at one of our fixed robotic platform in the bay.

12V battery fuse block which is recharged through a wind turbine. The sensor suite currently includes a particle sizer (LISST 100X, by Sequoia Sciences), a DO sensor

(Optode, by Aanderaa), a CTD (Conductivity, Temperature and Depth) sensor (SBE 37 SIP “Microcat”, by Sea-Bird Electronics, Inc.) and a fluorosensor (Eco-FL3, by WETLabs). The profiler is deployed off a tall pylon with an arm reaching over the side of the platform overlooking the water. Two suspension cables connect the payload to this arm, and an electric motor is responsible for winching the payload up and down. This motor is operated by an electronic controller module, which in turn is operated by control software developed as part of our research effort. This software is installed in the wincube which is a customized ruggedized PC/104 computing module. We have added multiport serial cards (Xtreme -8/104/RS-232 by Connect Tech Inc.) and 1.8 GB flash drive with this module. As PC/104 systems are small and have low power requirements, they have been used on various applications to meet the needs of an embedded system. Also, most of the development programs used in personal computer (PC) can also be used in this system. The operating system of the wincube is WINDOWS 2000 server. File Transfer Protocol (FTP) server in a Microsoft Windows 2000 environment has been used to transfer data from the fixed robotic platforms to the base station. Remote access and control of robotic profiler systems are also achieved through the remote control software (Real VNC) which has been installed in the wincube.

The control software operates the profiler and payload to provide vertical profiles of the water column by raising and lowering the payload into the water column and gathering measurements. The control software is designed in such a way so that it first captures the reading from the fastest sensor and then sequentially records readings from other sensors based on their stable response times. Laboratory experiments were

performed to determine the response time for each sensor on the profiler. Different instruments require different amount of time and differing numbers of measurements per sample to register a stable reading. For example, the LISST-100 particle sizer needs approximately three seconds to register a stable reading, whereas the DO sensor (Optode) requires seven seconds. The CTD sensor (Microcat) and Flurosensor (ECO-FL3) have faster response times, requiring approximately two and one seconds, respectively. The optimal sampling scheme for this robotic system was designed considering this information. The control software is also flexible to handle adaptive sampling scheme considering the dynamics of the system. Data collected from each sensor are written on text files and stored to a folder in the wincube for the transfer to our shore-based research facility at SERF. All software developed for this system is written using the dynamic programming language PERL. Data collected from our fixed robotic platforms are available to stakeholders in real time through the web server at SERF which hosts web services. The availability of data in real time also facilitates the quality assurance and quality control (QAQC) testing of sensors.

The current payload capability of our robotic system allows for four instruments, but can house additional sensors with minor modification. The control software is also designed in such a way so that it can accommodate future inclusion of more heterogeneous instruments with diverse data streams like ASCII, binary, image . It is configured through plain-text configuration files, making administration separate from programming maintenance. Along with the robotic profiling system, an upward-looking 1200 KHz workhorse Acoustic Doppler Current Profiler (ADCP by Teledyne RD

Instruments) has been installed at the base of each fixed platform to measure water column currents and a Meteorological sensor system (Windbird Monitor-MA R.M. Young) is configured on the platform to measure parameters including wind speed and direction, wind gust, air temperature, and barometric pressure. Vendor software for these sensors is not able to generate individual files for certain duration of measurements. Therefore, we have developed data collection software that can generate individual data files for the user-defined duration of measurements. As soon as these files generated, they are stored in the temporary folder from where they are periodically imported to the base station.

Power is the most critical factor for maintaining our long-term autonomous system. The necessary power to maintain our fixed robotic platform is generated from the small wind turbine (AIR-X by Southwest Windpower Inc.). It can generate 38 kWh/mo at a wind speed of 12 mph. Bio-fouling is another important issue for the long-term deployment of sensors systems in the marine environment. Our robotic profiling system helps to control sensor bio-fouling which can significantly deteriorate sensor performance. As the profiler system keeps the sensor suite in a stationary position above the water surface between measurement cycles, this allows the sensors to dry through air contact and ultra-violet sunlight exposure. This prevents the growth of microorganisms on the sensor and, therefore, the instrument duty cycle is longer. For our robotic sensor system, the instrument duty cycle is around six months. The control of bio-fouling through this method is more-efficient compared to other available methods such as the use of copper-based materials, tributyl tin- (TBT-) based products, slowly dissolving

chlorine (trichloroisocyanuric acid), underwater UV-lights and bromine tablets etc. Manov et.al. (2003) has discussed the limitation of these methods in controlling bio-fouling of optical sensors. We have also tested many of these strategies and found that air drying and sunlight exposure (UV) worked the best.

Description of the Developed Cyberinfrastructure

Measurements of water quality, hydrodynamic and meteorological parameters through in-situ sensors at our fixed robotic platforms need to be made available to stakeholders (i.e., public, scientific community, resource managers and planners) in near real time. We have developed cyberinfrastructure which can be described as a computing and communications technology infrastructure system to acquire and publish those data in real time. Figure 2.3 presents the schematic diagram of our cyber- infrastructure system used to transfer data from the fixed robotic platform to the user community.

All data collected from our robotic profiler system, Acoustic Doppler Current Profiler (ADCP) and meteorological sensor are stored in a temporary folder on the WINCUBE prior to being telemetried to our research facility at SERF (shown in Figure 2.1). Wireless data transceivers (FGR-115RE, Freewave Technologies, Inc) with directional antenna have been installed at platform P1 and P3 for establishing radio links with platform P2. Also, wireless data transceiver with omni-directional antenna has been installed at Platform P2 for receiving signals from platforms P1, P3. The other wireless data transceiver with directional antenna has been installed on platform P2 to relay data

to an intermediate radio relay station. Since wireless (radio) links are subject to distance limitations, intermediate radio relay stations have been established for the data telemetry

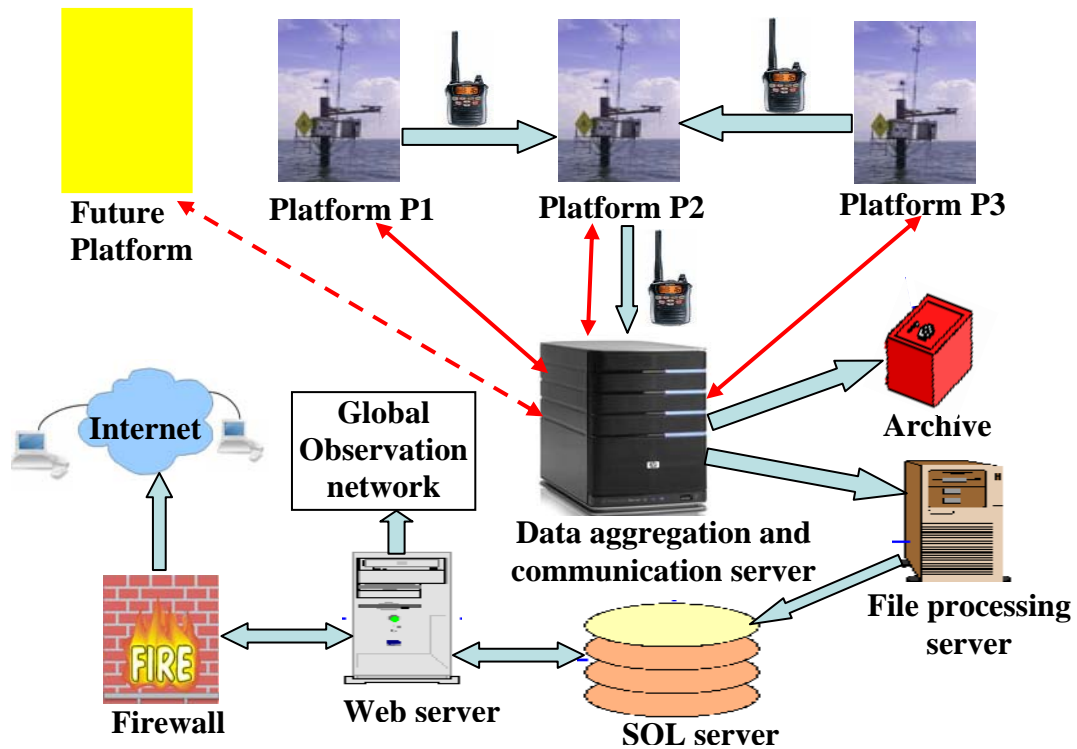


Fig 2.3 Schematic diagram of cyberinfrastructure for fixed robotic profiler system.

to SERF. The wireless data transceiver with omni-directional antenna at SERF is then connected with the data aggregation and communication server through which the administrator can control all geographically distributed platform sites. The remote control software (Real VNC) has also been installed on the server to get access to the wincube at different platforms. This remote access will serve different purposes from instrument management to quality assurance of the data. It is expensive to visit the

platform sites for activities such as troubleshooting instruments, detecting instrument failure, upgrading the data acquisition software. The remote access facilitates to reduce the number of such field visits, and also provides opportunity to develop event-based sampling schemes for our robotic profiler system. During windy conditions, the wind turbine at the platforms can generate higher power and so our robotic profiler systems will not be limited by power constraint. We can then schedule to run robotic profiler control software at higher frequency to collect data at greater resolution and thereby to capture wind-dominated processes such as sediment resuspension events, turbulent mixing. This system has been applied to collect data at greater temporal resolution during oil-spill response studies in CC Bay using remotely configured adaptive sampling scheme.

We have developed a program (named “Transbot”) which is installed on the data aggregation and communication server for the scheduled transfer and archival of real time data from an arbitrary number of fixed robotic platforms to a file processing server. While originally conceived to gather environmental data from a variety of remote platforms, Transbot is also transparent and generic, i.e., it is capable of managing any arbitrary data stream like ASCII, binary, image. It is configured through plain-text configuration files, making administration separate from programming maintenance. This software uses file transfer protocol (FTP) to download data from the remote sensor sites. The software is also robust enough to control data transfer in the case of network failure. This ensures continuous operation of our robotic platforms in the case of communication loss with one or more platforms due to various reasons like data-

transceiver failure, disruptions in line-of-sight, power failure. The data collected from each robotic sensor systems are then going to be stored in the temporary folder of the wincube and will be relayed to data aggregation and communication server as soon as the network will be up again. Once data are transferred to the file processing server, they are processed for the conversion into meaningful units and are then standardized for the insertion into the relational database system. The management of diverse datasets into the relational database server provides long-term storage facility and also helps to determine the interrelated processes that contribute to event of interest. The Microsoft database management system (Structured Query Language, SQL) server has been selected as the relational database system to manage water quality, hydrodynamic and meteorological datasets collected from the platforms. The web server at SERF hosts the web services through which researchers, educators, policymakers, natural resource managers and the general public can get data in real-time. Also, developed software for near real-time visualization of measured datasets was installed on the web server which facilitates quality assurance quality control (QAQC) testing. If any anomaly in the dataset is noticed, then those data are analyzed further to determine whether it arises from a sensor defect or from a change in the actual bay conditions. A platform service trip may be required to make the determination. If necessary, a faulty sensor can be replaced with a newly calibrated sensor and the original sensor is returned to the laboratory for post-calibration and diagnosis of the problem. All sensors on each profiler are pre- and post-calibrated before and after deployment. We have also developed and installed the software on our web server through which data requests from other

organization and observational network are queried into our SQL database and then converted into the XML (Extensible Markup Language) format to facilitate the sharing of structured data on the web. This helps to integrate our observation network with other local and global sensor networks.

Results and Discussions

Along with meteorological sensors and ADCPs, our robotic profiler system is operational at three fixed platforms for the continuous monitoring of hydrodynamic, meteorological and water quality condition of the bay. As a sampling scheme for the regular monitoring of CC Bay, the robotic profiler system at each platform is set to hourly measure water quality data at five equi-distant depth levels in the water column. This sampling scheme is designed to minimize power consumption especially when wind conditions are very low. However, the sampling frequency can easily be increased depending on the availability of power especially during windy periods. Our robotic profiler system is operational with minimum down time and it significantly reduces bio-fouling of sensors. The reduction in bio-fouling increases the instrument duty cycle for our platform and saves resources on platform service. The instrument duty cycle for our robotic sensor systems is around six months whereas sensors are normally biofouled on the order of days or weeks in a productive system like CC Bay and would require more frequent cleaning, calibration and field visits to replace the bio-fouled sensors. Also the “Transbot” software developed in this research work is very robust to handle network

failure, and monitoring activities at the platform will not be disrupted due to this kind of failure.

Figure 2.4 shows the time gap between robotic profiler measurements and user availability of those measurements collected at platform P2 from January 01 to August 31, 2007. Since the software, installed on the data aggregation and communication server, is set to import data from the fixed robotic platforms at ten minute intervals, measured data is normally available within then minutes. This is clear from the figure as time gap is close to zero (in terms of days, i.e., ten minute) during most of the time period. Each sudden spike represents the duration of a communication network failure during which measured data is not available. The subsequent reduction in the height of

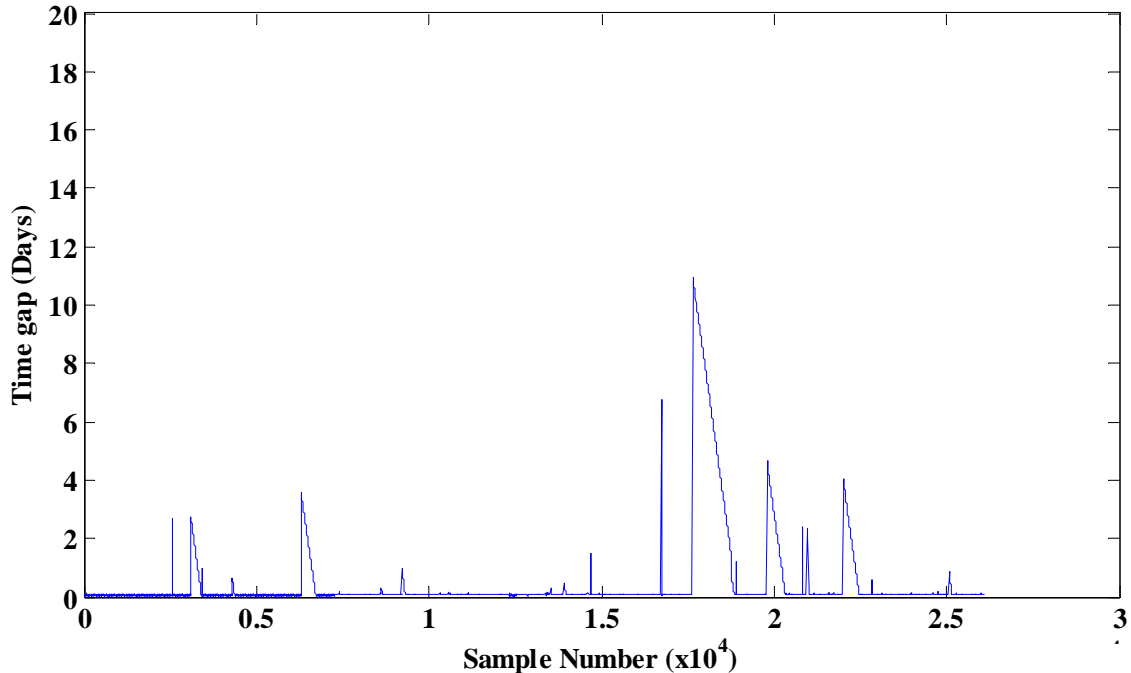


Fig. 2.4 Time gap between in-situ sensor measurements and data availability for various samples collected at platform P2 from January 01-August 31, 2007.

each spike illustrates the ability of our cyberinfrastructure to reliably import the data as soon as the communication network is re-established again. Since the robotic profiler system continues to operate during a period of network failure, the data is stored in the platform wincube. As soon as the network becomes online again, these stored data are then imported into our database. Once all the stored data is imported, then the time gap between measurements and data availability resumes to ten-minute intervals.

This research works also involves the development of relational SQL database and thereby, provides long-term storage facility for measured environmental datasets. The analysis of these datasets helps to clarify interrelated processes that control the event of interest and will characterize the long-term trend in various environmental processes. The integration of these datasets with other data collected from different monitoring systems can be used to determine the extent and frequency of hypoxia event in CC Bay. The development of other monitoring systems and their integration has been discussed detail in Islam et al. 2009b and Islam et al. 2009c. Also, the development of the cyberinfrastructure in this study facilitates the availability of the observed data to researchers, educators, policymakers, natural resource managers and the general public in real-time. This helps in emergency response activities for various events such as oil spills, storm surges and provides opportunities to environmental science education outreach through real-time analysis and display of observed data.

In this chapter, a snapshot of observational data is shown to illustrate the capability of our robotic monitoring system to capture various phenomena that will help to clarify the processes that can affect the hypoxic condition of CC Bay. A significant

vertical salinity gradient can be considered as a precursor to hypoxic events. When this gradient is high and the vertical water current structure is weak, the denser, more saline bottom water cannot mix with fresher (less dense) water at the surface where DO levels are higher due to re-aeration. Due to lack of mixing, DO levels at the bottom decrease as respiration and other biological processes continue. The CTD sensor at our robotic profiling system can provide variation of this salinity gradient with time. In Figure 2.5, the color-coded lines indicate the relative salinity variation (salinity corresponding to the observed peak value) at five different depths at Platform 'P3' on July 23-25, 2007. There exists a significant salinity gradient (salinity difference over 2m depth, $\Delta S > 4$ psu) between the first and fifth level of measurements overtime (0.00d ~1.60 d on x-axis) whereas this gradient is typically low (< 2 psu) most of the year. The blue line in this

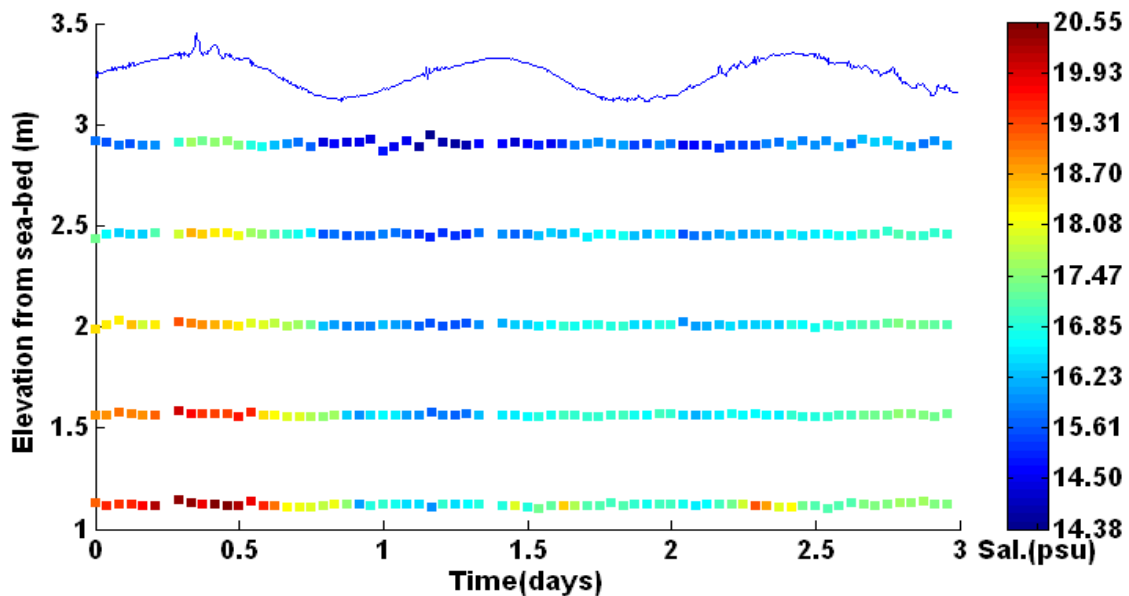


Fig. 2.5 Vertical variation of salinity in the water column at platform 'P3' during July 23-25, 2007 (■: salinity data points; —: water surface elevation).

figure represents variation of water surface elevation which was recorded by the pressure sensor installed on the ADCP. This snapshot indicates the capability of our robotic profiler system in capturing a significant vertical salinity gradient.

The understanding of particle dynamics can also provide insight about the DO distribution in the bay. The longer the oxygen consuming particles (e.g., Particulate Biochemical Oxygen Demand) remain in the water column, the greater the oxygen demand they will exert on the aquatic system. Various sensors installed on our profiler system will help to shed light on the particle dynamics of the bay. Figure 2.6 displays measurements of various parameters on June 15 that help to elucidate particle dynamics around our platform 'P2'. Fig. 2.6(a) presents the five depth measurements and Figures 2.6(b), 2.6(c) and 2.6(d) depict corresponding variation of salinity, total particle concentration and dissolved oxygen, respectively. From figure 2.6(c), one can think that a sediment re-suspension event might occur between 10:00 and 15:00 (GMT) as particle concentration at the lower levels of water column dramatically increases during that time period. But the salinity variation on the same time period showed the corresponding increases in the salinity level at the lower water column. This suggests that highly saline and turbid water might come towards our platform 'P2' through underflows of hypersaline water from two shallow neighbor water bodies (e.g., Oso Bay and Upper Laguna Madre). Laguna Madre is one of the most hypersaline lagoons in the world (Gunter, 1967) as the inflow of freshwater into this system is less than the evaporation rate and the system is also separated from the Gulf of Mexico by a barrier island. Oso Bay also suffers from hypersalinity as neighboring power plants draws cooling water

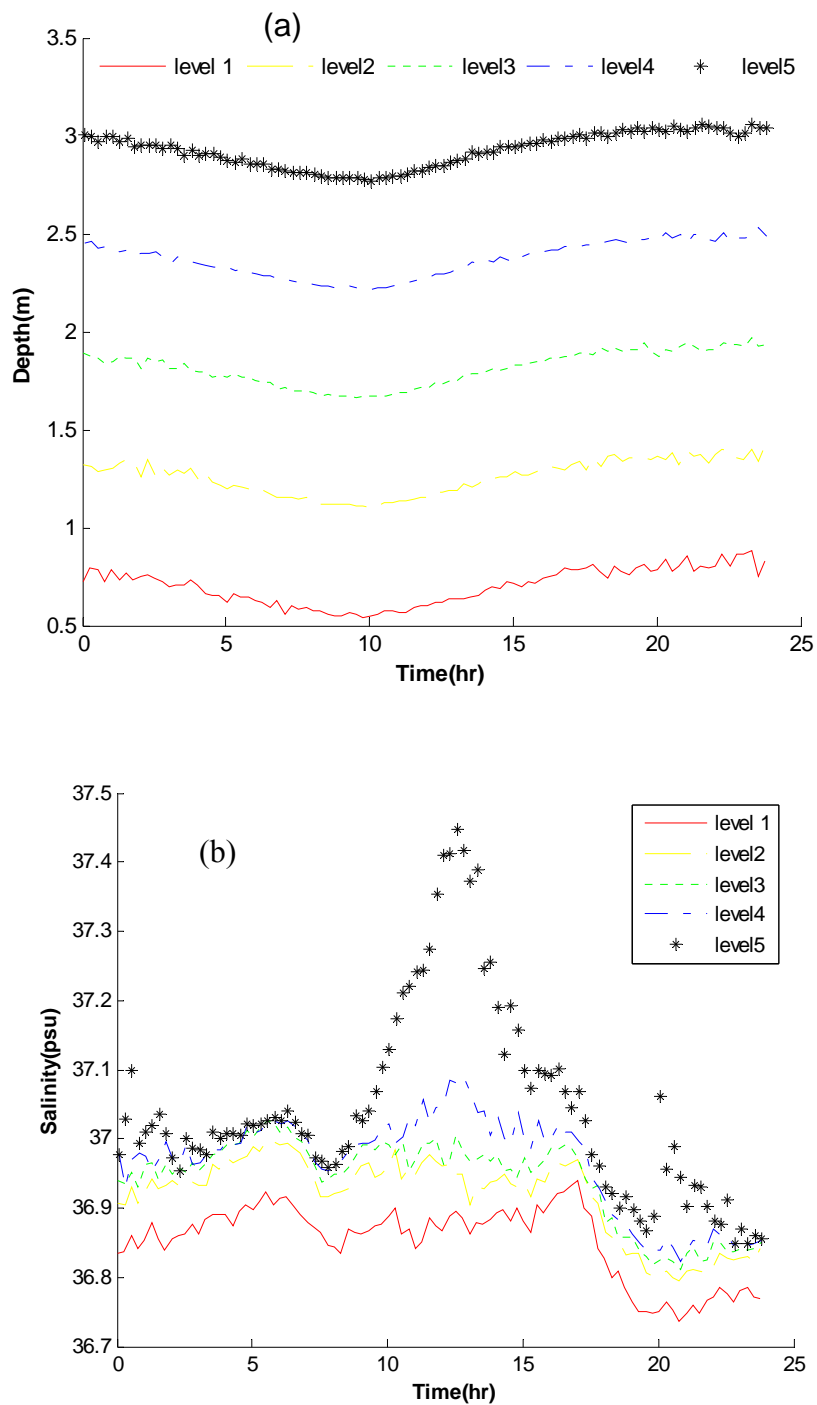


Fig. 2.6 a) Variation of robotic profiler measurement depths and corresponding measurements of b) salinity, c) total particle concentration and d) dissolved oxygen on June 15, 2006, respectively.

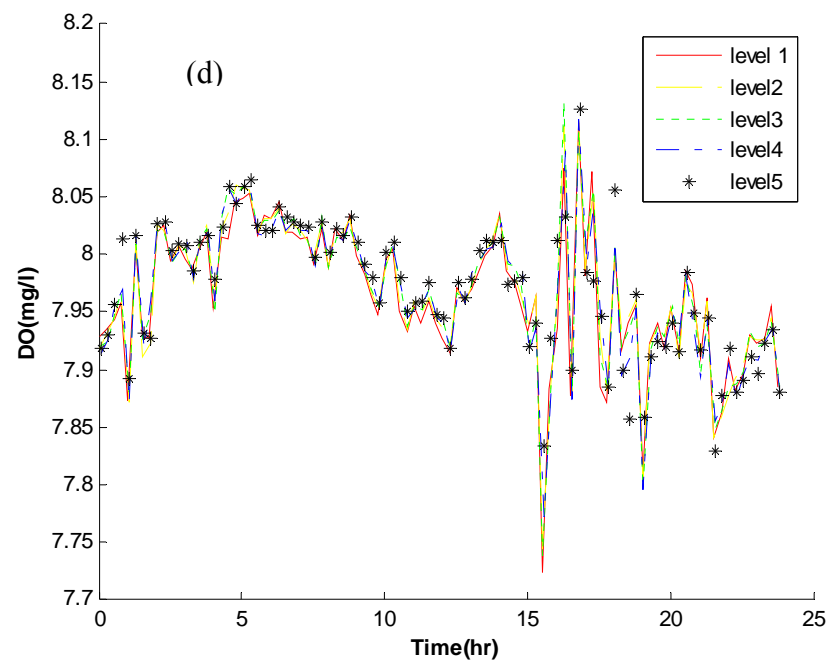
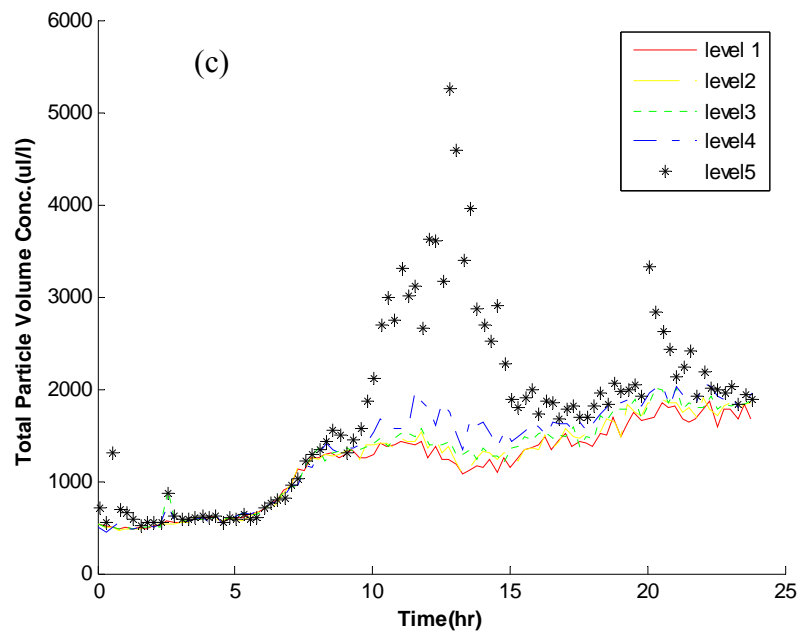


Fig. 2.6 Cont'd

from the upper Laguna Madre and discharges brine water into Oso Bay. Although DO did not vary significantly during that time period as shown in figure 2.6(d), the fluctuation of DO level was observed following that time period. Long term analysis of all parameters measured at our fixed robotic platforms can shed more light on important processes controlling DO dynamics in the bay. Data collected from this system can also drive various numerical models which can help to clarify important processes associated with hypoxia. For example, meteorological data measured at our fixed robotic platform is used to generate the wind field necessary to drive our two-dimensional depth integrated hydrodynamic model of CC Bay. The development of this numerical model to understand the hydrodynamic condition of the bay has been described detail in Islam et al. (2009d). The output of the hydrodynamic model can then be used to simulate our water quality model and can predict water quality of the bay. Therefore, the robotic monitoring system developed in this study is a valuable tool for the observatory in capturing and investigating various events that significantly impact the coastal environment.

Conclusions

The robotic profiler system developed in this study can measure vertical variation of various water parameters at a greater temporal resolution. This system also prevents bio-fouling of sensors and therefore it can be deployed for long-term autonomous monitoring of the bay. The developed cyberinfrastructure makes sensor data available to various stakeholders like researchers, educators, policymakers and general public in real

time. This system is also robust enough to handle the communication loss in the case of network failures and can reliably deliver measured dataset from the fixed robotic platforms to the user. The developed CI also allows us to remotely access to our fixed robotic platforms. This remote access serves different purposes such as instrument management, quality assurance of the data, implementation of event based-sampling scheme, reduction of field visits for troubleshooting. Also, the development of a relational database system in storing observational datasets will be useful for the exploration of the interrelated processes that control the event of interest and the determination of long-term trends in the variation of those processes. Observational data from our fixed robotic platforms can be used to drive various numerical models (Ernest et al. 1991; Garton et al. 1996; Lee et al. 2002; Sterling et al. 2004 & Ojo et al. 2007) developed in our research group to predict and understand various episodic events predominant in this energetic system.

CHAPTER III
A MOBILE MONITORING SYSTEM TO UNDERSTAND THE PROCESSES
CONTROLLING EPISODIC EVENTS IN CORPUS CHRISTI BAY

Overview

Corpus Christi Bay (TX, USA) harbors the nation's seventh largest port and numerous petrochemical facilities. This shallow wind-driven bay, which has significant affect on the national economy, is characterized as a highly pulsed system. It cycles through various episodic events such as sediment resuspension, flooding, water column stratification, hypoxia. The understanding of processes that control these events requires an efficient observation system that can measure various hydrodynamic and water quality parameters at the multitude of spatial and temporal scale of interest. As part of our effort to implement an efficient observation system for Corpus Christi Bay, a mobile monitoring system was developed that could acquire and visualize data measured by various submersible sensors on an undulating tow-body deployed behind a research vessel. Along with this system, we have installed a downward-looking Acoustic Doppler Current Profiler (ADCP) to measure the vertical profile of water currents. Real-time display of the measured parameter intensity (measured value relative to a pre-set peak value) guides in selecting the transect route to capture the event of interest. In addition, large synchronized datasets measured by this system provide an opportunity to understand the processes that control various episodic events in the bay. To illustrate the capability of this system, datasets from two research cruises are presented in this chapter

that help to clarify processes inducing hypoxia at the bottom of the bay. These measured datasets can also be used to drive numerical models to understand various environmental phenomena that control the water quality of the bay.

Introduction

Bays are among the most productive ecosystems in the world. The variety of habitats and productivity of these systems nurture the diversity of wildlife, fish, plants and microscopic organisms. These systems also significantly contribute to the national economy as tourism, fisheries, recreation and other commercial activities thrive in and around coastal regions. Human populations are growing at a high rate in the coastal regions, and now more than half of the US population lives within fifty miles of a coastline (US CENSUS BUREAU 2002). The high levels of anthropogenic activities associated with this growth have significantly deteriorated the natural balance of these coastal ecosystems. In addition, natural perturbations such as precipitation, tropical storms, hurricanes, tsunami can dramatically alter physical, chemical and biological characteristics of these dynamic systems. Therefore, it is necessary to understand the processes that control the dynamics of these systems and to take proper steps to improve environmental conditions.

Corpus Christi Bay (Texas, USA) is home to the nation's seventh largest port with numerous petrochemical facilities. Considering its impact to the economy, the National Estuary Program (NEP) designated Corpus Christi (CC) Bay as a National Estuary in 1992 and created the Corpus Christi Bay National Estuary Program (CCBNEP) to protect

the health of this bay while supporting its economic growth. This enclosed shallow bay is wind-driven and can be described as highly-pulsed system. It cycles through various episodic events such as sediment resuspension, flooding, water column stratification, hypoxia, etc. One of the episodic events that draws national attention is the occurrence of hypoxia (dissolved oxygen <2 mg/l) in this shallow bay. Hypoxia was first reported in the south-east part of CC Bay in 1988 (Montagna and Kalke 1992) and has been observed every summer thereafter (Ritter and Montagna 1999). Hypoxic events that occur in this bay can last on the order of hours to days (Ritter and Montagna 2001). Therefore, understanding this phenomenon requires the development of monitoring systems that can capture the stochastic processes controlling water quality in the bay.

Monitoring of water quality parameters and environmental indicators that influence the physical processes of hypoxia poses a challenge due to the spatial extent and dynamics associated with CC Bay. There are various sampling methods available to measure water quality parameters; some methods are ex-situ whereas others are in-situ. Grab sampling and flow-through sampling have been used for ex-situ collection of water samples in routine monitoring where immediate results are not required, and/or analysis must be done through wet chemistry (Volpe and Esser 2002). These sampling types have limitations because of poor spatial and temporal resolution. With recent advances in technology, real-time measurements of water quality parameters are possible through the use of submersible in-situ sensors (Agrawal and Pottsmith 2000; Boss et al. 2007 and Visbeck & Fischer 1995). The advantage of in-situ sensors is that the parameter can be measured in real time, thereby omitting the time gap between sample collection and data

analysis. The real-time availability of the measured parameter has made it possible to invoke a paradigm shift in designing sampling strategies for environmental monitoring. Instead of selecting the transect route, sampling frequency and total number of measurements prior to the start of the monitoring study, it is now possible to implement adaptive/sequential plans that will guide the choice of sampling route where more information about the parameter of interest can be gathered (Thompson & Seber 1996). This adaptive sampling scheme has gained wider acceptance as a valuable tool for the sampling of the abundant but clustered population of data in natural sciences. As an example of the use of adaptive sampling scheme, Fiorelli et al. (2004) used a fleet of autonomous underwater gliders to track the feature in an uncertain environment. In addition of the implementation of adaptive sampling technique, the proper characterization of the spatial and temporal scale of the event also depends on the type of platforms where in-situ sensors are installed (e.g., mobile platforms, fixed platforms, bottom tripods, drifters, float) (Dickey 1991& Dickey et al. 1998). Remote platforms such as satellites, aircraft and shore-based platforms can also be used to deploy various types of sensors. Each type of platform has its advantages and disadvantages, for example, sensors installed on fixed platforms can collect data at greater temporal resolution but will be limited in spatial resolution. On the other hand, mobile platforms (e.g., autonomous underwater vehicles, remote-operated vehicles, gliders and towed undulators) can address this limitation by housing in-situ sensors and collecting data at greater spatial resolution (Blackwell et al. 2008 & Barth and Bogucki 2000). This data, however, will have limited temporal resolution. The advances in remote sensing

techniques help to capture physical and biological variabilities of the upper layer of the water column at greater temporal and spatial resolution but have not succeeded yet to capture the chemical species and sub-surface condition of the water column. Therefore, installation of sensors on a single type of platform will not be able to measure all parameters at proper resolution to capture the event of interest.

The advances in sensor systems, platform design and communication technology in this decade have provided an opportunity to develop an efficient observation system through the integration of the above mentioned platforms to measure water quality, hydrodynamic and meteorological parameters at the multitude of spatial and temporal scales of interest. The National Oceanographic and Atmospheric Administration (NOAA) is currently operating the Physical Oceanographic Real-Time System (PORTS) that provides real time data from several waterbodies to improve the safety and efficiency of maritime commerce and coastal resource management. Other observatory systems that have been deployed at various coastal environments are MYSound in Long Island Sound (Tedesco et al. 2003), the COlumbia River Environment (CORIE) (Baptista et al. 2005), the Chesapeake Bay Observing System (CBOS) and the Long-term Ecosystem Observatory (LEO-15) (Glenn et al. 2000). In addition, the National Science Foundation (NSF) has provided funding to establish WATER and Environmental Research Systems (WATERS) Network which tests various aspects of observatory design and operation at different test beds sites. This network will make available measured data from various observatories and will help in investigating multi-scale environmental phenomena (Montgomery et.al. 2007). Corpus Christi (TX, USA) has

been selected as one of the test bed sites of WATERS network. We have developed various monitoring systems to measure meteorological, hydrodynamic and water quality parameter at greater spatial and temporal resolution. Along with Acoustic Doppler Current Profilers (ADCP) and meteorological sensors, we have installed robotic profiler systems at three different fixed platforms to measure the vertical variation of hydrodynamic, meteorological and water quality parameters at greater temporal resolution. The details of this system have been discussed in Islam et al (2009a). We have also installed HF radar system on remote platforms to generate surface current maps of CC Bay at greater temporal resolution (Trujillo et al. 2004). The development of a mobile monitoring system that can measure various parameters at greater spatial resolution will complement our observation system.

Various types of mobile monitoring systems such as autonomous underwater vehicles (AUV), solar-powered autonomous underwater vehicles (SAUV) and tethered sensor systems are developed by various researchers (Wiebe et al. 2002; MacNaughton et al. 2004 and Chatila & Laumond 1985). Although AUVs have certain advantages such as autonomous control of the vehicle, operation without the host vessel, and higher operational range, these systems are expensive and need specialized personnel to maintain, program, and deploy. Also these systems are not flexible enough to conduct adaptive sampling and need to be taken out of the water frequently for battery recharging. Art Sanderson (professor of electrical, computer, and systems engineering at Rensselaer and principal investigator of the RiverNet project) has been working on SAUV development in collaboration with D. Richard Blidberg of the Autonomous

Undersea Systems Institute in Lee, N.H (SAUV 2009). This system will be recharged with solar power and will communicate with other AUVs. This system has the similar limitations as described for the AUVs except it does not need to be taken out of water for recharging. Wiebe et al. (2002) has developed BIOMAPPER-II, a tethered sensor system that can measure biological and physical parameters at greater spatial resolution and display the measured data in real time. All of these systems described here were deployed in the deep water and were not implemented for the measurements of various environmental parameters in shallow water like CC Bay where distinct vertical gradient exist in water quality parameters (Islam et al. 2008).

The research objective for this paper was to describe the design, construction, test deployment and evaluation of a mobile monitoring system that could address the limitation of the spatial scale of interest and could be deployed in shallow water. This system was installed on a mobile platform and is able to measure various parameters 'synchronously' over a highly-resolved horizontal and vertical regime. Besides collecting data at greater spatial resolution, this system is capable of displaying data in real time and thereby provides guidance on transect route selection during research cruises. This monitoring system was deployed in CC Bay for routine monitoring and for providing aid in understanding phenomena associated with episodic events in the bay. This mobile monitoring system was also integrated with the fixed robotic profiler system and the HF-radar system on remote platforms to develop an adaptive sampling scheme to capture the extent, frequency and duration of hypoxia and other episodic events in CC Bay. The integration of these real-time monitoring systems is discussed in detail in Islam

et al. (2009c). This integrated system also provides myriad datasets that can be used to drive numerical models which will help to understand the processes controlling dissolved oxygen variation in the bay.

Study Area

Corpus Christi Bay, depicted in Figure 3.1, is located on the Texas coastline and covers an area of approximately 432.9 sq. km (Flint, 1985). This bay is linked with the Gulf of Mexico through a narrow ship channel (15 m depth), which runs from east to west. Recently, Packery Channel, located at the southern reaches of the bay, has been

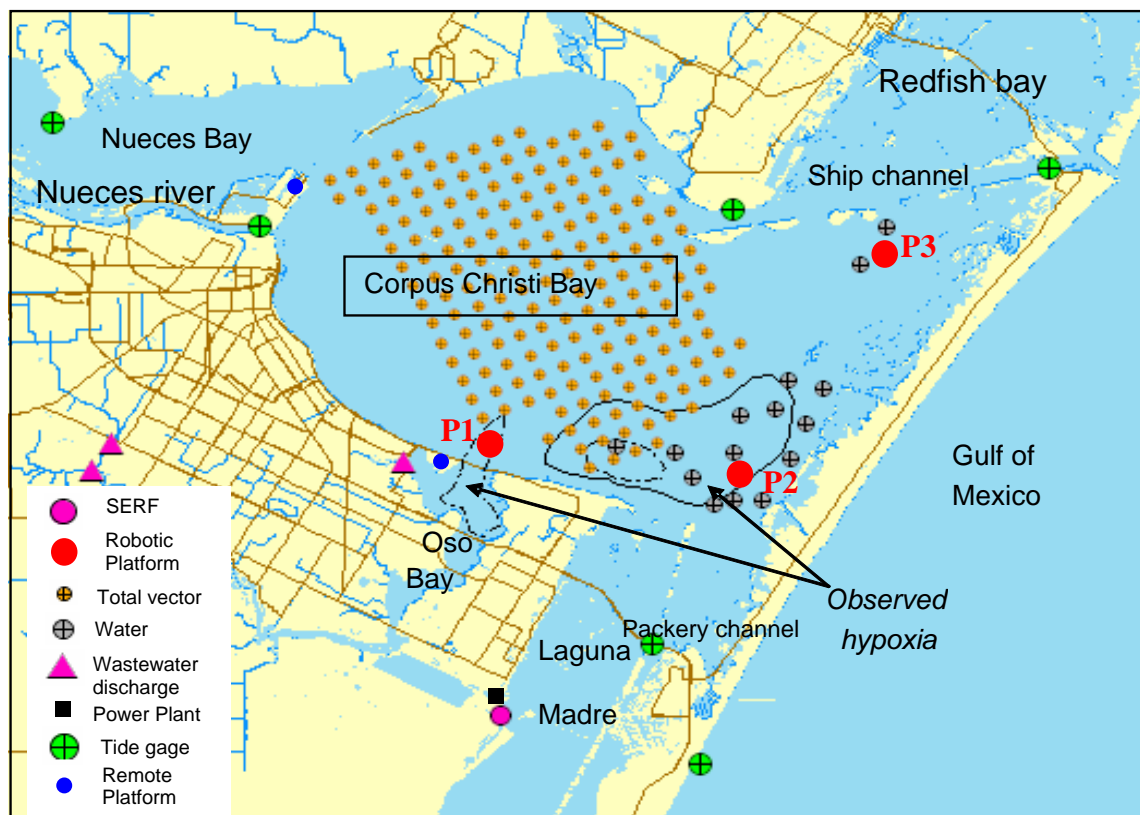


Fig. 3.1 Characteristics feature of Corpus Christi Bay.

opened and it is another source for the water exchange with the Gulf of Mexico. CC Bay is connected with four embayments namely Redfish Bay in the northeast, Nueces Bay in the northwest, Oso Bay in the southwest and Upper Laguna Madre in the south.

Freshwater enters CC Bay via the Nueces River and Nueces Bay, whereas high-saline water enters the bay during summer months from the shallow Upper Laguna Madre and Oso Bay. The Upper Laguna Madre is one of the most hypersaline lagoons in the world (Gunter, 1967). Our research facility (Shoreline Environmental Research Facility (SERF)) is located close to the Upper Laguna Madre and provides convenient field support for the regular monitoring of the bay (shown in as magenta-colored solid circle in figure 3.1).

This bay is mainly dominated by south-easterly winds although northerly winds occur periodically during the winter months. During some portions of the year, especially summer, the wind subsides and the bay becomes very quiescent. This condition can be altered and is well-mixed on the order of hours to days if wind condition changes. CC Bay experiences periodic episodes of hypoxia which has been reported to occur at the south-east part of the bay. The cross-hatched circles (Fig. 3.1) represent locations where hypoxia has been observed every summer (Ritter and Montagna 1999; Hodges and Furnans, 2007). The three solid red circles denote the strategic locations of our fixed robotic platforms in the bay. The solid blue circles represent the location of our remote platforms where HF-radar systems are installed, and tainted-yellow circles display the locations of total vector in CC Bay generated from our HF-radar system. The solid black rectangle denote the location of a power plant which draws cooling water from Upper Laguna Madre and discharges brine water into Oso Bay. The wastewater discharge

locations (denoted by magenta-colored triangle), tidal gage (represented by solid green circle), and water quality stations (displayed using grey circle) are shown here to indicate the areas of interest for collecting other important information and data, but are not used in this chapter.

Mobile Monitoring System

Ojo et al. (2007a) developed a portable Integrated Data Acquisition, Communication and Control (IDACC) system that was deployed on the mobile platform and could measure variation of water quality parameters ‘synchronously’ over a highly-resolved spatial regime. This system could acquire and visualize data measured by submersible sensors on an undulating tow-body (Acrobat LTV-50HB, by Sea Sciences Inc.) deployed behind the boat. Real time display of the parameter intensity (measured value relative to a pre-set peak value) provided guidance on transects route selection during each research cruise. However, this system had limited success in capturing vertical gradients of the parameters of interest, especially steep vertical gradients. As there exists a significant vertical gradient in dissolved oxygen (DO) concentration during the occurrence of hypoxia, this system was not able to characterize the processes that are dominant under this condition. Therefore, the IDACC system has been modified significantly in this study so that it can successfully capture vertical variations of the parameters and display them in real-time. Our research vessel serves as our mobile platform. Hardware upgrades to the IDACC system include use of a lightweight ruggedized laptop(s) to replace the previous bulky hardware components for data

acquisition and visualization, and use of a single Global Positioning System (GPS) as opposed to the original setup that required two GPS units. Software upgrades to the IDACC system include the expanded capability to capture the vertical concentration gradients of the parameters of interest. Modified hardware and software components are described in the following paragraphs.

Figure 3.2 shows the schematic diagram of the mobile platform with the modified IDACC system. In this system, three ruggedized laptop computers are set up in a local

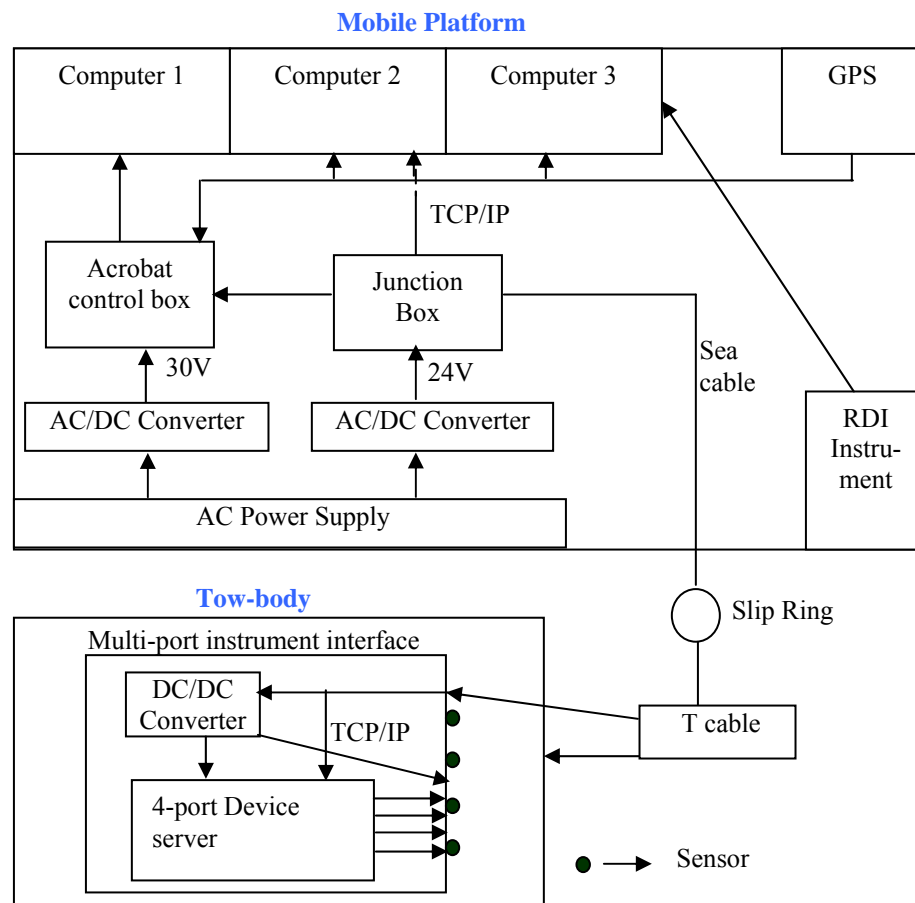


Fig. 3.2 Schematic diagram of real-time monitoring mobile platform system.

area network: a) a laptop to control the undulation of the tow-body, b) a laptop to acquire and visualize data from the sensor suite, and c) a laptop to determine the water current structure within the water column based on ADCP data. The laptops are situated on computer docking stations inside the boat cabin. A differential GPS (DGPS, Garmin, GPSMAP 3210C) is used to geo-reference the observed data and is serially connected with all three computers. Manufacturer software (Sea Sciences, Inc.) is used for the automatic control of the tow-body movement and the display of tow-body location within the water column. It can also be controlled manually through the tow-body control box that acquires 30V DC through the conversion of vessel's AC power. A downward-looking bottom-tracking 1200 KHz workhorse ADCP has been installed on the starboard side of the boat to measure a) water velocity, b) bathymetry, c) acoustic backscatter intensity which is indirectly related to particle concentration, and d) shear structure of the water column. The manufacturer software (WINRIVER I by RDI) presents the contour plot of real time variation of these parameters along the transect route. The computer designated to acquire and visualize sensor suite data is connected with different submersible sensors in the Acrobat tow-body cage through a subsurface multi-port sensor interface using transmission control protocol/internet protocol (TCP/IP). The instruments currently included are a particle sizer (LISST 100X, by Sequoia Sciences), a DO sensor (Optode, by Aanderaa), a CTD (Conductivity, Temperature and Depth) sensor (SBE 49 "FastCat", by Sea-Bird Electronics, Inc.) and a fluorosensor (Eco-FL3, by WETLabs).

The multi-port instrument interface shown on the lower left portion of Figure 3.2

serves as a power distribution, data communication unit for the submersible sensor suite. The details regarding the development of this submersible interface can be found in Ojo et al. (2007a). The interface acquires the power from the AC/DC power converter mounted on the mobile platform that supplies 24V DC output. The sea cable, made of stranded and twisted pair wires of power and communication lines from tow-body and multi-port instrument interface, is sent through the winch/slip ring assembly to the T-cable. It then diverges one set of power and communication wire to the tow-body whereas the other sets are connected to the submersible multi-port instrument interface. Data telemetry is facilitated through a network interface that connects two on-board laptops (e.g. Computer 1 and Computer 2 shown in Figure 3.2) with the subsurface device for data acquisition and sending command signals via TCP/IP to the sensors mounted on the tow-body.

Data measured by various submersible sensors were acquired and visualized previously in real time through the Multi-Parameter Instrument Array and Control System (MPIACS) software developed in our research group (Ojo et al. 2007a & Ojo et al 2006). It displayed horizontal variation of intensities of the measured parameters (measured value relative to a pre-set peak value) along the transect route and thereby aided in selecting the transect route ‘on the fly’ to capture the spatial extent of the parameters of interest. For this study, we have augmented the MPIACS software to acquire and display the vertical variation of water quality parameters along the transect route as well as the horizontal variation (i.e. upgrade of display from two-dimensional to three-dimensional). Figure 3.3 presents a snapshot of the graphical user interface (GUI)

generated by the modified MPIACS II software during one of our routine monitoring cruises in CC Bay. The lower left portion of the GUI gives the user the option to select the type/number of instruments to be used in each monitoring activity. At present, the system allows a maximum of six instruments to be included for synchronized measurements. The user also has the option to select the area to be monitored. Currently, Corpus Christi Bay, and other Texas coastline areas (Matagorda Bay, Galveston Bay, Galveston Offshore) have been loaded into the software so that user can use them directly as reference boundaries for their monitoring activities. The lower

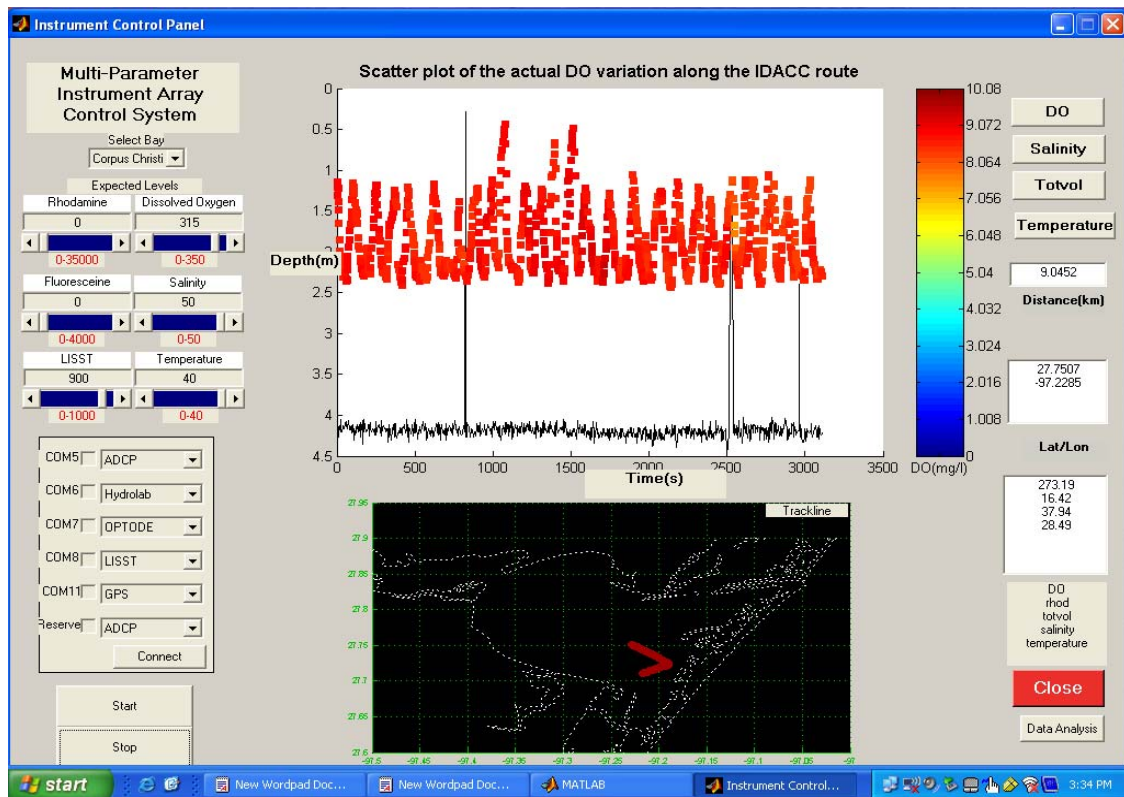


Fig. 3.3 Snapshot of Graphical User Interface (GUI) generated by our real time data acquisition and visualization software (MPIACS-II) in one of our routine monitoring activities in CC Bay.

middle panel of the GUI displays the color-coded trace line of the travel route whereas the upper middle panel shows the vertical variation of a water quality parameter along that route. In this snapshot, it shows the relative DO (measured DO with respect to preset peak DO values) variation along the travel route but the user can select other parameters (e.g., temperature, salinity, total particle concentration) for display. The real-time display capability of the system provides guidance when selecting the monitoring route to capture the event of interest. Along with the graphical displays, the system also presents the numerical values of the synchronized measurements and their location coordinates in the edit boxes at the lower right side of the GUI. The cycle time for each set of synchronized measurements is determined by considering the fastest stable response time of each sensor in the instrument suite. For this sensor suite, it takes approximately seven seconds to get a set of synchronized stable readings. The undulation speed of the tow-body is controlled in such a way so that it can collect sufficient amount of data to capture a significant change in vertical gradient of the measured parameters. All measured parameters are archived in a text-file format. The post analysis of this measured data will help to infer interrelated processes that control various episodic events in the bay.

Results and Discussions

Routine monitoring of CC Bay has been performed through periodic deployments of our mobile monitoring system. This system provides synchronized measurements of large hydrodynamic and water quality datasets. To illustrate the capability of this system

in capturing various environmental parameters and thereby to help in clarifying the processes controlling various episodic events, measured datasets from two research cruises made on November 29, 2006 and August 07, 2007 are presented here.

November 29, 2006 Cruise

On November 29, 2006, the cruise transect began at the mouth of the ship channel where it is connected to the Gulf of Mexico and moved in a westerly fashion along the ship channel. The deep ship channel serves as a conduit to exchange materials between the bay and the Gulf of Mexico. Therefore, various parameter measurements at the ship channel can shed light on the contribution of the Gulf of Mexico to the overall condition of the water quality of the bay. Figure 3.4 shows the actual transect route for the cruise made on November 29, 2006. The route line is color-coded and correlates with the horizontal color-coding along the top and bottom of Figures 3.5 and 3.7, thus

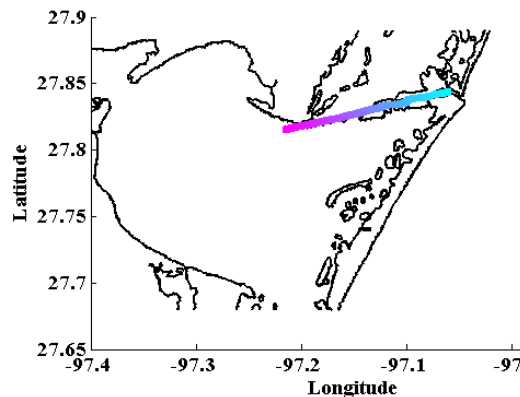


Fig. 3.4 IDACC transect route (in ship channel in CC Bay) on November 29, 2006 (Note: direction of transect was east-to-west).

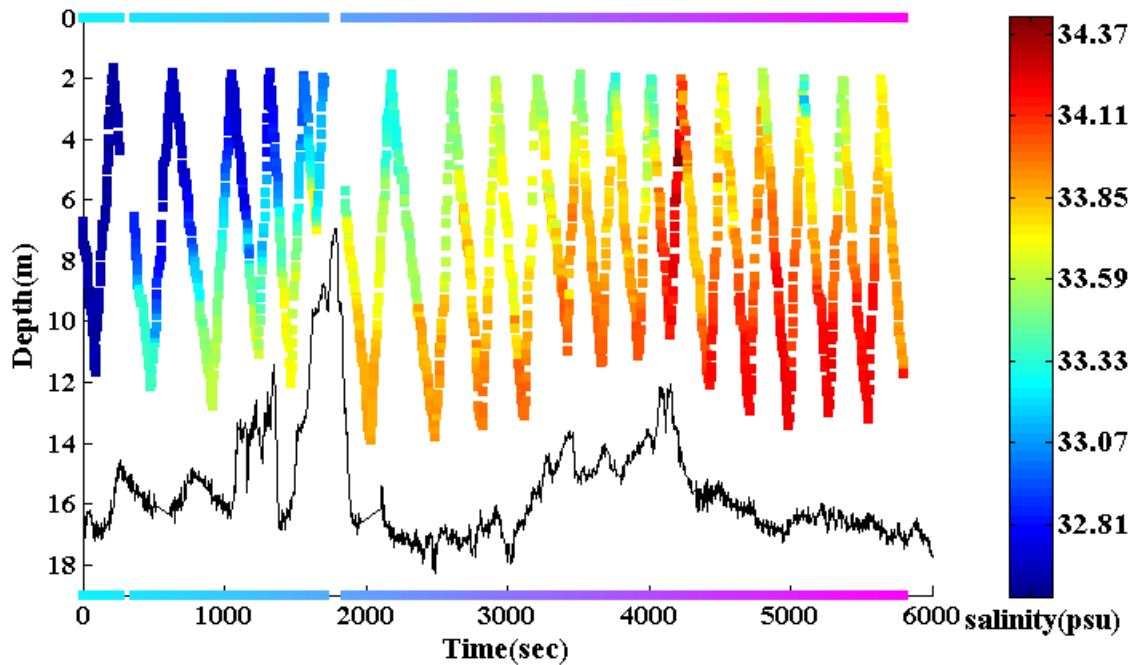


Fig. 3.5 Salinity variation along the IDACC route on Nov. 29, 2006 (Note: the colored horizontal lines at the top/bottom of the figure correlate to the transect route as presented in Figure 3.4).

matching the observed data with the spatial location in the bay. From the set of measured parameters, vertical variation of two parameters (salinity and particle concentration) along the transect route are presented here. This information provides evidence of the mobile monitoring platform capability in characterizing the water quality and the particle dynamics of the bay.

The color-coded scattered plot of Figure 3.5 depicts the vertical variation of salinity along our transect route while the solid black line represents the sea-bed profile. This data suggests that the inverse estuary situation existed in the ship channel, i.e., water became more saline and dense as the vessel moved from the mouth of the Gulf of

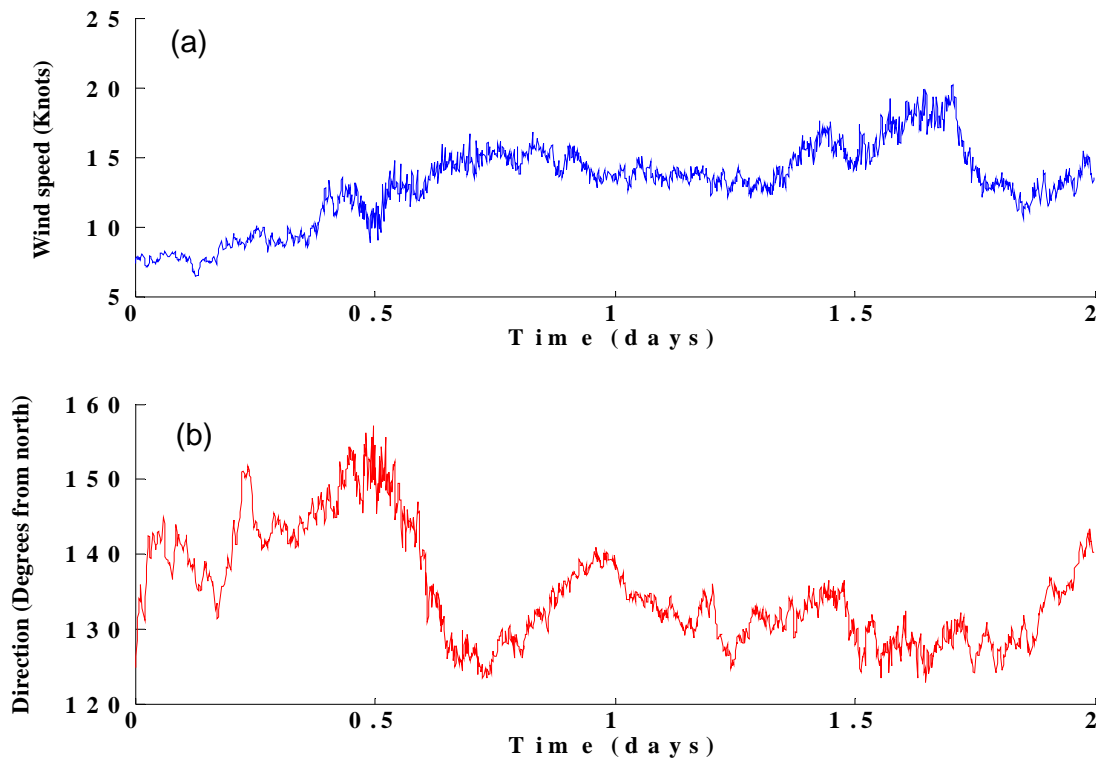


Fig. 3.6 Variation of wind speed (a) and direction (b) around the platform ‘P2’ on November 28-29, 2006.

Mexico towards the bay interior. Understanding the hydrodynamic conditions of the bay can provide insight about this salinity profile. Figure 3.6(a) and 3.6(b) displays the measured variation of wind speed and direction from our fixed robotic platform located in the observed hypoxic region during November 28-29, 2006 time frame, respectively. Wind blows persistently along the south-east direction during this time period; this wind may “push” high saline water from the mouth of the upper Laguna Madre and Oso Bay northward towards the ship channel. Low freshwater inflow and the dominance of evaporation over rainfall tend to increase the salinity levels in the shallow upper Laguna

Madre and the mouth of the Oso Bay as compared to the rest of the bay (Hodges and Furnans 2007). Our research collaborators at the University of Texas, Austin (Ben Hodge's research group) have been working on the development of a 3D hydrodynamic model of CC Bay. The preliminary results of their model showed a similar circulation pattern. Data collected from our mobile monitoring system can be integrated with the numerical model for greater understanding of various processes that occur in this dynamic bay.

Particle concentrations measured by a particle sizer (one of the instruments in our mobile monitoring system) are well correlated with the acoustic backscatter intensity measured by an ADCP (Thorne and. Hanes 2002; Gartner 2002, and Hay & Sheng 1992). This kind of relationship is very important because it provides a greater capability to characterize the particle dynamics of the bay. An ADCP can measure a vertical profile of the water column whereas a particle sizer measures the particle concentration at a given point. The synchronized measurements of particle concentration and acoustic backscatter intensity at our monitoring mobile platform provide opportunities to investigate this kind of relationship. Figure 3.7 presents the particle concentration while Figure 3.8 presents the acoustic backscatter intensity variation along the transect route. Note that Figure 3.8 presents only a portion of the transect data for the ADCP (from T=2100 sec through T=4800 sec). Comparing Figure 3.7 & Figure 3.8, it is clearly visible that higher particle concentrations (encircled in black, Figure 3.7) correspond to the higher acoustic backscatter intensity data (encircled in black, Figure 3.8). In order to interpret and understand a quantitative relationship between acoustic backscatter

intensity with the actual particle concentration, it is necessary to analyze other water quality parameter measurements such as salinity, temperature, and particle type and size distribution in the water column. Future research will provide more insight in clarifying the relationship between acoustic backscatter intensity and particle concentration with other water quality parameters measured with our monitoring mobile platform and therefore, will help to better understand the particle dynamics of CC Bay and other particle-mediated transport processes. Particles can transport ‘particulate BOD’ (biochemical oxygen demand), thus affecting hypoxia. Quantification of the particle influx/outflux to the Gulf of Mexico through the ship channel may help us to understand

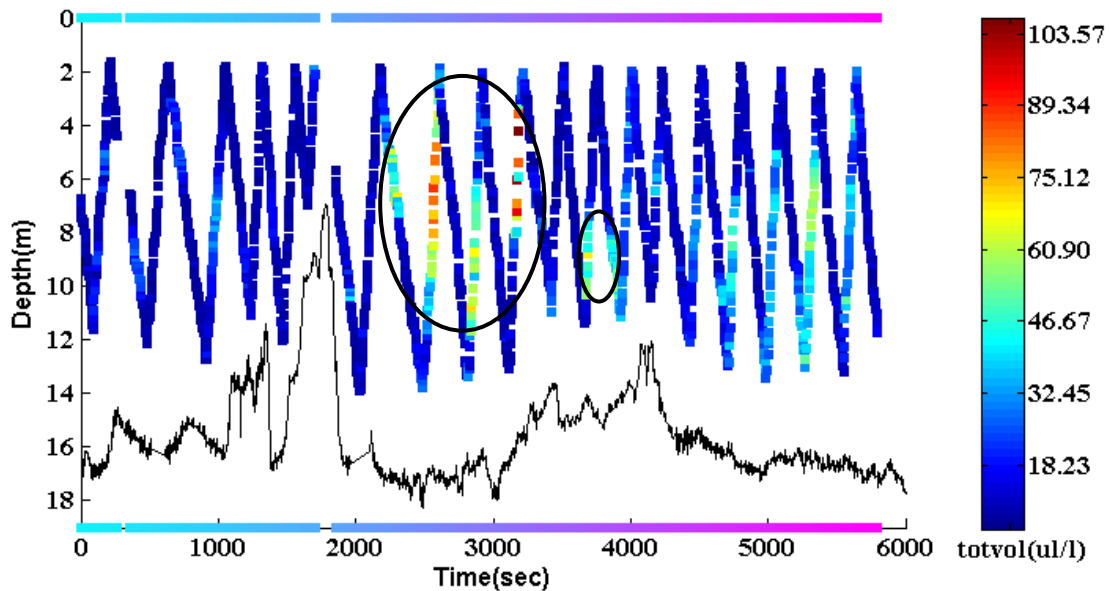


Fig. 3.7 Scatter plot of particle concentration variation along the transect route on November 29, 2006 (■: Total Particle concentration ($\mu\text{l/l}$); —: sea-bed profile; Note: the colored horizontal lines at the top/bottom of the figure correlate to the transect route as presented in Figure 3.4).

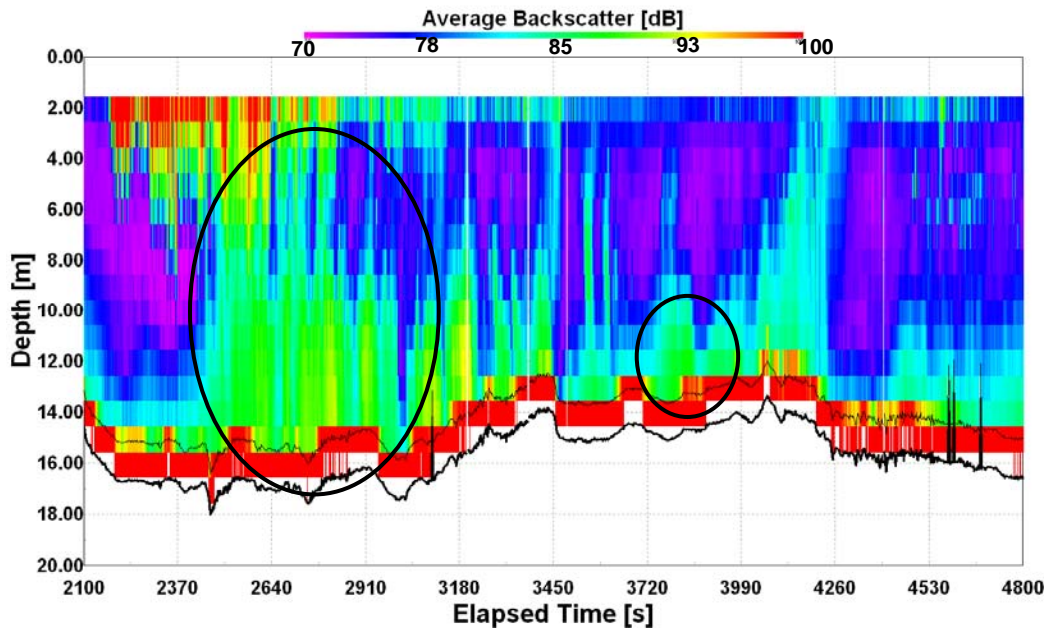


Fig. 3.8 Average acoustic backscatter intensity variation along the portion of transect route (time = 2100s~4800s) on November 29, 2006.

the contribution of the ship channel dynamics in affecting hypoxia of the bay.

August 07, 2007 Cruise

The second dataset collected from the research cruise made on August 07, 2007. In that cruise, the south-east part of the bay was monitored where hypoxia is observed at every summer (Ritter and Montagna 1999). Data collected from this cruise are plotted in Figures 3.9~3.13 and the actual cruise route is depicted on the inset plots in each figure. The relative concentrations of each measured parameters are displayed in color-coded points on these figures and thereby help to visually comprehend spatial variation of the parameters. It should be noted that at several points during this transect we had to stop

collecting data and pull our instrument suite onto the boat deck for inspection after inadvertent sea-floor hits. These data gaps are evident in Figures 3.9~3.13.

Figure 3.9 displays the vertical variation of dissolved oxygen (DO) along the transect route. DO levels were moderate (~ 6.5 mg/l) in the Upper Laguna Madre and it decreased gradually along the transect route from the Upper Laguna Madre towards Oso Bay. Finally, water was found hypoxic at the lower depths of the bay near the junction

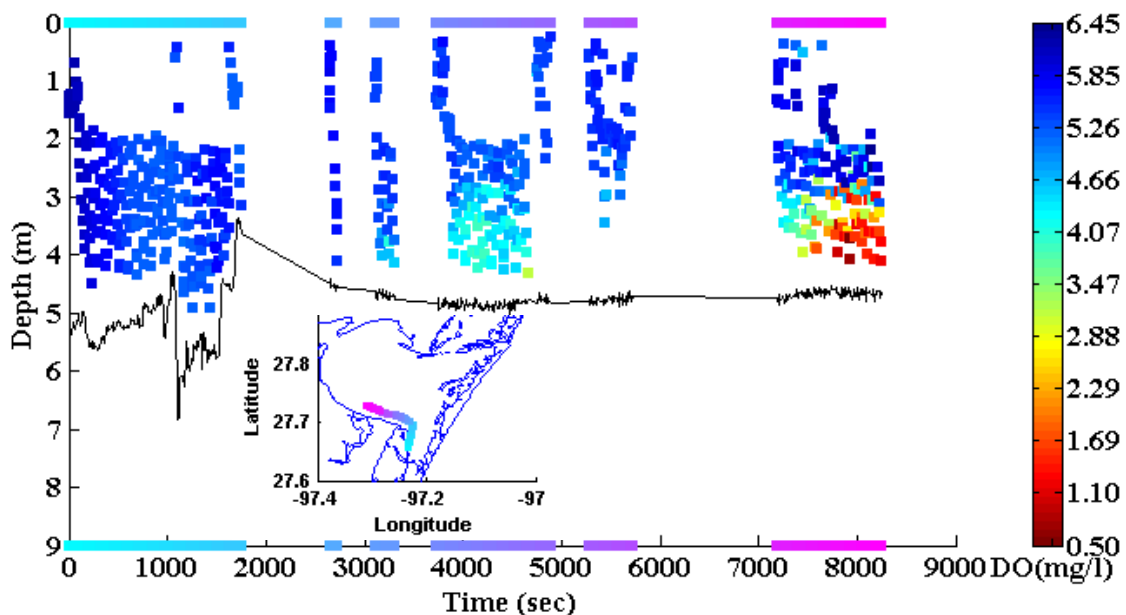


Fig. 3.9 Vertical DO variation along the transect route on August 07, 2007 (■: DO data points (mg/l); -: sea-bed profile).

point of Oso Bay and CC Bay. Real-time display of measured DO concentrations through mobile monitoring system guided us in transect route selection so that we could fully investigate the hypoxic area. The cruise was terminated at the mouth of Oso Bay.

Various factors might induce this hypoxic condition. For example, if the water column is stratified, aerated surface water may not mix with bottom water and thereby, significant vertical gradient in DO concentration develops (Turner et al. 1987). Also, high sediment oxygen demand and low rate of photosynthesis turns bottom water into hypoxic. The analysis of other parameters will help to test these hypothetical scenarios and will assist in the determination of the processes inducing hypoxia at the bottom of the bay.

The vertical variation of salinity along the same transect route is shown in Figure 3.10. The water was highly saline in the Upper Laguna Madre where the research cruise began. As the cruise progressed, a distinct and pronounced vertical salinity gradient was noted. The dominance of fresh water in the gradient became more pronounced at the end

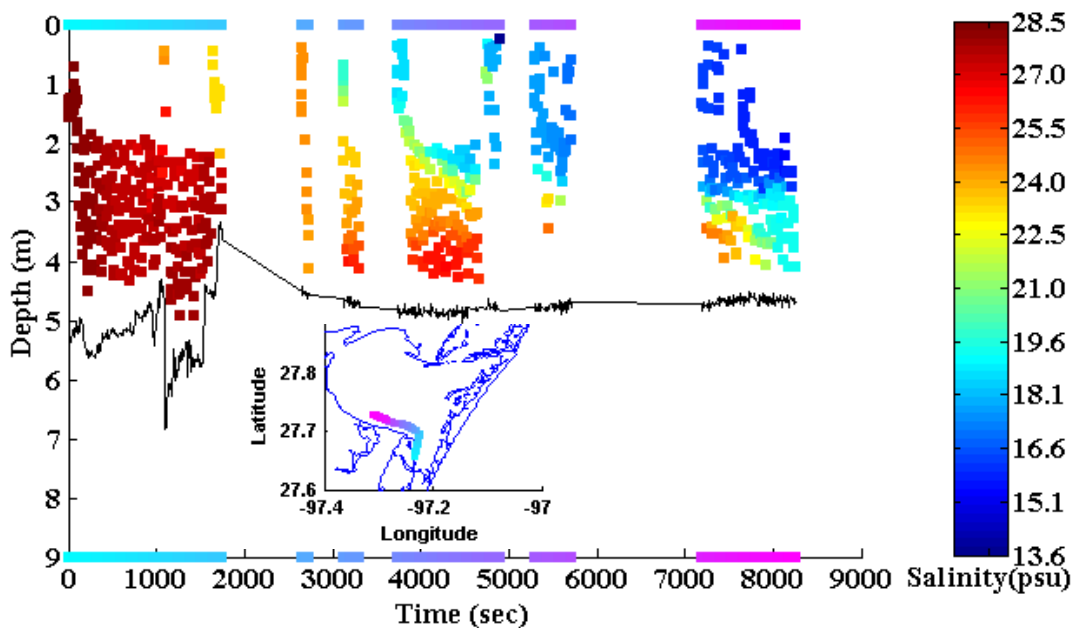


Fig. 3.10 Vertical salinity variation along the transect route on August 07, 2007 (■: Salinity data points (psu); -: sea-bed profile).

of the cruise transect. This trend might be due to the intrusion of high saline water from the upper Laguna Madre which is one of the most hypersaline lagoons in the world (Gunter, 1967). The inflow of freshwater into this system is less than the evaporation rate and the system is also separated from the Gulf of Mexico by a barrier island. This significantly increases the salinity level in the water column. If fresh water lies above the dense saline water, the water column may remain stratified until the vertical shear structure is strong enough to mix the water column. The ADCP sensor installed on the mobile monitoring platform can measure the vertical current structure of the water column. The examination of water current structure and density profile along the transect route provided insight into the stability of the stratified water column.

The gradient Richardson number (Ri) is used as an indicator of the stability of the stratified water column. Ri is the ratio of the amount of work required to resist mixing of the stratified water column to the amount of kinetic energy available from the existing shear current structure of the water column. Mathematically, it can be described by the following equation (3.1):

$$R_i = \frac{-\frac{g}{\rho} \frac{d\rho}{dz}}{\left(\frac{\partial u}{\partial z}\right)^2 + \left(\frac{\partial v}{\partial z}\right)^2} \quad (3.1)$$

where, ρ is water density, g is gravity acceleration, z is the depth from the water surface, u and v are the east-west (u) and north-south (v) velocity components. Water density is calculated from the temperature and salinity profile captured by the CTD sensor on the instrument suite whereas vertical profile of u , v are measured by the ADCP. The

sampling frequency of the CTD sensor is different than that of ADCP. Therefore, a suitable interpolation scheme was developed in this study to synchronize these two different datasets. The ADCP was configured to measure a vertical profile every 2 seconds from an ensemble of 11 pings. It measured water currents at several vertical bins. Each bin was separated by 25 cm and the first measured “good” bin was at a depth of 2m after considering the blanking distance from the transducer head and the depth of transducer from the water surface. Since there was no good water current data for the top two-meters of the water column, Ri values were calculated at different points below that level. The vertical profile of measured density was interpolated into the regular grid using a triangle-based linear interpolation algorithm. Both ADCP-measured water currents and density data were interpolated at a regular grid consisting of 25 cm increments in depth and 30 sec increments in time. Once both datasets were synchronized in depth and time, the vertical distribution of the Richardson (Ri) number was calculated using equation (3.1). Miles (1961) and Howard (1961) have demonstrated that $Ri > 0.25$ is sufficient conditions for stability in a shear layer with linearly varying water current and density. When the nonlinear interactions are considered, sufficient conditions for stability in a three-dimensional stratified parallel shear flow becomes $Ri > 1$ (Abarbanel et al. 1984). The color-coded variation of the Richardson number along the transect route is plotted in Figure 3.11, assigning the Richardson number greater than unity as red. This representation helps to differentiate the areas where the water column was stabilized. From Figure 3.11, it is clear that water column remained stratified in the upper water column near Oso Bay (time= \sim 4000-8200sec) and the lower water column

near the mouth of Upper Laguna Madre (time= \sim 2800-3600sec). Interestingly, the water was hypoxic in the lower water column near the mouth of Oso Bay (Figure 3.9) where the Richardson number was high in the upper water column (Figure 3.11) in that area of the bay. This substantiates the hypothesis that highly aerated surface water may not mix with bottom water where the consumption of dissolved oxygen continued through respiration and decomposition of organic matter. Although the water did not become hypoxic at the lower depths where Richardson number was high (time= \sim 2800-3600sec), dissolved oxygen level was somewhat lower as compared to the upper region of the

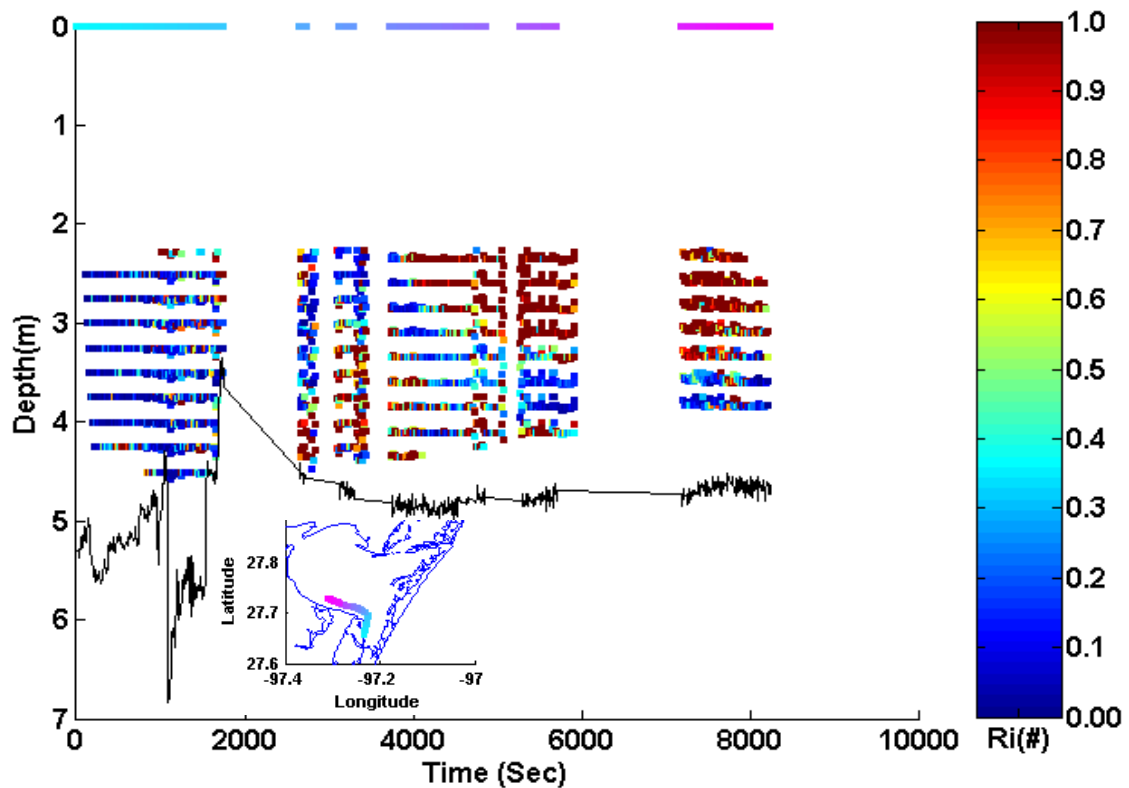


Fig. 3.11 Vertical variation of Richardson number (Ri) along the transect route on August 07, 2007 (■: Ri; - : sea-bed profile).

water column. The measured vertical profile of chlorophyll concentration and total particle concentration along the transect route may further shed light in clarifying the processes causing hypoxia at the bottom of the bay.

The measured vertical profile of chlorophyll concentration, an indirect measure of phytoplankton biomass, is shown in figure 3.12. The chlorophyll concentration was significantly higher in the upper Laguna Madre compared to the bay. Vertical profile of total particle concentration was also higher in the upper Laguna Madre (Figure 3.13). This suggests the existence of high amount of biogenic particles around this region. Biogenic particles such as phytoplankton can produce DO through photosynthetic activities in the day light. This may be the one of the reasons for the presence of higher DO levels in this area. Also, the water column was not stratified around the upper Laguna Madre (Fig. 3.11) and so aerated surface water may also transfer DO into the lower levels of water column. One interesting point to notice from Fig. 3.10, Fig. 3.12 and Fig. 3.13 is that a salt wedge was moving from the upper Laguna Madre towards the bottom of Oso Bay and carried high amount of particles. As particles traveled from upper Laguna Madre towards Oso bay, they started to settle and high amount of particles were found around the mouth of the Oso Bay (shown in Figure 3.13) where low DO concentration was also observed. The decomposition of dead biogenic particles may exert oxygen demand in the water column. Also, density stratified water column at the mouth of Oso Bay prevents high aerated surface water to mix with low DO water. These two possible factors might turn lower levels of water column into hypoxic.

The datasets presented here from two cruises provide evidence of the capability of our mobile monitoring system in capturing and clarifying processes inducing hypoxia in CC Bay.

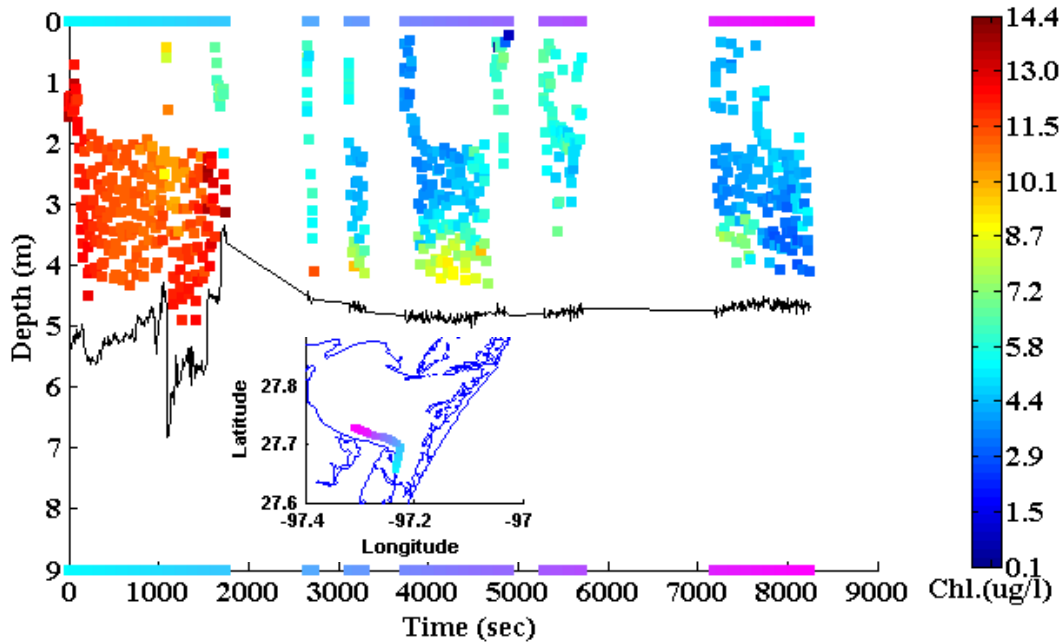


Fig. 3.12 Vertical profile of chlorophyll along the transect route on August 07, 2007 (■: Chlorophyll concentration ($\mu\text{g/l}$); -: sea-bed profile).

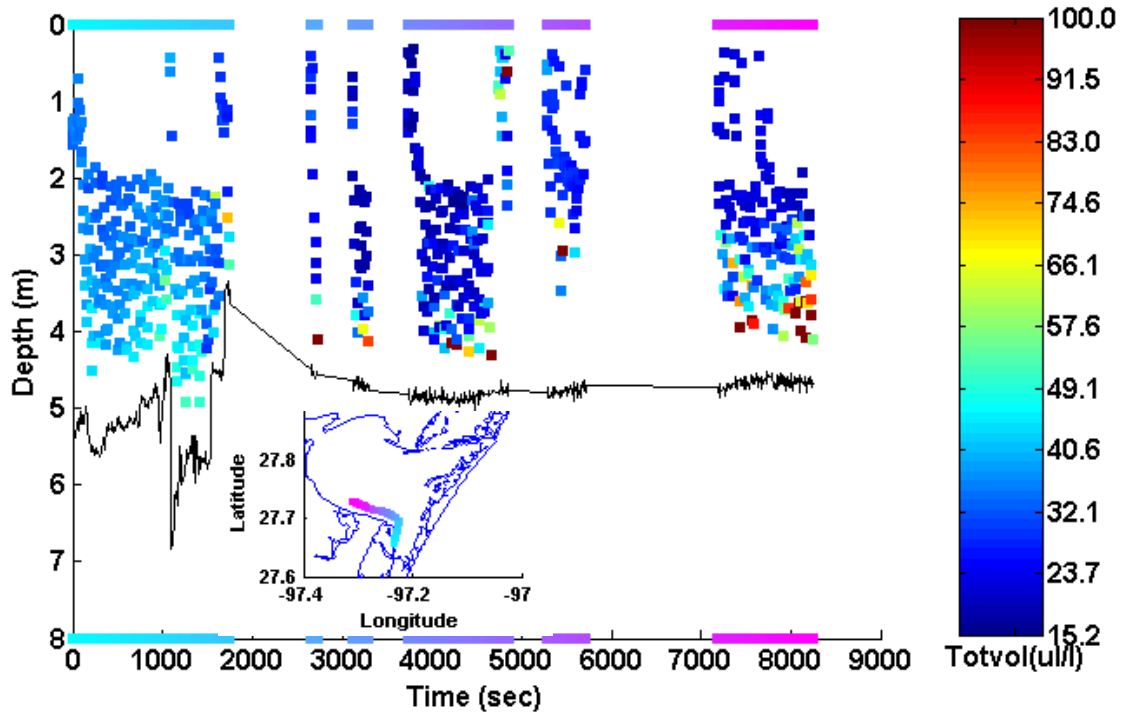


Fig. 3.13 Vertical profile of total particle concentration along the transect route on August 07, 2007 (■: total volume of particle concentration ($\mu\text{l/l}$); -: sea-bed profile).

Conclusions

The mobile monitoring system developed in this study was able to measure hydrodynamic and water quality parameters at greater spatial resolution. The real-time display capability of this system can provide guidance in selection of the transect route to capture the event of interest. Data provided in this chapter illustrates the capability of our monitoring systems in measuring various parameters which can shed light on important processes like stratification, hypoxia, and particle dynamics. The occurrence of the inverse estuary situation in the bay might occur due to the inflows of the hyper-saline water from the Laguna Madre and Oso Bay. The observed significant vertical salinity

gradient might keep the water column stratified as long as the vertical shear structure is weak enough to mix them. The analysis of the measured dataset suggests that hypoxic conditions can occur at the bottom of the bay due to the density-stratified water column associated with high amount of dead-biogenic particles which can exert oxygen demand during their decomposition. Also, aerobic aquatic organisms deplete oxygen at the lower level of water column through their respiration. The positive correlation between acoustic backscatter intensity measured by the ADCP and particle concentration measured by the LISST-100 allows us to develop a quantitative relationship between these two parameters and potentially with the other observed data as measured by our mobile monitoring system. The development of these kinds of quantitative relationships is the subject of our future research, which will then facilitate better understanding of particle dynamics of the bay that significantly affect hypoxia through the transport of the particulate BOD in/out of the bay. Also the development of water quality and three-dimensional hydrodynamic models with observed-data integration will assist in greater understanding of the processes that control hypoxia in this shallow wind-driven bay.

CHAPTER IV
INTEGRATED REAL TIME MONITORING SYSTEM TO INVESTIGATE THE
HYPOXIA IN A SHALLOW WIND-DRIVEN BAY

Overview

Corpus Christi Bay (Texas, USA) is a shallow wind-driven bay which has been designated as part of the National Estuary Program, due to its impact on the local and national economies. During the summertime, this bay experiences hypoxia (dissolved oxygen < 2mg/l) at the south-east part of the bay near the upper Laguna Madre and the mouth of the Oso Bay. Since Corpus Christi (CC) Bay is very dynamic system, the processes that control the hypoxia can last on the order of hours to days. Monitoring systems installed on a single type of platform will not be able to fully capture these processes at the spatial and temporal scales of interest. Therefore, we have integrated monitoring systems installed on three different platform types: 1) Fixed Robotic, 2) Mobile, and 3) Remote. On the fixed robotic platform, an automated profiler system vertically moves a suite of water quality measuring sensors within the water column for continuous measurements. An Integrated Data Acquisition, Communication and Control (IDACC) system has been configured on our mobile platform (research vessel) for the synchronized measurements of hydrodynamic and water quality parameters at greater spatial resolution. In addition, a high frequency (HF) radar system has been installed on remote platforms to generate surface current maps for CC Bay and its offshore area. Data presented in this paper provide evidence of the potential capacity of our integrated

system to determine the extent and timing of hypoxia in CC Bay. In summer 2007, we captured evidence of an hypoxic event; moreover, we detected low dissolved oxygen conditions in a part of the bay with no previously-reported history of hypoxia. Our integrated system can also provide large sets of hydrodynamic, meteorological and water quality data that can be used to drive water quality and hydrodynamic models, thereby providing greater understanding and prediction of hypoxia in the bay.

Introduction

Corpus Christi Bay harbors the nation's seventh largest port and a large complex of petroleum facilities. In 1992, the National Estuary Program (NEP) designated Corpus Christi (CC) Bay as a National Estuary and created the Corpus Christi Bay National Estuary Program (CCBNEP) to protect the health of this bay while supporting its economic growth. This shallow bay has an average depth of 3.6 m (Ward 1997) and is connected to the Gulf of Mexico through a narrow inlet. Therefore, the hydrodynamic conditions of the bay are primarily wind-driven as opposed to tidally-dominated. However, this dynamic bay has reoccurring hypoxia, which can be described as the condition of the water column when dissolved oxygen (DO) levels dip below 2 mg/l. Most aerobic aquatic organisms cannot survive under this condition. Hypoxia was first observed in the south-east portion of CC Bay in Summer 1988 (Montagna and Kalke 1992) and has been reported every year thereafter (Ritter and Montagna 1999).

Factors such as eutrophication, water column stratification, geomorphology of the bay, meteorology etc. may contribute to the development of hypoxia (Buzzelli et al.

2002). Texas researchers have concluded that eutrophication is not the likely cause for hypoxia in CC Bay since over the past 14 years, freshwater inflow rates into the bay have decreased and nutrient levels have not changed significantly (Ritter et al. 2005).

Although water column stratification is a possible cause for hypoxia, CC Bay would not be considered a likely candidate for stratification because it is a shallow wind-driven bay with an expected high level of mixing. However, stratification does occur, and this phenomenon has been observed in other shallow bays such as Mobile Bay in Alabama (Turner et al. 1987) and Pamlico River estuary in North Carolina (Stanley & Nixon 1992) where oxygen-depleted waters were found at the bottom of the bays during low-wind conditions. Ritter and Montagna (2001) observed hypoxic events in CC Bay usually at night or early morning, which typically lasted on the order of hours. Therefore, understanding hypoxic events in this energetic system requires the development of real time monitoring systems (i.e., collection of data at greater spatial and temporal resolution) to capture the stochastic processes that control water quality in the bay.

Monitoring of water quality parameters and environmental indicators that influence the physical processes of hypoxia poses a challenge due to the spatial extent and dynamics associated with this bay. With recent advances in technology, real-time measurements of various water quality parameters are possible through the use of submersible in-situ sensors (Agrawal and Pottsmith 2000; Boss et al. 2007 and Visbeck & Fischer 1995). The advantage of in-situ sensors is that the parameter of interest can be measured in real time, thereby omitting the time gap between sample collection and data analysis. This real-time high-resolution data can expedite decision making in the case of

emergency responses. The in-situ sensors can be installed on fixed platforms for continuous environmental and oceanographic measurements. Although real-time data collected from in-situ sensors on fixed platforms provide information at a high temporal resolution, the spatial resolution is limited. Mobile platforms (e.g., autonomous underwater vehicles, remote-operated vehicles, gliders and towed undulators) can address this limitation by housing in-situ sensors and collecting data at greater spatial resolution (Blackwell et al. 2008 and Barth & Bogucki 2000). This data, however, will have limited temporal resolution. The technical advances in remote sensing help to capture physical and biological variability in the upper layer of the water column at greater temporal and spatial resolution but have not succeeded yet in capturing the chemical species and sub-surface condition of the water column. Therefore, it is optimum to deploy monitoring systems on different platform types and develop an integrated sampling scheme to better capture the dynamics of CC Bay.

The advances in communication technology, relational database management system (RDBMS) and World Wide Web applications provide an opportunity to access the data from various systems in real-time and thereby, help to develop an integrated adaptive sampling scheme for monitoring systems in capturing the events of interest. The research objective for this paper was to develop a cyberinfrastructure which will support real time data acquisition, storage, visualization, management and dissemination for the greater understanding of hypoxic events in CC Bay, as well as other episodic events. Once developed, it helps to implement a coordinated sampling scheme for our monitoring systems in capturing an episodic event. We have developed and installed

different monitoring systems on three different types of platform. A robotic profiler system installed on fixed robotic platform can measure vertical variation of various water quality parameters at high temporal resolution. Other sensors installed on the fixed robotic platform are an Acoustic Doppler Current Profiler (ADCP) to measure current structure of the water column and meteorological sensors to determine wind speed, direction, atmospheric pressure, air temperature. A monitoring system configured on a mobile platform (i.e., research vessel) can measure variation of various water quality parameters ‘synchronically’ over a highly-resolved horizontal and vertical regime. Besides collecting data at greater spatial resolution, this system is capable of displaying data in real time and thereby providing guidance on transect route selection during a research cruise. In addition to these two types of in-situ monitoring systems, four high frequency(HF) radar units were installed on remote platforms to generate surface current maps for the bay and its offshore area (Trujillo et al. 2004; Ojo et al. 2002 and Ojo et al. 2007b). The development of the robotic profiler system and the mobile monitoring system are discussed in detail in Islam et al. (journal manuscript in preparation, 2009a) and Islam et al. (journal manuscript in preparation, 2009b), respectively. These three monitoring platform types (i.e., fixed robotic, mobile, and remote) have been integrated, and the successful implementation of this integrated system to capture the extent and timing of an hypoxic event in CC Bay is described in this chapter.

Site Description

Corpus Christi Bay is located on the Texas coastline and covers an area of approximately 432.9 sq. km (Flint 1985). It is connected with the Gulf of Mexico through a narrow ship channel (15 m depth), which runs from east to west. Freshwater enters the bay via the Nueces River and Nueces Bay, whereas high-saline water enters the bay during summer months from the shallow Upper Laguna Madre and Oso Bay (Figure 4.1). Recently, Packery Channel, located at the southern reaches of the bay, has been opened and it is another source for water exchange with the Gulf of Mexico. CC Bay is mainly dominated by south-easterly winds although northerly winds occur periodically during the winter months. Figure 4.1 shows characteristic features of the bay. The cross-hatched circles represent locations where hypoxia has been reported (Ritter and Montagna 1999; Hodges and Furnas (manuscript submitted to *Environmental Fluid Mechanics*, in review, 2007)). The three large red circles denote the strategic locations of our fixed robotic platforms in the bay. Platform 'P1' ($27^{\circ}43.531'N$, $97^{\circ}18.412'W$) is positioned 100m from the mouth of Oso Bay to characterize the effects of Oso Bay inflow, which has been reported to trigger hypoxia in that part of the bay. Platform 'P2' ($27^{\circ}43.375' N$, $97^{\circ}11.403'W$) is positioned in the south-east portion of the bay where hypoxia has been documented since 1988 (Ritter and Montagna 1999). Some of the ship channel effects on CC Bay may be captured through our Platform 'P3' ($27^{\circ}48.560' N$, $97^{\circ}08.513' W$) in the north-east part of the bay. The data collected from this platform will also provide the necessary boundary conditions for simulation of our three-dimensional mechanistic model to predict the dissolved oxygen (DO) distribution

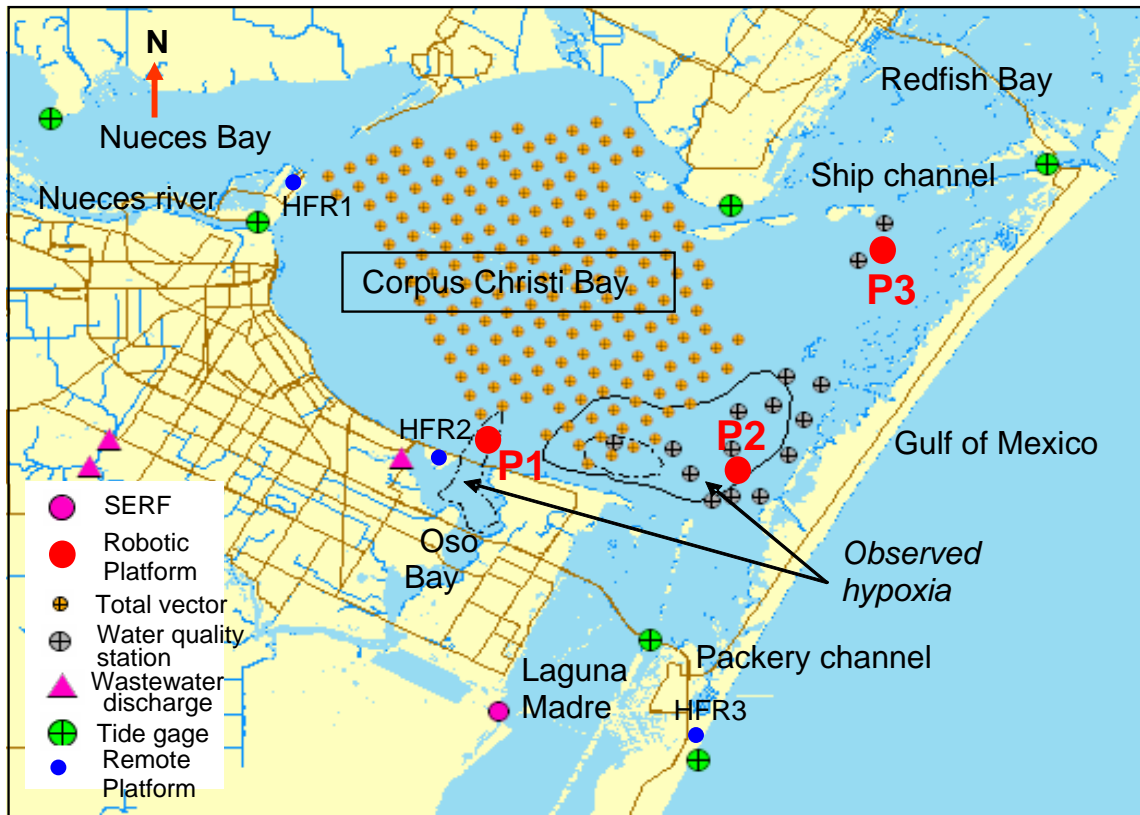


Fig. 4.1 Features of the study area and platform locations.

in the bay.

Along with the fixed robotic platforms, we have installed HF-radar systems on remote platforms which are shown as blue circles in Figure 4.1. Two of them are located on CC Bay shoreline (HFR1 27.832° N, 97.38° W, and HFR2, $27^{\circ}.714'$ N, $97^{\circ}.321'$ W) and generate the surface current map for CC Bay. The other two HF radar systems (HFR3, 27.587° N, 97.218° W, and HFR4, 28.067° N, 96.476° W, not shown in Figure 4.1) capture surface current patterns of offshore CC Bay. The radial current vectors measured by HF-radar system at sites (HFR1 and HFR2) are combined on regular grids (amber-

yellow solid circles in Fig. 4.1) to generate hourly surface current maps for the bay. The amber-yellow circles in Figure 4.1 depict the coverage within the bay. Moreover, Our research facility (Shoreline Environmental Research Facility (SERF) is located close to the Upper Laguna Madre and provides convenient field support for the regular monitoring of the bay (shown in as magenta-colored solid circle in figure 4.1). In addition, the wastewater discharge locations (denoted by magenta-colored triangle), tidal gage (represented by solid green circle), and water quality stations (displayed using grey circle) are shown here to indicate the areas of interest for collecting other important information and data, but are not used in this chapter.

Materials and Methods

The robotic profiler system installed on each fixed robotic platform moves the sensor suite from mean low-water level to the bottom of the bay within 2.5 minutes and measures water quality parameters at five equi-distant depth levels. It then pulls the instrument suite and keeps it in a stationary position above the water column. The cycle time of profiling is currently set for one hour but it can be set to any user-defined interval. The instruments currently deployed on this profiler are a particle sizer (LISST 100X, by Sequoia Sciences), a DO sensor (Optode, by Aanderra), a CTD (Conductivity, Temperature and Depth) sensor (SBE 37 SIP, by Sea-Bird Electronics, Inc.) and a fluorometer (Eco-FL3, by WETLabs). Along with these water quality sensors, an upward-looking 1200 KHz workhorse acoustic Doppler Current Profiler (ADCP, by Teledyne RDI) and meteorological sensors are installed on each fixed robotic platform.

Each ADCP is configured to measure a vertical profile at every five minutes, where each profile is measured from an ensemble of 45 pings, and the time between pings is one second. In addition to water currents, the ADCP can also measure acoustic backscatter intensity, waves and other hydrographic information.

The mobile monitoring platform contains the similar suite of instruments as those installed on the robotic profiler system. In addition, a Global Positioning System (GPS) has been used to geo-reference the synchronized measurements of water quality parameters. All instruments are pre- and post-calibrated for each research cruise and the data collected from the mobile platform are screened to remove outliers before performing any kind of post data analysis. MATLAB® toolboxes have been used for the post processing of observed data.

The HF-radar system at each remote platform generates radial vectors. The transmitting antenna at each radar site sends out radio waves which are scattered off from the ocean surface. The return of these sea-echo signals have been captured by the receiving antenna and processed to determine the range, bearing and radial velocity of the ocean surface toward/away from it (Barrick et al. 1977& Barrick and Lipa 1999). All radial vectors collected from the sites are processed in the computer at our Corpus Christi base station (Shoreline Environmental Research Facility, SERF, Fig. 4.1) through manufacturer software to generate hourly surface current maps on regular grid.

All measurements from our monitoring systems are stored in a structured query language (SQL) database server and are retrieved using a MATLAB® database toolbox for post-processing. These data are shown on our web server in real time and are

checked daily by a research staff member to ensure data quality. If any anomaly in the dataset is noticed, then those data are analyzed to determine whether it arises from a sensor defect or from a change in the actual bay conditions. Sensor or other technical malfunctions may require a platform service trip, whereas changes in bay conditions may serve as a prompt for a research cruise (e.g., mobile platform deployment) to further investigate the phenomenon. All sensors on each profiler are pre- and post-calibrated before and after deployment.

Description of the Developed Cyberinfrastructure

Measurements of water quality, meteorological and hydrodynamic parameters through in-situ sensors at our fixed robotic platforms and HF radar units at our remote platforms need to be made available to stakeholders (i.e., public, scientific community, resource managers and planners) in near real time for taking the full advantage of these deployed sensors. We have developed cyberinfrastructure which can be described as a computing and communications technology infrastructure system to acquire and publish those data in real time. Figure 4.2 presents the schematic diagram of our cyberinfrastructure system. The data flow and various components of this diagram are described in subsequent paragraphs.

All water quality sensors on the robotic profiler system are serially connected with the WINCUBE (i.e., PC/104 computer platform standard; customized and ruggedized in our labs), which acquires data from these sensors through the data acquisition software developed in this study. The manufacturer-supplied software for the

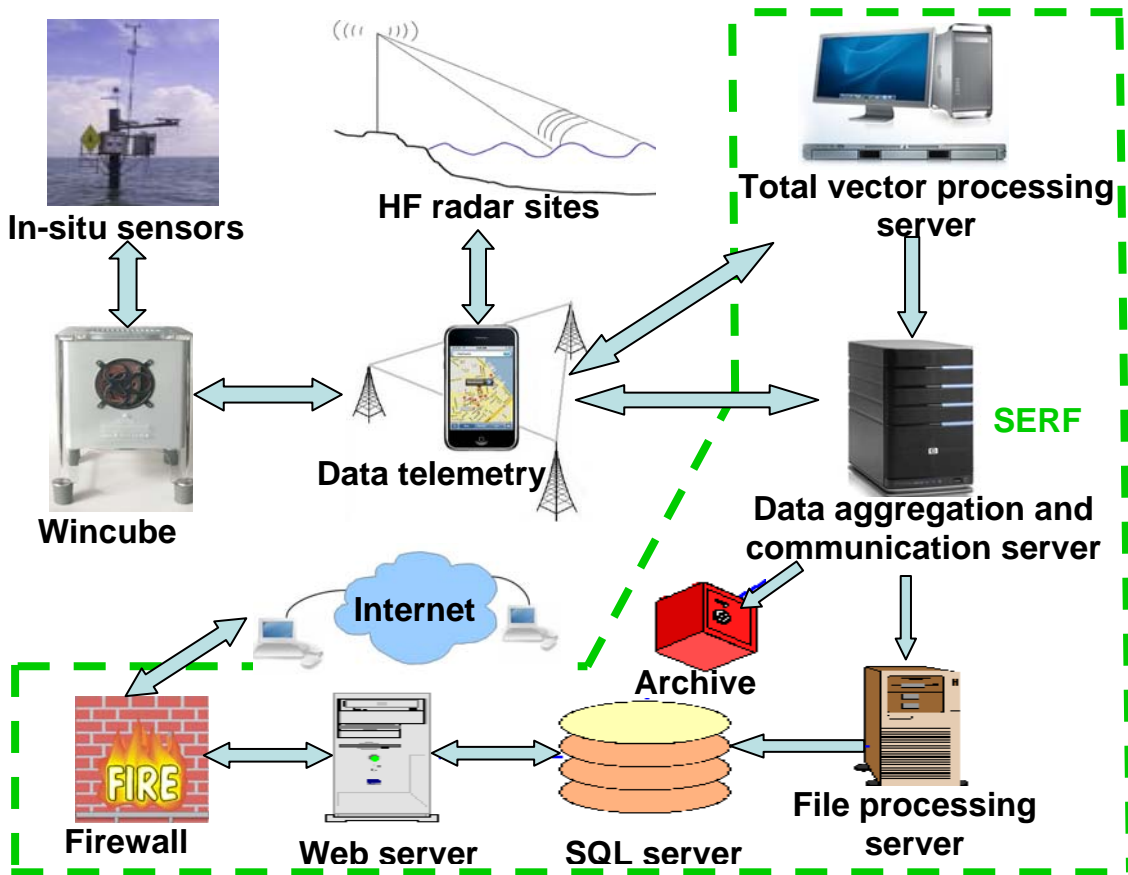


Fig. 4.2 Schematic diagram of SERF cyberinfrastructure.

meteorological sensors and the ADCP have also been installed on the WINCUBE to collect data. The collected data are stored in a temporary folder on the WINCUBE prior to being telemetried to base station, SERF. A wireless data transceiver (FGR-115RE, Freewave Technologies, Inc) with directional antenna has been installed at each fixed robotic platform for establishing radio links to the shore-based network. Since wireless (radio) links are subject to distance limitations, intermediate radio relay stations have also been established for the data telemetry to SERF. The wireless data transceiver with omni-directional antenna at SERF receives data comes from our fixed robotic platforms

and offshore HF radar sites. The Corpus Christi offshore HF radar sites are connected with SERF through cellular networks whereas the Corpus Christi Bay radar sites (HFR1 and HFR2, Figure 4.1) communicate with SERF through DSL and radio relay. Radial vectors collected from all HF radar sites are processed in the “total vector processing server” to generate total vectors. The surface current map generated from this server is then imported to the data aggregation and communication server. We have developed a program (named “Transbot”) which is installed on this server for the scheduled transfer and archival of real time data from an arbitrary number of remote stations (fixed robotic platforms, total vector processing server) to a file processing server. While originally conceived to gather environmental data from a variety of remote sites, Transbot is transparent and generic, i.e., it is capable of managing any arbitrary data stream. It is configured through plain-text configuration files, making administration separate from programming maintenance. Once all data are in the file processing server, they are processed for the conversion into meaningful units and are then standardized for the insertion into the relational database. The Microsoft database management system (Structured Query Language, SQL) server has been used to manage this myriad of water quality, hydrodynamic and meteorological datasets. The web server at SERF hosts the web services through which researchers, educators, policymakers, natural resource managers and the general public can get data in real-time. We have developed and installed the software on our web server through which requested data are queried into our SQL database and then converted into the XML (Extensible Markup Language) format to facilitate the sharing of structured data on the web.

Results and Discussion

The profiling system on each fixed robotic platform provides continuous measurements of water quality parameters and current structure of the water column at a given spatial location, while the HF radar system on remote platforms continuously measures the surface currents for the entire bay and its offshore area. The Integrated Data Acquisition, Communication and Control (IDACC) system on the mobile platform provides a temporal snapshot of the water column condition for the larger spatial portion of the bay. These systems have been integrated in this study to capture the extent and timing of a hypoxic event in CC Bay. Any unusual (i.e., non-baseline) measurements from a fixed robotic platform can alert our research group regarding a potential ‘critical’ condition of the water column and trigger the demand for further investigation. At that point in time, our research scientist(s) can further investigate /analyze the observed data (e.g., dissolved oxygen level, density gradient, surface current map and current structure of the water column). If water column conditions appear favorable for hypoxia or have already turned hypoxic, then a mobile platform deployment is warranted for further investigation.

With this integrated real time monitoring system, we were able to detect and investigate the extent of hypoxia in CC Bay in Summer 2007. Our findings included hypoxic conditions in a new region of the bay, which had not been reported previously for hypoxia. The following paragraphs illustrate the success of our integrated systems in capturing the hypoxic event at greater spatial and temporal resolution.

Investigation of a Hypoxic Event (July 22-25, 2007)

In-situ sensors associated with the robotic profilers on our three fixed robotic platforms can provide baseline observations for CC Bay throughout the year. The following figures (Figures 4.3~4.10) provide examples for some of the water quality and hydrodynamic information available during Summer 2007. A snapshot in time (July 22-25, 2007) illustrates the capability of our fixed robotic platform monitoring system to alert researchers as to a potentially critical condition of the water column, thus allowing us to potentially capture an episodic event (such as hypoxia). In each of the figures associated with our fixed robotic platforms, the data points are color coded to indicate the range of the measurements at five water depths. The wavy blue line at the top of these figures represents the actual water surface elevation at the fixed robotic platforms. The temporal variation of several water quality and hydrodynamic parameters is shown starting at 00:00 hours on July 22, 2007 through 24:00 hours on July 25, 2007.

In Figure 4.3, the color-coded lines indicate the relative salinity variation (salinity corresponding to the observed peak value) at five different depths at Platform 'P3'. There exists a significant salinity gradient (salinity difference over 2m depth, $\Delta S > 4$ psu) between the first and fifth level of measurement on July 22 to July 23 (0.00d ~1.60 d on x-axis) whereas this gradient is typically low ($\Delta S < 2$ psu) most of the year. This is an example of the type of unusual (non-baseline) measurement which alerts our research group and requires further investigation for a clarification of this anomaly. We then analyze all water quality and hydrodynamic information collected at our fixed robotic platforms and remote platforms. Park et al. (2007) observed significant correlation

between hypoxic conditions and the bottom-surface salinity gradient. They found 65-78% of their collected dissolved oxygen data at the bottom of shallow Mobile Bay remained below 2 mg/l when the salinity gradient (over 2.5m depth) was greater than 4psu. The dissolved oxygen data collected from platform ‘P3’ did not indicate any condition of hypoxia above one meter from the sea-bed, though it is possible that dissolved oxygen levels dropped below 2 mg/l closer to the bottom. Salinity and vertical current profile measured at the fixed robotic platforms together with the surface current map generated by the HF-radar system shed light on the condition of the water column

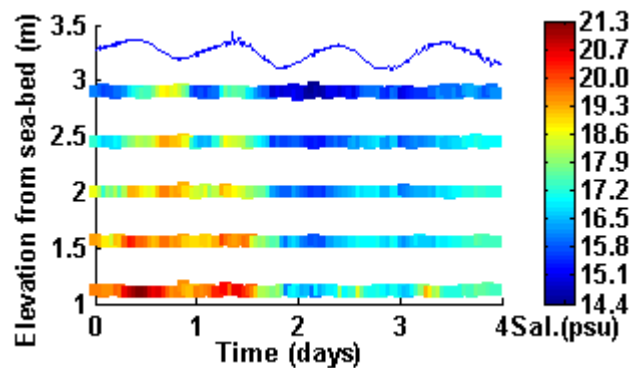


Fig. 4.3 Vertical variation of salinity at platform ‘P3’ during July 22-25, 2007 (■: salinity data points; —: water surface elevation).

and thereby helped evaluate the status of hypoxia in the bay. The analysis of these measured parameters is discussed in detail in the following paragraphs.

Stratification created by the salinity gradient suppresses the vertical mixing of oxygen-rich surface water with the low-DO bottom waters whereas the vertical shear produced from the velocity gradient enhances the mixing. The salinity and water current

structure provide necessary information to determine the relative importance of the mechanisms in controlling the vertical mixing, and thereby help to infer the dissolved oxygen condition in the bay. The salinity profile on July 22-25, 2007 at platform ‘P2’ is shown on Figure 4.4. It should be noted that the profiler mechanism was not operating properly in this time frame; as such, the data measurement collection did not occur at five equi-distant depths which is our preferred mode of operations. Nevertheless, the data is insightful for assessing the potential for hypoxia during this timeframe. Salinity levels at Platform ‘P2’ were higher at all measurement depths compared to levels at

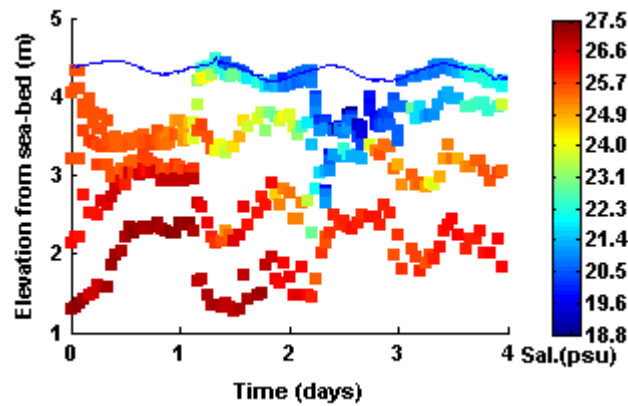


Fig. 4.4 Vertical salinity variation at platform ‘P2’ during July 22-25, 2007 (■: salinity data points; -: water surface elevation).

Platform ‘P3’ during the July 22 to July 23 timeframe (0.00d ~1.60 d on x-axis). This may be due to the inflow of high saline water from the shallow Oso Bay and the upper Laguna Madre which is one of the most hypersaline lagoons in the world (Gunter, 1967). In addition, precipitation data collected from the National Weather Service station at Port

Aransas (just north of 'P3') indicates that significant rainfall occurred during July 17-20 and July 23, 2007 and thereby, it may contribute to lower salinity level around our platform 'P3'. Under this condition, the water circulation pattern may be controlled by gravity flow, i.e., denser saline water moves towards platform 'P3' through the bottom whereas fresher water moves along the surface towards platform 'P2'. The vertical salinity profile shown on Figure 4.4 supports this hypothesis as there existed a significant salinity gradient ($\Delta S > 8\text{psu}$) at platform 'P2' on July 24 (2.25d ~2.75d on x-axis), whereas the salinity level was low at all depths at Platform 'P3' during this time.

The HF-radar system on remote platforms can shed more light on bay's hydrodynamic conditions as it determines surface water current velocities by analyzing the backscattering of radar pulses from the moving ocean surface (Barrick et al.1977). If the bay is calm, this system is not able to capture this information. The surface current maps generated by HF-radar system are presented in Figure 4.5 at successive days from July 21, 2007 to July 24, 2007. During much of this timeframe, the water remained calm as inferred from low values of surface current and data gaps (particularly in the eastern portion of the bay). On July 22, the HF-radar system captured the clockwise circulation pattern, i.e. water moved at the surface from platform 'P3' to platform 'P2' and this further substantiates our hypothesis of the gravity flow. Our HF-radar system generated only one hourly surface current map from 23:00 on July 22 to 09:00 on July 23 due to the calm condition of the bay. Same condition happened from 22:00 July 23 to 06:00 July 24. Therefore, the circulation maps at midnight (00:00 hr) are missing for July 23 and July 24 from the set of surface current maps presented here. If the less-saline water

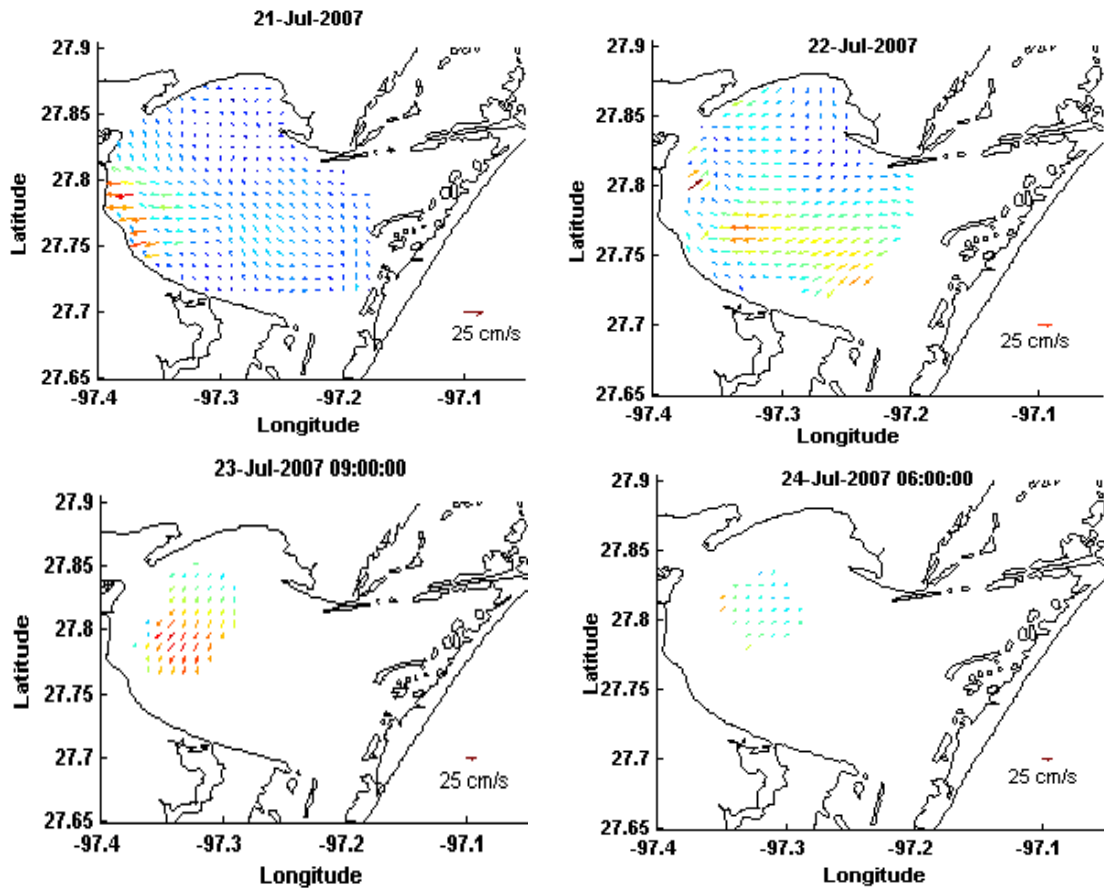


Fig. 4.5 Surface current velocity of CC Bay as captured by our HF-radar system at successive days from July 21 to July 24, 2007 (top left to bottom right). Note: colored-arrow is scaled by color magnitude (cm/s).

overlays the more-saline water and the bay is calm, the water column then may be stratified and the oxygen-rich surface water may not mix with less oxygenated water at the bottom. This may induce hypoxia at the bottom of the bay.

The kinetic energy generated from the vertical shear structure will indicate the mixing potential of the water column. The shear rate (S) can be calculated using the equation (4.1):

$$S^2 = \left(\frac{\partial u}{\partial z} \right)^2 + \left(\frac{\partial v}{\partial z} \right)^2 \quad (4.1)$$

The east-west (u) and north-south (v) velocity components used in this equation are measured by the ADCP at the fixed robotic platforms. Figure 4.6 shows the vertical variation of shear rate at platform ‘P2’ from July 22-25, 2007. There was not a significant amount of shear to mix the water column except at the later part of the day on July 23, 2007 (X-axis 1.4~2.0d). On the other hand, the amount of work required to mix density stratified water column can be determined through the quantification of the buoyancy frequency (N) which can be described by the following equation (4.2):

$$N^2 = - \frac{g}{\rho} \frac{d\rho}{dz} \quad (4.2)$$

Where, ρ is water density, g is gravity acceleration and z is the depth from the water surface. The vertical density profile captured by our CTD sensors can be used to determine N . Figure 4.7 displays the vertical variation of buoyancy frequency at platform

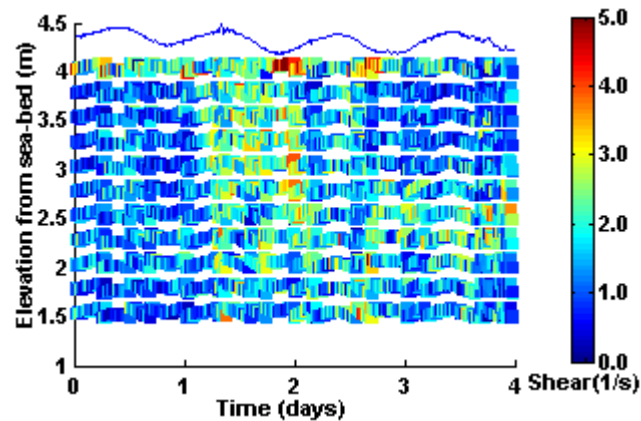


Fig. 4.6 Vertical variation of shear at platform P2 during July 22-25, 2007 (■: shear magnitude (1/sec) data points; —: water surface elevation).

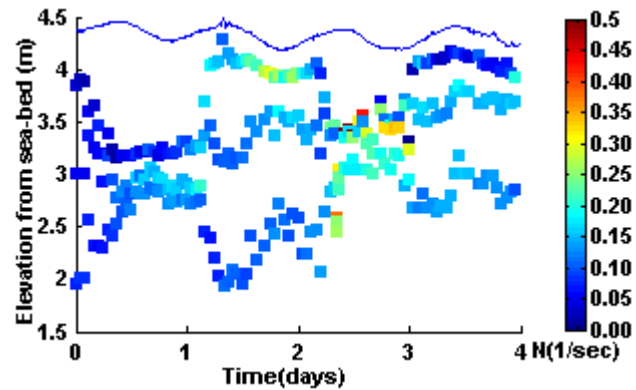


Fig. 4.7 Vertical variation of buoyancy frequency at platform ‘P2’ during July 22-25, 2007 (■: buoyancy data points (1/sec); -: water surface elevation).

‘P2’ on July 22-25, 2007. The buoyancy frequency is high from the morning to the end of the day on July 24, 2007(x-axis 2.3d~3.0d). Therefore, the amount of work required to mix the water column is high and so the water column may remain stratified if the shear is not high enough to mix this column.

The mixing potential of the water column can be understood by determining the Richardson number (Ri) which is the ratio of the above mentioned buoyancy frequency and shear rate. Mathematically, this number can be defined by the following formula (4.3):

$$Ri = \frac{N^2}{S^2} \quad (4.3)$$

According to Abarbenal et al. (1984), the water column remains stable in a three-dimensional stratified parallel shear flow if Ri is greater than unity. Figure 4.8 depicts the vertical variation of Richardson numbers at Platform ‘P2’ and it can be seen from this figure that the water column was stratified from mid-day July 22 to early morning of July

23 (x-axis:0.6d~1.2d), and became restratified again from the early morning of July 24 (x-axis ~2.15 d). Therefore, the water column at the bottom of the bay may turn hypoxic if this condition prevails. The observed vertical dissolved oxygen profile at platform ‘P2’ (Figure 4.9) does not indicate any hypoxic condition above 2m from the sea-bed at that time frame. However, the dissolved oxygen level close to the bottom (0~1.0m) may be hypoxic depending on the duration of the stratified conditions and the presence of the amounts of organic matter at the bottom. The fluorosensor deployed on the profiler determines the chlorophyll concentration which is a measure of phytoplankton biomass available in the water column. This sensor detected insignificant amounts of chlorophyll (Chl. a < 5 $\mu\text{g/l}$) in the water column and so phytoplankton would not produce noticeable changes in the dissolved oxygen condition in the water column through photosynthesis. However, the particle sizer on the robotic profiler system at platform ‘P2’ detected a noticeable amount of particles in the water column (Figure 4.10). These particles include

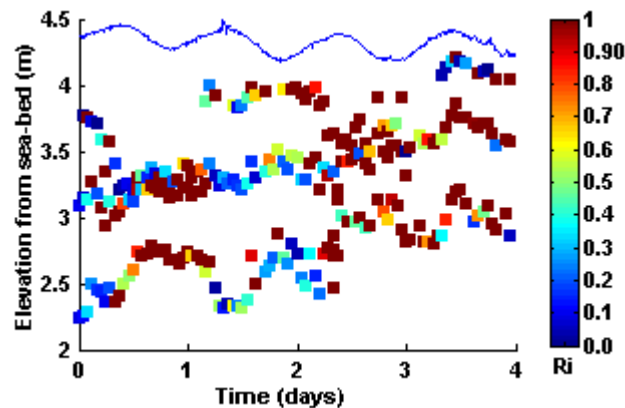


Fig. 4.8 Vertical Richardson number (Ri) variation at platform ‘P2’ during July 22-25, 2007 (■: Richardson number; —: water surface elevation).

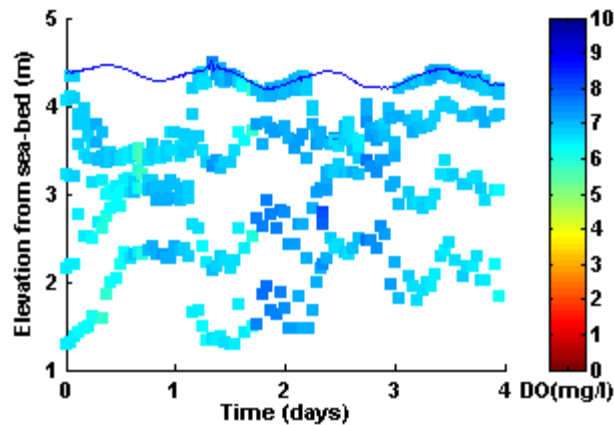


Fig. 4.9 Vertical dissolved oxygen (DO) variation at platform 'P2' during July 22-25, 2007 (■: DO data points (mg/l); -: water surface elevation).

silt, clay, sand and biogenic particles etc. If the concentration of dead biogenic particles is significant, they may potentially reduce DO levels in the water column through consuming oxygen during decomposition. We collected water samples at several bay locations in the month of July 2007 and found that the biochemical oxygen demand (BOD) was significant (5~7.5 mg/l) in the upper Laguna Madre and around our platform

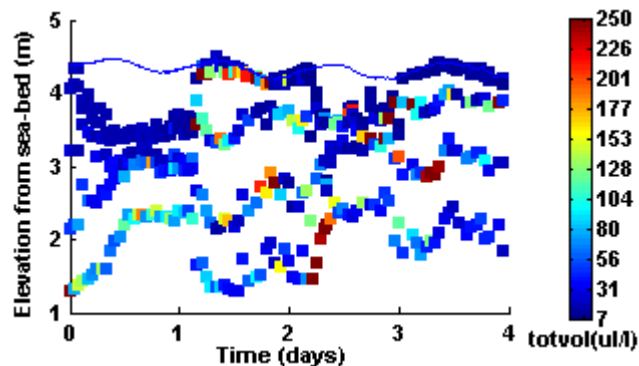


Fig. 4.10 Vertical variation of particle concentration at platform 'P2' during July 22-25, 2007 (■: total particle concentration (µl/l); -: water surface elevation).

'P2; whereas BOD was undetectable (<2 mg/l) in other portions (e.g. near the mouth of Oso Bay, around platform 'P3' etc.) of the bay (Islam et al. 2008). This suggests the presence of oxygen consuming particles in the water column near platform 'P2'. Since the fixed robotic platform data suggests the possibility of low DO water at the bay bottom, it was deemed necessary to collect samples at greater spatial resolution (both vertical and horizontal direction) to determine the extent of the DO levels in the hypoxia-prone regions of CC Bay. As such, the mobile platform was deployed.

The mobile platform (research vessel and tow body with sensor suite) was deployed in the morning of July 24, 2007. The real-time display of relative concentration of measured parameters guided the cruise transect direction to capture the extent of hypoxia, if indeed it was occurring. Data results are presented as color-coded scatter points in Figures 4.11-4.17, and the actual cruise route is depicted on the inset plots in each figure. The route line is color-coded and correlates with the horizontal color-coding along the top and bottom of each figure, thus matching the observed data with the spatial location in the bay. The black solid line in each of these figures represent the sea-bed profile along our transect route. The first transect began in the upper Laguna Madre and headed north towards Platform 'P2' where a sharp salinity gradient and favorable stratified conditions had been detected by our fixed robotic platform systems (Fig. 4.4).

Figure 4.11 presents the vertical dissolved oxygen variation during our first transect. The red solid circle on the inset shows the location of Platform 'P2'. Unfortunately, there were ongoing field activities by a commercial seismic company in

the proximity of our platform, and the crew had posted warning signs requesting no interruption of their activities. Therefore, we towed our instrument array away from our platform in the depth range of 0-2m ($t \approx 3500-3800$ sec). Once we moved out of the area, we began towing again in the full depth range of our IDACC system (near-surface levels to approximately one meter above the bay bottom to avoid impact). Dissolved oxygen levels at the bottom of the water column around Platform P2 were low ($t = 2800-4000$ sec). Ritter and Montagna observed hypoxia at the lower depths of this region in previous years (Ritter and Montagna 1999).

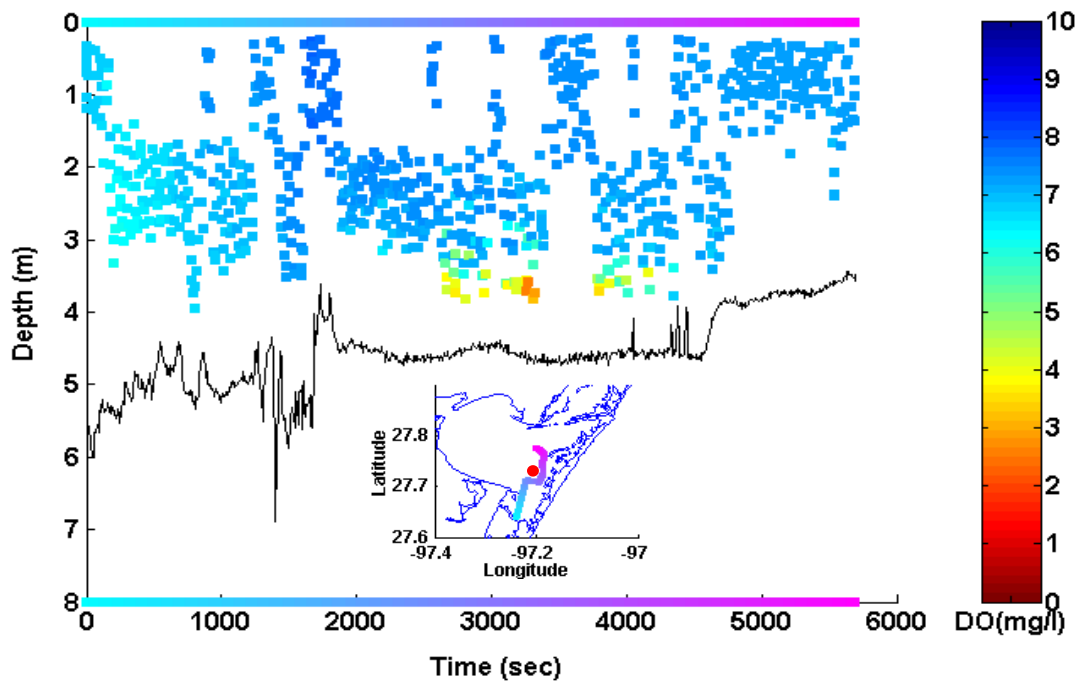


Fig. 4.11 Scatter plot of actual DO variation along the first transect route on July 24, 2007 (■: DO data points (mg/l); ●: Platform 'P2' location; —: sea-bed profile).

Figure 4.12 displays the vertical variation of salinity along the transect route. Salinity levels at all depths were higher at the Upper Laguna Madre (early part of the cruise, $t = 0$ -1300 seconds) as compared to salinity levels in CC Bay (mid and latter parts of the cruise, $t = 1300$ -5800 seconds). The temperature profile (Figure 4.13) varied in a similar pattern along the travel route. It may be hypothesized from these temperature and salinity profiles that a salt edge might move from the shallow upper Laguna Madre towards the Platform 'P2' area and induce a significant vertical salinity gradient around this platform. The salinity level at the shallow upper Laguna Madre (depth < 1 m) is generally very high at summer due to the higher evaporation rate and low freshwater inflow (Texas Department of Water Resources, 1983). The salinity and vertical current

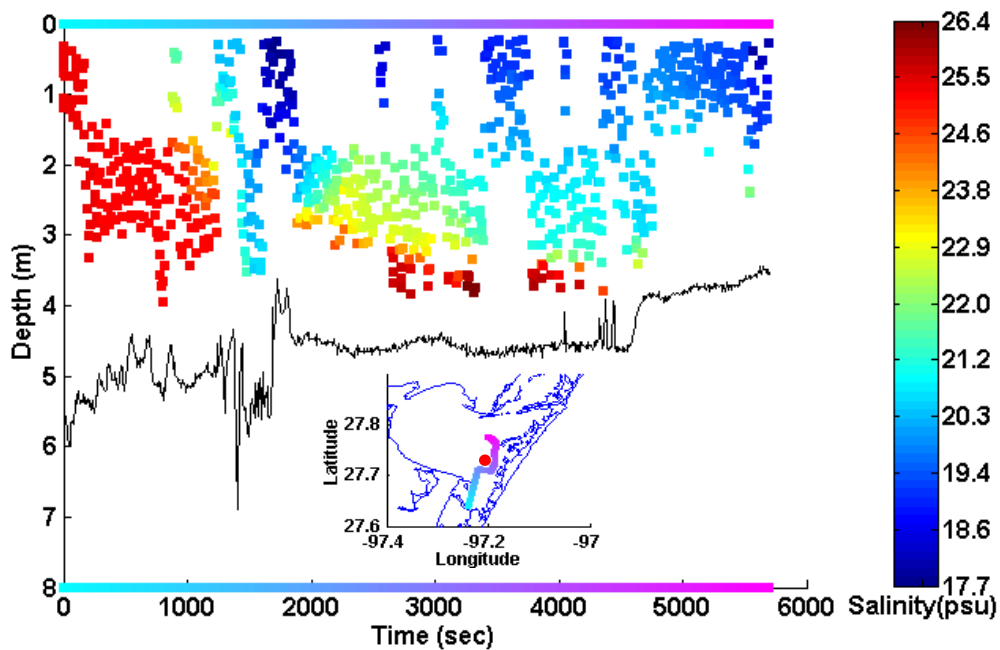


Fig. 4.12 Scatter plot of actual salinity variation along the first transect route on July 24, 2007 (■: Salinity data points (psu); ●: Platform 'P2' location; -: sea-bed profile).

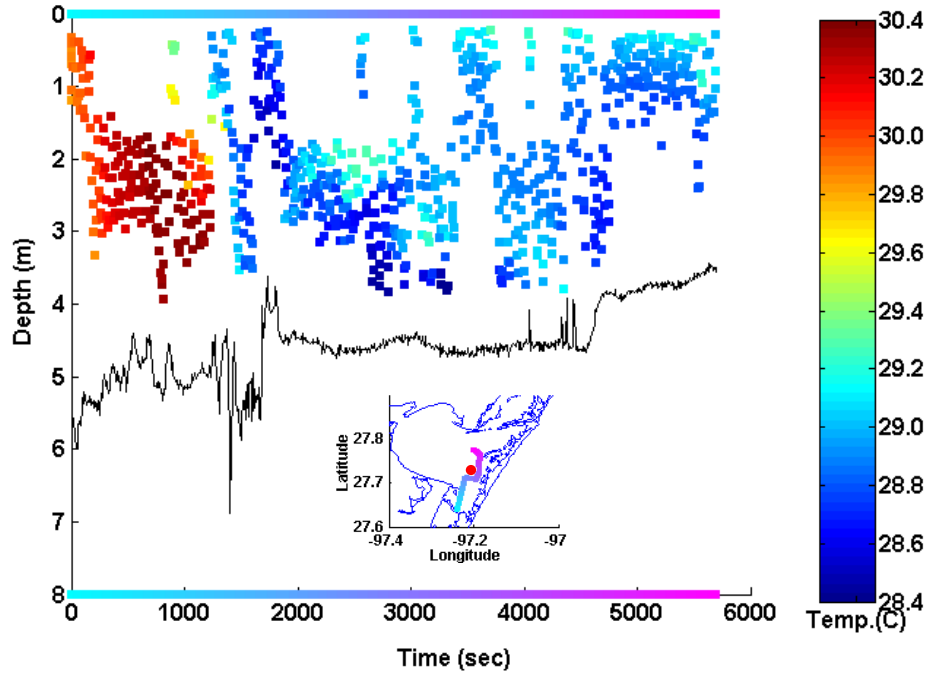


Fig. 4.13 Scatter plot of actual temperature variation along the first transect route on July 24, 2007 (■: Temperature data points ($^{\circ}\text{C}$); ●: Platform ‘P2’ location; —: sea-bed profile).

profile can shed light on the vertical mixing condition along the transect route. Due to higher cruise speeds (~ 6 knots) and calm bay conditions, measured water current profile data was not reliable on that day and so is not used in the analysis.

The vertical variation of chlorophyll along the transect route is presented in Figure 4.14. Chlorophyll concentration was much higher in the upper Laguna Madre compared to the bay area. On the other hand, total particle (organic and inorganic) concentrations (Figure 4.15) did not change significantly along the transect except in the region near Platform ‘P2’, where the low dissolved oxygen conditions were observed (Fig 4.11). The increase in particle concentration in the lower depths around the

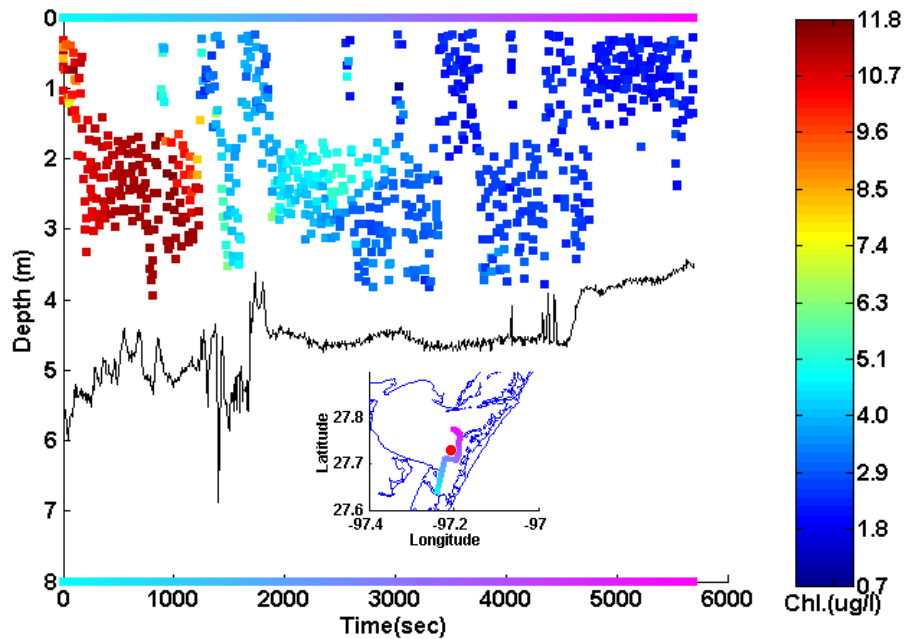


Fig. 4.14 Scatter plot of actual chlorophyll (Chl. a) variation along the first transect route on July 24, 2007 (■: Chlorophyll (Chl. a) concentration ($\mu\text{g/l}$); ●: Platform 'P2' location; -: sea-bed profile).

platform area ($t = 2800\text{-}3800$ seconds, red box region) may be due to the increase of dead non-fluorescing biogenic particles, as chlorophyll concentrations did not change and remained very low ($2\text{-}4$ $\mu\text{g/L}$, Fig.4.14). Since there was a fairly sharp salinity gradient at the lower depths near the platform 'P2', the denser bottom water column may not have mixed with the less-dense more-aerated waters in the upper water column. If the water column cannot vertically mix, oxygen levels at the bottom of the bay may decrease due to the decomposition of biogenic particles detritus. On the other hand, the higher oxygen levels in the upper Laguna Madre may be due to the un-stratified water column and

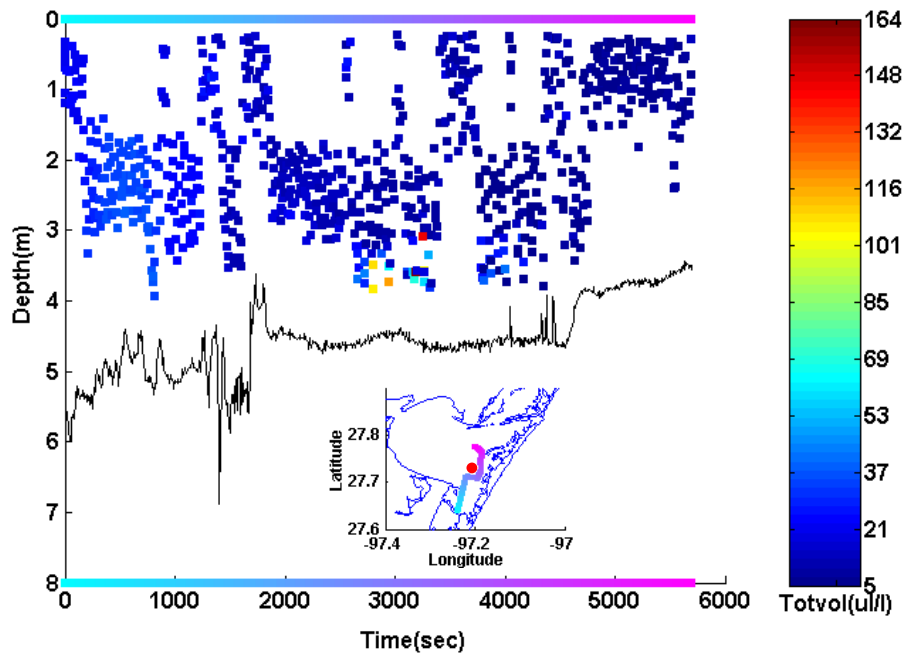


Fig 4.15 Scatter plot of actual particle concentration variation along the first transect route on July 24, 2007 (■: Total Particle concentration ($\mu\text{l/l}$); ●: Platform ‘P2’ location; –: sea-bed profile).

presence of relatively high levels of phytoplankton that can produce oxygen through photosynthesis. These speculative statements are examples of possible explanations which can be hypothesized and tested when large datasets such as those provided by our integrated monitoring system are available. Ultimately, this information can shed light into understanding of environmental processes associated with hypoxia and other phenomena.

A primary objective of this study was to determine the extent of hypoxia and this was achieved through the selection of a relevant transect route, as guided by our mobile monitoring system. The observed data from the profiler at Platform ‘P3’ showed high

dissolved oxygen concentrations (~ 8 mg/l) and uniform salinity level at all depths of measurement. Therefore, we completed our first transect after we had completely transversed the pocket of hypoxic waters near Platform 'P2'. At that point, we changed our direction of travel and headed southwest towards Oso Bay where hypoxia had been observed previously (Hodges and Furnans 2007). However, as we moved towards Oso Bay, we found another pocket of low dissolved oxygen levels, and changed directions, moving northwest towards Nueces Bay.

Figure 4.16 shows the vertical variation of dissolved oxygen concentrations along our second transect. Low dissolved oxygen levels continued in the lower water column (3-4m depths) along our cruise transect, and surprisingly, very low dissolved oxygen conditions were observed at the mouth of Nueces Bay ($t \sim 7000$ seconds). Hypoxia in this area of the bay has not been reported previously. It should be noted that at two points during this transect we had to pull our instruments onto the boat deck and stop collecting data due to the sudden gradient in sea-bed levels where the tow body with instrument suite struck the bottom. The first brief gap in the data set ($t = \sim 4500$ seconds) occurred when we crossed the ship channel and the tow-body was not capable of undulating in a sharp seabed gradient; the second gap ($t = 4800$ to 5500 seconds) occurred when the tow body hit the seabed. The vertical salinity variation along our second transect is shown on Figure 4.17 and it has two distinct water layers. The top layer (0-2.5m) was much less saline than the bottom layer (2.5-4.0 m depth). The precipitation data, recorded by the National Weather Service station at Corpus Christi Airport (approximately 10 km from the mouth of the Nueces Bay), indicated a

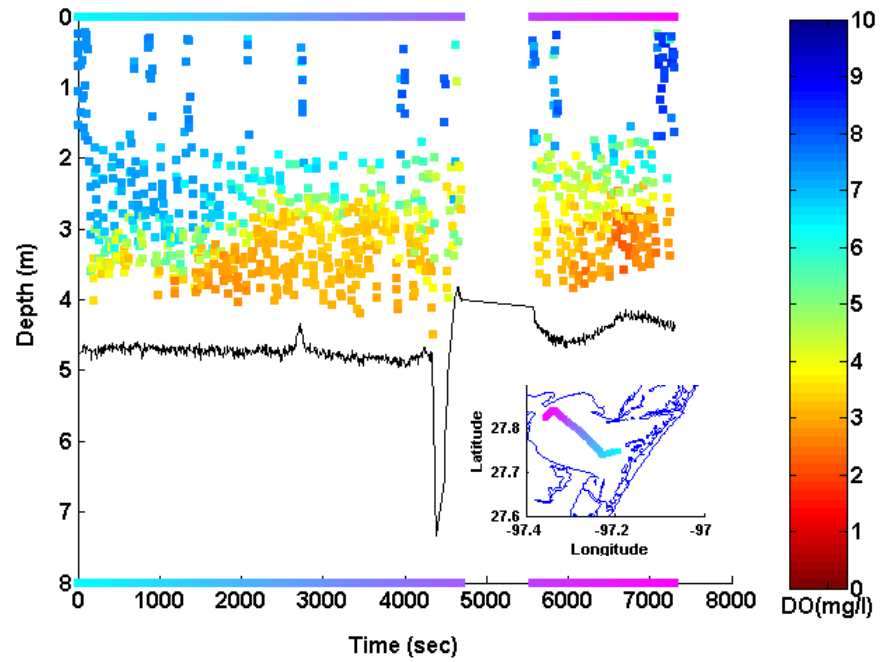


Fig. 4.16 Scatter plot of actual DO variation along the second transect route on July 24, 2007 (■: DO data points (mg/l); ●: Platform 'P2' location; -: sea-bed profile).

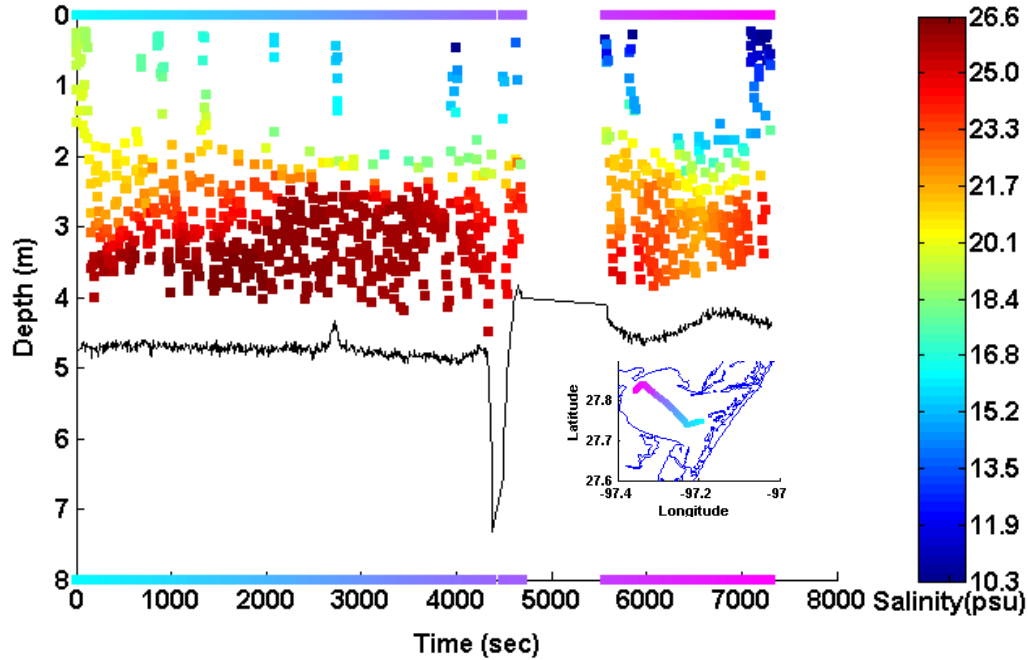


Fig. 4.17 Scatter plot of actual salinity variation along the second transect route on July 24, 2007 (■: Salinity data points (psu); ●: Platform 'P2' location; -: sea-bed profile).

significant rainfall event on July 23 which might contribute to a large freshwater input into the upper waters of this bay. As proposed before, the denser bottom water layer may not mix with less dense more-aerated upper water layer, and so the dissolved oxygen level may be reduced as respiration and decomposition of organic matter exerted oxygen consumption in the lower water depths. The other measured parameters (e.g., total particle volume, chlorophyll concentration, temperature) did not change significantly along this transect; therefore, no results are presented in this paper.

Conclusions

Hypoxia poses a severe threat to coastal ecosystem as most aerobic aquatic organisms cannot survive under this condition. Monitoring of water quality parameters and environmental indicators that influence the physical processes of this event poses a challenge due to the spatial extent and dynamics involved. Profiling systems installed on fixed robotic platforms can measure various parameters at greater temporal resolution but limited spatial resolution. A mobile monitoring platform can address the limitation of the spatial coverage but has limited temporal resolution. HF-radar systems installed on remote platforms can generate continuous surface current maps for CC Bay. The integration of these monitoring systems can help in characterizing the various environmental processes at a multitude of spatial and temporal scales of interest. The development of cyberinfrastructure in this study helps to integrate these systems and makes data available in real time to stakeholders. The real time availability of this data provides an opportunity to develop coordinated sampling scheme for capturing hypoxia or other episodic events in the bay. All data presented in this paper provide evidence of the potential capacity of our integrated systems to determine the extent and timing of hypoxia in CC Bay, and help to better understand the processes that control hypoxic events in this ecosystem. With our integrated system, we were able to capture a hypoxic event in Summer 2007 and found a new area of the bay with low dissolved oxygen conditions that had no previously-reported history of hypoxia. This integrated system can also be used for regular monitoring of the water quality of the bay and thereby to characterize/monitor other episodic events such as oil spills, harmful algal blooms,

sediment re-suspension events, etc. Data collected from these monitoring systems can be used to drive water quality and hydrodynamic models (Islam et al. 2008; Ojo et al. 2007b & Islam et al. 2006c) which are valuable resource tools for predicting water quality of the bay.

CHAPTER V
DEVELOPMENT AND INVESTIGATION ON THE RELIABILITY OF A 2-D
HYDRODYNAMIC MODEL FOR CORPUS CHRISTI BAY

Overview

Hydrodynamic information is critical to the implementation of our Coastal Margin Observation and Assessment System (CMOAS) which can be conceptualized as an environmental observatory that will supply surface current maps, vertical profiles of currents, meteorological observations and other real-time physical, chemical and biological measurements within the water column. Two-dimensional depth-integrated hydrodynamic models have long been used to successfully predict hydrodynamic information such as storm surges and tidal elevation in a shallow wind-driven bay. The key assumption of this model is the well-mixed condition of the water column. Corpus Christi (CC) Bay (TX, USA), a test bed for the CMOAS implementation, is connected to two shallow water bodies which bring highly saline water into the bay. This can induce significant vertical gradients in the hydrodynamic and water quality conditions of the bay, and so the key assumption of a depth-averaged model may not be applicable for CC Bay. The development of a 2-D barotropic hydrodynamic model of CC Bay and its comparisons with realtime observations provides an opportunity to verify the applicability of this model in capturing hydrodynamic information of the bay. The numerical model used in this study is the ADvanced CIRCulation (ADCIRC) model which is a two-dimensional depth-integrated finite-element model. This model was

simulated under the influence of wind and tidal forces. The wind-field was generated for the entire computational domain using the meteorological data measured at our observational platforms in the bay whereas tidal elevation determined using the Le Provost Database was specified at the open ocean boundary. Model simulation results are then compared with the data collected from our observation system and National Oceanographic Atmospheric and Administration (NOAA)'s water level observation stations in CC Bay and onshore of the Gulf of Mexico. The model was able to successfully capture water surface elevation (WSE) variation in the station at the Gulf of Mexico although it was limited in capturing WSE variation within the bay. This limitation may be mainly attributed to omission of baroclinic forces, two-dimensional representation of water currents, and to some extent other factors such as erroneous parameterization of bottom frictional stress, assignment of a constant bottom roughness coefficient throughout the computational domain and ignorance of non-linear tidal effects, etc. Discrepancies in model-computed depth-averaged water currents with that of high frequency (HF) radar measured surface currents and observed vertical gradients in water current structure suggest that the depth-averaged model will not be able to capture detailed water current conditions of the bay. The development of a three-dimensional hydrodynamic model can help to resolve the actual water current structure of the bay. The output of this 3-D model will then provide useful information to drive various numerical models which will help to assess water quality of the bay.

Introduction

A new scientific paradigm is evolving which involves real time environmental observations and assessment. State and federal research organizations are spearheading the development of large-scale environmental assessment systems designed to facilitate environmental research. The National Science Foundation's Biological, Geoscience and Engineering directorates have taken the lead with the development of their respective programs (NEON- National Ecological Observatory Network, ORION-Ocean Research Interactive Observatory Networks, CUAHSI-Consortium of Universities for the Advancement of Hydrologic Science, Inc., CLEANER- Collaborative Large-scale Engineering Analysis Network for Environmental Research and WATERS- Water and Environmental Research Systems network). The National Oceanic and Atmospheric Administration (NOAA) also developed a coastal monitoring system, Integrated Ocean Observation System (IOOS). Among the environmental observation and forecasting systems currently developed in the United States, the Physical Oceanographic Real-Time System (PORTS) maintained by NOAA, and CORIE (Baptista et. al. 1999) are mentionable. These systems are used for various purposes like navigation safety, tsunami warning, hydropower management, habitat restoration and coastal marine resources protection, etc. With the support of both state and federal funding, our research group implemented the Coastal Margin Observation and Assessment System (CMOAS). The CMOAS is conceptualized as an environmental observatory that will supply surface current maps, vertical profiles of currents, meteorological observations and other real-time chemical and biological measurements within the water column. These

measurements can be integrated with model predictions for immediate use in coastal monitoring. This will facilitate oil spill response, natural resources recovery, and a host of applications for state and federal agencies. Corpus Christi (CC) Bay (TX, USA) is used as our test bed for the implementation of CMOAS.

The key information that needs to be measured and assessed by CMOAS is hydrodynamic condition (water current and surface elevation) of the bay which gives an indirect indication of the quality of the ecosystem. It has significant influence on the extent and duration of various environmental phenomena and anthropogenic events like sediment re-suspension, hypoxia, harmful algal blooms, contaminant spills (e.g., oil spills), advection and dispersion of various contaminants, nutrients etc. in the bay. Water currents can be measured by mooring a current meter (e.g., Acoustic Doppler Velocimeter (ADV), Acoustic Doppler Current Profiler (ADCP)) in the water or by tracking floating objects (Ojo et al. 2006 & Shenoi et al. 1999). However, these sensors cannot capture the dynamics of the bay at both greater spatial and temporal resolution. High frequency (HF) radar systems measure surface currents at greater spatial and temporal resolution through the analysis of return signals from the ocean surface (Barrick et al. 1977). The accuracy of this instrumentation in measuring surface currents has been explored by many researchers, and has been concluded that it measures the surface current within an acceptable range of error (Chapman, Shay et al. 1997; Graber, Haus et al. 1997; Kelly 2003; Mau, Wang et al. 2007). The real time measurement capabilities of this system establish it as an essential tool for the coastal ocean observation system in this decade (Kelly 2002; Ojo 2002; Liu, Weisberg et al. 2007; Breivik and Saetra 2001;

Coulliette, Lekien et al. 2007). In spite of its greater spatial and temporal coverage, this system is not able to capture the vertical water current structure and may provide no/erroneous information under certain conditions such as calm weather, ship movement in the bay, etc. (Aguilar et al. 2003 & Ojo et al. 2007b). As CC Bay is a wind-driven bay, there are several times in the year when wind conditions are low and the bay remains calm. During those periods, there are significant gaps in the surface current maps. Also if there exists a significant gradient in the vertical water current structure, it may dramatically change the water column condition of the bay. Therefore, it is necessary to develop a numerical model that can capture the hydrodynamic condition of the bay at greater spatial and temporal resolution. Moreover, it will be cost-effective compared to the efforts and instrumentation involved in measuring the sparse water current data sets. This model will also serve as a necessary and complementary tool of the observation system through its prediction of important hydrodynamic information to decision makers in the case of emergency events like oil spills, storm surges, and contaminant releases (Westerink et al. 2008 & Chen et al. 2007). Breivik and Saetra (2001) have assimilated observed currents with model-computed currents to provide real time current analyses and forecasts to local vessel traffic services for monitoring the ship traffic around two oil terminals on the coast of Norway. The development of a hydrodynamic model for CC Bay will contribute significantly to explore and understand the hydrodynamic conditions of the bay and to achieve our implementation of CMOAS to better understand episodic events in this bay.

The hydrodynamic model computes water current and surface elevation through the solution of the conservation of mass and momentum equation. The accuracy of the model-computed output depends on various factors such as boundary conditions, initial conditions, bathymetric information, tidal and wind forces, turbulence closure scheme, bottom frictional stress, numerical dispersion and stability. The uncertainty associated with these factors may significantly affect model output. Also, the complexity in developing a model increases geometrically with the order of computational domain. Although higher-order models may capture the fine scale physical processes well, they may provide erroneous results if the aforementioned factors are not assigned properly. Moreover, determination of these factors is more difficult, expensive and challenging for higher-order models. Therefore, the numerical model which represents hydrodynamic processes within the domain of interest and involves less computational time and complexity is a suitable candidate for the choice. Two-dimensional depth integrated hydrodynamic model has been long used for predicting the hydrodynamic conditions which are used in various policy making decisions such as allocation of total maximum daily load for the watershed management, setting the maximum nutrient level of wastewater discharge and guidelines to maintain the water quality of aquatic systems, etc. The determination of the reliability of 2-D model output through comparisons with observations sheds light on the limitations of a 2-D model (if any) in predicting reliable hydrodynamic information and thereby, assists in making sound judgment in setting environmental policy.

Pandoe and Edge (2008) have successfully captured water surface elevation variation of Matagorda Bay (TX) through the development of a hydrodynamic model using a depth-integrated two-dimensional numerical model. They ignored the baroclinic terms since Matagorda Bay is a shallow wind-driven bay and so water density is considered uniform throughout the water column. CC Bay and Matagorda Bay share some similar features like shallow bathymetry with a deep ship channel, enclosed and connected with the Gulf of Mexico through narrow inlets, and are wind-driven. Therefore, the processes that control hydrodynamic conditions of CC Bay may be represented using a 2-D depth-integrated hydrodynamic model. But one significant difference in terms of hydrodynamic conditions in CC Bay is the inflow of highly saline water from two neighboring shallow water bodies (Oso Bay and Upper Laguna Madre) that may induce vertical density gradients within the water column (Hodges & Furnans 2007). This may change the circulation pattern of the bay. Therefore, the development of a 2D hydrodynamic model of CC Bay, assuming a barotropic condition, provides an opportunity to determine the limitation of the two-dimensional model in capturing the dynamics involved from the movement of highly saline water from the neighboring water-bodies. Also, water quality and hydrodynamic data measured by our real-time monitoring systems can provide additional insight into the hydrodynamic condition of the bay (Islam et al. 2009a, Islam et al. 2006a & Islam et al. 2009b). Moreover, this information will be useful to explore the necessity of the development of a higher-order complex numerical model against a depth-integrated 2-D model for capturing details of the water current structure of the bay.

The model-computed hydrodynamic information is compared with observed data to quantify the error associated with model predictions. Various efforts have been conducted previously on the comparison and verification of the model with the observed data (Baptista et al. 2005; Sankaranarayanan et al. 2003 & Cuiger & Hir 2002). However, most of them compared model-predicted WSE and water current values with observed values at a fixed location. These comparisons are difficult to interpret because the model determines the average currents and WSE over a larger spatial domain whereas current meter observations, water level measurements represent fixed-length temporal averages at a single point in the water column. The dynamics of ocean currents with motions on a variety of spatial and temporal scales will further accentuate these differences between model-predicted values and measured data. HF radar, which maps surface currents, can be used to validate the model as both capture currents at greater spatial and temporal resolution. Mau et al. (2007) compared the model-predicted tidal velocity ellipses with that determined from HF radar surface current maps. To our knowledge, there are no previous studies to date that quantify the error associated with model-predicted currents through comparison with HF-radar-measured currents for wind-driven bays. Although HF radar measures average surface currents for the upper one meter-depth of the water column, these currents may represent depth-integrated current patterns if the bay is shallow and uniformly mixed in the vertical direction and the circulation pattern is controlled by barotropic forces. This comparison will shed light on the error associated with the model due to the omission of baroclinic forces and the contribution of highly saline water from two neighboring water bodies on the bay

circulation patterns. In addition, measured vertical current profiles and water quality parameter variation along our research cruise transect routes will help to test the validity of the main assumption of our 2-D model, i.e., vertically well-mixed water column.

This chapter contains details regarding the development of the two-dimensional depth-integrated hydrodynamic model of CC Bay. Data collected from our CMOAS observational system and from NOAA's water level observation stations in CC Bay and the Gulf of Mexico are used to investigate the reliability of the developed model to capture the hydrodynamic conditions of the bay. As such, the research objectives are:

- to develop a two-dimensional depth-integrated hydrodynamic model for CC Bay, and
- to verify the reliability of the model using observational data.

The specific datasets used to investigate model reliability include water surface elevation data from the nearby NOAA stations (predicted from tidal forces only as well as observed), wind speed and wind direction data from a CMOAS monitoring station in the bay, surface current measurements from CMOAS HF radar stations, as well as water current data and salinity data from two CMOAS research cruises.

Study Area

Corpus Christi (CC) Bay is located on the Texas coastline and covers an area of approximately 432.9 sq. km (Flint, 1985). It is a shallow bay with an average depth of 3.6m (Ward, 1997) (Figure 5.1). It is connected with the Gulf of Mexico through a narrow ship channel of 15 m deep (which runs from east to west) and an intra-coastal

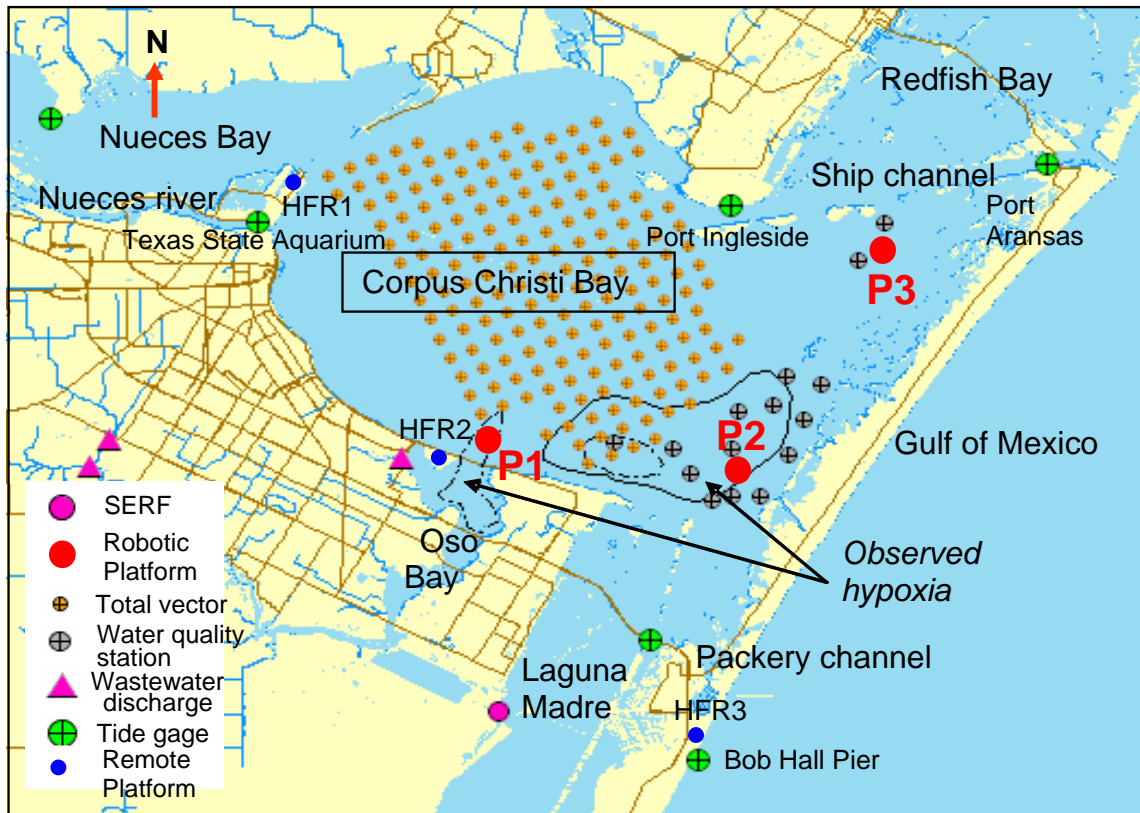


Fig. 5.1 Site description of study area in Corpus Christi Bay.

waterway (which runs north to south). Four embayments are connected with CC Bay: Oso Bay from the southwest, Nueces Bay from the northwest, Upper Laguna Madre from the south and Redfish Bay from the northeast. CC Bay is mainly wind-driven; south-easterly winds dominate throughout the year although northerly winds occur periodically during the winter months. The location of our base research facility (Shoreline Environmental Research Facility, SERF) is denoted as solid magenta circle in the figure; several wastewater discharge facilities around CC Bay are denoted by magenta-colored triangles. The cross-hatched circles represent locations where hypoxia has been reported (Ritter and Montagna 1999; Hodges and Furnas (manuscript submitted

to Environmental Fluid Mechanics, in review)). The wastewater discharge locations and observed hypoxic areas are shown here to indicate the areas of interest for collecting other important information and data, but are not used in this paper. Specific information on the CMOAS monitoring platforms and the NOAA stations is provided in the Materials and Methods section.

Numerical Model and Governing Equations

Various numerical models are available which can be used to develop a hydrodynamic model in the scale of river to ocean. Among them, POM (Blumberg & Mellor 1987), ADCIRC (Luettich et al.1991), ELCIRC (Zhang et al. 2004 & Baptista et al. 2005), ROMS (Haidvogel et al. 2000), SEOM (Iskandarani et al. 2003) and QUODDY (Lynch, et al. 1996) are popular ones. These models vary in their choice of numerical schemes, inclusion of baroclinic terms, turbulence closure schemes, grid structure, representation of boundary conditions and forcing functions, stretched or unstretched vertical co-ordinate system and level of complexities (2D/3D), etc. The numerical model that can capture the dominant physical processes controlling the hydrodynamics of the domain of interest is most desirable; the numerical model used in this study for the development of a hydrodynamic model of CC Bay is the ADvanced CIRCulation (ADCIRC) model. It is a two-dimensional depth-integrated finite-element model that solves the conservation laws for mass and momentum through a Generalized Wave Continuity Equation (GWCE) in non-conservative form. GWCE is derived by combining the time derivative form of the continuity equation with the spatial gradient of

the momentum equation and the details have been described by Luetlich et al.(1991). GWCE helps to avoid spurious oscillation associated with the galerkine finite element formulation of the governing equation. The computational domain of ADCIRC model is represented through the unstructured grid which helps to better capture the details of the coastline and topographical features (Blain et al. 2002). This feature is extremely important for capturing the hydrodynamic characteristics of CC Bay which has an irregular coastline boundary and sudden slope in topography near the ship channel. The computational costs are also reduced as the grid resolution is fine in the area of highly variable hydrodynamic conditions whereas it is moderate or coarse in other areas. This model has been used extensively in predicting tide and storm surges in coastal waters (Blain et al. 1994; Westerink 1994; Luetlich 1999) and has a good algorithm for controlling wet and dry conditions of the coastal areas.

The ADCIRC model solves the shallow water equations subject to incompressibility and hydrostatic pressure approximation on an unstructured grid. Neglecting the lateral mixing and baroclinic terms, the following set of governing equations expressed in spherical coordinates in a primitive non-conservative form are used in the model (Kolar et al. 1994):

$$\frac{\partial \zeta}{\partial t} + \frac{1}{R \cos \phi} \left[\frac{\partial UH}{\partial \lambda} + \frac{\partial (UV \cos \phi)}{\partial \phi} \right] = 0 \quad (5.1)$$

$$\frac{\partial U}{\partial t} + \frac{U}{R \cos \phi} \frac{\partial U}{\partial \lambda} + \frac{V}{R} \frac{\partial U}{\partial \phi} - \left[\frac{\tan \phi}{R} U + f \right] V = -\frac{1}{R \cos \phi} \frac{\partial}{\partial \lambda} \left[\frac{p_s}{\rho_0} + g(\zeta - \eta) \right] + \frac{\tau_{s\lambda}}{\rho_0 H} - \tau_* U \quad (5.2)$$

$$\frac{\partial V}{\partial t} + \frac{U}{R \cos \phi} \frac{\partial V}{\partial \lambda} + \frac{V}{R} \frac{\partial V}{\partial \phi} - \left[\frac{\tan \phi}{R} U + f \right] U = -\frac{1}{R \cos \phi} \frac{\partial}{\partial \phi} \left[\frac{p_s}{\rho_0} + g(\zeta - \eta) \right] + \frac{\tau_{s\phi}}{\rho_0 H} - \tau_* V \quad (5.3)$$

Where, λ , ϕ are the degrees longitude and latitude respectively, ζ = free surface elevation relative to geoid, U , V = depth-averaged horizontal velocities, p_s = atmospheric pressure at free surface, H = total water column thickness, f = Coriolis parameter, R = radius of the earth, t = time, g = gravity and η = effective Newtonian equilibrium tidal potential. $\tau_{s\lambda}$, $\tau_{s\phi}$ are the applied free surface stresses whereas bottom shear stress, τ^* is given by the following expression:

$$\tau^* = \frac{C_f (U^2 + V^2)^{1/2}}{H} \quad (5.4)$$

where C_f is bottom friction coefficient. This model computes water surface elevation (WSE), depth-averaged velocities through the solution of GWCE and Equations 5.2~5.3.

Model Development

The schematic diagram of the model development is shown in Figure 5.2. Surface-water Modeling System (SMS) software is used to generate the grid and to control ADCIRC model simulation. Finite element grid originally developed by the Scheffner et al. (2003) is modified in the areas of interest with details added using the software. The coastline dataset for this model has been obtained from the GEOPhysical DATA System (GEODAS) and National Oceanic Atmospheric and Administration (NOAA) databases, and they were smoothed before use in the grid generation. Bathymetric data were collected from the grid developed by Scheffner et al. (2003), GEODAS, United States Army Corps of Engineers (USACE) survey, Texas A&M

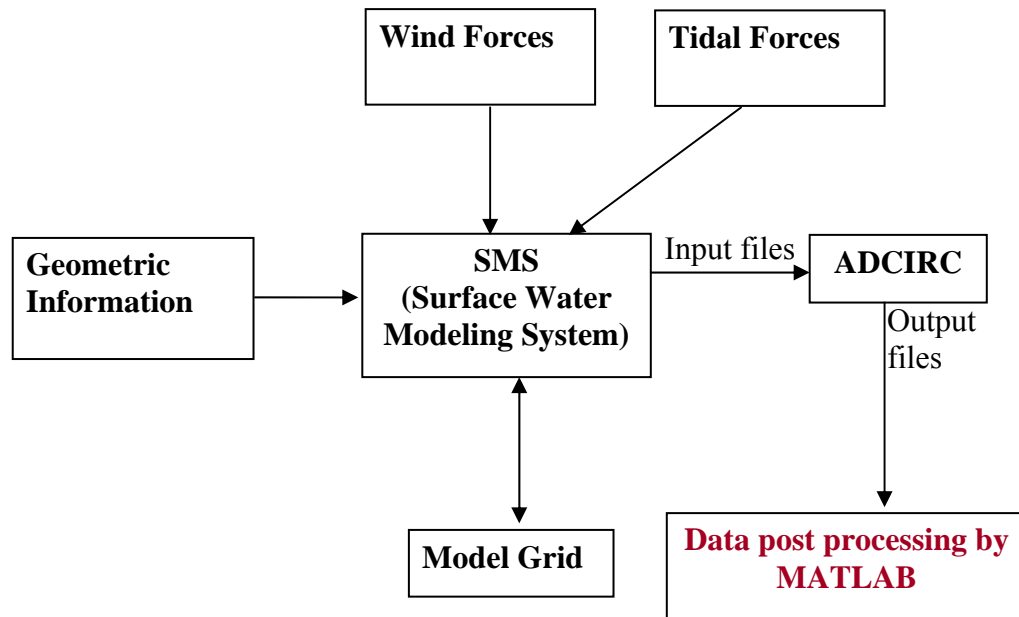


Fig. 5.2 Schematic diagram of model development.

University survey of the area of interest and the USGS terrain data. Boundary conditions were assigned into the model through the SMS graphical interface. Three types of boundary were considered in the model development: mainland boundary, island boundary and elevation-specified tidal boundary at the open ocean. These boundaries are shown in Figure 5.3, which describe the computational domain of our model. It includes part of the Gulf of Mexico, Baffin Bay and Copano Bay along with our study area of CC Bay and its neighboring water-bodies. The grid consists of 8,887 triangular elements with 5,354 nodes. The model was simulated under tidal and wind forces, and a hyperbolic tangent ramp function was applied to both boundary and direct forcing functions over a period of two days. The optimal time step for the simulation of the model was found to be six seconds considering the Courant Number criteria.

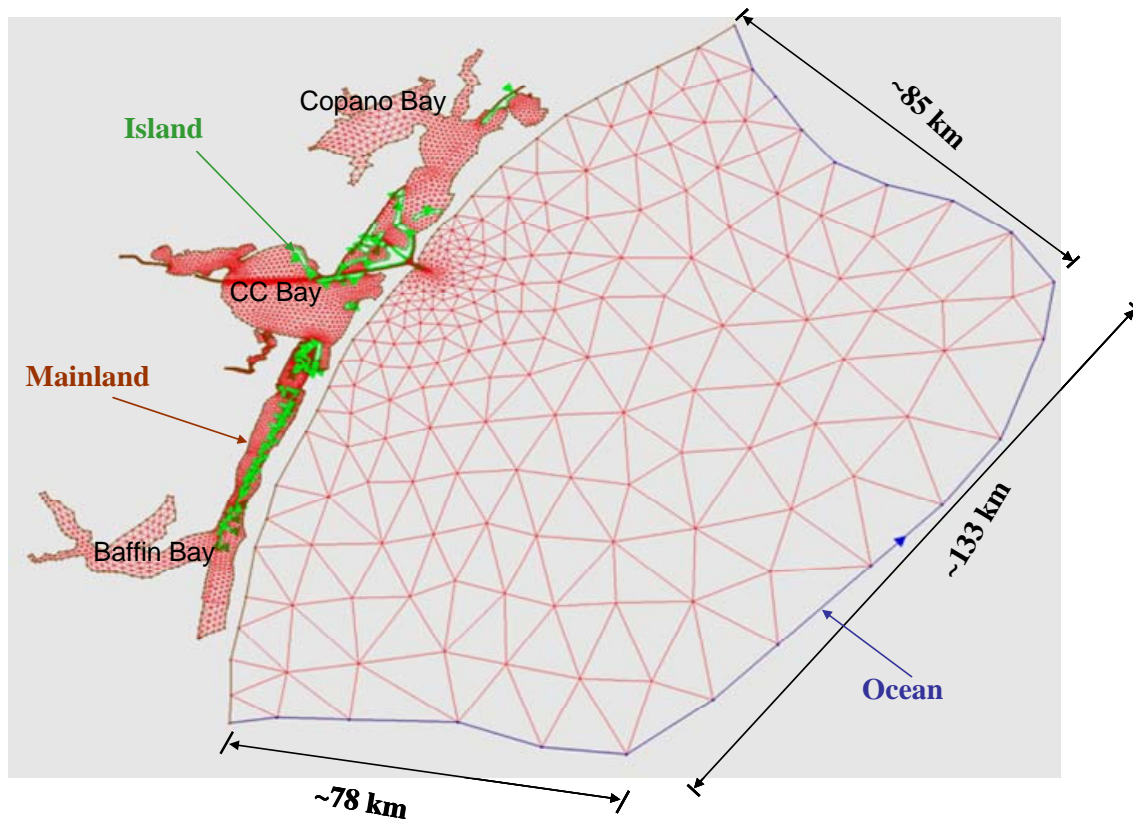


Fig. 5.3 Computational domain of the developed hydrodynamic model.

Model Forcing Functions

Water circulation of CC Bay was studied for the effect of atmospheric and tidal forces. The river discharge into CC Bay is very small and so was neglected in the model simulation (Ritter et al. 2005). Meteorological sensors (Wind Monitor-MA instruments by R.M. Young Company) installed at each CMOAS monitoring station in the bay collect atmospheric and wind information at two-minute intervals. This data is used to generate a wind field for the entire computational domain. Wind stress was calculated from the measured wind data by using the following formula:

$$\tau_{s\lambda} = C_D * 0.001293 * |W| * W_\lambda \quad \text{and}$$

$$\tau_{s\phi} = C_D * 0.001293 * |W| * W_\phi$$

where, $\tau_{s\lambda}$ and $\tau_{s\phi}$ are the surface wind stresses in λ and ϕ direction respectively. W is the magnitude of wind velocity and W_λ , W_ϕ are the components of wind velocity in λ , ϕ directions, respectively; C_D is the drag coefficient. Tidal elevation was specified at the open ocean boundary by generating tidal time series based on the main eight harmonics of tidal constituents which comprise most of the tidal energy (Aggarwal 2004). These constituents are M_2 , S_2 , N_2 , K_2 , K_1 , O_1 , P_1 and Q_1 . The amplitude, frequency and other parameters of tidal potential constituents were determined using the Le Provost Database (Westerink et al. 1993) incorporated in the SMS. Based on finite element hydrodynamic modeling, this database has been developed to help the scientific community in predicting the sea surface variation due to tidal effects. Additionally, tidal potential terms are specified at each node of the computational grid.

Materials and Methods

Hydrodynamic, meteorological and water quality data collected from our CMOAS observation system can help to evaluate the reliability of the developed numerical model in characterizing the key processes that control the hydrodynamics of the bay. This information also provides guidance in selecting the criteria of a suitable numerical model that captures the detail of the hydrodynamic condition of CC Bay. CMOAS consists of three types of monitoring platforms: a) Fixed Robotic, b) Remote and c) Mobile.

The locations of the three CMOAS fixed robotic monitoring platforms in CC Bay are depicted in Figure 5.1 as red solid circles. The platform 'P1' ($27^{\circ}43.531'N$, $97^{\circ}18.412'W$) is positioned 100m from the mouth of Oso Bay to characterize the effects of Oso Bay inflow, which has been reported to trigger hypoxia in that part of the bay. Platform 'P2' ($27^{\circ}43.375' N$, $97^{\circ}11.403'W$) is located in the south-east portion of the bay where hypoxia has been documented since 1988 (Montagna & Kalke 1992). The ship channel effects on CC Bay can be monitored by Platform 'P3' ($27^{\circ}48.560' N$, $97^{\circ}08.513' W$) platform in the north-east part of the bay. Various instruments populate these platforms to measure water quality, hydrodynamic, and meteorological conditions; details are described in Islam et al. (2009a). The meteorological sensors installed on each of these platforms were used to develop wind field that drove the developed hydrodynamic model. The nearest-neighbor interpolation scheme was used in generating the wind field for our computational domain. As wind forces have normally low spatial gradients, this scheme may be a reasonable approximation for our model.

Two 25-MHz HF radar units installed on CMOAS remote platforms generate hourly surface current maps of CC Bay. The locations of these two sites (HFR1 and HFR2) are depicted in Figure 5.1; one is installed near the ship channel bridge (HFR1, 27.831600 N, 97.379733 W) while the other is located near Texas A& M University Corpus Christi (HFR2, 27.713783 N, 97.320467 W). The HF-radar system was used to generate surface current maps of CC Bay. These surface current maps are compared with model-computed depth-averaged water currents in the bay. This comparison may shed light on the vertical gradient of water currents in the bay. If the gradient is negligible, these two parameters will agree each other.

On the CMOAS mobile platform (i.e., research vessel), we installed four water quality measuring sensors, namely a particle sizer (LISST 100X, by Sequoia Sciences), a DO sensor (Optode, by Aanderaa), a CTD (Conductivity, Temperature and Depth) sensor (SBE 37 SIP, by Sea-Bird Electronics, Inc.) and a fluorometer (Eco-FL3, by WETLabs) on an undulating tow body which is deployed behind the boat. This system ‘synchronously’ measures various water quality parameters over a highly-resolved spatial regime. In addition, a downward-looking bottom-tracking 1200 KHz workhorse Acoustic Doppler Current Profiler (ADCP by Teledyne RD Instruments) was installed on the mobile platform to measure water current structure. Large datasets collected from this monitoring system are post-processed with MATLAB toolboxes for use in model validation. Further details on all components of the CMOAS observation system are discussed in Islam et al. (2009a) and Islam et al. (2009b).

In addition to measured datasets from the CMOAS observational platforms, data

from water level stations in CC Bay were also used for model validation. The green solid circles on Figure 5.1 denote the location of several NOAA water level stations, which are maintained by Texas Coastal Ocean Observation Network (TCOON; Division of Nearshore Research, Conrad Blucher Institute for Surveying and Science, Texas A&M University-Corpus Christi). Data from four of the stations (ie., Bob Hall Pier, Port Aransas, Port Ingleside, and Texas State Aquarium) were used in the model verification.

Results and Discussions

The model skill assessment for the prediction of water surface elevation (WSE) is considered as the primary step for the determination of model accuracy. The forces that significantly control water surface variation are tidal forces, wind forces and river discharges. The contribution of tidal forces in changing the WSE at a point can be determined through the harmonic analysis of observed time series data. The calculated characteristic features (amplitude and phase) of various harmonic constituents can then be used to determine tidal variation at that point. NOAA's Center for Operational Oceanographic Products and Services (CO-OPS) publishes tidal water levels at various TCOON stations through the analysis of observed water levels (CO-OPS 2009). The comparison of ADCIRC model-computed tides with the NOAA's observed tides at these stations will help to understand model performance in simulating tidal circulation. Presented in this chapter are two sets of model simulation results with comparative NOAA data. The first set consists of the model results for the simulation time period from May 11, 2007 to June 10, 2007, whereas

the second set of results from July 7, 2007 to August 10, 2007. In both of these simulations, two days of spin up time were used to reproduce the tide acceptably.

Model-predicted Tides vs. Observed Tides

Figure 5.4 show comparisons of our model-predicted tides with that of NOAA's observations at four different stations in CC Bay and the onshore of the Gulf of Mexico for the time period of May 13 to June 10. The blue line in Figure 5.4(a) represents model-predicted tidal levels whereas the red line denotes the observed tidal levels at Bob Hall Pier station (onshore station in the Gulf of Mexico). It is clear from this figure that the model was able to successfully capture the tidal variation at this station. Tidal range in this station varied from 0.9m during the spring tide to 0.2m during the neap tide. The comparison of tidal elevations at the Port Aransas station (Figure 5.4(b)) also indicates reasonable agreement with the observed tide and the model-computed tide level. Figure 5.4(c) and Figure 5.4(d) display similar tidal comparisons for stations at Port Ingleside and Texas State Aquarium, respectively. The observed tidal ranges are much higher than the model predicted values. The error associated with various tidal model predictions in coastal areas and semi-enclosed seas are usually higher in comparison to similar predictions in the deep ocean (He et al. 2004) as such, a second model simulation was conducted to better understand the pattern of these errors, and reasons for the discrepancies are hypothesized. These hypotheses can be tested in future model development efforts for greater understanding of hydrodynamic conditions in this shallow bay.

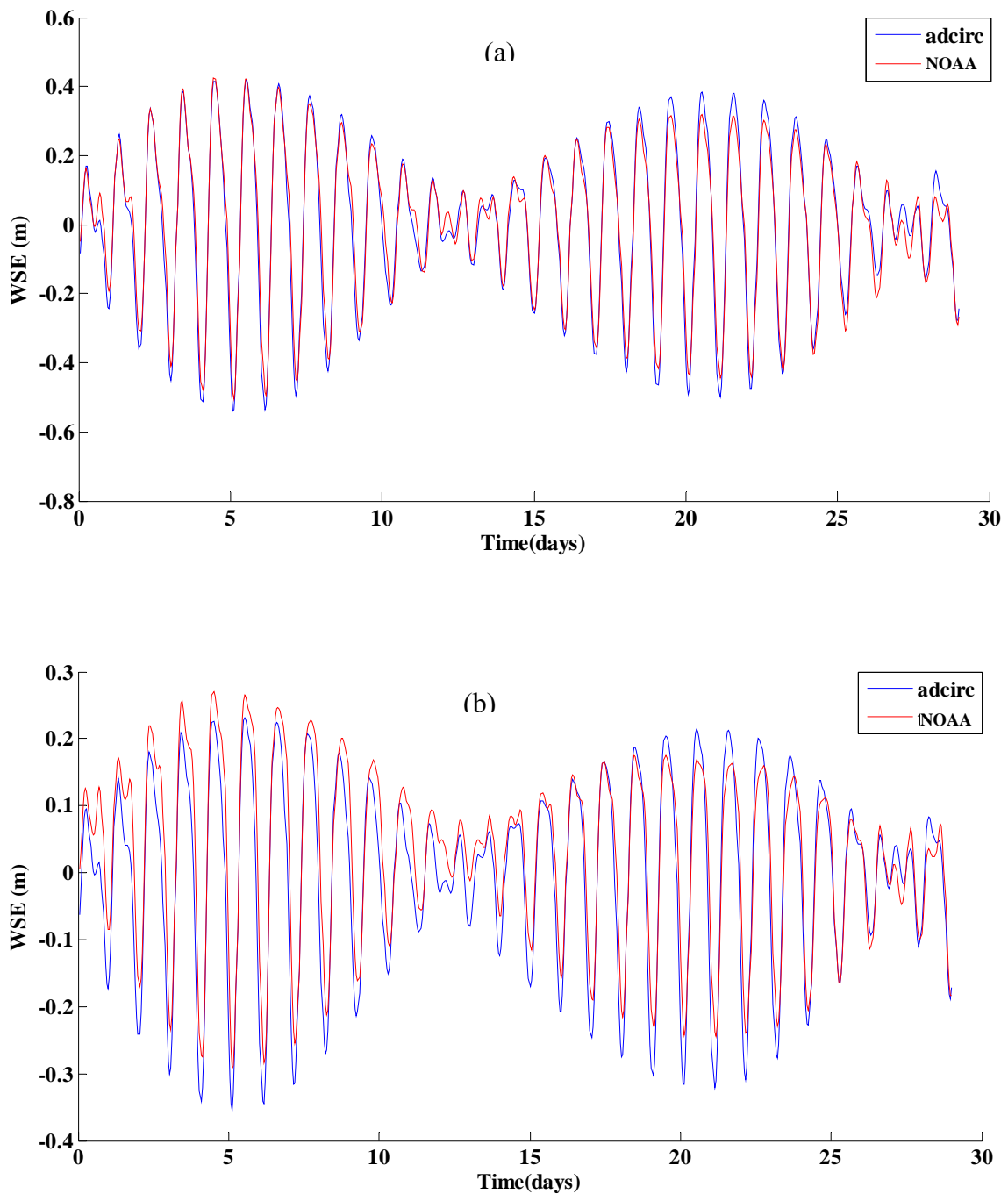


Fig. 5.4 Tidal water surface elevation from ADCIRC model results (blue line) and from NOAA's published time series (red line) at a) Bob Hall Pier, b) Port Aransas, c) Ingleside and d) Texas State Aquarium stations from May 13, 2007- June 10, 2007.

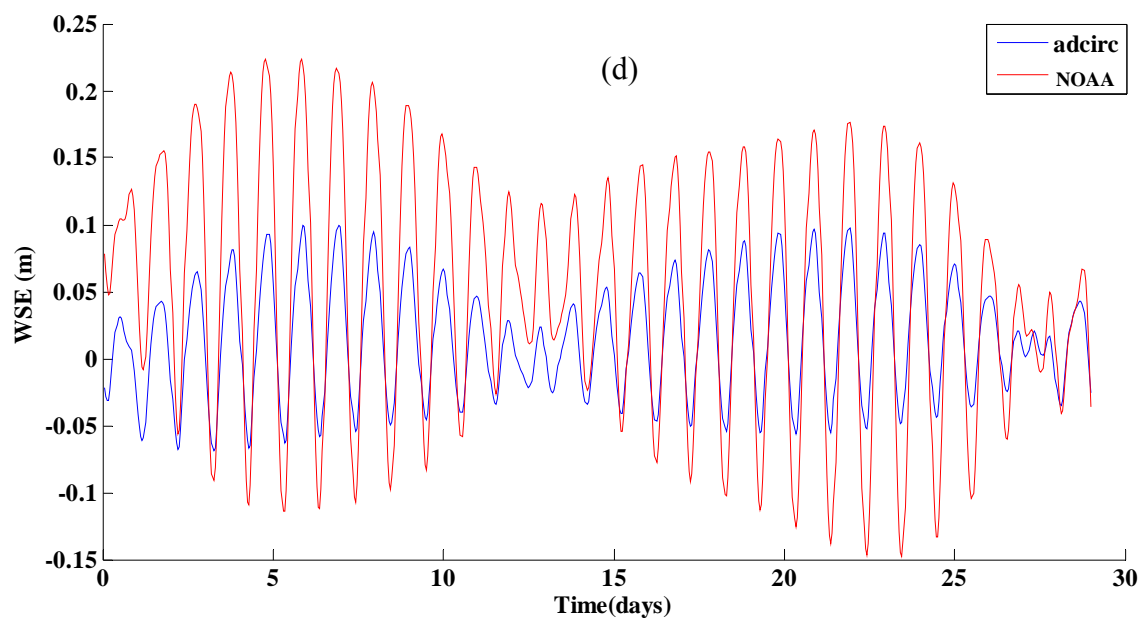
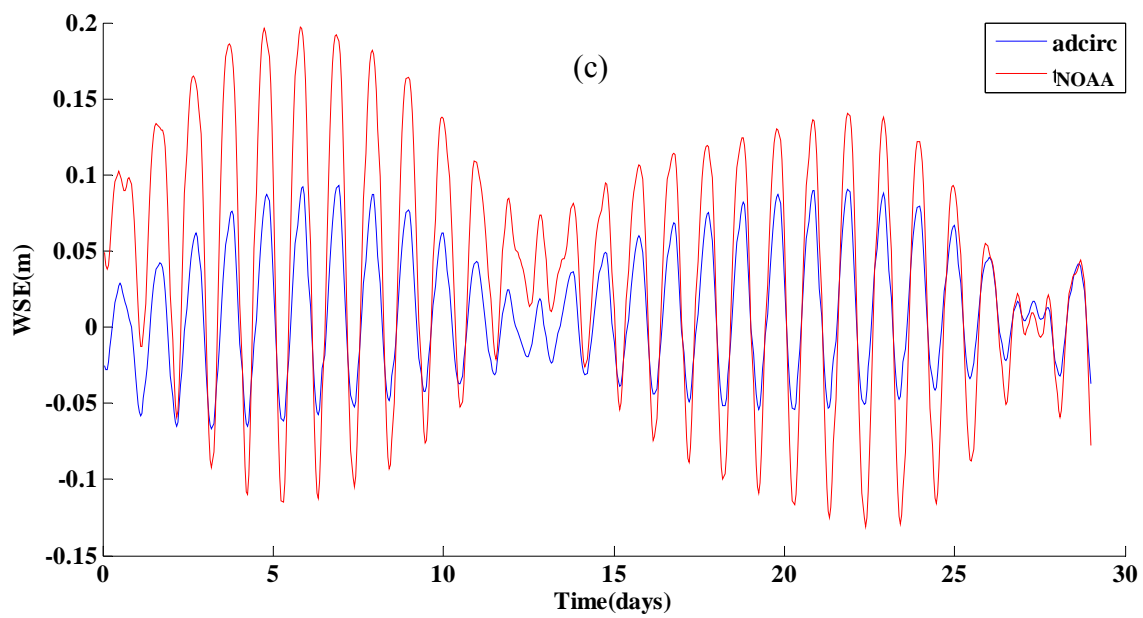


Fig. 5.4 Cont'd.

Figure 5.5 illustrates similar tidal comparisons for the time period of July 10 to August 10. The comparison of tidal elevation at Bob Hall Pier station is shown in Figure 5.5(a) whereas comparisons at Port Aransas, Ingleside and the Texas State Aquarium stations located within CC Bay are shown in Figures 5.5(b), 5.5(c), and 5.5(d), respectively. As found in the previous simulation results, ADCIRC model predictions agreed well with the observations at the Bob Hall Pier station, whereas discrepancies were more dramatic when comparing the model predictions with the data from the stations within CC Bay. Observed tidal ranges were much higher at stations Port Ingleside (Figure 5.5c) and Texas State Aquarium (Figure 5.5d) than that of the model predictions. The lower prediction of tidal ranges at both simulations suggests that model might not correctly represent all factors that influence tidal variation inside the bay. In addition, observed tidal time series may not resolve the tidal harmonic components accurately and may include some harmonic components from the wind forces.

Compound tides and overtides resulted from the nonlinear interaction between harmonic constituents may be important since nonlinear phenomena such as bottom friction, wind forces, etc are dominant in the shallow regions of the bay. These tides are commonly known as shallow water tides. A good representation of bathymetry and a high resolution computational grid are necessary to resolve these tides. These factors must be properly accounted for in future model development. The discrepancy can also be attributed to the under representation of tidal harmonic constituents. Our 2-D model only considers eight harmonic constituents whereas

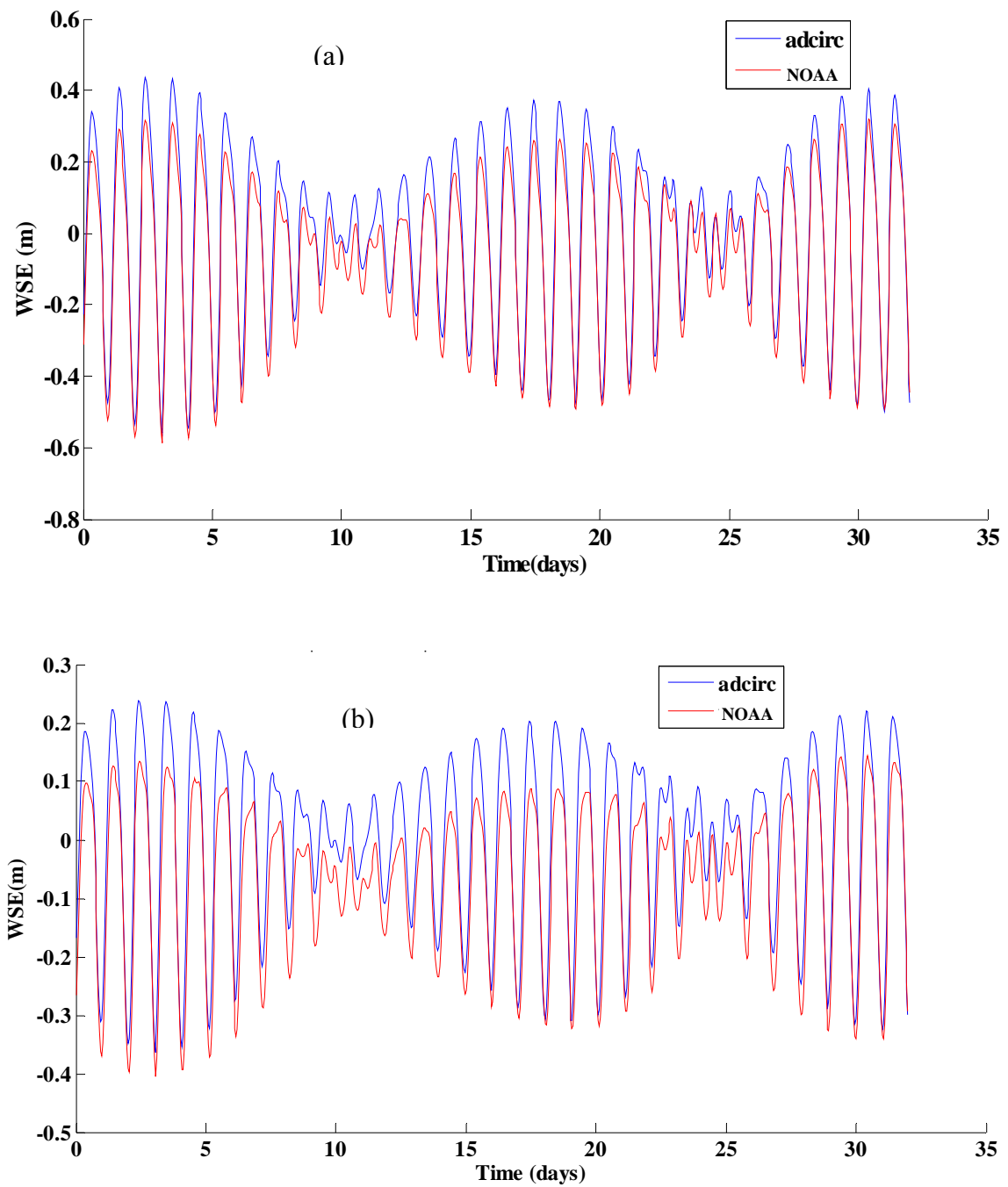


Fig. 5.5 Tidal water surface elevation from ADCIRC model results (blue line) and from NOAA's published time series (red line) at a) Bob Hall Pier, b) Port Aransas, c) Ingleside and d) Texas State Aquarium stations from July 10~August 10, 2007.

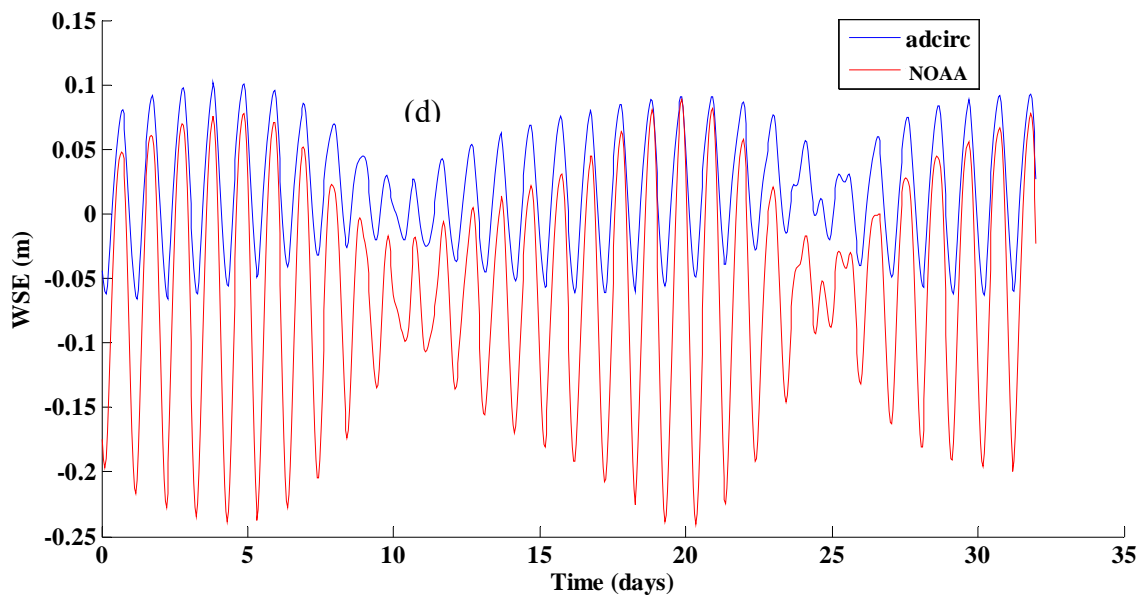
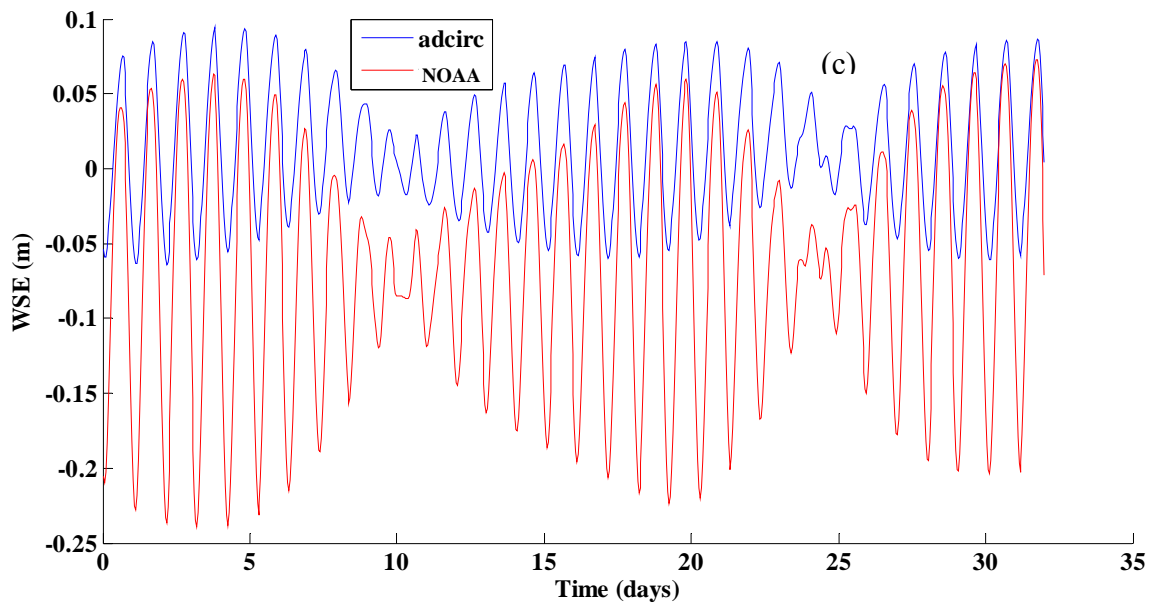


Fig. 5.5 Cont'd.

NOAA uses thirty seven constituents to establish tidal levels at each station. Also, the use of eastcoast 2001 tidal database (Mukai et al.2001) instead of LeProvost database may help to reduce error in model prediction. In addition, poor representation of bottom frictional stress may cause error into model prediction (Grenier et al. 1995). A constant bottom roughness coefficient was used throughout the computational domain of our model to generate bottom frictional stress. However, there are significant differences in the bottom topography of the bay, and so the roughness coefficient value will differ at various locations of the bay. Higher amounts of sea grass were observed at the upper Laguna Madre in compare to the rest of the bay (NOAA Coastal Services Center 2009). The presence of seagrass increases the bottom roughness and so the frictional roughness coefficient is higher at the Upper Laguna Madre compared to the rest of the bay. Therefore, it is necessary to consider a variable friction coefficient for better characterization of the hydrodynamic condition of the bay. More importantly, depth-averaged velocity was used to determine the frictional force in the two-dimensional depth-averaged model whereas bottom current velocity is actually responsible for inducing frictional stress. There exists a significant difference in velocity magnitude between bottom current and the depth average velocities if the vertical current pattern is bi-directional. The observed vertical current profile along the transect route of the cruise may illuminate the actual water current pattern in the bay. Development of a three-dimensional hydrodynamic model can resolve bottom current velocity which can be used to determine frictional forces as such, will capture the frictional effect reliably for better characterization of water surface elevation.

Observed vs. Model-predicted WSE

The hydrodynamic condition of CC Bay is expected to be highly wind-driven as it is a shallow enclosed bay. The change in WSE due to combined tidal forces and wind forces were computed in the model, and model-predicted WSE were compared to observed values at several NOAA's water level observation stations. It should be noted that there were no WSE data recorded at Port Ingleside and Texas State Aquarium stations for the simulation time period of July 10 to August 10, so WSE comparisons at these stations are presented for another simulation run (May 13 ~ June 10) when observational data were available.

The variation of observed and model predicted WSE at Bob Hall Pier and Port Aransas stations (July 10 ~ August 10) are shown in Figure 5.6(a) and 5.6(b), respectively. Model-predicted WSE agreed reasonably well for the Gulf of Mexico water level observation station (i.e., Bob Hall Pier) and the maximum difference between observed and model predicted WSE was less than 10 cm. The model also successfully captured WSE variation at the Port Aransas station for the first nine days of simulation (July 10~ July 18) although differences between observation and model prediction were significant for the rest of the simulation time period (July 19~ August 10). The comparisons of WSE and wind data may provide some insight into this discrepancy. Measured wind data at fixed robotic platform "P3", which is closest to the Port Aransas station, is shown in Figure 5.7. In this figure, the blue line denotes wind speed variation whereas the red line represents wind direction variation for the time period of July 10 ~ August 10. The higher wind activity (strong wind (7~11.5

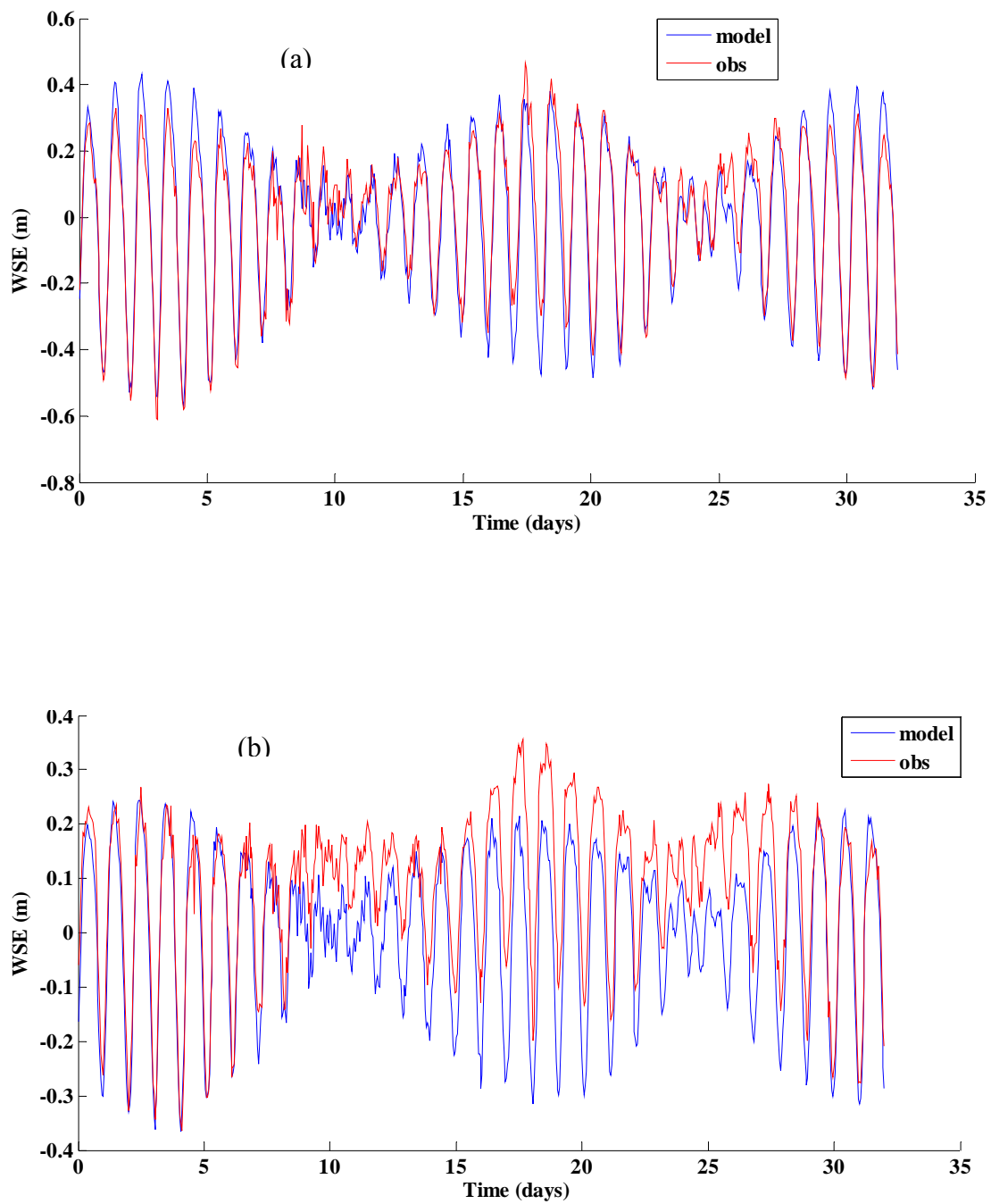


Fig. 5.6 Comparisons of observed (red line) and model predicted (blue line) WSE variation at a) Bob Hall Pier and b) Port Aransas from July 10~August 10, 2007.

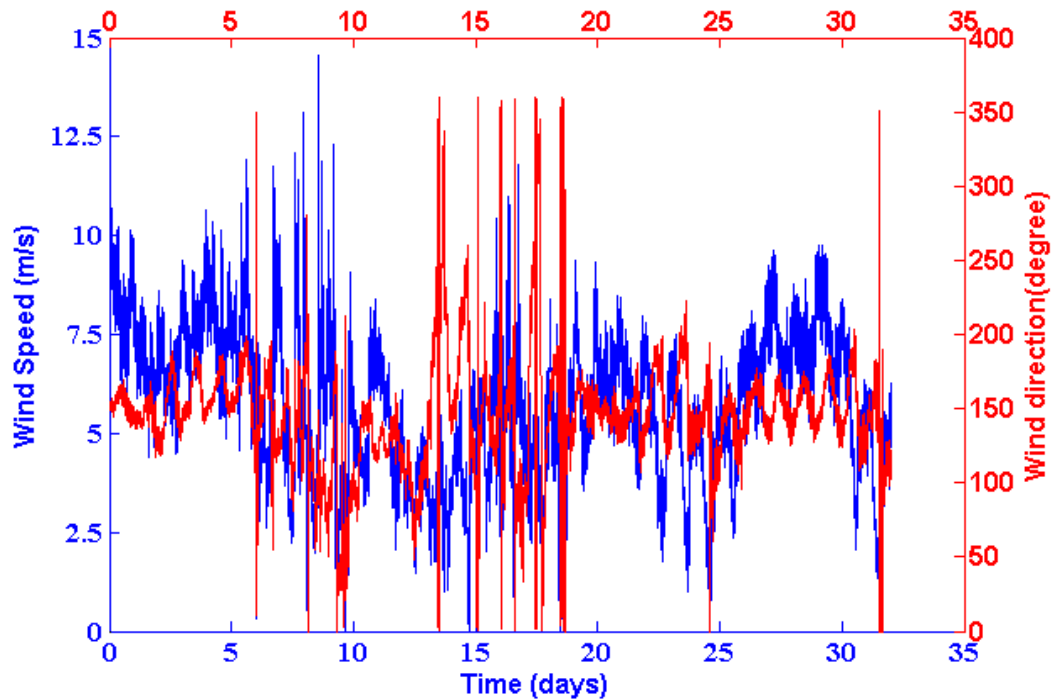


Fig. 5.7 Wind speed (blue line) and direction (red line) variation at platform “P3” from July 10~ August 10, 2007.

m/s) from south-east direction) prevailed during the earlier part of simulation (first eight days) when observations are in close agreement with the model prediction. The wind changed its course several times for the following eleven days (9~19 days) and then blew steadily from the south-east direction for the rest of the simulation time period. Although model-predicted WSE at the Port Aransas station compared well during the strong wind conditions for first eight days of simulation, this was not the case for the later part of simulation when the wind was blowing steadily. Therefore, the error associated with the model prediction may be related to other factors.

Figure 5.8(a) and 5.8(b) display model-computed and observed WSE

variation at the Port Ingleside and Texas State Aquarium stations during May 13~June 10, respectively. The observed WSE is much higher as compared to the model prediction at both stations. The larger discrepancies suggest that the model may not correctly capture all factors contributed to WSE variation in the bay. The model was simulated under the assumption of barotropic condition which might induce error if the water column was densely-stratified. In that case, the baroclinic condition must be considered in the model simulation. The inflow of highly saline water from Upper Laguna Madre and Oso Bay may induce a density gradient in the bay. The density gradient may induce gravity flow which will cause water currents to flow in opposite directions at top and bottom levels of the water column. Depth-averaged water currents then induce error in the calculation of inflow/outflow of a finite element which will impose error in the solution of WSE. The CTD sensor and ADCP installed on the mobile monitoring system can aid in understanding the vertical structure of salinity and water current pattern in the bay, and is discussed later in this paper. Moreover, unusual occurrences of high precipitation in 2007 and resulted high freshwater inflow (originated at Nueces River and Nueces bay), ignored in the model, may contribute to discrepancies between observations and model predictions. Also, as discussed previously, improper characterization of the bottom frictional stresses might introduce error in model computation of wind-induced WSE changes in the more shallow areas of the bay.

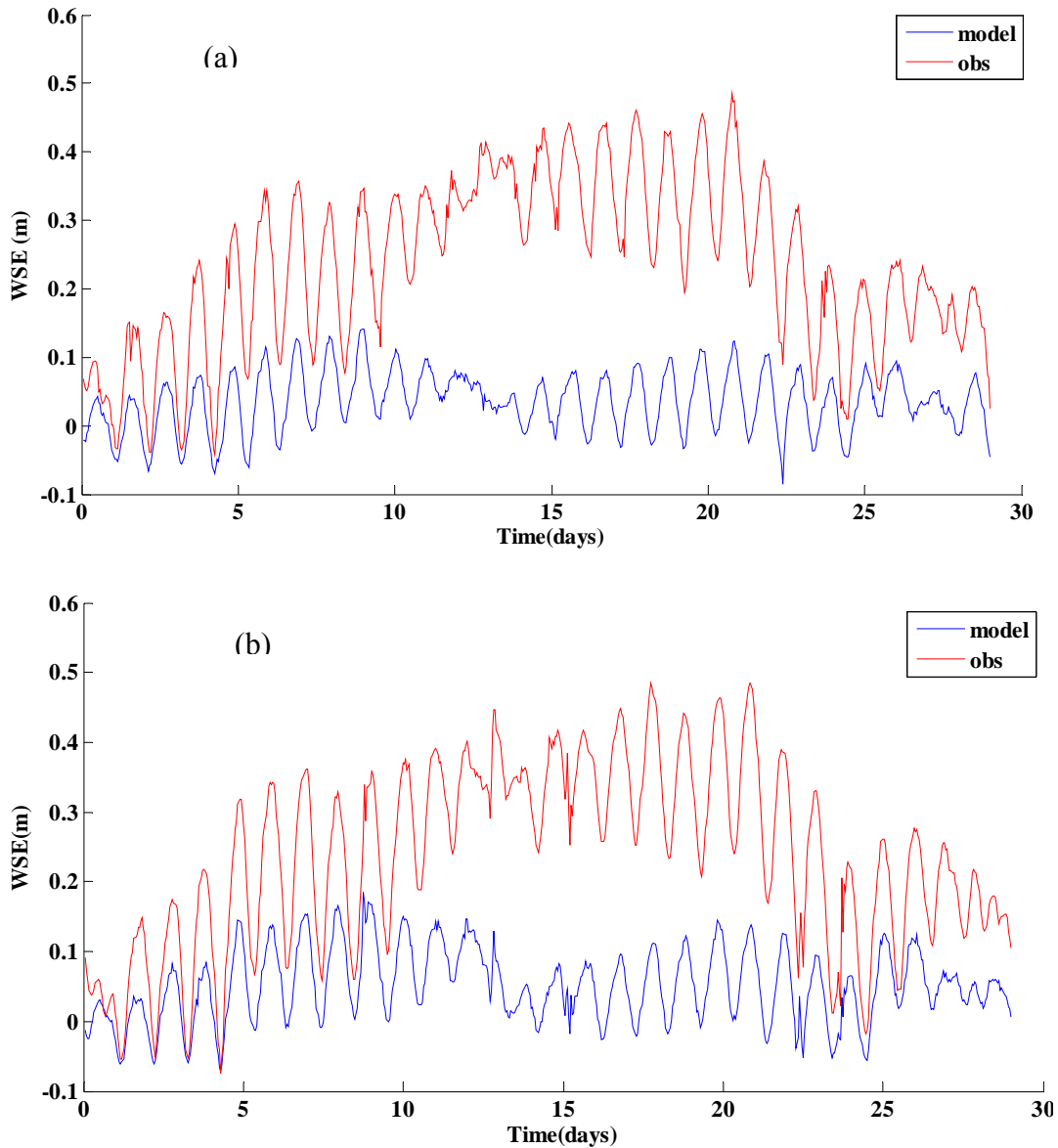


Fig. 5.8 Comparisons of observed (red line) and model predicted (blue line) WSE variation at a) Ingleside and b) Texas State Aquarium stations from May 13~June 10, 2007.

Model-computed Velocities vs Observed Velocities

Advection and dispersion coefficients can be determined from the water current structure of the bay (Ojo et al 2006). These coefficients are supplied as input parameters

to various constituent transport and water quality models developed in our laboratory (Ojo et al. 2007b; Sterling et al. 2005 & Lee et al. 2000). The successful implementation of these numerical models depends on the accurate determination of these coefficients. Therefore, model-computed water currents are compared with the observed surface current maps to understand the reliability of the 2-D hydrodynamic model in capturing water currents of the bay. Although the model computes depth-averaged water currents whereas HF-radar measures averaged surface currents for the top one meter of the water column, these two parameters will agree each other if the water column is well-mixed. Figure 5.9 compares the model-computed current velocity magnitude with HF radar measured surface currents magnitude. This figure presents the comparison as a ratio defined as the velocity magnitude difference between observation and model prediction, divided by the observed velocity magnitude (i.e. (predicted current magnitude-observed current magnitude)/observed current magnitude). Figures 5.9(a), 5.9(b), 5.9(c), 5.9(d) present the ratios for mid day on July 12, July 18, July 24 and July 30, 2007, respectively. The ratios are plotted as color coded points at different locations of observation within the bay. The red color indicates greater difference between observation and model prediction, i.e. higher error, whereas the blue color indicates the opposite. If the ratio is greater than one, it was plotted as red color. From these color plots, it is clearly visible that there exists a significant difference in velocity magnitude between observation and model prediction. The similar plots are presented on Figures 5.10(a), 5.10(b), 5.10(c), 5.10(d) for the directional differences between observed and model-predicted velocity direction at mid day of July 12, July 18, July 24 and July 30,

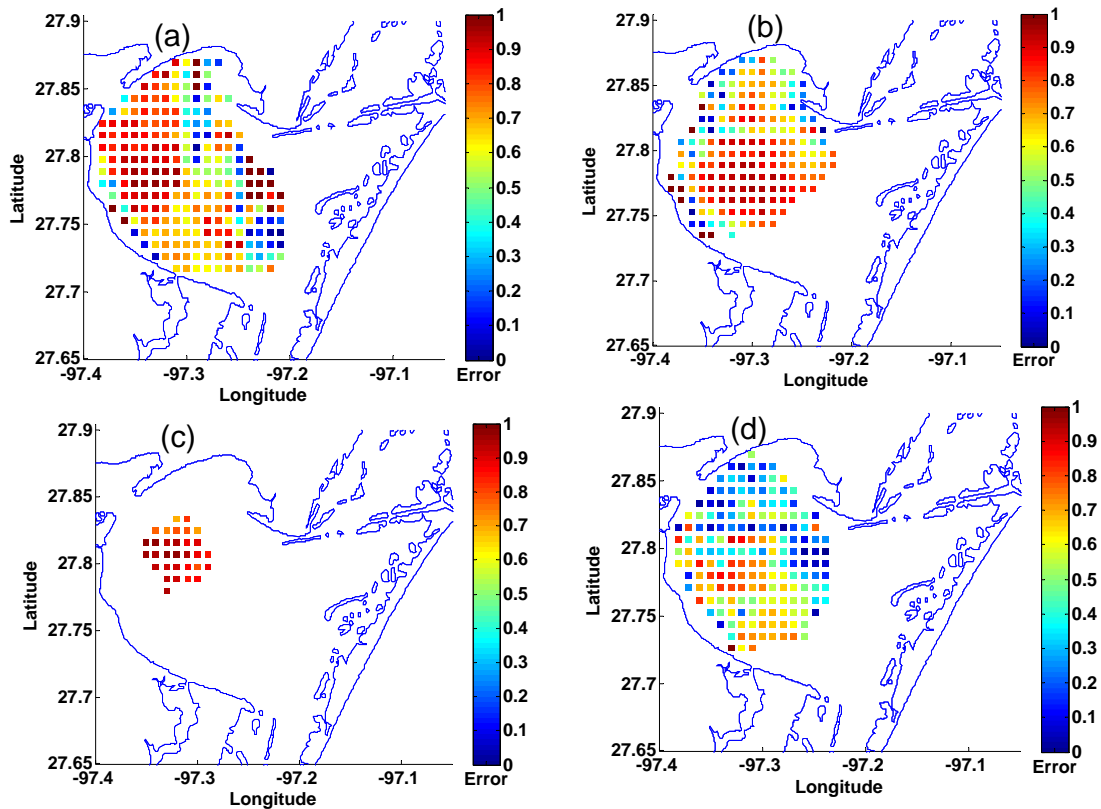


Fig. 5.9 Comparison of model-computed velocity magnitude with that of HF-radar measured surface current at mid day of July 12,2007(a), July 18,2007 (b), July 24,2007 (c) and July 30,2007(d) , respectively.

2007, respectively. These differences are shown as color coded plots in these figures.

The fewer data points in Figure 5.10(c) and 5.9(c) are due to gaps in HF-radar measurements. It is clearly visible from Figures 5.9 and 5.10 that there were significant differences between model prediction and observation. These differences suggest that the bay might not be well-mixed and a significant gradient in water current might have occurred in the vertical direction. If the water column is not vertically well-mixed, then depth averaged velocities do not represent the surface currents which are measured by our HF-radar system. The existence of a vertical current gradient reduces the depth

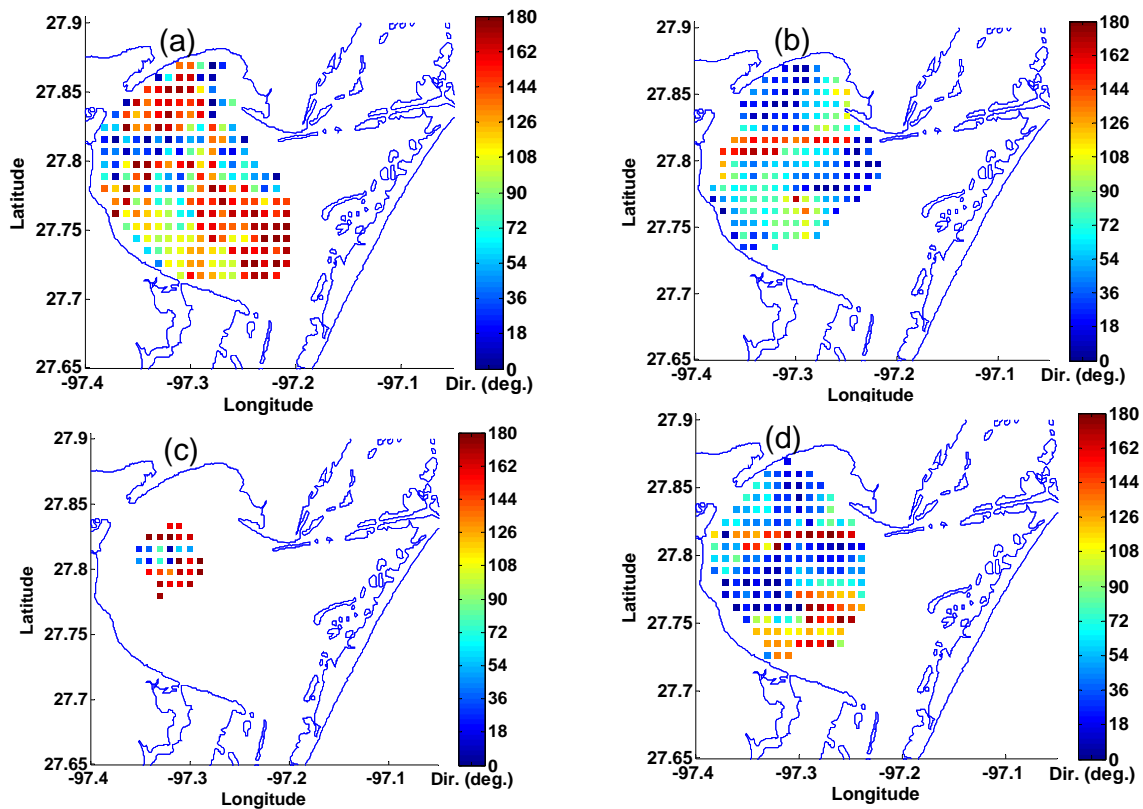


Fig. 5.10 Comparison of model-computed velocity direction with that of HF-radar measured surface current at mid day of July 12,2007(a), July 18,2007 (b), July 24,2007 (c) and July 30,2007(d) , respectively.

averaged velocities and thereby, discrepancies between model-computed velocities and observed surface currents might grow larger. The hydrodynamic and water quality parameters measured by our mobile monitoring system may provide information on vertical gradients of these parameters in the bay; these results are presented in the next section.

Results from Mobile Platform Cruises

Two cruises in CC Bay occurred during the simulation time frame of July 10~ August 10. The first cruise was made on July 24. Salinity data measured at this cruise is presented in the color-coded plot (Figure 5.11) and the transect route is depicted on the inset plot. The route line is color coded and correlates with the horizontal color-coding along the top and bottom of the figure, thus matching the observed data with the measurement location in the bay. The two red rectangular boxes shown in the figure represent the time period during this cruise when we had to pull our instruments onto the boat deck and stops collecting data. These data gaps are evident in the figure. The first data gap ($t \approx 5800\sim 7500$ sec) occurred during the interval of the end of first transect and the beginning of second transect. The second data gap ($t \approx 12500\sim 13000$ sec) occurred when we crossed the ship channel; tow-body is not capable of undulating in a sharp seabed gradient. The water column was more saline at all depths at the beginning of our research cruise near the Upper Laguna Madre. As we headed towards the bay, we found salinity-stratified water column i.e., fresh water overlaying highly saline water. The observed distinct longitudinal and vertical salinity gradient in the bay suggests that the exclusion of baroclinic terms in the model might induce significant error in model predictions. The vertical profile of the water current along the cruise route might shed light on the limitation of the depth-averaged model in accurately predicting water currents in CC Bay. Unfortunately, current profiles measured by the ADCP on the boat were unreliable due to high travelling speeds. A higher speed was necessary (~ 6 knots) to keep the tow-body undulating in the water column during the calm bay conditions on

that day. Therefore, the ADCP data cannot be used to infer water current structure along the travel route. Also calm bay conditions justify the significant gaps in HF-radar measured surface current maps as obvious in Figures 5.9 (c) and 5.10 (c). Under this condition, uniform mixing of density-stratified water column is not expected. This is

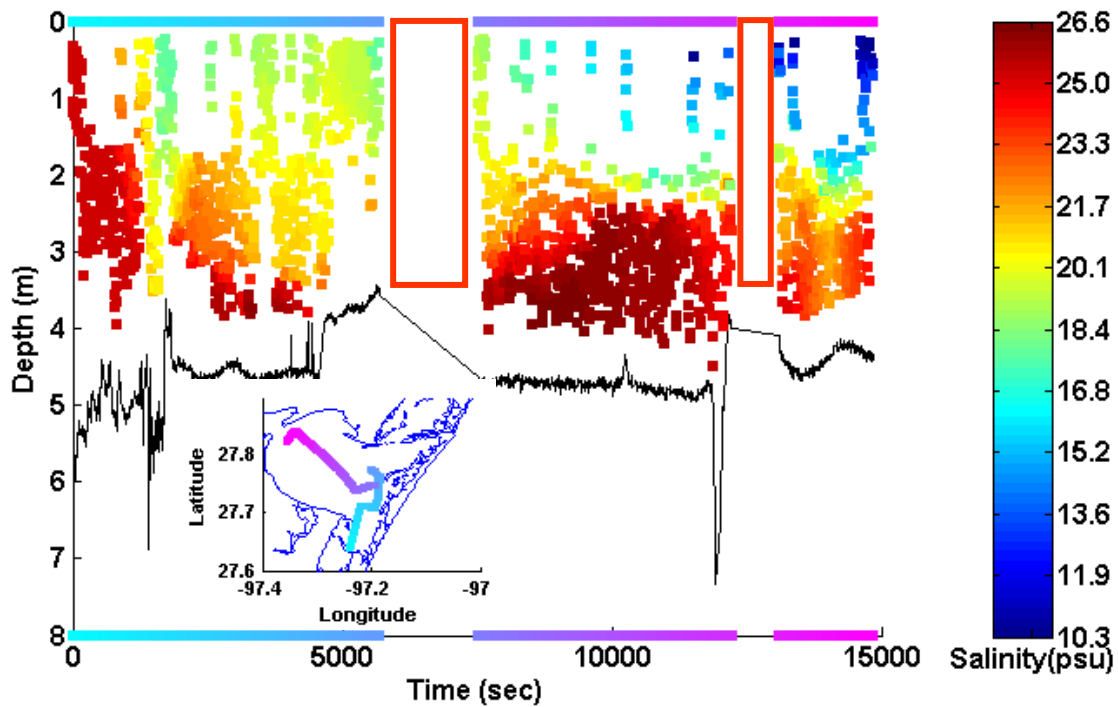


Fig. 5.11 Salinity variation along the transect route for the cruise made on July 24, 2007.

further speculated from the significant difference in model predictions and observations as shown in Figures 5.9 (c) and 5.10 (c) in all of the bay areas except in the ship channel. This substantiates the limitation of depth-integrated model in capturing the water current structure of CC Bay.

On the second cruise (August 07, 2007), the water quality parameters and vertical profile of water currents along the transect route were captured. The vertical salinity profile along the transect route of the cruise is presented in Figure 5.12 and the cruise route is depicted on the inset plot of the figure. It should be noted that at several points during this transect we had to pull our instruments onto the boat deck and stops collecting data for servicing and potential bottom hits. These data gaps are evident in the figure. As found in the previous research cruise, water column was more saline at the upper Laguna Madre and became stratified in the bay. The hypersaline conditions occur at the upper Laguna because the inflow of freshwater into this system is less than the evaporation rate and the system is also separated from the Gulf of Mexico by a barrier island (Gunter, 1967). If the water column is stratified, denser bottom saline water may not be able to mix with less dense fresh water at the top of the water column. When currents at the top and bottom of the water column flow in the reverse direction, a depth-averaged model is not able to resolve the current structure of the water column. The observed vertical current structure along the transect route can clarify the water current pattern in the bay and thereby, help in determining the applicability of a 2-D model in capturing the water current structure of CC Bay.

Figure 5.13 displays observed water current vectors along the transect route of the cruise made on August 07, 2007 at successive depths of 1.5m, 1.75m, 2.0m, 3.0m, 3.25m and 3.5m, respectively (from top left to bottom right). It is evident from this figure that water currents in the Upper Laguna Madre flow at the same direction in different levels of water column, whereas the vertical water current pattern in the part of the

transect in the bay is bi-directional. The comparisons between Figure 5.12 and Figure 5.13 indicate that the water flow is unidirectional when the water column is not salinity-stratified, whereas the water currents travel in opposite directions above and below the level of stratification. This suggests that gravity flow has significant contribution in setting the current structure of the water column in this shallow bay. The distinct vertical gradient in water current direction further suggests that the depth-averaged model will induce significant error in predicting water currents. As long as the water column remains stable, this stratified water column will not be able to mix, and the vertical gradient in hydrodynamic and water quality parameters will remain.

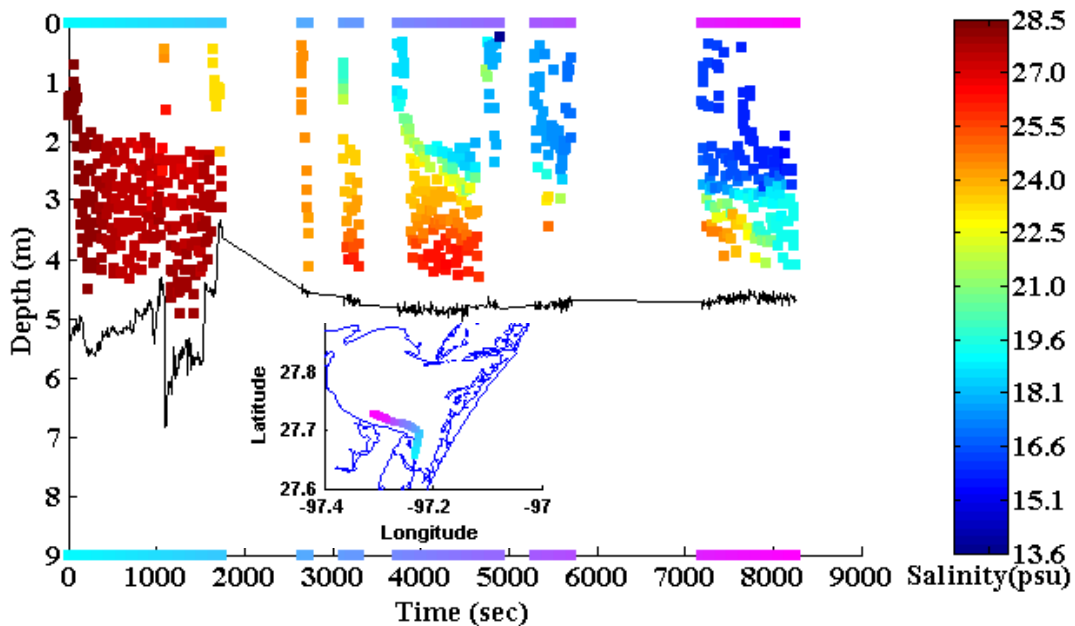


Fig. 5.12 Salinity variation along the transect route for the cruise made on August 07, 2007.

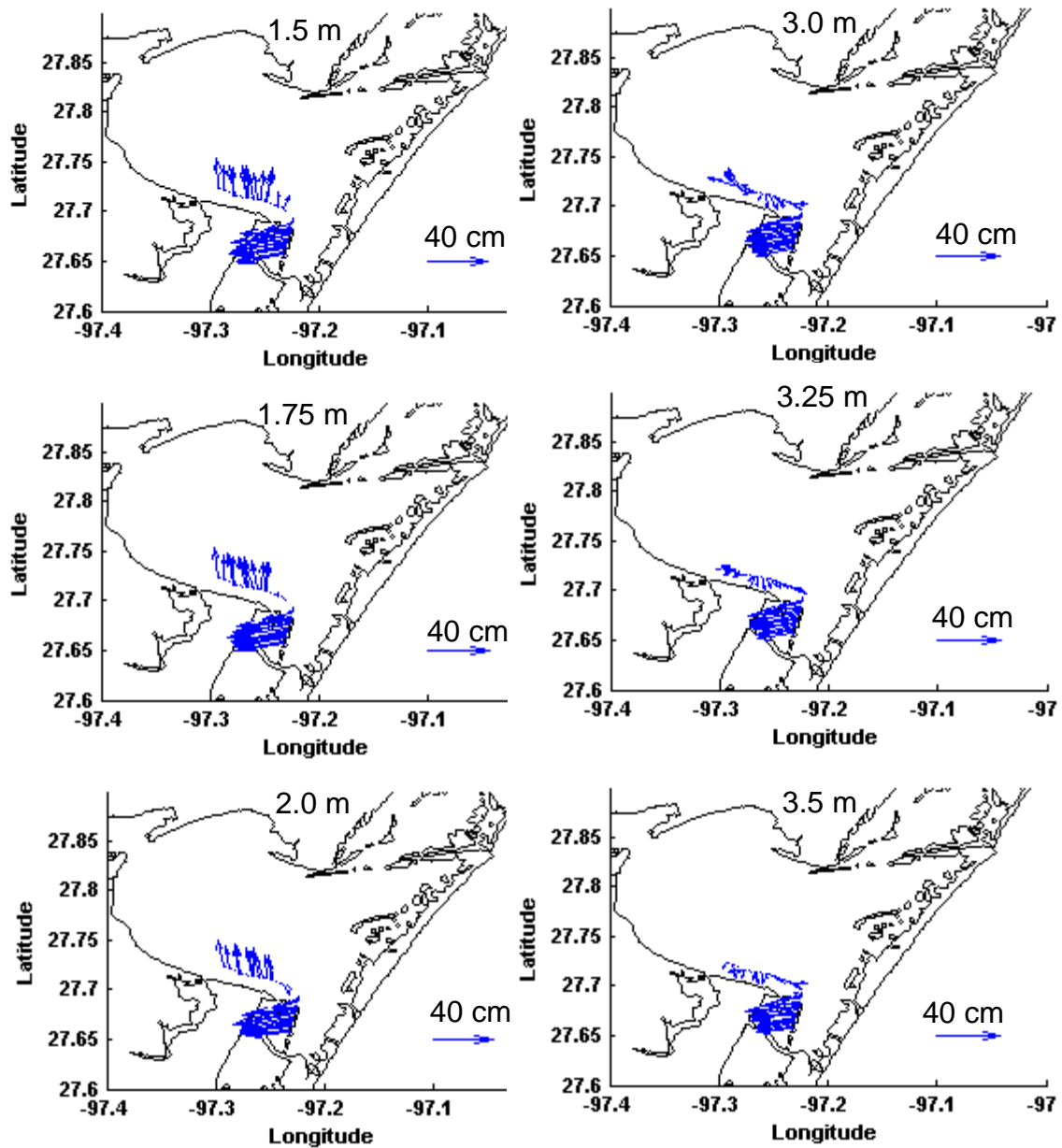


Fig. 5.13 Water current map along the transect route of the cruise made on August 07, 2007 at successive depths of 1.5m, 1.75m, 2.0m, 3.0m, 3.25m & 3.5m, respectively (from top left to bottom right).

The examination of water current structure and density profile along the transect route can provide insight regarding the stability of the water column. These profiles were

used to determine the gradient Richardson number (Ri) which quantifies stability condition of the water column. Miles (1961) and Howard (1961) have demonstrated that $Ri > 0.25$ is sufficient conditions for stability in a shear layer with linearly varying water current and density. When the nonlinear interactions are considered, sufficient conditions for stability in a three-dimensional stratified parallel shear flow becomes $Ri > 1$ (Abarbanel et al. 1984). For understanding stratification condition of water column, color-coded variation of the Richardson number along the transect route is plotted in Figure 5.14 assigning the Richardson number greater than unity as red. This representation helps to differentiate the areas where the water column was stabilized. From Figure 5.14, it is clear that water column remained stratified in the upper water column near Oso Bay (time= ~ 4000 - 8200 sec) and in the lower water column near the

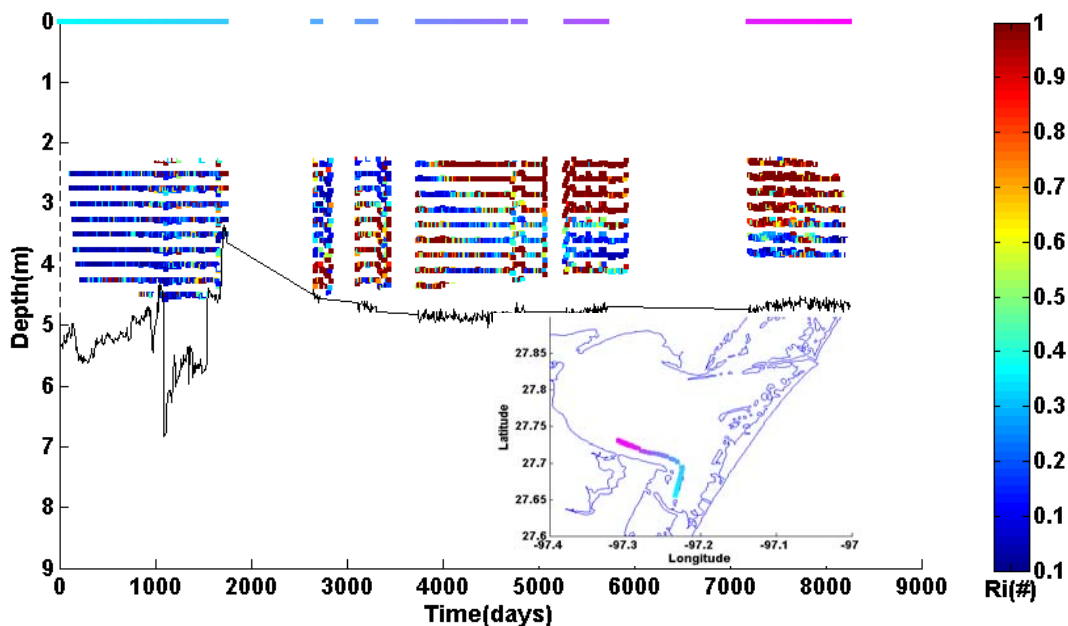


Fig. 5.14 Variation of Richardson (Ri) number along the transect route on August 07, 2007.

mouth of Upper Laguna Madre (time= \sim 2800-3600sec). This stable condition prevented mixing within the water column. If water column is not vertically well mixed, the depth-averaged model cannot capture the water current patterns of the bay. Therefore, it is necessary to develop a three-dimensional hydrodynamic model to resolve the actual water current structure of this shallow bay.

Conclusions

Development of a 2-D hydrodynamic model of CC Bay and comparisons of its output with observations provide insight about the dominant processes that control the hydrodynamics of this shallow bay. It also helped to understand the limitation of the depth-averaged model in capturing the certain hydrodynamic condition of the bay. Although the developed 2D model was able to successfully capture tidal variation at the Gulf of Mexico water level observation station, there exists a significant difference between observed and model-computed tidal WSE within the shallow bay. This discrepancy may be mainly attributed to omission of baroclinic forces, a two-dimensional representation of water currents, and to some extent other factors such as erroneous parameterization of bottom frictional stress, assignment of constant bottom roughness coefficient throughout the computational domain, coarse grid resolution, bathymetric inaccuracies and ignorance of non-linear tidal effects, etc. Also, the significant differences in the model-computed WSE with that of observed values at various water level observation stations inside CC Bay suggests that omission of baroclinic terms and the approximation of depth-averaged velocities in the model might

induce error. The observed distinct vertical and longitudinal salinity gradient in the bay further substantiates this hypothesis. Discrepancies in the model-computed depth-averaged water currents with that of HF-radar measured surface currents imply the existence of a vertical gradient in the water currents. The vertical current profile along the transect route as captured during one of our research cruises also showed a sharp gradient in the water current direction. Moreover, analysis of the salinity profile and water current structure along the transect route revealed that the water column remained stable at the existing condition. If this stable water column is not vertically well mixed, the depth-averaged model cannot capture water current pattern of the bay. Development of three-dimensional hydrodynamic model may help to resolve the actual water current structure of this shallow bay. This 3-D model can then provide useful information to drive various numerical models which will help to understand various important environmental phenomena controlling water quality in this bay.

CHAPTER VI

A MECHANISTIC DISSOLVED OXYGEN MODEL OF CORPUS CHRISTI BAY TO
UNDERSTAND CRITICAL PROCESSES CAUSING HYPOXIA***Overview**

Corpus Christi Bay (TX, USA) is a shallow wind-driven bay which experiences hypoxia (dissolved oxygen < 2 mg/L) during the summer months in the southeast region of the bay. We have developed and installed real-time monitoring systems in the bay to measure various water quality, meteorological and hydrodynamic parameters. These systems can aid in determining the extent and frequency of hypoxic events in this energetic bay. A three-dimensional mechanistic dissolved oxygen model has been developed in this study to investigate the key processes that induce hypoxia in Corpus Christi (CC) Bay. This model includes variable advection and dispersion coefficients so that it can be driven by real-time monitoring hydrodynamic data. The results from model simulations indicate that hypoxia may occur at the lower depths of the bay when both stratification and higher biological activity conditions exist. The water column in the south-east part of the bay becomes stratified during calm wind conditions when there is inflow of hyper-saline water from the neighboring Laguna Madre waterbody. This

* [2008] IEEE. Reprinted, with permission, from (A Mechanistic Dissolved Oxygen Model of Corpus Christi Bay to Understand Critical Processes Causing Hypoxia” by Islam, M.S., Bonner, J., Ojo, T. & Page, C., 2008. Oceans '08 MTS/IEEE Quebec Technical Program).

condition, when combined with higher biological activity during the summer months, induces hypoxia at the lower depths of the bay. The simulation results also point out that physical transport processes have more pronounced effect on the DO distribution within the water column than the effects of biological activity. Therefore, it is necessary to develop suitable sampling strategies that will measure hydrodynamic data at greater spatial and temporal resolution. The integration of this data with our developed model will provide a useful tool to the stakeholders to assess the water quality of the bay in real time.

Introduction

Dissolved oxygen (DO) is an important indicator of aquatic ecosystem health. Hypoxia develops when DO concentration in the water column dips below 2 mg/l and most aerobic aquatic organisms cannot survive under this condition (Diaz et al. 2008). According to the National Water Quality Inventory report (USEPA report, 2000), oxygen-depleting substances in U.S. rivers, lakes and estuaries are identified as one of the five leading causes of water quality impairment in these systems. CC Bay, home to the nation's seventh largest port with numerous petrochemical facilities, suffers from hypoxia during the summer months. Ordinarily, CC Bay would not be considered a likely candidate for hypoxia because it is a shallow wind-driven bay with an expected high level of mixing with aerated-surface water. However, hypoxia was first observed in the south-east portion of this bay by Montagna and Kalke (1992) in summer 1988 and has been reported every year thereafter (Ritter & Montagna 1999). This phenomenon

has been detected in other shallow bays such as Mobile Bay in Alabama (Turner 1979) and Pamlico River estuary in North Carolina (Stanley & Nixon 1992). Oxygen-depleted waters were found at the bottom of these bays during low-wind conditions.

Hypoxia develops when oxygen sinks exceed the oxygen sources in the system. The sources of oxygen in a water body are re-aeration from the atmosphere, photosynthetic oxygen production and the inflow of oxygen from neighboring waterbodies whereas the sinks are oxygen consumption through decomposition of organic matter (particulate and dissolved), respiration, oxidation of inorganic matter, outflow of oxygen into the oxygen-deficient neighboring bays, etc. Organic matter and nutrients are released into the rivers from the watershed during precipitation events and can ultimately enter the bay with freshwater flow. As the precipitation events occur randomly, the concentrations of organic matter and nutrient in the bay can vary accordingly. There are two different but not mutually exclusive hypotheses on the causes of hypoxia (Rowe 2001). Many biologists and chemists think that increased nutrient concentrations in the water column yield excessive primary production in the system. After the death of these primary products, the detritus settles to the bottom of the bay, are decomposed, thus consuming oxygen. This may significantly reduce the dissolved oxygen levels in the bottom of the bay and may induce hypoxia. On the other hand, the physicists argue that inflow of freshwater into the bay creates stratification in the water column and thereby, prevents the mixing of highly aerated surface water with the bottom waters where respiration dominates. If the stratification is not interrupted by the wind events, the bottom water may not be refreshed and may become hypoxic. Texas

researchers found that freshwater inflow rates into CC Bay have decreased in recent years (Ritter et al. 2005) and the stratification observed in the south-east part of the bay occurs due to the inflow of highly saline water from neighboring water bodies, not from the inflow of freshwater from the Nueces River (Hodges & Furnans 2007). This creates an inverse estuary situation. Therefore, the complex interplay of physical and biological processes that occur in CC Bay may be different from other typical shallow bays, and so it is necessary to monitor water quality, meteorological and hydrodynamic parameters in real time to understand these processes.

Monitoring of water quality parameters and environmental indicators that influence the physical processes of hypoxia poses a challenge due to the spatial extent and dynamics associated with CC Bay. Ritter and Montagna (2001) noticed that hypoxic events in CC Bay usually occur at night or during the early morning, and typically lasted on the order of hours. With the support of both state and federal funding, our research group has developed monitoring systems to measure various water quality and hydrodynamic parameters at greater spatial and temporal resolution (Islam et al. 2006a). Data collected from these systems are used to understand the processes that affect hypoxia. Due to logistics and costs involved, it is not feasible to measure all water quality parameters at extremely high spatial and temporal resolution; therefore, it is necessary to determine the key processes that control hypoxia and thereby, develop suitable monitoring schemes to capture the variation of the related parameters that will help to characterize these processes. Development of a dissolved oxygen model will help

to understand the internal dynamics of the ecosystem, and thereby will assist in determining the key processes of hypoxia.

Models can vary from the empirical statistical model to the three-dimensional complex deterministic numerical model. The empirical models are simple to apply as they establish relationships among various parameters through correlating measured parameters, and do not consider the actual physical and bio-geochemical processes involved in the ecosystem. On the other hand, a complex mechanistic model considers the processes actually involved in the ecosystem and thereby aid in understanding the internal dynamics associated with the ecosystem (Scavia et al. 2006). James (2002) comprehensively reviewed of the present status of deterministic water quality models and found that the most important factor that limits the progress of the operational coastal water quality model is the lack of observed data. The deployment of various monitoring systems in CC Bay provides us a unique opportunity to collect a myriad of datasets which can be used in developing a mechanistic dissolved oxygen model and thereby assists in understanding the dissolved oxygen dynamics in the bay. In this study, a three-dimensional mechanistic dissolved oxygen model was developed and the sensitivity analysis of this model was performed to determine the key processes causing hypoxia. This information will help in developing suitable sampling strategies for our monitoring system so that it can capture hypoxic events.

Study Area

CC Bay is located on the Texas coastline and covers an area of approximately

432.9 sq. km (Flint 1985). It is connected to the Gulf of Mexico through a narrow ship channel (15 m depth), which runs from east to west. Figure 6.1 shows the characteristic features of the bay. It is also surrounded by four water bodies, namely Oso Bay in the southwest, Nueces Bay in the northwest, Upper Laguna Madre in the south and Redfish Bay in the northeast. Freshwater enters the bay via the Nueces River and Nueces Bay, whereas high-saline water enters the bay during summer months from the shallow Upper

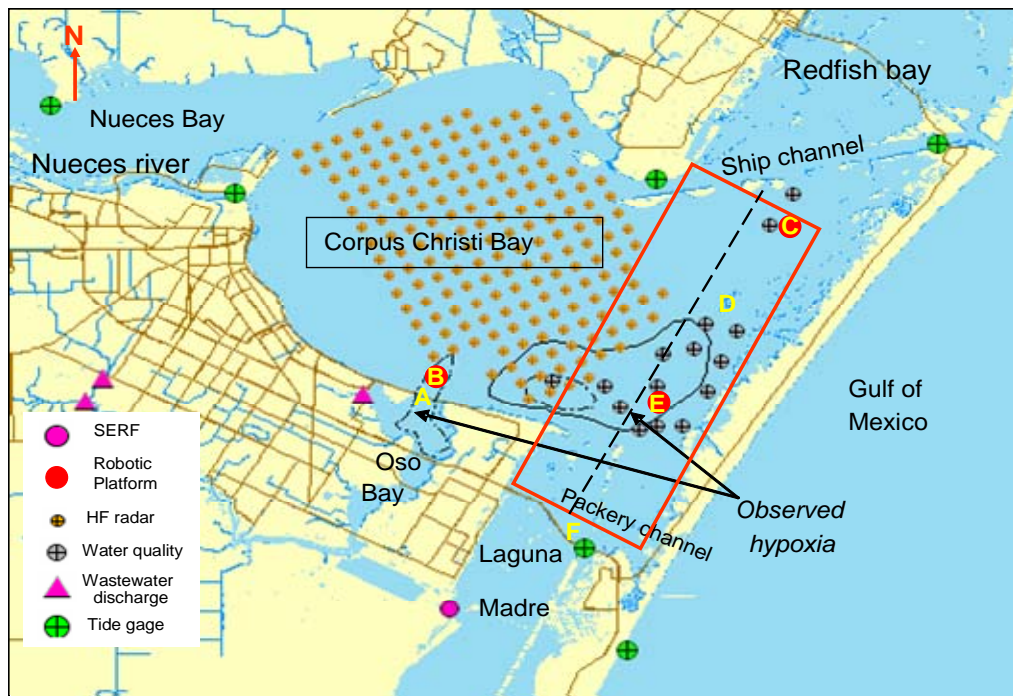


Fig. 6.1 Characteristic features of Corpus Christi Bay.

Laguna Madre and Oso Bay (Fig. 6.1). Recently, Packery Channel, located at the southern reaches of the bay, has been opened and it is another source for the water exchange with the Gulf of Mexico. CC Bay is mainly dominated by south-easterly

winds although northerly winds occur periodically during the winter months. The black-colored polygons represent locations where hypoxia has been reported (Ritter & Montagna 1999; Hodges & Furnans 2007). The three red solid circles represent the location of our fixed robotic platforms in the bay. Platform 'B' ($27^{\circ}43.531'N$, $97^{\circ}18.412'W$) is positioned 100m from the mouth of Oso Bay to characterize the effects of Oso Bay inflow, which has been reported to trigger hypoxia in that part of the bay. Platform 'E' ($27^{\circ}43.375' N$, $97^{\circ}11.403'W$) is positioned in the south-east portion of the bay where hypoxia has been documented since 1988 (Ritter & Montagna 1999). Some of the ship channel effects on CC Bay may be captured through our Platform 'C' ($27^{\circ}48.560' N$, $97^{\circ}08.513' W$) in the north-east part of the bay. The brown circles denote the grid where total current vectors are measured by the high frequency (HF) radar systems installed at our remote platforms.

Materials and Methods

We have developed a monitoring system that measures various water quality, hydrodynamic and meteorological parameters at greater spatial and temporal resolution. Our monitoring system includes three observational platform types: 1) Fixed Robotic, 2) Mobile, and 3) Remote. An automated vertical profiling system installed on each fixed robotic platform moves a suite of in-situ sensors within the water column and measures various water quality parameters at five different depths. Along with this profiling system, an 1200 Khz workhorse Acoustic Doppler Current Profiler (ADCP) and meteorological sensors are also installed at each fixed robotic platform to measure water

currents and meteorological parameters, respectively. An Integrated Data Acquisition, Communication and Control (IDACC) system has been configured on our mobile platform (research vessel) for the measurement of various water quality parameters ‘synchronously’ over a highly-resolved spatial regime. This system can acquire and visualize data measured by submersible sensors on an undulating tow-body deployed behind the vessel. Along with the fixed robotic and mobile platforms, four high frequency (HF) radar units have been installed on our remote platforms to measure surface currents of CC Bay and its offshore area. Also periodically, we collected grab water samples at different locations (labeled A, B, C, D, E, F in Fig. 6.1) in the bay to determine bio-chemical oxygen demand (BOD). Grab water samples were chilled immediately, and processed within six hours of collection (ANALYSYS, Inc). The laboratory followed standard methods (SM 5210B) for BOD analysis and reported as 5-day BOD. Table 6.1 lists spatial BOD variation as captured during one of our routine monitoring activities in CC Bay. There was a significant amount of BOD at the Laguna Madre (sampling location F) and the area close to our platform “E”. The value of BOD was undetectable or very low at the other sampling locations. This information is used to initialize and to provide boundary conditions for our model.

Description of the Model Development

Two primary state variables considered in this model are DO and BOD. BOD is used as a surrogate to indicate the total amount of oxygen required for biochemical degradation of organic matter and oxidation of inorganic materials such as sulfides and

Table 6.1 Spatial BOD variation in CC Bay as captured by grab sampling

Location symbol	Date	Time of Collection (local time)	Depth (m)	BOD ₅ (mg/L)
F	July 11,2007	8:30 AM	3	7.6
F	July 11,2007	8:35 AM	1.5	5.7
E	July 11,2007	9:45 AM	3	7.5
E	July 11,2007	9:45 AM	2	<2
E	July 11,2007	9:45 AM	1	<2
D	July 11,2007	10:25 AM	3	<2
D	July 11,2007	10:25 AM	1.5	<2
C	July 11,2007	11:15 AM	3	<2
C	July 11,2007	11:15 AM	1.5	<2
C	July 11,2007	11:15 AM	0.5	<2
A	July 11,2007	12:50 PM	1.25	<2
A	July 11,2007	12:50 PM	0.25	<2
B	July 11,2007	1:20 PM	1.25	<2
B	July 11,2007	1:20 PM	0.25	<2

ferrous iron. This term is derived out of convenience in the water quality model development since it is not feasible to include all the kinetics involved in the dissolved oxygen dynamics of the bay. For example, dissolved inorganic substances are converted into organic material through photosynthesis and release dissolved oxygen in the water column. This process requires nutrient such as nitrogen, phosphorus and silicate.

Nitrogen is available in the water column as free nitrogen, nitrite (NO₂⁻), nitrate (NO₃⁻)

and ammonia (NH_4^+) whereas phosphorous is available as phosphate (PO_4^-). The availability of this nutrients control the rate of growth of organic matter. Therefore, it is necessary to quantify each component of the nutrient distribution in the bay to characterize the photosynthesis. Also, the rate of decomposition of organic matter depends on its type, size, structure etc. These are few examples of the processes involved in the dissolved oxygen dynamics of the bay, and so the use of BOD will help to quantify the total amount of oxygen consumed through the overall processes involved in the dissolved oxygen dynamics. The following differential equations are used in the model to characterize the DO-BOD kinetics involved in the bay:

$$\left(\frac{\partial L}{\partial t} = -\frac{\partial uL}{\partial x} - \frac{\partial vL}{\partial y} - \frac{\partial wL}{\partial z} + \frac{\partial(K_x \frac{\partial L}{\partial x})}{\partial x} + \frac{\partial(K_y \frac{\partial L}{\partial y})}{\partial y} + \frac{\partial(K_z \frac{\partial L}{\partial z})}{\partial z} - K_r L \right) \quad (6.1)$$

$$\left(\frac{\partial C}{\partial t} = -\frac{\partial uC}{\partial x} - \frac{\partial vC}{\partial y} - \frac{\partial wC}{\partial z} + \frac{\partial(K_x \frac{\partial C}{\partial x})}{\partial x} + \frac{\partial(K_y \frac{\partial C}{\partial y})}{\partial y} + \frac{\partial(K_z \frac{\partial C}{\partial z})}{\partial z} + K_a(C_s - C) + P - K_d L - S_B - R \right) \quad (6.2)$$

Where, L is the BOD, K_x, K_y and K_z are the dispersion coefficients whereas u, v, w are the velocities in the x, y and z direction respectively. K_a is the re-aeration coefficient, K_d is the de-oxygenation rate, C is the dissolved oxygen concentration, C_s is the saturated oxygen concentration, S_B is the sediment oxygen demand, P and R the photosynthesis and respiration rate, respectively. The partial differential equations (6.1) and (6.2) will be solved through discretization into solvable equations using Thomann's finite segment

method (Thomann 1972). In this method, the bay is divided into a series of segments and the mass balance equation is written for each segment assuming the insignificant gradient within it. The discretized equations are then solved using fourth order Runge-Kutta method to capture the time evolution of DO and BOD dynamics in the bay.

The advective and dispersive transport of organic matter and DO are highly variable in a wind-driven shallow bay due to the stochastic nature of the wind forces. Ojo et al. (2006) conducted several dye study experiments in CC Bay and found the significant variation in the spatial distribution of the dispersion coefficient within the bay. This difference in the vertical dispersion coefficient may be more pronounced during the stratified condition when there is a greater probability of the occurrence of hypoxia in the bay. Therefore, our mechanistic model is developed in such a way so that it can handle variable advection and dispersion coefficients. A staggered grid is considered in the model development, i.e., advection and dispersion are assigned at the interface of each segment whereas the concentration of state variables is calculated at the center of the segment. The data collected from our monitoring systems are used to define the computational domain, and to provide initial and boundary conditions for the model.

Fig. 6.2 shows the salinity variation along the transect route during the cruise made with our mobile monitoring platform system on July 24, 2007. The actual cruise route is depicted on the inset plot of the figure. The route line is color-coded and correlates with the horizontal color-coding along the top and bottom of each figure, thus matching the observed data with the spatial location in the bay. Salinity levels at all depths were higher at the Upper Laguna Madre (early part of the cruise, $t = 0-1300$

seconds) as compared to salinity levels in CC Bay (mid and latter parts of the cruise, $t = 1300\text{-}5800$ seconds). It is clear from this salinity profile that a salt edge moved from the shallow Laguna Madre towards Platform “E” and there existed a significant vertical salinity gradient around this platform. Laguna Madre most probably contributes to this salinity gradient as it is one of the hypersaline estuary systems in the world (Sharma et al. 1999). Also, BOD data collected at several locations in the bay indicates that BOD concentration was high at the Laguna Madre whereas BOD concentrations were undetectable at the mouth of Oso Bay. Therefore, the characterization of the BOD-DO

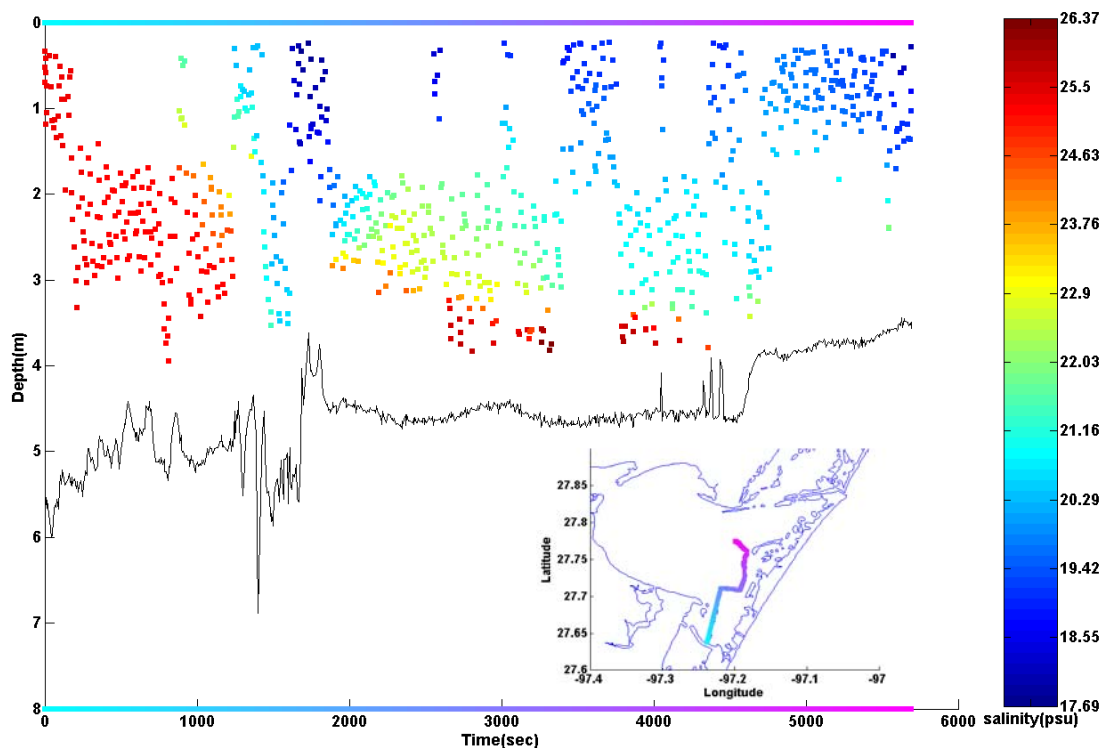


Fig. 6.2 Salinity variation along the transect route on July 24, 2007. (Note: the colored horizontal lines at the top/bottom of the figure correlate to the transect route as depicted in the inset plot of the figure).

kinetics in the rectangular computational domain (Fig. 6.1) will help to investigate the contribution of two important processes (biological and physical transport) that may induce hypoxia at this part of the bay. The dimension of the computation domain is 21km x 4km x 4.5m.

In shallow wind-driven water bodies like CC Bay, wind may have significant effect in oxygen transfer through producing internal turbulence and thereby, may increase the re-aeration rate. Banks (1975) and Banks and Herrera (1977) have investigated the wind effect on re-aeration and suggested the following relationship for the determination of a wind-driven oxygen transfer coefficient (K_L):

$$K_L = 0.728U_W^{1/2} - 0.317U_W + 0.0372U_W^2 \quad (6.3)$$

Where U_W is the wind speed (m/s) at 10 m above the water surface. The volumetric re-aeration coefficient (K_a) can then be determined by dividing K_L with the depth of the surface layer. The wind speed measured at our monitoring platforms can be plugged into the model for the determination of re-aeration co-efficient. The BOD concentration at the south boundary (boundary at Laguna Madre) was held invariable with time and the vertical profile of constant BOD was determined from BOD measured at location “F”. The surface boundary condition for BOD was considered as reflective whereas an adsorptive boundary condition was assigned at the bottom boundary. Therefore, BOD cannot move into/out of the domain at the surface layer whereas the BOD that settles into the bottom will stay in the sea-bed. The net exchanges of dissolved oxygen at the surface layer will be due to the re-aeration only whereas these changes at the bottom boundary will be due to sediment oxygen demand (SOD). The initial value of BOD was assigned

zero everywhere at the domain whereas a saturated condition was considered as the initial condition for DO.

Results and Discussion

The level of disturbance that hypoxia can create in this ecosystem depends on its spatial extent, frequency and duration. Understanding of the key processes that control dissolved oxygen dynamics in the bay will help to quantify these disturbances. The developed model was simulated under different conditions to examine the effects of physical and biological processes on DO distribution in the bay. The change in the biological activity in the water column can be mimicked by changing the de-oxygenation rate (K_d) of BOD. The K_d value depends on the temperature, types of organic material, microbial activity etc. In the summer, the K_d value is higher due to higher biological activity. As an approximation, the K_d value can vary in the range of 0.1~0.5/day for deeper water bodies (depths greater than 1.5m) (Thomann & Mueller 1987). We have simulated our model at different K_d values while keeping the hydrodynamic conditions and other parameters constant to understand the biological effect on the BOD distribution in the bay. Also, SOD, which represents the total sediment oxygen consumption from biological activity and oxidation of inorganic materials, was kept constant, and the water column was simulated as un-stratified assuming the same vertical dispersion coefficient throughout the computational domain. Fig. 6.3(a) and fig. 6.3(b) shows the vertical and spatial BOD distribution (one snapshot of our simulation results) along the black dotted line (Fig.6.1) after 15 hr of simulation for K_d values of 0.1/d and 0.5/d, respectively. It is

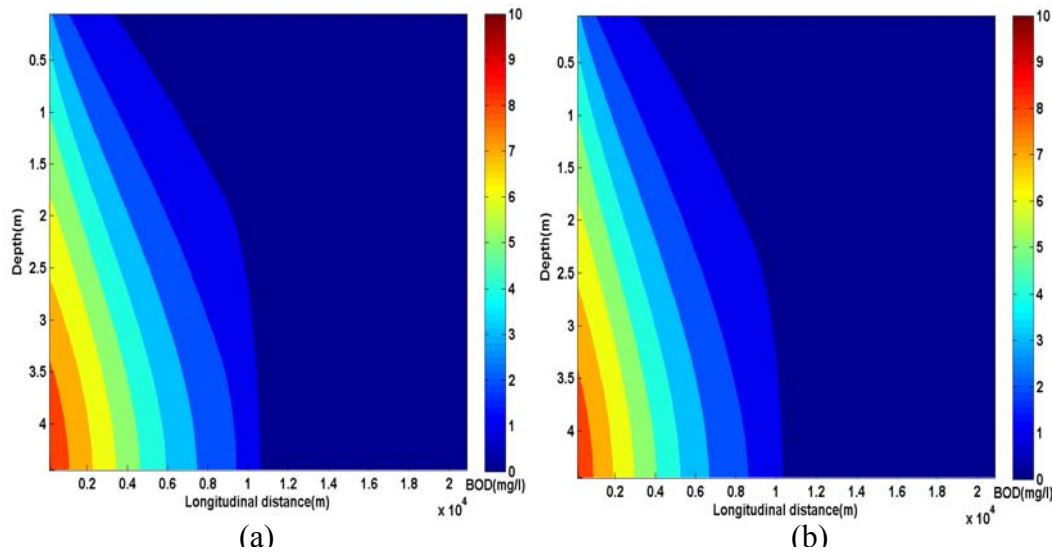


Fig. 6.3 Modeled BOD variation along the black dotted line in Fig. 6.1 after 15 hr of simulation for a) $K_d=0.1/d$ and b) $K_d=0.5/d$. The hydrodynamic conditions and other model parameters held constant.

clear from these two figures that the BOD distribution in CC Bay is not significantly affected with changes in the rate of biological activity (K_d). The spatial extent of BOD materials remains the same in both cases. The concentration of BOD is highest at the bottom of the bay near the mouth of the Laguna Madre (approximately 5 km from the south boundary).

The physical transport processes may significantly effect the BOD distribution in the bay. CC Bay is mainly driven by the south/south-east wind during the summer time. The inflow of hypersaline water from the shallow upper Laguna Madre (<1m) produces the inverse estuary situation, and the water column at the south-east part of the bay (near platform “E”) can become stratified. This phenomenon was captured by our mobile monitoring platform (Fig. 6.2). Therefore, the model was simulated under different

hydrodynamic conditions to understand the effect of transport processes on the BOD distribution in the bay. Two different vertical dispersion coefficients were used to simulate stratified conditions in the bay. The vertical dispersion coefficient of $1 \text{ cm}^2/\text{s}$ was considered for the upper 3m of the water column whereas the coefficient of $0.01 \text{ cm}^2/\text{s}$ was considered for the lower portion of the water column. Fig. 6.4(a) and fig. 6.4(b) shows the BOD distribution (one snapshot of our simulation results) under stratified conditions along the black dotted line in Fig. 6.1 after 15 hr of simulation for longitudinal advection velocity of 10 cm/s and 30 cm/s , respectively. K_d values were kept constant in both cases. It is clear from these two figures that the transport processes have significant effect on the spatial distribution of the BOD materials. Sudden changes in the vertical gradient of BOD at a level of 3m are due to the stratification effect. The

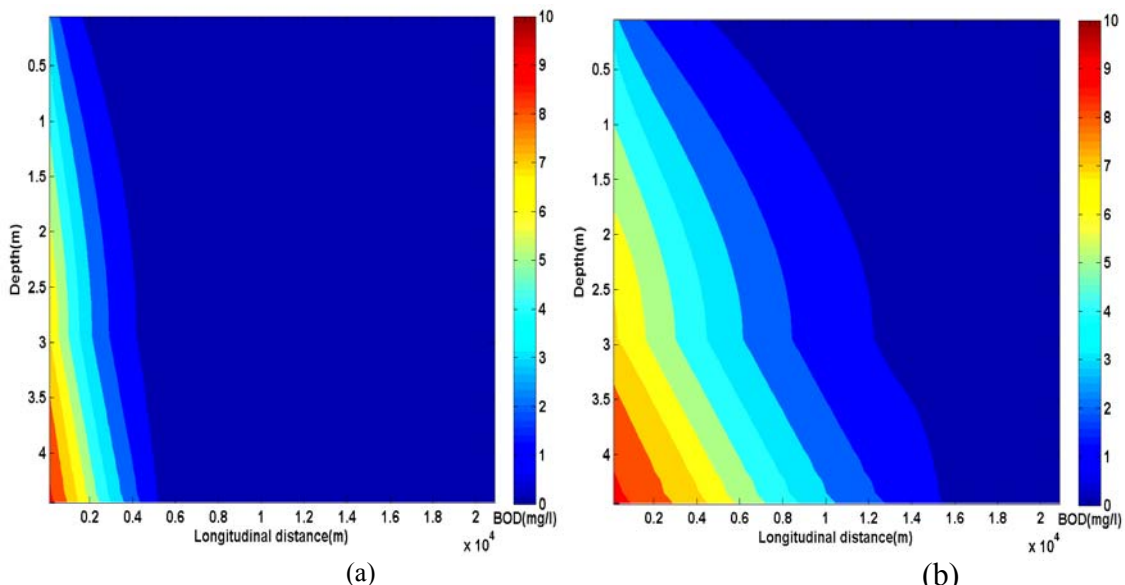


Fig. 6.4 Modeled BOD variation along the black dotted line in Fig. 6.1 after 15 hr of simulation for a) $V=10 \text{ cm/s}$ and b) $V=30 \text{ cm/s}$. $K_d=0.3/\text{d}$ and stratification of water column at a depth of 3m is considered.

advection has notable effect on the distribution of BOD materials within the bay. As the longitudinal velocity increases, the spatial extent of BOD material increases. Under normal hydrodynamic conditions in the summer, the longitudinal velocity component in our computational domain varies from 0 to 30 cm/s (calculated from data generated by our HF-radar system). Model predicts that detectable amount of BOD material will be found between Laguna Madre and our platform “E” under this hydrodynamic condition. We collected water samples to determine BOD levels on several occasions in the bay and always found the highest concentrations between Laguna Madre and platform “E”. The concentrations of BOD were undetectable at other part of the bay. Therefore, the developed model is successful in capturing the trend of BOD distribution in the bay.

Stratification of water column affects the distribution of BOD and so it is expected that this process will also contribute in the DO distribution in the bay. Therefore, the developed model was simulated under stratified conditions with low biological activity (low K_d and zero SOD values). Fig. 6.5 shows model-computed vertical DO variation under low biological activity conditions (SOD = 0 g-O₂/m².day, K_d =0.1/day). The dissolved oxygen levels at the bay bottom decreased since the lower water column waters were not able to mix with higher-aerated surface waters, and oxygen was partially consumed at the lower depths due to biological activity. Although DO level was reduced at lower depths, it did not reach hypoxic conditions (DO <2 mg/L) due to the lower rate of biological activity (K_d =0.1/day). A high rate of biological activity coupled together with stratification may induce hypoxia at the bay’s

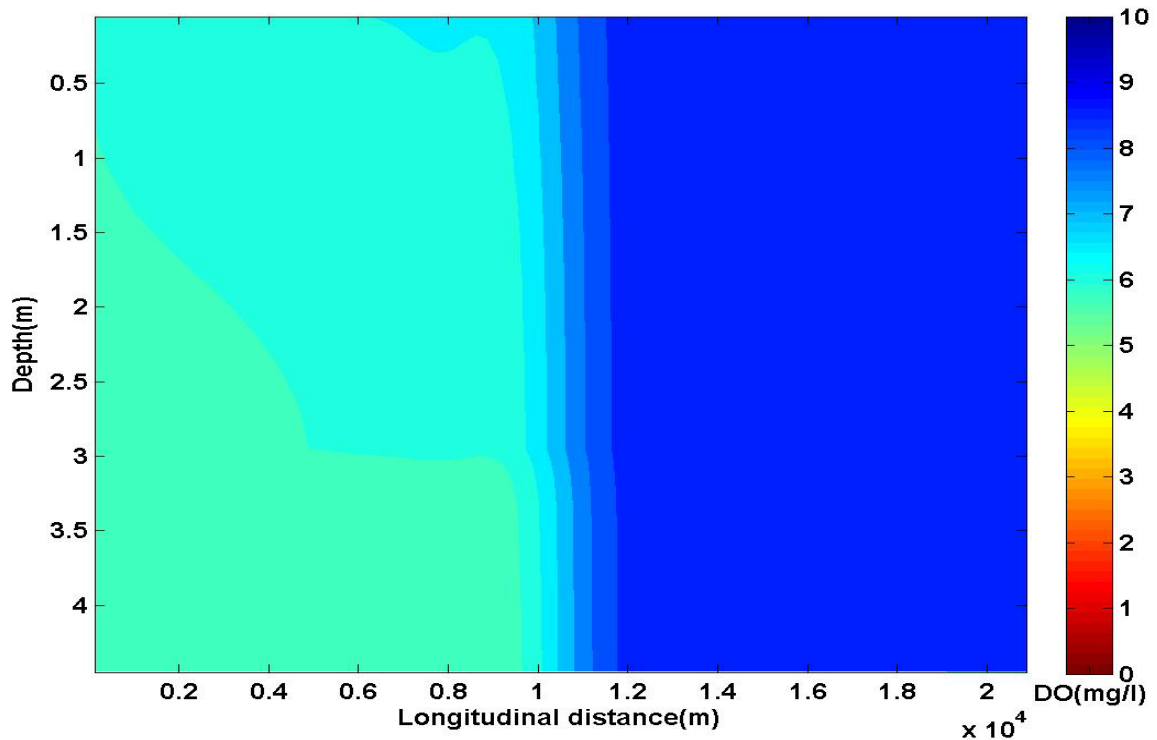


Fig. 6.5 Snapshot (15 hr simulation) of DO variation along the black dotted line in Fig. 6.1 under stratified condition with low biological activity conditions ($SOD = 0 \text{ g O}_2/\text{m}^2 \cdot \text{day}$, $K_d = 0.1/\text{day}$).

lower depths. Kemp et al. (1992) examined the relative importance of biological and physical processes in inducing seasonal depletion of oxygen at the bottom of Chesapeake Bay and argued that these processes are coupled to each other at the bay bottom. If biological activity increases, physical transport of DO at the bottom will increase and vice-versa. The higher rate of biological activity at the bottom will consume more oxygen and thereby a vertical oxygen concentration gradient will be higher. This will increase the physical transport of DO. Although these processes may be coupled at the bottom of the bay, this may not be the case for the whole system. The dispersion coefficient can vary on the orders of magnitude in vertical direction during stratified

conditions and it will limit the transfer rate of aerated surface DO water to the bottom of the bay where biological activity and oxidation of inorganic matter occur. Therefore, we have simulated our mechanistic DO model under stratified conditions while keeping the biological activity and other parameters reasonable for an estuary like CC Bay.

The following values were assumed for the simulation of the model considering both physical and biological processes: a) $SOD = 1.5 \text{ g O}_2/\text{m}^2/\text{day}$ for estuarine mud (Thomann & Meller 1987), b) $K_d = 0.3/\text{day}$. Hydrodynamic information and re-aeration rates were determined using the hydrodynamic and meteorological data measured at our monitoring platforms. Also, the water column was assumed stratified at a level of 3m from the surface. The model predicted that hypoxic condition will occur at the bottom of the bay under these conditions (Fig. 6.6). This conditions prevailed from the mouth of the Laguna Madre towards platform "E" (6~10 km). Dissolved oxygen data collected from our mobile monitoring platform (July 24, 2007 cruise) agree with this result (Fig. 6.7). The dissolved oxygen levels are low (lower depth range; $t = 2800\text{-}4000 \text{ sec}$) around our platform "E". Although the dissolved oxygen level was higher at the Laguna Madre compared to model-predicted dissolved oxygen level, this might occur due to the uncertainties in the determination of the model parameters and limitation of boundary condition. The BOD was kept constant at the south boundary which might not be the actual case. The rate of biological activities (SOD and K_d) may vary spatially, and thereby could differently influence model output. The dispersion coefficient can also vary in time and space and thereby significantly change the location of hypoxic conditions in the bay. Although the developed model is capable of handling spatial and

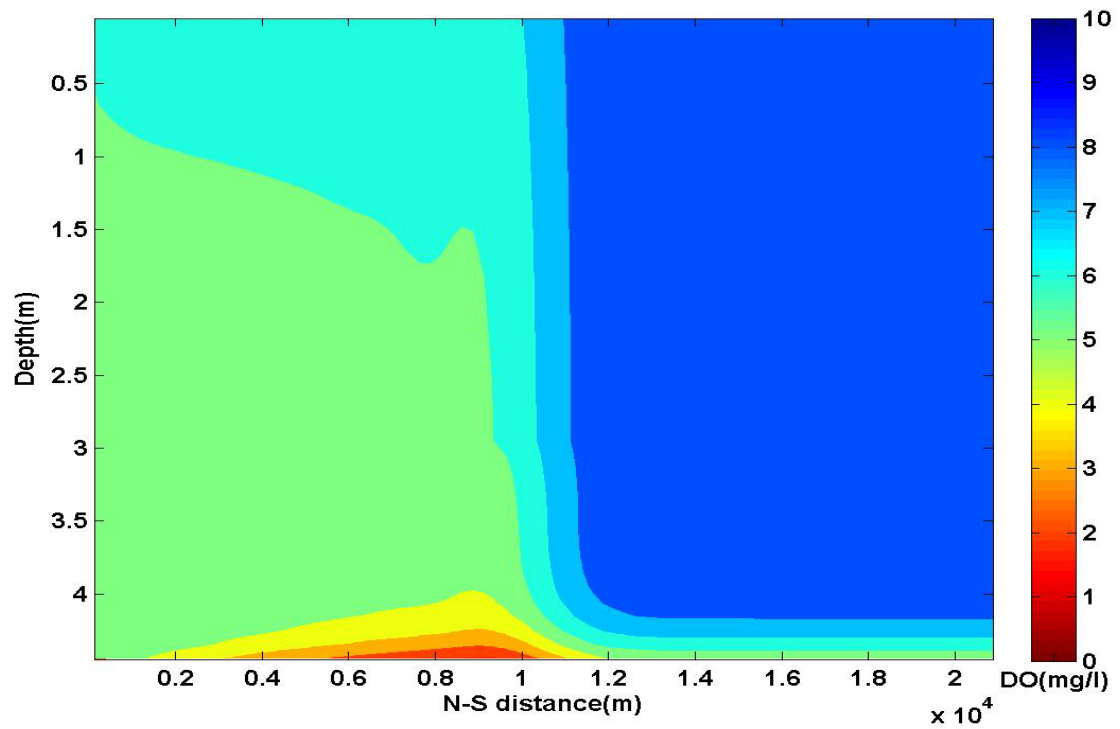


Fig. 6.6 Snapshot (15 hr simulation) of DO variation along the black dotted line in Fig.6.1 under stratified condition with normal biological activity conditions ($SOD = 1.5 \text{ g O}_2/\text{m}^2\cdot\text{day}$, $K_d=0.3 \text{ /day}$).

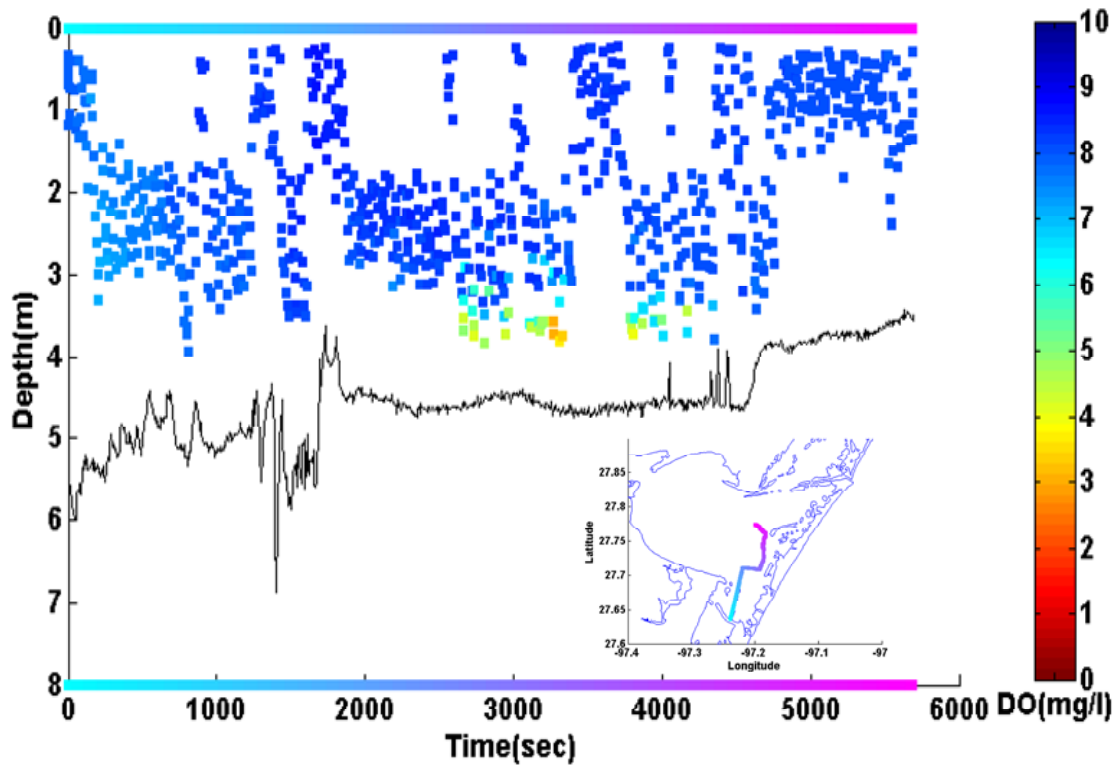


Fig. 6.7 DO variation along the transect route on July 24, 2007. (Note: the colored horizontal lines at the top/bottom of the figure correlate to the transect route as depicted in the inset plot of the figure).

temporal variation of dispersion coefficients, the model was simulated with a constant spatial dispersion coefficient (except in vertical direction) because of limited observed hydrodynamic data. Therefore, more emphasis needs to be given on the collection of hydrodynamic data with our monitoring platforms at greater spatial and temporal resolution. This will help to characterize the stratification phenomena well and thereby assist in better understanding of the hypoxia phenomenon. Also, our simulation results indicate that an hypoxic event only occurs when both biological activity and physical transport processes are favorable for this condition. Therefore, biological processes need

to be better characterized through developing proper monitoring schemes. The frequency of monitoring biological processes may be less compared to that of physical transport processes as changes in the rate of biological processes appear to have less effect on dissolved oxygen dynamics. This information will help to allocate our resources efficiently and thereby, to develop efficient monitoring plans for our platforms.

Conclusions

The developed three-dimensional mechanistic dissolved oxygen model is able to shed light on the processes that have significant effects on dissolved oxygen dynamics in CC Bay. Both the physical and biological processes need to be favorable for inducing hypoxic conditions in the bay. The inflow of hypersaline water from the Upper Laguna Madre produced a vertical salinity gradient along the south-east part of the bay and this gradient may prevent the mixing of aerated surface water with bottom water if wind conditions remain calm. This condition, when combined with higher biological activity in the summer months can induce hypoxia at the bottom of the bay. As physical transport processes have more pronounced effects on the dissolved oxygen distribution in the bay, it is necessary to develop suitable sampling schemes that will capture hydrodynamic condition at greater spatial and temporal resolution. Also, resources need to be allocated to investigate the actual rate of various biological processes that occur in the bay. The integration of real time monitoring data with the developed model can be used as a valuable tool for the real time assessment of water quality in the bay.

CHAPTER VII
DEVELOPMENT OF A THREE-DIMENSIONAL (3-D) PARTICLE AGGREGATION
AND TRANSPORT MODEL TO CHARACTERIZE PARTICLE DYNAMICS IN
CORPUS CHRISTI BAY

Overview

The characterization of particle dynamics assists in greater understanding of the processes that control water quality of aquatic ecosystems. Particles can be transported in the aquatic environment as discrete ones or aggregated particles interacting with each other. Transport mechanisms of discrete particles can be described using an advective-dispersive transport model whereas aggregated particle dynamics can be captured through the inclusion of aggregation kinetics in the advective-transport model. Particles in aquatic systems may need to be characterized through fractal geometry as most of them are fractal in nature. Using the up-to-date fractal theories for coagulation kinetics, a three-dimensional particle aggregation and transport model has been developed in this study. The governing partial differential equations describing particle size dynamics in three-dimensions are discretized using a finite segment method which is essentially a finite difference approximation of differential equations. The discretized equations are then numerically integrated using the fourth-order Runge-Kutta method to determine particle size spectra in the computational domain. The developed model performance is evaluated against the analytical solution for the transport of polydispersed particles in a three-dimensional water column. Model predictions agree reasonably well with that of

the analytical solution. Field-scale application of this model helps to test various hypotheses in understanding the processes causing hypoxia (dissolved oxygen < 2mg/l) in Corpus Christi Bay. Observational data from our monitoring platforms provide guidance in setting the initial and hydrodynamic conditions for the model simulation. Simulation results illustrate the importance of the vertical transport process and aggregation in controlling particle residence time in the water column. It was predicted that oxygen-consuming particles can settle at the bottom of the bay on the order of hours and thereby, bottom water may turn hypoxic within a short time frame under stratified conditions. The future extension of this model for a multiple-particle-type system may help to better characterize the particle dynamics, and thereby leads to the greater understanding of particle-mediated processes and their contributions to the water quality of an aquatic system.

Introduction

Particles play a significant role in maintaining balance and health of natural aquatic systems. They exist in different forms, and affect water quality of the system depending on their types, source of origin, sizes, shapes, density, etc. The decomposition of organics particulates can induce lower dissolved oxygen (DO) level in the water column through consuming oxygen. In addition of organic particles, inorganic particles such as sand, clay, silt, nutrients etc. are abundantly available in the aquatic system. These inorganic particles can directly or indirectly affect water quality of the system. They can act as a carrier for the transport of various contaminants within the water

column. The tidal and wind activity move sand particles along the shore and erode the natural beach. The characterization of sand particles kinetics is necessary for the implementation of beach nourishment which helps to preserve the beach environment. Accidental oil spills in coastal regions disperse oil in the aquatic system as 'particles'. If oil particles are not degraded faster, the longer these oil particles will stay in the water column, greater detrimental effects will be incurred on the environment. Inorganic particles can also be associated with organic particles and thereby change the transport dynamics of the organic particles. The understanding of particle dynamics will help in water quality prediction, tracking of contaminants in the system, emergency response activities such as design of dispersant use or other counter measures in the case of accidental oil spill and providing insights about other processes that control ecosystem health.

Particle dynamics in the natural system can be understood through characterization of particle transport as discrete particles and as aggregated particles (Faisst 1976; Morel and Schiff 1980; Hunt and Pandya 1984). If particles are not able to aggregate due to the existing hydrodynamic and particulate surface conditions, particle transport then can be modeled using a set of uncoupled simple advective-dispersive transport equations. Also, if it can be assumed that all particles settle at the same settling velocity, then one advective-dispersive equation can be used to model them all.

However, particles in the water column can be aggregated depending on the combined effect of electrostatic repulsion and van der Waals attraction between two particles as described by DLVO theory (Deryaguin and Landau 1941; Verwey and Overbeek 1948)

and settle in different settling velocities. In that case, heterogeneous particle interactions terms must be included in the transport model (Bonner et al. 1994). Several investigators (Kihara and Matijevic, 1992; Van de Ven and Mason, 1977) have incorporated DLVO theory into aggregation transport models. Considering complex chemical and biological characteristics of particles in the natural systems, collision efficiency (α) term which represents the level of destabilization has been used in particle aggregation and transport (PAT) model development (Ernest, et al. 1995; Han and Lawler 1991). α is resolved through the determination of the probability of a successful collision between two particles for the formation of aggregates. Ernest, et al. (1995), Lee et al. (2002) and Sterling et al. (2005) calculated α through minimization of variation between observed particle concentration and model prediction.

The core of almost all flocculation modeling available to date is based on the basic equation 7.1 developed by Smoluchowski (1917) for the determination of particle size distribution (PSD) (Ernest et al. 1995):

$$\theta_k = \frac{1}{2} \alpha \sum_{i+j=k} \beta(i,j) n_i n_j - \alpha n_k \sum_{i=1}^c \beta(i,k) n_i \quad (7.1)$$

Where i, j , and k denote particle size categories; c is the maximum number of size categories; n_i, n_j , are the number concentration of particle sizes i and j , respectively and θ_k is the generation rate of particle size category k from the successful collision of particle size category i and j ; $\beta(i,j)$ is the collision frequency. The first term on right hand side of the equation represents the rate of generation of particle size category k from the collision of particle size class i and j whereas the second term represents loss of particle

size class k due to the collision with other size categories. The first term is multiplied by the $\frac{1}{2}$ to avoid double counting (Ernest et al. 1995; Lawler 1979; Logan and Kilps 1995).

According to Equation (7.1), the rate of particle aggregation depends not only on the collision efficiency but also on the collision frequency. Collision frequency depends on the hydrodynamic condition of the water column that determines the contact mechanisms through which particles collide with each other. Three types of contact mechanisms are dominant in the aquatic environments: a) Brownian motion which leads to random movement of particles in the water column, b) fluid shear, i.e., velocity gradient, and c) differential sedimentation arisen from the differential settling velocity of individual particles which forces particles to come close together. Total collision frequency is assumed to be the sum of contributions from each mechanism. Collision frequency introduced through these mechanisms depends on particle's type, size, shape and density, water temperature, etc.

Most of the flocculation model uses Euclidian geometry to describe both primary and aggregated particles. But aggregated particles in natural systems are fractal objects (Li and Ganczarczyk 1989). Therefore, their kinetics needs to be characterized through fractal geometry. The density of fractal aggregates decreases as aggregate size increases whereas aggregate porosity increases as the size of the aggregate increases, under the fixed fractal dimension. These are the core characteristics of fractal aggregate. Jiang and Logan (1991) have developed set of equations for the characterization of aggregates using fractal geometry. These equations together with the Equation (7.1) describe the aggregation kinetics of fractal aggregates which need to be modeled for understanding

the particle dynamics in field scale settings.

Corpus Christi (CC) Bay (TX, USA), a National Science Foundation-sponsored test bed for implementation of Coastal Margin Observation and Assessment System (CMOAS), experiences periodic hypoxia during summer months (Montagna and Kalke 1992; Ritter and Montagna 1999; Hodges and Furnas 2007). Islam et al. (2008) found higher biochemical oxygen demand (BOD) around the area of the bay where hypoxia was observed. The longer the oxygen-consuming particles remain in the water column, greater amounts of oxygen will be consumed. Therefore, understanding of particle dynamics can provide insight regarding the dissolved oxygen condition in the water column. Various researchers use natural radionuclide such as ^{234}Th , ^7Be as tracers for the determination of particulate flux and particle residence time in the water column (Schmidt et al. 2002 ; Amiel et al. 2002; Feng et al. 1999) . Since residence time depends on the hydrodynamic condition of the system, it may change quite frequently in a dynamic system like CC Bay. In addition, the use of tracer in resolving particle dynamics will not be able to clarify particle size dynamics and aggregation phenomenon which have greater implications for understanding the health of ecosystems.

Therefore, a three-dimensional PAT model was developed and thereby, particle transport behavior can be studied under the normal hydrodynamic condition of CC Bay. The model performance is evaluated against the analytical solution for the transport of polydispersed particles in the water column. In addition, several simulation studies were conducted to understand the significance of aggregation processes in controlling residence time of particles in the water column. These studies shed light on the

importance of vertical transport processes in inducing vertical dissolved oxygen gradients in the south-east part of the bay.

Modeling Background

Ernest et al. (1995) developed the framework for modeling aggregation dynamics of particles where they used Euclidian geometry to characterize particles. But estuarine sediment particle's aggregation kinetics need to be described using fractal geometry as most of the natural aggregates are fractal in nature. The mass of fractal aggregates can be described using the power law relationship (7.2):

$$m \propto l^{D_F} \quad (7.2)$$

Where m is the aggregate mass, D_F is the fractal dimension and l is the characteristic length of aggregate. Fractal dimension (D_F) signifies the structure of the aggregate. A higher value of D_F indicates a more compact structure of the aggregate. The value of D_F varies in the range of 1.0 to 3.0 for aquatic aggregates (Jiang and Logan 1991; Li and Ganczarczyk 1989; Logan and Wilkinson 1991; Wiesner 1992, Jackson et al. 1997). According to Jiang and Logan (1991), the characteristic length of a fractal aggregate is the longest aggregate length. The number (N) of spherical monomers with diameter d_0 that can combine together to form fractal aggregates of encased diameter d can be described by the following Equation (7.3) (Feder 1988):

$$N = \zeta \left(\frac{d}{d_0} \right)^{D_F} \quad (7.3)$$

Where ζ is a packing factor indicating how monomers are packed. This equation applies

only in the limit $d/d_0 \gg 1$. The value of ζ depends on shapes of both fractal aggregates and monomers, and on the way of packing.

Lee et al. (2000) used coalesced fractal sphere (CFS) assumption to model the kinetics of estuarine sediment particles where he considered $\zeta=1$ (i.e., no pore space in the aggregate due to packing effects). However, there will still be pore spaces within the aggregate due to fractal nature which relies on the fundamental aggregation process. This source of pore spaces is more significant than that is induced from the packing factor (Lee et al. 2000). Others CFS assumption include: a) the fractal aggregate consist of a single type of compact spherical particles, b) aggregates have same fractal dimension irrespective of particle sizes and c) the aggregate formed from the collision of two aggregates has the same fractal dimension as the colliding aggregates and the solid volume of new aggregate equals the sum of solid volumes of the colliding aggregates. Lee et al.(2000) simplified Jiang and Logan's (1991) original governing equations for fractal aggregates through these assumptions and the assignment of particular values to the following parameters: primary particle shape factor, $\zeta_0=\pi/6$, aggregate area shape factor, $\zeta_2=\pi/4$, fractal frequency functions constants 'a' and 'b' as $a=24$ and $b=1$. This simplification permits to describe the complex real aggregates with simple governing equation as shown in Table 7.1 and allows to use Jiang and Logan's (1991) extensive fractal theory for the application of real-world coagulation kinetics model.

Table 7.1 Basic equations for fractal aggregates under the coalesced fractal sphere assumption (Lee et al. 2000)

Description	Equations
Solid mass	$m = \frac{\pi}{6} \rho_0 d_0^{3-D_F} d^{D_F}$
Solid volume	$v_s = \frac{\pi}{6} d_0^{3-D_F} d^{D_F}$
Aggregate diameter	$d = \left(\frac{\pi}{6}\right)^{-1/3} v_0^{1/3-1/D_F} v_s^{1/D_F}$
Density	$\rho = \rho_0 \left(\frac{d}{d_0}\right)^{D_F-3}$
Porosity	$\varepsilon = 1 - \left(\frac{d}{d_0}\right)^{D_F-3}$
Settling velocity	$U = \frac{g}{18\mu} \left(\frac{\rho_0 - \rho_w}{\rho_w}\right) d_0^{3-D_F} d^{D_F-1}, (2 \leq D_F \leq 3)$ $U = \frac{g}{18\mu} \left(\frac{\rho_0 - \rho_w}{\rho_w}\right) d d_0, (D_F \leq 2)$

Under CFS assumption, collision frequency due to three different contact mechanisms (i.e., Brownian motion, fluid shear and differential settling velocity) can be described by the equation (7.4) (Lee et al. 2000) :

$$\beta_{BR}(v_i, v_j) = \frac{2kT}{3\mu} \left(v_i^{1/D_F} + v_j^{1/D_F} \right) \left(v_i^{-1/D_F} + v_j^{-1/D_F} \right) \quad 7.4(a)$$

$$\beta_{SH}(v_i, v_j) = \frac{G}{\pi} v_0^{1-3/D_F} \left(v_i^{1/D_F} + v_j^{1/D_F} \right)^3 \quad 7.4(b)$$

$$\beta_{DS}(v_i, v_j) = \frac{g}{12\mu} \left(\frac{\pi}{6}\right)^{-1/3} \left(\frac{\rho_0 - \rho_w}{\rho_w}\right) v_0^{1/3-1/D_F} \left(v_i^{1/D_F} + v_j^{1/D_F}\right)^2 \quad 7.4 (c)$$

$$\times \left| v_i^{(D_F-1)/D_F} - v_j^{(D_F-1)/D_F} \right| \quad (2 \leq D_F \leq 3)$$

$$\beta_{DS}(v_i, v_j) = \frac{g}{12\mu} \left(\frac{\pi}{6}\right)^{-1/3} \left(\frac{\rho_0 - \rho_w}{\rho_w}\right) v_0^{4/3-3/D_F} \left(v_i^{1/D_F} + v_j^{1/D_F}\right)^2 \quad 7.4 (d)$$

$$\times \left| v_i^{1/D_F} - v_j^{1/D_F} \right| \quad (D_F \leq 2)$$

Where, β_{BR} , β_{SH} and β_{DS} are collision frequencies due to Brownian motion, fluid shear and differential settling, respectively. Here k is the Boltzmann's constant, T is absolute temperature (K), μ dynamic viscosity, ρ_0 and ρ_w are density of primary particles and density of water, respectively; G average velocity gradient, g is the gravitational constant, and v_0 , v_i and v_j are the solid volumes of the primary particle, particle size i and j , respectively.

Ernest et al. (1991) developed a nonlinear parameter estimation algorithm (PARAMEST) to extract model collision efficiency (α) through the minimization of variation between model predictions and observations via the iterative numerical determination of the functional minima of the model with respect to α . Sterling et al. (2005) used this algorithm to determine α values for crude oil, silica and clay particles. They also extended Lee's (2000) fractal aggregation model for the incorporation of primary particles of different densities, and estimated collision efficiencies for two-particle type systems using the PARAMEST algorithm (Sterling et. al 2004). Once α and β are determined, the aggregation rate then can be resolved using Equation (7.1).

Model Development

Lee et al. (2000) combined the fractal aggregation kernel with the transport equation to characterize the particle dynamics in a lab-scale experimental settling water column. Their model is extended in this research work for application in the field. The governing equation for the PAT model to simulate the particle dynamics in three-dimensions can be described as follows in Equation (7.5):

$$\frac{\partial n_k}{\partial t} = -\frac{\partial un_k}{\partial x} - \frac{\partial vn_k}{\partial y} - \frac{\partial (w+w_s)n_k}{\partial z} + \frac{\partial (K_x \frac{\partial n_k}{\partial x})}{\partial x} + \frac{\partial (K_y \frac{\partial n_k}{\partial y})}{\partial y} + \frac{\partial (K_z \frac{\partial n_k}{\partial z})}{\partial z} + \theta_k \quad (7.5)$$

Where n_k is the number concentration of particulate at size k and θ_k represents the net rate of generation of particle size class k from the successful collision of particle size class i and j as described in equation (7.1); K_x, K_y and K_z are the dispersion coefficients whereas u, v, w are the fluid velocities in the x, y and z direction, respectively and w_s is the particle settling velocity. The major assumptions considered in the formulation of PAT model come from the assumption of Smoluchowski's equation and the CFS assumption. They are as follows: i) particles are aggregated due to the binary collisions only; ii) no breakage of particles occur; iii) α does not depend on particle size and is constant in the system; iv) particle collision mechanisms are modeled using the CFS assumption and v) rectilinear motions are assumed for the determination of collision functions while curvilinear effects (Han and Lawler 1992) due to hydrodynamic and inter-particle forces between colliding particles are neglected. In addition, it is considered that the particle volume of the largest size category is conserved after attachment with the same or smaller size particles. This kind of attachment leads to the increase in the

volume of the largest category by some fractional number equivalent to the volume of smaller particle.

The partial differential equation (7.5) is converted into an algebraically-solvable equation for each particle size category using Thomann's finite segment method which is essentially a finite difference approximation of differential equations (Thomann 1972). one of the advantages of this method is that it can be applied for systems of variable segment size or many coupled state variables. In this method, the entire computational domain is subdivided into several finite segments, and the gradient within each segment is assumed insignificant to conserve mass. The Forward-Time Central-Space (FTCS) scheme is used to discretize the governing equation to eliminate numerical dispersion. Moreover, dispersion coefficients are considered variable in discretizing the transport part of the governing equation as Ojo et al. (2006) found from their dye study experiments in Corpus Christi Bay that dispersion coefficients significantly vary within spatial and temporal scale of interest for transport processes. The discretised equations for each size category are then numerically integrated using the fourth-order Runge-Kutta method to determine particle size spectra in the computational domain.

The selection of suitable time step and segment size is critical in maintaining the solution stability and increasing the solution accuracy while keeping the computational time reasonable. A common practice in the development of time-variable finite-segment models is to fix the spatial grid first and then select the time step (Thoman 1973). The segment size of spatial grid in this model was selected by considering the solution positivity constraint which requires positive concentration at every point. Thomann and

Mueller (1987) showed the positivity criteria for the one dimensional estuary as described in Equation (7.6):

$$\Delta x < 2 \frac{K_x}{u} \quad (7.6)$$

where Δx is the segment size in the x-direction. For the three-dimensional case, the grid size in each direction can be selected using this relationship while considering values of dispersion coefficients and velocities in the respective direction.

The stability of the solution needs to be considered while selecting the time step. Hindmarsh et al. (1984) used von Neumann stability analysis to determine the conditions of a stable solution for the transport of conservative material and suggested the following condition (7.7) for the stable solution:

$$\frac{K_x * \Delta t}{\Delta x^2} + \frac{K_y * \Delta t}{\Delta y^2} + \frac{K_z * \Delta t}{\Delta z^2} \leq \frac{1}{2} \quad (7.7)$$

This condition resulted a stable solution where error will not grow, but oscillate. Setting the right hand side of the inequality value to 1/4 will prevent oscillation (Chapra and Canale 1988) and assignment of the inequality value to 1/6 will minimize truncation error (Carnahan et al. 1969). The time step determined from this restriction is used as the maximum time step. The minimum time step is set up considering the computational power used and the simulation time period. The actual time step for our particle aggregation and transport model is optimized using maximum and minimum time step that yield positive concentration between successive integration.

Study Area of Interest

Three-dimensional PAT model developed in this study has been applied to understand the particle dynamics in the southeast part of CC Bay (Montagna and Kalke 1992; Ritter and Montagna 1999). This bay is located on the Texas coastline and covers an area of approximately 432.9 sq. km (Flint 1985). Figure 7.1 shows the characteristic features of the bay. The study area where the model has been applied to characterize particle dynamics is indicated by the black rectangle in the figure. This bay is connected to the Gulf of Mexico through a narrow ship channel (15m depth), which runs from east

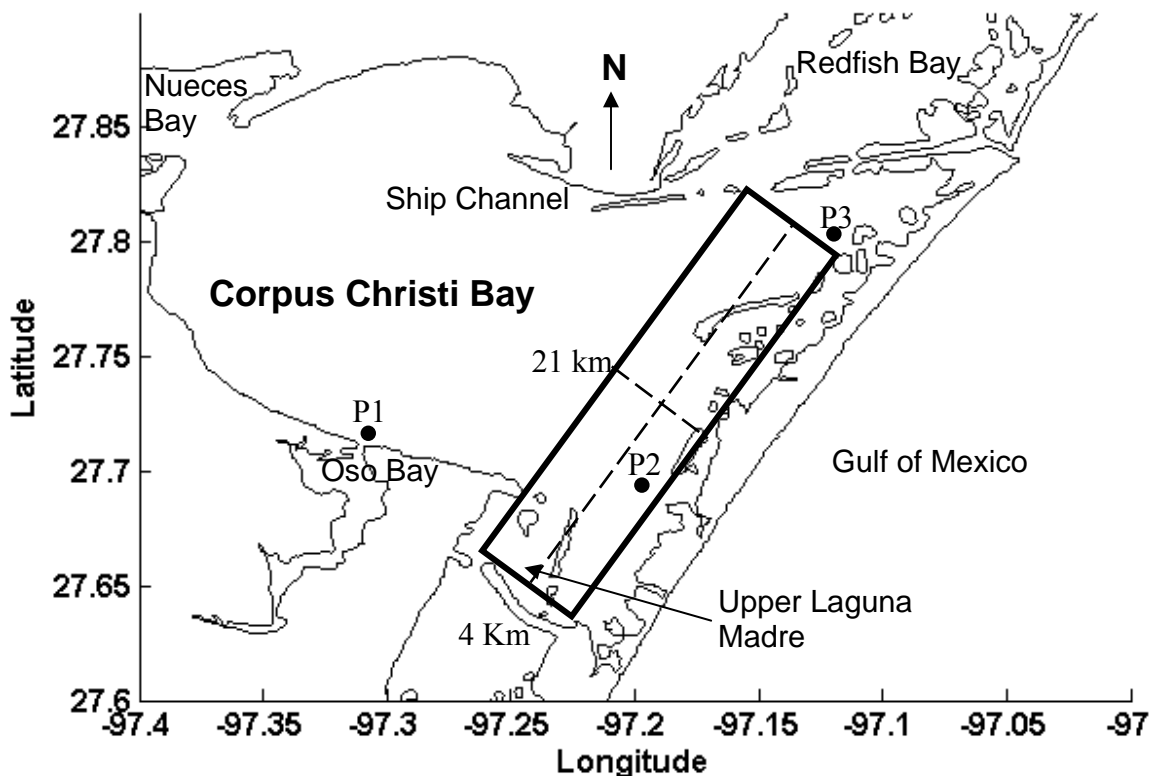


Fig.7.1 Map of Corpus Christi Bay and surrounding water bodies. Note: The black rectangle indicates the study area for particle aggregation and transport model development; ●- location of fixed robotic monitoring platforms.

to west. It is surrounded by four water bodies, namely Oso Bay in the southwest, Nueces Bay in the northwest, Upper Laguna Madre in the south and Redfish Bay in the northeast. The three solid circles on the figure denote the locations of our fixed robotic monitoring platforms in the bay. Sensor systems are installed on those platforms (labeled 'P1', 'P2' and 'P3') for the continuous measurements of hydrodynamic, meteorological and water quality parameters. Islam et al. (2008) suggested that the characterization of particle dynamics in the southeast portion of the bay (rectangular box area shown in Fig. 7.1) will help in the greater understanding of the processes causing hypoxia in this part of CC Bay. They found significant levels of biochemical oxygen demand (BOD) at several locations in the upper Laguna Madre (lower portion of the rectangular box area) whereas BOD values were insignificant at the other areas of the bay. Also, they showed significant particle load gradients which were correlated to BOD and DO dynamics. Moreover, they observed a salinity gradient along the longitudinal axis of the rectangle box area which suggests that gravity induced flow dominant in this part of the bay. This gravity flow causes denser saline water to flow from the upper Laguna Madre towards the bay along the seafloor, whereas less saline water moves along the water surface in the reverse direction. Therefore, understanding particle dynamics in the rectangular box will help to elucidate the effect of dominant transport mechanisms on particle residence time and size distribution in the water column.

Data Observation Methods

We have developed a robotic profiler system for the continuous measurements of

water quality parameters at different levels of water column. This profiler system is installed on each of our fixed robotic platforms in Corpus Christi Bay (Fig. 7.1). The instruments currently deployed on this profiler are a particle sizer (LISST 100X, by Sequoia Sciences), a DO sensor (Optode, by Aanderaa), a CTD (Conductivity, Temperature and Depth) sensor (SBE 37 SIP, by Sea-Bird Electronics, Inc.) and a fluorometer (Eco-FL3, by WET Labs). Along with these water quality sensors, an upward-looking acoustic Doppler Current Profiler (ADCP, by Teledyne RDI) and meteorological sensors are installed on each fixed robotic platform. Each ADCP is configured to measure a vertical profile at every five minutes, where each profile is measured from an ensemble of 45 pings, and the time between pings is one second. In addition to water currents, the ADCP can also measure acoustic backscatter intensity, waves and other hydrographic information. The details of the monitoring systems installed on fixed robotic platform are discussed in Islam et al. (2009a).

Another type of monitoring system was configured on our mobile platform (research vessel) that could acquire and visualize data measured by various submersible sensors on an undulating tow-body deployed behind a research vessel. The mobile monitoring platform contains the similar suite of instruments as installed on the robotic profiler system. In addition, a Global Positioning System (GPS) has been used to georeference the synchronized measurements of measured parameters. Along with this system, we have installed a downward-looking ADCP on the vessel to measure the vertical profile of water currents. Real-time display of the measured parameter intensity (measured value relative to a pre-set peak value) guides in selecting the transect route to

capture the event of interest during the research cruises in CC Bay. Islam et al. (2009b) discusses details about the development and implementation of this system in monitoring water quality and hydrodynamic parameters in the bay.

Model Error Analysis

The understanding of the error associated with model predictions is essential for assessing model performance in simulating real-world conditions of the water column. There are two kinds of errors associated with model prediction: i) errors involved due to the assignment of erroneous model coefficients and ii) errors resulted from the discretization of the governing equations which introduce error due to numerical approximation of the differencing. The former error can be reduced through the determination of accurate model coefficients such as velocity and dispersion coefficients whereas the later one can be reduced through the selection of proper time step, segment size and discretization algorithm. The error involved from the second source can be quantified through comparison of model predicted value against the analytical solution of the closed-form which does not contain any discretization error. Ojo et al. (2007b) evaluated the performance of his conservative constituent transport model in tracking the transport of a dye patch through the comparisons of model results against the analytical solution of the closed form. Since there are concerns regarding the transport of various particle sizes, the PAT model prediction has been evaluated against the analytical solution for the transport of polydispersed particles in a three-dimensional water column.

The analytical solution for a pulse discharge of mass, M (sc) of particle size, sc in a domain with infinite boundary can be described by the equation (7.8) (Ojo et al. 2007b):

$$C(sc, x, y, z, t) = \frac{M(sc)}{8(\pi)^{3/2} (K_x K_y K_z)^{1/2} t^{3/2}} \exp \left[-\frac{1}{4} \left\{ \frac{(x-ut)^2}{K_x t} + \frac{(y-vt)^2}{K_y t} + \frac{(z-wt-w_s(sc)t)^2}{K_z t} \right\} \right] \quad (7.8)$$

where C (sc, x, y, z, t) is the concentration of particle size sc at a distance of x, y, z , from the point of discharge. If polydispersed particles are not allowed to aggregate, the total concentration of particles at a point will be the sum of the concentration determined at that point for each size category using Equation (7.8). The comparison of this concentration at different points of the domain with that of the model-predicted value gives an idea about the amount of numerical error involved in model discretization, and thereby assists in understanding the model accuracy limit.

The analytical solution described in the previous paragraph was used to validate the numerical accuracy of the PAT model developed in this study. The PAT should be simulated under specific conditions to imitate the analytical problem. The boundaries of the computational domain must be at an infinite distance from the point of discharge. The dimension of the CC Bay study area is 4 km x 21 km x 4.6 m (Fig. 7.1). The vertical dimension is much smaller than that of horizontal dimensions and pulsed discharge of particles can be transported to the bottom in short time. This violates the infinite boundary requirement for the analytical solution. Therefore, we considered the larger vertical dimension (15.2m) than the actual depth of the water column. A certain mass of polydispersed particles are pulsed discharged at a point (2km x 10.25km x 4.6m)

of the computational domain, and model results are compared with that of calculated from the analytical solution. This comparison between analytical and model results is valid as long as particles remain far away from the boundary which guarantees the infinite boundary requirement of the analytical solution. Also, the collision efficiency must be assigned to zero, and fractal dimension D_F is set to 3.0 for the simulation of the analytical problem. In addition, the particle shape is considered spherical in the model. This satisfies the requirement for the use of Stoke's equation in calculating the particle settling velocity.

Particles considered for the simulation studies are estuarine sediments collected at three different sites in New Bedford Harbor, MA, and particle density was experimentally determined as 1.7 gm/cm^3 (Sanders 1990). This density ensures representation of lighter biogenic particles (e.g., phytoplankton, $p_p \approx 1.05 \text{ gm/cm}^3$) as well as heavier estuarine particles of inorganic origin (e.g., clay, $p_p \approx 2.5 \text{ gm/cm}^3$). Sixteen discrete size categories over a particle size range of $2.0\text{--}67 \mu\text{m}$ are used in the simulation. The mass of particles in each size category used in simulation is set using the experimentally determined particle size distribution for New Bedford Harbor estuarine sediments (Lee, D.G. 1996). Although advection and dispersion coefficients are variable in the bay (Ojo et al. 2006), constant representative values of these coefficients in CC Bay are used to simulate the analytical problem. The longitudinal and lateral dispersion coefficients used are $3 \times 10^5 \text{ cm}^2/\text{s}$ and $3 \times 10^4 \text{ cm}^2/\text{s}$, respectively. These are the median values of the coefficients derived from a previous dye study in CC Bay (Ojo et al. 2006). Since there are no data for the vertical dispersion coefficient in CC Bay, this coefficient

is set to $3.2 \text{ cm}^2/\text{s}$ which was determined by Lee, D.G. (1996) through settling column experiments in the laboratory under the velocity gradient (G) of 20 S^{-1} . The parameters u, v, w are assigned as $5.0 \text{ cm/s}, 10.0 \text{ cm/s}$ and 0.05 cm/s , respectively. The segment size for each cell of the computational domain is set to $100\text{m} \times 250 \text{ m} \times 0.2\text{m}$ considering the numerical stability and accuracy constraint as described by Equations (7.6) and (7.7). The centers of model segments were initialized with particle concentrations for each size category at ten minutes after the pulsed discharge of particles at location of $2\text{km} \times 10.25\text{km} \times 4.6\text{m}$. These concentrations are calculated using the analytical solution. Figure 7.2(a) and Figure 7.2(b) show the initial ($t=10 \text{ min.}$) vertical profile of the total particle concentration along the longitudinal and lateral line (shown as dotted line in study area, Figure 7.1), respectively.

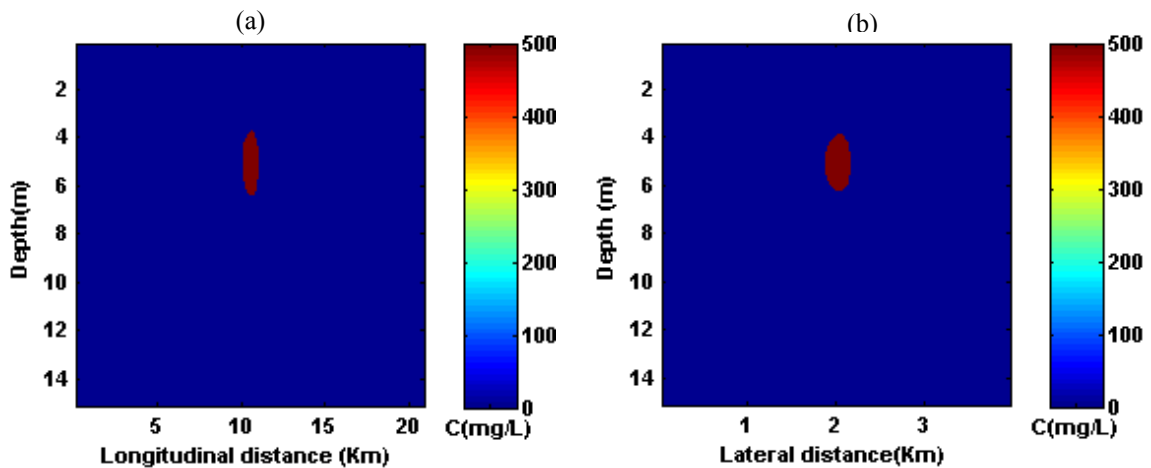


Fig. 7.2 Initial ($t = 10 \text{ min.}$) vertical profile of the total particle concentration along the longitudinal and lateral line (shown as dotted line in Figure 7.1), respectively.

The model was simulated under the conditions outlined in the previous paragraphs and model results are compared with the analytical solution. Figure 7.3(a), 7.3(b) and 7.3(c) show total particle concentration distribution along the longitudinal line after 20 min., 40 min., and 60 min. of model simulations, respectively. Figures 7.3(d), 7.3(e) and 7.3(f) show the similar variation as calculated using the analytical solution at 20 min., 40 min. and 60 min., respectively. From these figures, it is evident that model was able to successfully capture the vertical particle variation along the longitudinal direction. Although it seems from these figures that vertical dispersion is much greater than that of the longitudinal dispersion, the opposite is the reality. In these figures, horizontal scale is in kilometer whereas vertical scale is in meter. In spite of smaller vertical dispersion coefficient, vertical transport is very significant as this mechanism dominates the contaminant exposure time in the water column. In the above figures, particles dispersed in a significant area of the water column and reached closer to the boundary of the computational domain within sixty minutes of simulation.

Model-predicted particle distributions along the lateral direction at 20 min., 40 min. and 60 min. are shown in Figures 7.4(a), 7.4(b), 7.4(c), respectively; whereas the similar distribution obtained from the analytical solution are shown in Figures 7.4(d), 7.4(e) and 7.4(f), respectively. Again, model predicted concentrations agree reasonably well with that of analytical solution and this proves the capability of the developed numerical model in capturing the particle dynamics in three-dimensional field. The analysis of the model performance under the influence of the aggregation process will

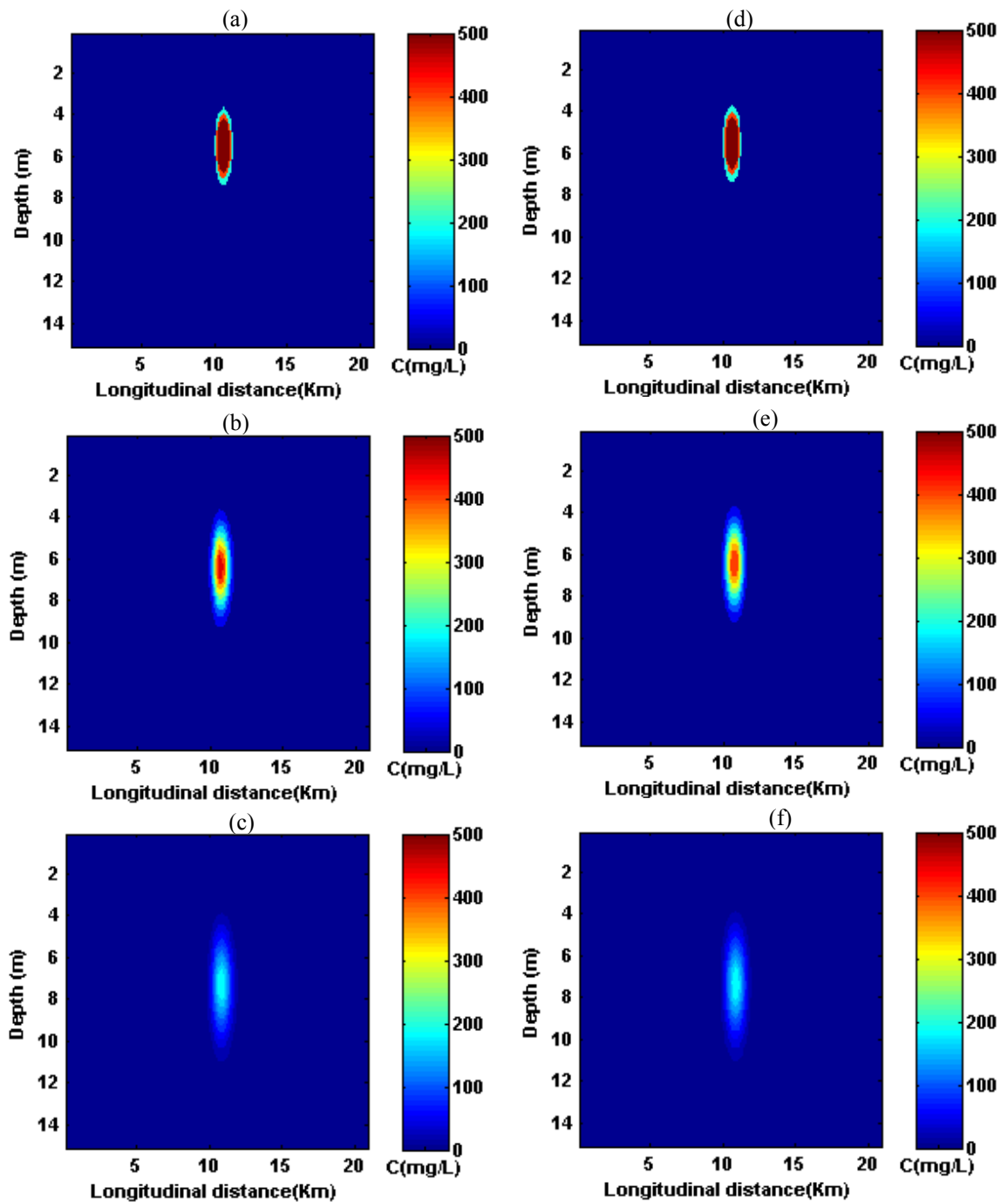


Fig. 7.3 Vertical profile of model-computed total particle concentration along the longitudinal line (shown in Fig. 7.1) at simulation time of a) 20 min., b) 40 min., and c) 60 min., respectively; Similar profile calculated using analytical solution at d) 20 min., e) 40 min. and f) 60 min., respectively.

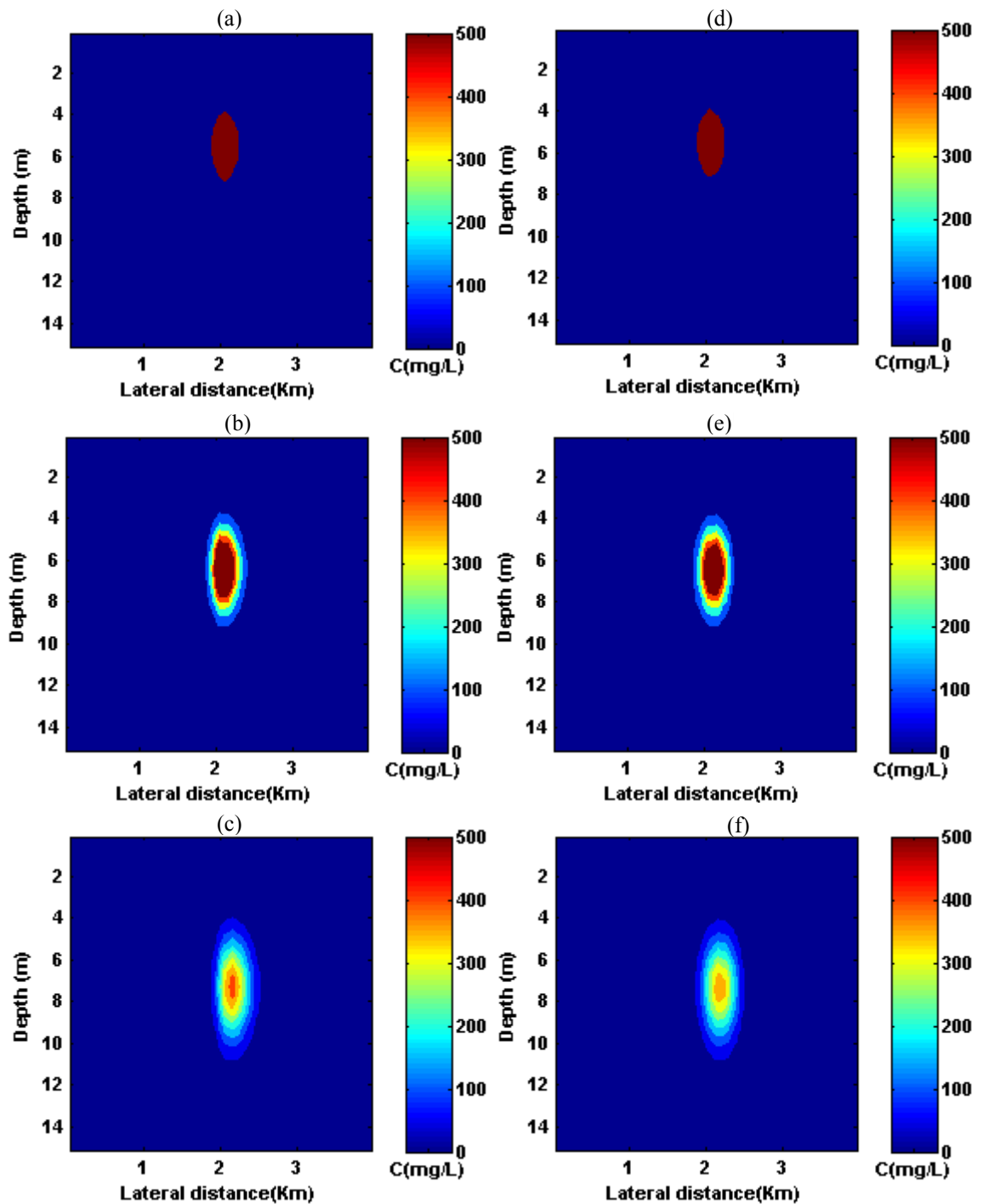


Fig. 7.4 Vertical profile of model-computed total particle concentration along the lateral line (shown in Fig. 7.1) at simulation time of (a) 20 min., (b) 40 min., and (c) 60 min., respectively; Similar profile calculated using analytical solution at (d) 20 min., (e) 40 min. and (f) 60 min., respectively.

shed more light about the capability of the model in predicting real time dynamics of particle distribution in the bay.

Results and Discussion

We have performed several simulation studies with the developed PAT model to understand the aggregation effect on particle residence time in the water column. The observational data from our monitoring platforms provide guidance in setting the initial and hydrodynamic condition for the model simulation. The vertical variation of total particle concentrations along the transect route of the research cruise (July 24, 2007) is shown on Figure 7.5; the actual cruise route is depicted on the figure inset plot. The route line is color-coded and correlates with the horizontal color-coding along the top and bottom of Figure 7.5, thus matching the observed data with the spatial location in the bay. Observed particle concentrations are displayed in a color range from blue to red, assigning particle concentrations ≥ 70 $\mu\text{l/l}$ as dark red. From this figure, it is clear that particle concentrations are high (~ 40 $\mu\text{l/l}$) in the upper Laguna Madre (x-axis: $t=0\sim 1000$ sec) whereas the concentrations are low (~ 10 $\mu\text{l/l}$) in the other part of the bay except near the bottom around platform 'P2' (x-axis: $t=3000\sim 4000$ sec). Using an average particle density as 1.7 gm/cm^3 , a particle volume concentration of 40 $\mu\text{l/l}$ is then converted into 68 mg/l in weight unit whereas 10 $\mu\text{l/l}$ is converted into 17 mg/l . This particle concentration distribution was used in initialization of the model for each simulation. Neglecting particle concentration variation along the lateral direction, the initial condition assigned in the model for the vertical distribution of particle

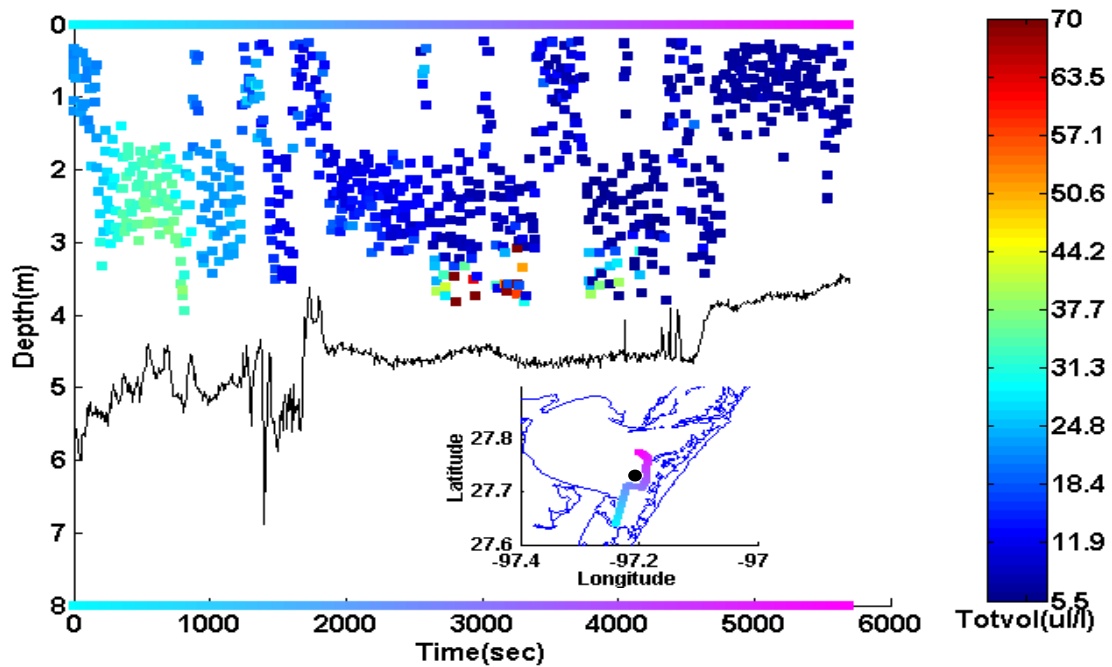


Fig. 7.5 Vertical profile of total particle concentration along the transect route of the July 24, 2007 research cruise; inset plot displays the transect route; (color-coded ■: Total Particle concentration ($\mu\text{l/l}$); ●: Platform 'P2' location; —: sea-bed profile).

concentration along the longitudinal direction is shown in Figure 7.6. The value of the fractal dimension (D_F) is selected as 2.5, considering the range of fractal dimension variation in aquatic systems as reported by previous researchers. Logan and Wilkinson (1991) determined the value of the fractal dimension for microbial aggregates as high as 2.66 and 2.99 whereas Jackson et al. (1995) estimated this value for algal aggregates as 2.3. The past researchers in our group found fractal dimension values for clay and silica to vary in the range between 2.6 and 3.0 (Sterling et al. 2005). The other important parameter, alpha (α), can take any value between 0 to 1.0 depending on the degree of particle destabilization which relies on many factors ranging from the nature of particle

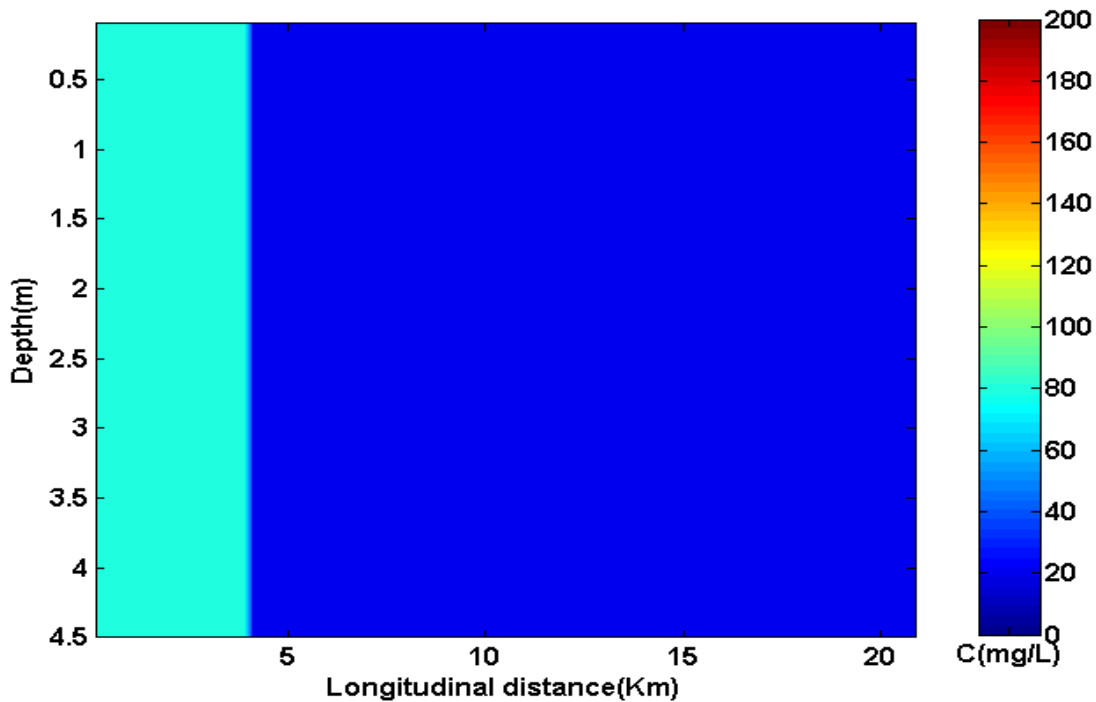


Fig. 7.6 Initial vertical profile of total particle concentration along the longitudinal line (shown in Fig. 7.1) for the model simulation.

to the environmental condition such as salinity level, flow regime etc. Using the estuarine sediment particles in batch flocculation and vertical settling studies, Sanders (1990) determined the value of α that varied from 0.002 to 0.4. In our simulation studies, we varied the value of α and tried to understand the aggregation effect on particle dynamics.

We conducted several simulation studies with our PAT model and are presenting results from two simulations that shed light regarding the effect of particle aggregation in controlling particle residence time within the water column. In addition to model simulation conditions outlined in the previous paragraph, α was assigned to zero in the first simulation. This ensures that the particles are not able to aggregate and are

transported as non-interacting particles in the water column. Under this condition, transport dynamics are controlled by advection and diffusion processes only. Figures 7.7(a), 7.7(b), 7.7(c) and 7.7(d) present the model-computed vertical variation of total particle concentrations along the longitudinal line (shown in Figure 7.1) after 20 min., 40 min., 90 min. and 180 min. of simulation, respectively. Vertical profiles of particle concentrations shown in these figures clearly emphasize the importance of the vertical

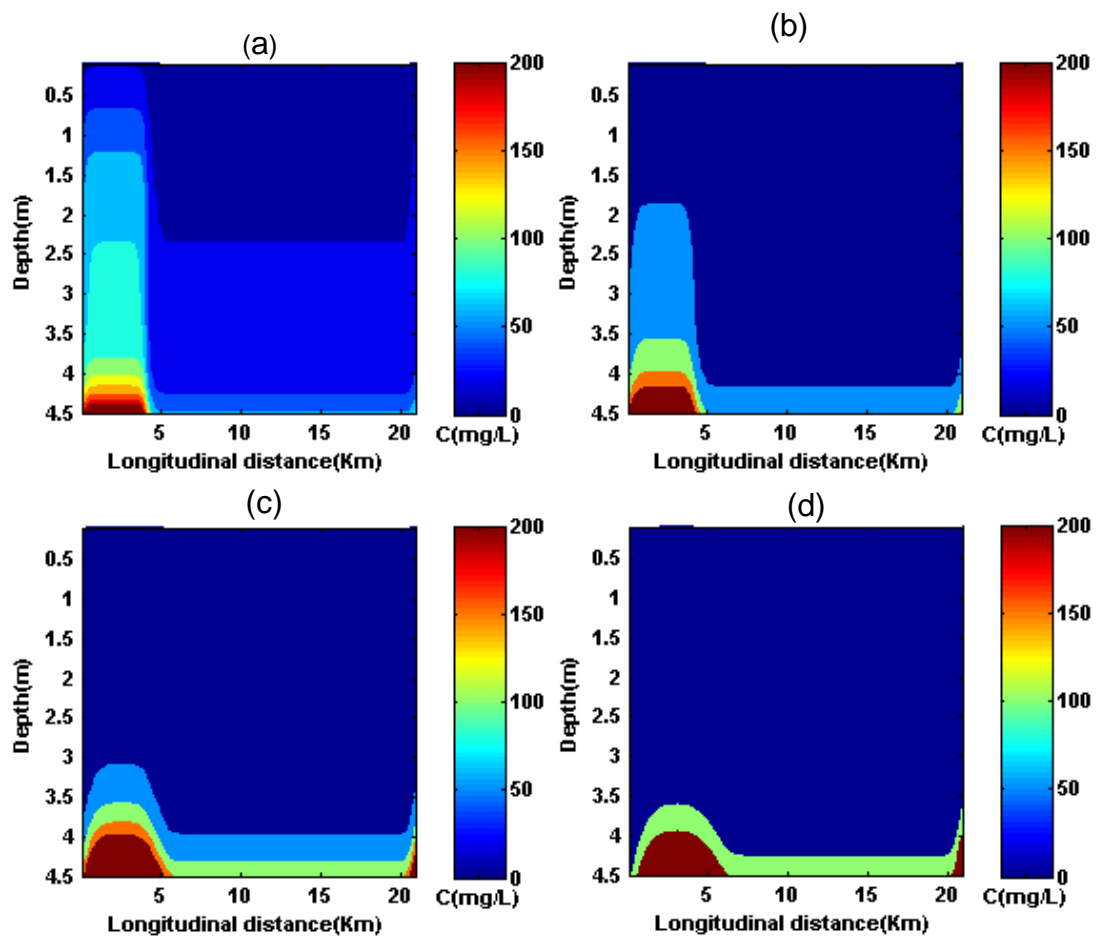


Fig. 7.7 Model-computed vertical variation of total particle concentration along the longitudinal line (shown in Fig. 7.1) after a) 20min., b) 40 min., c) 90 min. and d) 180 min. of simulation, respectively; $\alpha=0$.

transport process in determining the particle residence time in the water column. Most of particles settle close to the bottom within hours of simulation (i.e., 180 min.). Therefore, resolving the vertical advection and dispersion coefficients are key for the successful implementation of the PAT model in predicting particle dynamics in the bay.

Figure 7.8 displays the profile of the measured vertical component of fluid velocity at platform 'P2' for 38 hours from the beginning of our model simulation. The starting time of our model simulation was 10:00 am on July 24, 2007, when we started our cruise from the upper Laguna Madre. In this figure, the positive velocity magnitude represents the downward direction of the velocity component whereas the negative velocity magnitude indicates the opposite. There is a wide fluctuation in observed velocity magnitude which can significantly impact model stability and output. Measurement errors associated with low vertical velocity and the effect of turbulent eddies on instantaneous velocity measurements suggest that observed vertical velocity cannot be used directly in the model simulation. The post-processing of instantaneous observed velocities and their assimilation with the numerical hydrodynamic model provide representative hydrodynamic conditions of the bay for simulation of the PAT Model. However, time series of instantaneous observed data can still provide insight regarding the average hydrodynamic condition of the bay, which can be used for various hypotheses testing for greater understanding of the processes controlling particle dynamics in the bay. A vertical velocity of 0.5 mm/s was used in the model simulation.

In the second simulation, all conditions remained same as in the first simulation, except particles were allowed to interact with each other; the value of α was assigned as

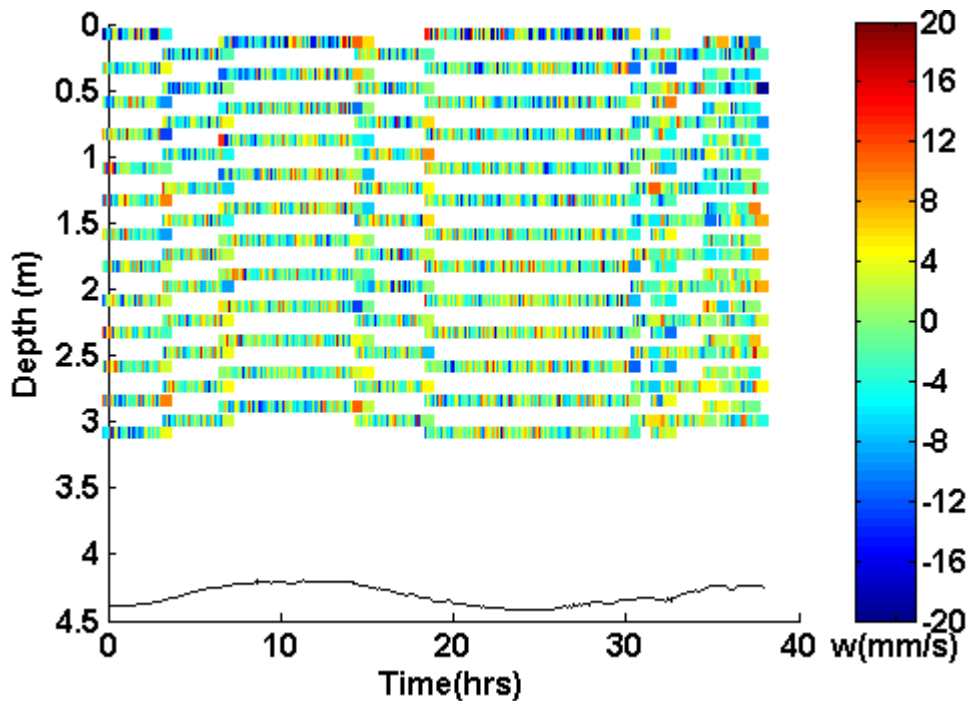


Fig. 7.8 Observed vertical component of fluid velocity at Platform ‘P2’ for 38 hours (starting at 10 am) on July 24, 2007; the wavy solid line denotes the depth of the sea-bed at platform ‘P2’.

0.1. As smaller particles aggregate into larger ones, their settling velocities change and so does the particle residence time in the water column. Figures 7.9(a), 7.9(b), 7.9(c) and 7.9(d) display the vertical variation of particle concentrations along the longitudinal line (shown in Fig. 7.1) after 20 min., 40 min., 90 min. and 180 min. of simulation, respectively. Comparing Figures 7.7 and 7.9, it is evident that the aggregation process has significantly controlled the particle water column residence time. Most particles settle close to the bottom within forty minutes of simulation for the aggregation case, whereas they take more than ninety minutes to reach the bottom if not allowed to aggregate. Settled particles may remain at the bottom or can be transported as bed load.

The existence of high concentrations of dead organic particles at the bottom may induce hypoxia as oxygen is consumed during decomposition. When the water column is stratified, highly aerated surface water may not reach the bottom while high concentrations of organic particles continue to exert oxygen demand on the bottom water and reduce oxygen levels. Simulation results from this study also help to explain the transitory nature of observed hypoxic events at the south-east part of the bay that have

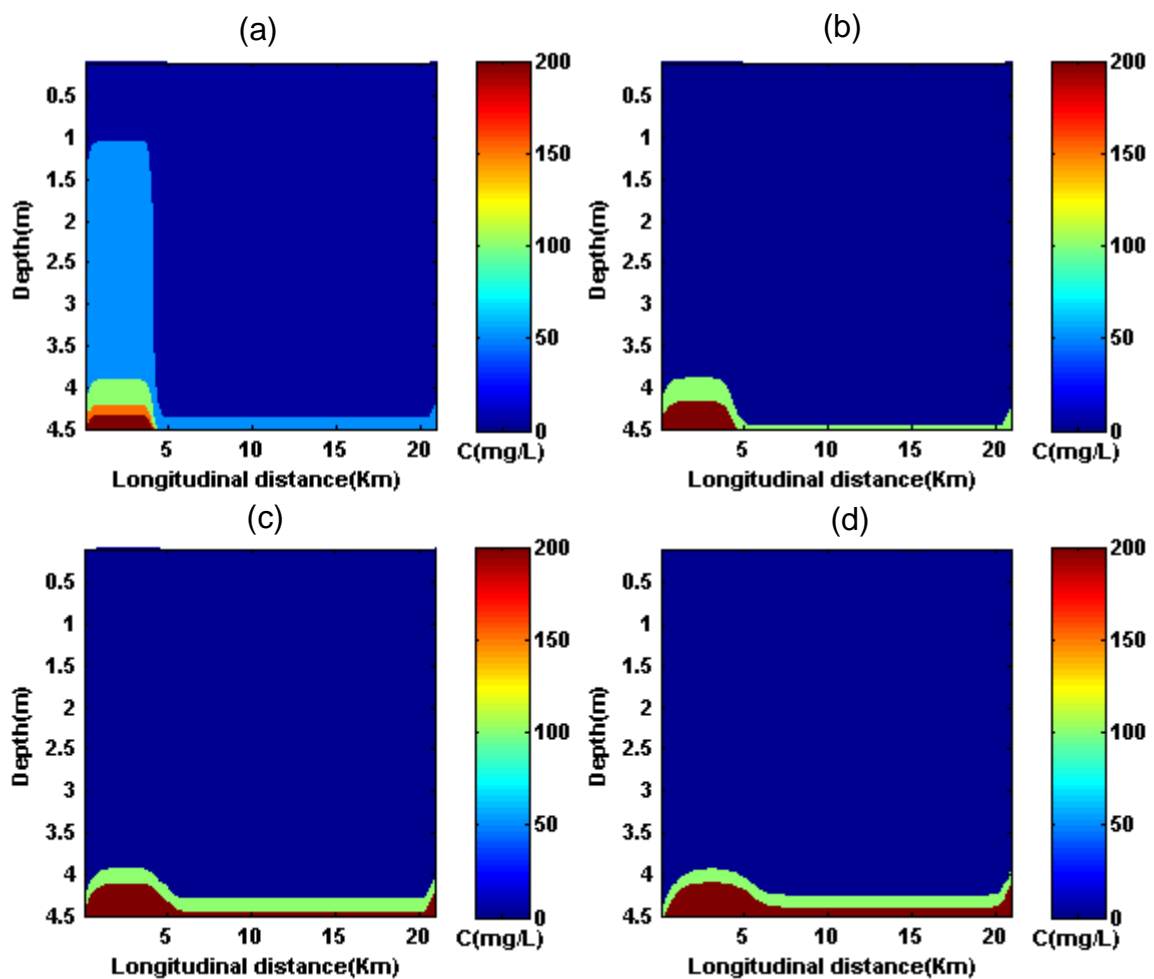


Fig. 7.9 Model-computed vertical variation of total particle concentration along the longitudinal line (shown in Figure 7.1) after a) 20min., b) 40 min., c) 90 min. and d) 180 min. of simulation, respectively; $\alpha=0.1$.

been reported by Ritter and Montagna (2001). According to model simulation results, oxygen-consuming particles can settle at the bottom of the bay on the order of hours and therefore, bottom waters may turn hypoxic within a short time frame under stratified conditions. In addition, the simulation results help to hypothesize the reason for the existence of high biochemical oxygen demand (BOD) in the south-east part of the bay. As vertical transport processes are dominant, high BOD material released from the upper Laguna Madre remains within a limited horizontal extent of the south-east part of the bay.

The vertical profiles of chlorophyll levels and total particle concentrations measured at our robotic platform 'P2' can aid in evaluating the model performance and the limitations of the developed model in capturing the detailed particle dynamics of the bay. Figure 7.10(a) and Figure 7.10(b) present the vertical profile of measured chlorophyll and total particle concentration variation, respectively, at platform 'P2' for 38 hours starting from our model simulation time (i.e., 10 am on July 24, 2007). Although the observed chlorophyll concentration is low ($< 6\mu\text{g/l}$) at all depths, the concentrations at the lower depths are consistently higher than that of the upper layer. On the other hand, significant levels of total particle concentrations are observed at different depths of the water column whereas our model predicts high levels of particle concentrations close to the sea-bed only. This discrepancy between model results and observations may arise due to various model assumptions. For example, the model considers the direction of the average vertical fluid velocity downward whereas vertical fluid velocity is variable and can move in both directions. The upward vertical velocity

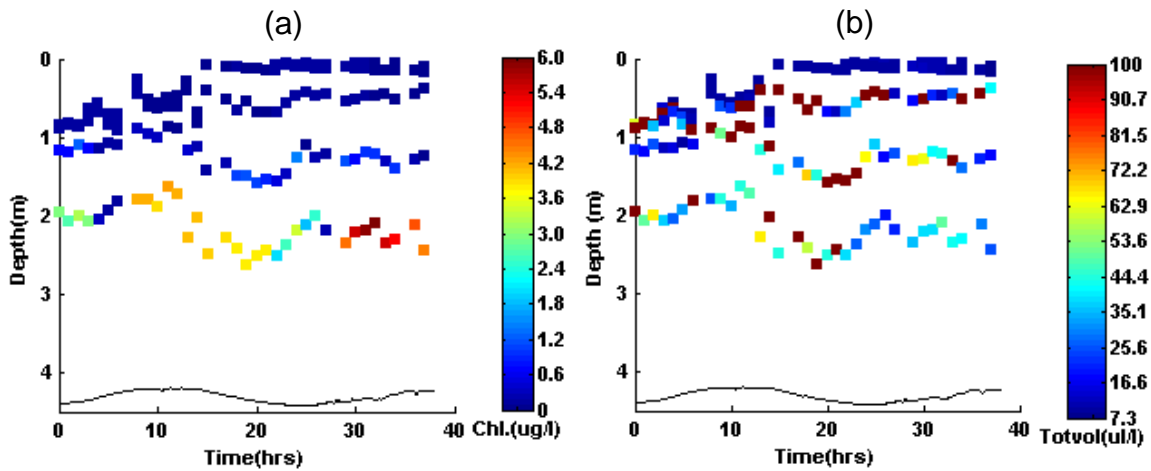


Fig. 7.10 Vertical profile of measured (a) chlorophyll concentration and (b) total particle concentration variation at platform 'P2' for 38 hours starting from 10 am on July 24, 2007; the wavy solid line denote the depth of the sea-bed.

can counteract with the gravitational settling speed of particles, especially particles of a smaller size class, and keep them in the upper levels of the water column. Also, aggregated particles are not permitted to disintegrate once they are formed. However, in reality, particle size and mass distributions are controlled through the balance of aggregation and break-up phenomena (Spicer and Pratsinis 1996). Moreover, an average particle density and constant collision efficiency were considered in the model. However, particle density can vary depending on the types of particles. For example, phytoplankton has much lower density ($\sim 1.05 \text{ gm/cm}^3$) than that of clay particles ($\sim 2.5 \text{ gm/cm}^3$) and therefore, their settling velocities will be different. The value of α can also vary depending on the types of particles involved in the collisions. Sterling et al. (2005) determined the value of α for dual-particle-type system using his modified coalesced fractal sphere (mCFS) model. The possible extension of our PAT model considering

multiple particle type system may help to better characterize the particle dynamics in the aquatic system. The field application of PAT model in this study opens up a new venue for future research in understanding the particle-mediated processes and their contributions to the water quality of aquatic systems.

Conclusions

The characterization of particle kinetics within the water column assists in greater understanding of the processes controlling water quality and health of aquatic ecosystems. A three-dimensional particle aggregation and transport model was developed in this study using the advection-dispersion transport equation and the recently proposed fractal theories for the aggregation kinetics. The model performance was evaluated against the analytical solution for the transport of polydispersed particles in a three-dimensional water column. Simulation results indicate that model predictions agree reasonably well with that of the analytical solution. In addition, field-scale application of this model helps to test various hypotheses in understanding the processes causing hypoxia in CC Bay. Vertical transport and aggregation processes are the key mechanisms controlling particle residence time in the water column which has greater implications in understanding the dissolved oxygen condition in the bay. Discrepancies between observed and model-predicted particle concentrations can be attributed to the constraints imposed by model assumptions. These constraints can be relaxed through the extension of the PAT model for multiple particle type system and the use of observational data assimilated hydrodynamic model for driving the advective-dispersive

transport of the PAT model. These modifications will help in better characterization of particle dynamics, and thereby lead to the greater understanding of particle-mediated processes and their contributions to the water quality of aquatic system.

CHAPTER VIII

SUMMARY AND CONCLUSIONS

Human populations are growing at a high rate in the coastal regions, and now more than half of the US population lives within fifty miles of a coastline (US census report, 2000). The high density of coastal populations and increased growth rate puts coastal areas vulnerable from various anthropogenic activities in addition to natural perturbations. Various episodic events such as hypoxia, harmful algal blooms (HAB), accidental oil spill, storm surges etc. are frequently occurring in coastal regions around the world and pose severe threats to the coastal ecosystems. Integrated sensor deployment platforms in conjunction with numerical modeling framework can be used to investigate the processes causing these events. In this study, the Coastal Margin Observation and Assessment System (CMOAS) has been implemented through installation of sensor systems on different types of platforms and development of numerical models to understand the processes causing hypoxia in shallow wind-driven CC Bay. This CMOAS can be used as template for the design and implementation of observation and assessment system in other energetic coastal ecosystems.

A sensor system installed on a single type of platform is not able to measure environmental parameters at proper spatial and temporal resolution to capture the episodic events. Therefore, monitoring systems developed in this study were installed on three different types of platforms: a) Fixed Robotic, b) Mobile and c) Remote. On the fixed robotic platform, an automated profiler system vertically moves a suite of water

quality measuring sensors within the water column for continuous measurements. This system prevents bio-fouling of sensors and therefore, it can be deployed for long-term autonomous monitoring of the bay. In addition, this system can be accessed remotely and thereby it allows troubleshooting and implementation of an adaptive sampling scheme based on frequency of the event of interest. On the other hand, an integrated data acquisition, communication and control system configured on mobile monitoring platform can measure vertical variation of hydrodynamic and water quality parameters along the transect route of travel. The real-time display capability of this system provides guidance in transect route selection to capture the event of interest. In addition of these two monitoring platforms, HF-radar systems installed on remote platforms generate hourly surface current maps of CC Bay and its offshore area. The large datasets collected from these monitoring platforms assist in providing insight regarding the possible processes inducing hypoxia at the bottom of CC Bay.

Data collected from monitoring platforms are made available to stakeholders in real time for the best use of the observational datasets. This is made possible through the development of cyberinfrastructure which includes establishment of a communications network, software development, web services and database development, etc. As monitoring platforms are normally located in the harsh remote areas, the network is often subjected to poor communication link between central data aggregation station and monitoring platforms. The developed efficient data collection and transport software allows sensor systems to monitor water quality of the bay in the case of network failure and sends measured data as soon as a communication link is reestablished. The relational

database developed in this study stores measured data from different platforms and assists in exploring interrelationship among various parameters to understand the processes causing hypoxia in the bay. In addition, real-time availability of measured datasets stored in our database assists in implementing an integrated sampling scheme for our monitoring systems installed at different platforms. With our integrated system, we were able to capture evidence of an hypoxic event in Summer 2007; moreover, we detected low dissolved oxygen conditions in a part of the bay with no previously-reported history of hypoxia.

Observational datasets from different monitoring platforms were used to drive and validate various numerical models developed in this study. The analysis of observational datasets and developed 2-D hydrodynamic model output provided insight about the dominant processes that control hydrodynamics of this shallow bay. The observed gradient in vertical salinity and water current direction along the transect route of our research cruises suggests that the depth-averaged model is not able to capture the dominant current structure of the water column. The development of a three-dimensional baroclinic hydrodynamic model can help in resolving the hydrodynamic conditions that prevail in CC Bay. The output of this 3-D model can then be used to drive our developed numerical models (e.g., mechanistic DO model and PAT model) in understanding the processes causing hypoxia and other episodic events in the bay.

The developed three-dimensional mechanistic dissolved oxygen model sheds light on the important processes controlling dissolved oxygen distribution in the bay. The sensitivity analysis of the model indicates that stratification and oxygen consumption

through decomposition of organic matter are the two key processes responsible for the induction of hypoxia at the bottom of the bay. Three-dimensional particle aggregation and transport (PAT) model was also developed in this study for the characterization of particle dynamics which can help to elucidate particle-mediated processes and their contributions to the water quality of aquatic system. The PAT Model performance is evaluated against the analytical solution for the transport of polydispersed particles in the water column, and simulation results suggest that model predictions agree reasonably well with that of the analytical solution. Field-scale application of this model helps to test various hypotheses in comprehending the processes causing hypoxia in the bay, and opens up a new venue for future research in exploring particle-mediated processes and their contributions to the water quality of aquatic ecosystem.

The various numerical models and monitoring systems developed in this study will remain as valuable tools for the understanding and prediction of various episodic events dominant in other dynamic ecosystems.

Future Works

The accurate hydrodynamic information is the key for the successful implementation of our developed mechanistic DO and PAT model in understanding the processes causing hypoxia in the bay. A three-dimensional hydrodynamic model of CC Bay may provide better hydrodynamic information that can be used to drive the developed numerical models. Also, future research may focus on the implementation of smart sampling scheme for our robotic profiler system. This scheme will enforce the

robotic profiler system for automatic adjustment of the sampling frequency depending on the occurrence of event of interest. In addition, our observational database needs to be integrated with the observational database of other communities such as the observational data model (ODM), developed by hydrologic community, for the effective sharing of the information. This will help to bridge various communities and to establish diverse collaborative research team for the exploration of the solution of scientific problems.

REFERENCES

- Abarbanel, H.D., Holm, D.D., Marsden, J.E. and Ratiu, T. (1984). Richardson number criterion for the nonlinear stability of three-dimensional stratified flow. *Physical Review Letters*, 52, 2352-2355.
- Aggarwal, M. (2004). Storm surge analysis using numerical and statistical techniques and comparisons with NWS model slosh. MS thesis, Texas A&M University, College Station, TX.
- Agrawal, Y.C., and Pottsmith, H.C. (2000). Instruments for particle size and settling velocity observations in sediment transport. *Marine Geology*, 168, 89–114.
- Aguilar, H., Fitzgerald, R., Barrick, D., Bonner and J., Perez, J. (2003). Fitting normal modes to HF radial and total surface current vector data over enclosed bays and estuaries. Reviewed Long Manuscripts for Proceedings IEEE/OES on Current Measurement Technology, March 2003.
- Amiel, D., Cochran, J.K. and Hirschberg, D.J. (2002). $^{234}\text{Th}/^{238}\text{U}$ disequilibrium as an indicator of the seasonal export flux of particulate organic carbon in the North Water, *Deep-Sea Research, II*, 49, 5191–5209.
- Banks, R.B. (1975). Some features of wind action on shallow lakes. *Am. Soc. Civ. Eng., J. Environ. Eng. Div.*, 101(EE5), 813-827.
- Banks, R.B. and Herrera, F.F.(1977). Effect of wind and rain on surface reaeration. *Am. Soc. Civ. Eng., J. Environ. Eng. Div.* 103(EE3), 489-504.
- Baptista, A.M., Zhang, Y., Chawla, A., Zulauf, M., Seaton, C., Myers, E.P., Kindle, J., Wilkin, M., Burla, M. and Turner, P.J.(2005). A cross-scale model for 3D baroclinic circulation in estuary-plume-shelf systems: II. Application to the Columbia River. *Continental Shelf Research*, 25, 935-972.
- Baptista, A. M. , Wilkin, M., Pearson, P. , Turner, P. , McCandlish, C. and Barrett, P. (1999). Coastal and estuarine forecast systems: A multi-purpose infrastructure for the Columbia River. *Earth System Monitor*, 9(3), National Oceanic and Atmospheric Administration, Washington, D. C., March 1999.
- Barrick, D.E. and Lipa, B.J. (1999). Radar angle determination with MUSIC direction finding. *U.S. Patent 5 990 834*.

- Barrick, D. E., Evans, M. W. and Weber, B.L. (1977). Ocean surface currents mapped by radar. *Science*, 198(4313), 138-144.
- Barth, J.A. and Bogucki, D.J. (2000). Spectral light absorption and attenuation measurements from a towed undulating vehicle. *Deep Sea Research, Part I*, 47(2), 323-342.
- Blackwell, S.M., Moline, M.A., Schaffner, A., Garrison, T. and Chang, G.(2008). Sub-kilometer length scales in coastal waters. *Continental Shelf Research*, 28(2), 215-226.
- Blain, C.A., Preller, R.H. and Rivera, A.P. (2002). Tidal prediction using the Advanced Circulation Model (ADCIRC) and relocatable PC-based system. *Special Issue: Navy Operational Models: Ten Years Later*, 15(1), 77-87.
- Blain, C. A., Weterink, J.J. and Luettich, R.A. (1994). The influence of domain size on the response characteristics of a hurricane storm surge model. *J. Geophys. Res.* 99(C9), 18467-18479.
- Blumberg, A.F. and Mellor, G.L. (1987). A description of a three-dimensional coastal ocean circulation model. *Three-Dimensional Coastal Ocean Models*, N. Heaps. Washington, D.C., AGU 4, 1-16.
- Bonner, J.S., Ernest, A.N., Autenrieth, R.L. and Ducharme, S.L. (1994). Parameterizing models for contaminated sediment transport. In DePinto, J.V., Lick, W. and Paul, J. eds., *Transport and transformation of contaminants near the sediment-water interface*. Chelsea, MI.: Lewis Publishers.
- Boss, E., Collier, R., Larson, G., Fennel, K. and Pegau, W. S. (2007). Measurements of spectral optical properties and their relation to biogeochemical variables and processes in Crater Lake, Crater Lake National Park, OR. *Hydrobiologia*, 574,149-159.
- Breivik, O. and Saetra, O. (2001). Real time assimilation of HF radar currents into a coastal ocean model. *Journal of Marine Systems* 28(3-4), 161-182.
- BRTT (2009). Boulder Real Time Technologies (BRTT) antelope real-time system. <http://www.brtt.com/>, accessed February 01, 2009.
- Buzzelli, C.P., Luettich Jr., R.A., Powers, S.P., Peterson, C.H, McNinch, J.E., Pinckney, J.L. and Paerl, H.W. (2002). Estimating the spatial extent of bottom-water hypoxia and habitat degradation in a shallow estuary. *Marine Ecology Progress Series*, 230,103-112.

- Carnahan, B., Luther, H.A. and Wilkes, J.O. (1969). *Applied numerical methods*. New York: Wiley.
- Carter, R.W.G. (1998). *Coastal environments*. London: Academic Press.
- Chapman, R. D., Shay, L. K., Graber, H. C., Edson, J. B., Karachintsev, A., Trump, C. L. and Ross, D. B. (1997). On the accuracy of HF radar surface current measurements: Intercomparisons with ship-based sensors. *Journal of Geophysical Research-Oceans* 102(C8), 18737-18748.
- Chapra, S.C. and Canale, R.P. (1988). *Numerical methods for engineers*. New York: McGraw-Hill Book Company.
- Chatila, R. and Laumond, J.P. (1985). Position referencing and consistent world modeling for mobile robots. *Proc. IEEE Int. Conf. Robotics and Automation*, pp. 138-145.
- Chen, Q., Wang, L.X., Zhao, H. and Douglass, S.L. (2007). Prediction of storm surges and wind waves on coastal highways in hurricane-prone areas. *Journal of Coastal Research* 23(5), 1304-1317.
- CO-OPS (2009). NOAA's Center for Operational Oceanographic Product and Services. <http://tidesandcurrents.noaa.gov/>, accessed February 02, 2009.
- Coulliette, C., F. Lekien, Paduano, J., Haller, G. and Marsden, J. (2007). Optimal pollution mitigation in monterey bay based on coastal radar data and nonlinear dynamics. *Environmental Science & Technology*, 41(18), 6562-6572.
- CREON (2009). Coral Reef Environmental Observatory Network. <http://www.coralreefeon.org/>, accessed February 01, 2009.
- Cugier, P. and Hir, P.L.(2002). Development of a 3D hydrodynamic model for coastal ecosystem modelling. Application to the plume of the Seine River (France). *Estuarine, Coastal and Shelf Science*, 55, 673-695.
- Deryaguin, B.V. and Landau, L.D. (1941). A theory of the stability of strongly charged lyophobic sols and of the adhesion of strongly charged particles in solutions of electrolytes. *Acta Physicochim*, 14, 633-662.
- Diaz, R.J. and Rosenberg, R. (2008). Spreading dead zones and consequences for marine ecosystems. *Science*, 321, 926-929.
- Dickey, T. (1991). The emergence of concurrent high-resolution physical and bio-optical measurements in the upper ocean. *Reviews of Geophysics*, 29, 383-413.

- Dickey, T., Frye, D., Jannasch, H., Boyle, E., Manov, D., Sigurdson, D., McNeil, J., Stramska, M., Michaels, A., Nelson, N., Siegel, D., Chang, G., Wu., J. and Knap, A. (1998). Initial results from the Bermuda Testbed Mooring Program. *Deep-Sea Research*, 45, 771-794.
- Ernest, A. N., Bonner, J.S. and Autenrieth, R.L. (1991). Model parameter estimation for particle transport. *Journal of Environmental Engineering-ASCE* 117(5), 573-594.
- Ernest, A. N., Bonner, J.S. and Autenrieth, R.L. (1995). Determination of Particle Collision Efficiencies for Flocculant Transport Models. *Journal of Environmental Engineering-ASCE* 121(4), 320-329.
- Faisst, W.(1976). *EQL Rep. 13*, Environmental Quality Laboratory, California Institute of Technology, Pasadena, CA.
- Feder, J. (1988). *Fractals*. New York: Plenum Press.
- Feng, H., Cochran, J.K. and Hirschberg, D.J. (1999). ^{234}Th and ^7Be as tracers for the transport and dynamics of suspended particles in a partially mixed estuary. *Geochim. Cosmochim. Acta* 63, 2487–2505.
- Fiorelli, E., Leonard, N. E., Bhatta, P. Paley, D. A., Bachmayer, R. and Fratantoni, D. M. (2006). Multi-AUV control and adaptive sampling in Monterey Bay. *IEEE Journal of Oceanic Engineering* 31(4), 935-948.
- Flint, R.W. (1985). Long-term estuarine variability and associated biological response. *Estuaries*, 8, 158–169.
- Gartner, J. W. (2002). Estimation of suspended solids concentrations based on acoustic backscatter intensity. Theoretical Background, Turbidity and Other Sediment Surrogates Workshop, April 30 – May 2, 2002, Reno, NV.
- Garton, L.S., Bonner, J.S., Ernest, A.N., and Autenrieth, R.L. (1996). Fate and transport of PCBs at the New Bedford Harbor superfund site. *Environmental Toxicology and Chemistry*, 15(5), 736-745.
- Glenn, S.M., Boicourt, W., Parker, B. and Dickey, T.D. (2000). Operational observation networks for ports, a large estuary and an open shelf. *Oceanography*, 13, 12-23.
- GLEON (2009). Global Lake Ecological Observatory Network. www.gleon.org, accessed February 01, 2009.
- Graber, H. C., Haus, B. K., Chapman, R. D. and Shay, L. K. (1997). HF radar comparisons with moored estimates of current speed and direction: Expected

- differences and implications. *Journal of Geophysical Research-Oceans*, 102(C8), 18749-18766.
- Grenier, R. R., Luettich, R. A. and Westerink, J. J.(1995). A comparison of the nonlinear frictional characteristics of two-dimensional and three-dimensional models of a shallow tidal embayment. *Journal of Geophysical Research*, 100(C7), 13719-13736.
- Gunter, G. (1967). Vertebrates in hypersaline water. *Contributions in Marine Science*, 12, 230-241.
- Haidvogel, D.B., Arango, H.G., Hedstrom, K., Beckmann, A., Malanotte-Rizzoli, P. and Shchepetkin, A.F. (2000). Model evaluation experiments in the North Atlantic Basin: simulations in nonlinear terrain-following coordinates. *Dynamics of Atmospheres and Oceans*, 32, 239–281.
- Han, M.Y. and Lawler, D.F. (1991). Interactions of two settling spheres: settling rates and collision efficiencies. *Journal of Hydraulic Engineering, ASCE*, 117,1269-1289.
- Han, M. and Lawler, D.F. (1992). The (relative) insignificance of G in flocculation. *Journal AWWA*, 84(10), 79-91.
- Hay, A. E. and Sheng, J. Y. (1992). Vertical profiles of suspended sand concentration and size from multifrequency acoustic backscatter. *Journal of Geophysical Research-Oceans*, 97(C10), 15661-15677.
- He Y., Lu X., Qiu, Z. and Zhao J.(2004). Shallow water tidal constituents in the Bohai Sea and the Yellow Sea from a numerical adjoint model with TOPEX/POSEIDON altimeter data. *Continental Shelf Research*, 24 (13-14), 1521-1529.
- Hindmarsh, A. C., Gresho, P. M. and Griffiths, D. F. (1984). The stability of explicit Euler time-integration for certain finite-difference approximations of the multi-dimensional advection diffusion equation. *International Journal for Numerical Methods in Fluids* 4(9), 853-897.
- Hodges, B.R. and J.E. Furnans (2007). Linkages between hypoxia and thin-layer stratification in Corpus Christi Bay. Manuscript in revision for *Environmental Fluid Mechanics*.
- Honji, H., Kaneko, A. and Kawatate, K. (1987). Self-governing profiling system. *Continental Shelf Research* ,7, 1257-1265.

- Howard, L.N. (1961). Note on a paper of John W. Miles. *Journal of Fluid Mechanics*, 10, 509-512.
- Hunt, J.R. and Pandya, J. (1984). Sewage sludge coagulation and settling in seawater. *Environmental Science and Technology*, 18(2), 119-121.
- Isern, A.R. and Clark, H.L.(2003). The Ocean Observatories Initiative: A continued presence for Interactive Ocean Research. *Marine Technology Society*, 37(3), 26-41.
- Islam, M.S., Bonner, J., Ojo, T. and Page, C. (2006a). Using numerical modeling and direct observation to investigate hypoxia in a shallow wind-driven bay, Oceans '06 MTS/IEEE Boston Technical Program. September 18-24, 2006.
- Islam, M.S., Bonner, J., Ojo, T. and Page, C.(2006b). Integrating observation with numerical modeling for the exploration of hypoxia. In S. Starrett, J. Hong, W. Lyon, Editors, *Environmental Science and Technology Conference*. Houston, TX, Aug 19-23.
- Islam, M.S., Bonner, J.S., Ojo, T. and Page, C. (2006c). 2-D Hydrodynamic model for Corpus Christi Bay using ADCIRC: Model development and error analysis. Student paper for Texas water 2006, WEAT and Texas Section AWWA Annual Conference, April 4 – 7, 2006, Austin, TX.
- Islam, M.S., Bonner, J., Ojo, T. and Page, C. (2008). A mechanistic dissolved oxygen model of Corpus Christi Bay to understand critical processes causing hypoxia. Oceans '08 MTS/IEEE, Quebec Technical Program, September 15-18, 2008.
- Islam, M.S., Bonner, J., Ojo and T., Page, C. (2009a). A fixed robotic profiler system to sense real-time episodic pulses of the condition of Corpus Christi (CC) Bay, manuscript in preparation to be submitted to *IEEE Sensors Journal*.
- Islam, M.S., Bonner, J., Ojo, T. and Page, C. (2009b). Development of a mobile monitoring system to understand the processes controlling episodic events in Corpus Christi Bay, manuscript in preparation to be submitted to *Environmental Monitoring and Assessment*.
- Islam, M.S., Bonner, J., Ojo, T. and Page, C. (2009c). Integrated real time monitoring system to investigate the hypoxia in a shallow wind-driven bay. Manuscript in preparation to be submitted to *Environmental Monitoring and Assessment*.
- Islam, M.S., Bonner, J., Ojo, T. and Page, C. (2009d). Development and investigation on the reliability of a 2-D hydrodynamic model for Corpus Christi Bay. Manuscript in preparation to be submitted to *Estuarine, Coastal and Shelf Science*.

- Iskandarani, M., Haidvogel, D.B. and Levin, J. (2003). A three-dimensional spectral element model for the solution of the hydrostatic primitive equations. *Journal of Computational Physics*, 186 (2), 397–425.
- James, I. D. (2002). Modelling pollution dispersion, the ecosystem and water quality in coastal waters: a review. *Environmental Modeling & Software*, 17(4), 363-385.
- Jackson, G.A., Logan, B.E., Alldredge, A.L. and Dam, H.G. (1995). Combining particle size spectra from a mesocosm experiment measured using photographic and aperture impedance (Coulter and Elzone) Techniques. *Deep-Sea Research*, 42, 139-157.
- Jackson, G.A., Maffione, R., Costello, D.K., Alldredge, A.L., Logan, B.R. and Dam, H.G. (1997). Particle size spectra between 1 μ m and 1cm at Monterey Bay determined using multiple instruments. *Deep-Sea Research I*, 44 (11), 1739-1767.
- Jiang, Q. and Logan, B. E. (1991). Fractal dimensions of aggregates determined from steady-state size distributions. *Environmental Science & Technology*, 25 (12), 2031-2038.
- Kelly, F. J., Bonner, J.S., Perez, J.C., Adams, J.S., Prouty, D., Trujillo, D., Weisberg, R.H., Luther, M.E., He, R., Cole, R., Donovan, J. and Merz, C.R.(2002). An HF-radar test deployment amidst an ADCP array on West Florida Shelf. *Oceans '02 MTS/IEEE* 2, 692- 698.
- Kelly, F. J., Bonner, J.S., Perez, J.C., Trujillo, D., Weisberg, R.H., Luther, M.E. and He, R. (2003). A comparison of near-surface current measurements by ADCP and HF radar on the West Florida Shelf. *Proceedings of the IEEE/OES Seventh Working Conference on Current Measurement Technology*, San Diego, CA, 70-74.
- Kemp, W.M, Sampou, P.A., Garber, J., Tuttle, J. and Boynton, W.R. (1992). Seasonal depletion of oxygen from bottom waters of Chesapeake Bay: roles of benthic and planktonic respiration and physical exchange processes. *Marine Ecology Progress Series*, 85, 137-152.
- Kihara, H. and Matijevic, E. (1992). An assessment of heterocoagulation theories. *Advances in Colloid and Interface Science*, 42, 1-31.
- Kolar, R.L., Gray, W.G., Westerink, J.J. and Luettich, R.A. (1994). Shallow-water modeling in spherical coordinates - equation formulation, numerical implementation, and application. *Journal of Hydraulic Research*, 32(1), 3-24.

- Lawler, D.F. (1979). *A particle approach to the thickening process*. Ph.D. dissertation, University of North Carolina, Chapel Hill.
- Lee, D.G. (1996). *Mathematical modeling of particle aggregation and vertical transport in aquatic environments using fractal and curvilinear approaches*. Ph.D. dissertation, Texas A&M University, College Station, TX.
- Lee, D.G., Bonner, J.S., Garton, L.S., Ernest, A.N.S. and Autenrieth, R.L. (2000). Modeling coagulation kinetics incorporating fractal theories: A fractal rectilinear approach. *Water Research*, 34 (7), 1987-2000.
- Lee, D.G., Bonner, J.S., Garton, L.S., Ernest, A.N.S. and Autenrieth, R.L. (2002). Modeling coagulation kinetics incorporating fractal theories: comparison with observed data. *Water Research*, 36(4), 1056-1066.
- Li, D. and Ganczarczyk, J. (1989). Fractal geometry of particle aggregates generated in waste and wastewater treatment processes. *Environmental Science and Technology*, 23, 1385-1389.
- Logan, B.E. and Wilkinson, D.B. (1991). Fractal dimensions and porosities of *Zoogloea ramigera* and *Saccharomyces cerevisiae* aggregates. *Biotechnology and Bioengineering*, 38(4), 389-396.
- Logan, B.E. and Kilps, J.R. (1995). Fractal dimensions of aggregates formed in different fluid mechanical environment. *Water Research*, 29(2), 443-453.
- Luettich, R.A., Hensch, J.L., Fulcher, C.W., Werner, F.E., Blanton, B.O. and Churchill, J.H. (1999). Barotropic tidal and wind-driven larval transport in the vicinity of a barrier island inlet. *Fisheries Oceanography* 8, 190-209.
- Luettich, R.A., Kirby-Smith, W.W. and Hunnings, W. (1993). PSWIMS, a profiling instrument system for remote physical and chemical measurements in shallow water. *Estuaries*, 16, 190-197.
- Luettich, R.A., Westerink, J.J. and Scheffner, N.W. (1991). ADCIRC: an advanced three-dimensional circulation model for shelves, coasts and estuaries. Coast. Engrg. Res. Ct., US Army Engrs. Wtrways. Experiment Station, Vicksburg, MS.
- Lynch, D.R., Ip, J.T., Naimie, C.E. and Werner, F.E. (1996). Comprehensive coastal circulation model with application to the Gulf of Maine. *Continental Shelf Research*, 16 (7), 875-906.
- MacNaughton, A., White, R.H. and Bendzlowicz, M. (2004). Into the deep end: The Naval Oceanographic Office's Subsurface Autonomous Mapping System

- (SAMS) AUV. Resource document, Naval Oceanographic Office.
<https://savage.nps.edu/svn/nps/Savage/Robots/UnmannedUnderwaterVehicles/SamsMacNaughtonOctober2004.pdf>. Accessed February 9, 2009.
- Manov, D.V., Chang, G.C. and Dickey, T.D. (2003). Methods for reducing biofouling of moored optical sensors. *Journal of Atmospheric and Oceanic Technology*, 21, 958-968.
- Mau, J. C., Wang, D. P., Ullman, D.S. and Codiga, D.L. (2007). Comparison of observed (HF radar, ADCP) and model barotropic tidal currents in the New York Bight and Block Island Sound. *Estuarine Coastal and Shelf Science* 72(1-2), 129-137.
- Miles, J.W. (1961). On the stability of heterogeneous shear flows. *Journal of Fluid Mechanics*, 10, 496-508.
- Montagna, P. A. and Kalke, R. D. (1992). The effect of freshwater inflow on meiofaunal and macrofaunal populations in the Guadalupe and Nueces estuaries, Texas. *Estuaries*, 15, 307-326.
- Montgomery, J. L., Harmon, T., Kaiser, W., Sanderson, A., Haas, C. N., Hooper, R., Minsker, B., Schnoor, J., Clesceri, N. L., Graham, W. and Brezonik, P. (2007). The WATERS network: An integrated environmental observatory network for water research. *Environmental Science & Technology*, 41(19), 6642-6647.
- Morel, F.M. and Schiff, S. (1980). *Ocean disposal of municipal wastewater: The impact on estuary and coastal waters*. Cambridge, MA: MIT Sea Grant College Program.
- Mukai, A. Y., Westerink, J. J., Luettich Jr. and Mark, D. (2001). Eastcoast 2001, a tidal constituent database for the western North Atlantic, Gulf of Mexico and Caribbean Sea, US Army Corps of Engineers, Washington, DC .
- NEON (2009). National Ecological Observatory Network. <http://www.neoninc.org>, accessed February 01, 2009.
- NOAA Coastal Services Center (2009). NOAA coastal services center, <http://www.csc.noaa.gov/benthic/data/gulf/bend.htm>, accessed 12 January 2009.
- NRC (2001). *Grand challenges in environmental sciences*. Committee on Grand Challenges in Environmental Sciences, National Research Council (NRC), National Academy Press, Washington, DC.
- Ojo, T.O. (2005). *Development of environmental and oceanographic real-time*

assessment for the near-shore environment. Ph.D. dissertation, Texas A&M University, College Station, TX.

- Ojo, T.O. and Bonner, J.S. (2002). Three-dimensional self-calibrating coastal oil spill trajectory tracking and contaminant transport using HF radar. *Twenty-fifth Arctic and Marine Oilspill Program (AMOP) Technical Seminar*, Ottawa, Canada, Environment Canada.
- Ojo, T.O., Bonner, J.S. and Page, C. (2006). Studies on turbulent diffusion processes and evaluation of diffusivity values from hydrodynamic observations in Corpus Christi Bay. *Continental Shelf Research*, 26, 2629-2644.
- Ojo, T.O., Bonner, J.S. and Page, C. (2007a). A Rapid Deployment Integrated Environmental and Oceanographic Assessment System (IEOAS) for coastal waters: Design concepts and field implementation. *Environmental Engineering Science*, 24(2), 221-232.
- Ojo, T.O., Bonner, J.S. and Page, C. (2007b). Simulation of constituent transport using a reduced 3D Constituent Transport Model (CTM) driven by HF radar: Model application and error analysis. *Environmental Modeling and Software*, 22, 488-501.
- ORION (2009). Ocean Research Interactive Observatory Networks website http://www.oceanleadership.org/ocean_observing, accessed February 01, 2009.
- Park, K., Kim, C.K and Schroeder, W. W. (2007). Temporal variability in summertime bottom hypoxia in shallow areas of Mobile Bay, Alabama. *Estuaries and Coasts*, 30 (1), 54-65.
- Pandoe, W. W. and Edge, B. L. (2008). Case study for a cohesive sediment transport model for Matagorda Bay, Texas, with coupled ADCIRC 2D-transport and SWAN wave models. *Journal of Hydraulic Engineering-ASCE*, 134(3), 303-314.
- PORTS (2009). Physical Oceanographic Real-Time System website, National Oceanic and Atmospheric Administration. <http://tidesandcurrents.noaa.gov/ports.html>, accessed February 01, 2009.
- Purcell, M., Austin, T., Stokey, R., von Alt, C. and Prada, K. (1997). A vertical profiling system for making oceanographic measurements in coastal waters. *OCEANS '97. MTS/IEEE Conference Proceedings*, 1, 219 – 224, 6-9 Oct. 1997.
- Rabalais, N.N., Turner, R.E., Dortch, Q., Wiseman Jr, W.J. and Sen Gupta, B.K. (1996). Nutrient changes in the Mississippi River and system responses on the adjacent continental shelf. *Estuaries*, 19,366-407.

- Reynolds-Fleming, J.V., Fleming, J.G. and Luettich, R.A. (2002). Portable autonomous vertical profiler for estuarine applications. *Estuaries & Coast*, 25, 142-147.
- Ritter, C. and Montagna, P. A. (1999). Seasonal hypoxia and models of benthic response in a Texas estuary. *Estuaries*, 22(3), 7-20.
- Ritter, C., and Montagna, P. A. (2001). Cause and effect of hypoxia (low oxygen) in Corpus Christi Bay, Texas. *Technical Report 2001-001*, University of Texas at Austin, Marine Science Institute.
- Ritter, C., Montagna, P. A. and Applebaum, S. (2005). Short-term succession dynamics of macrobenthos in a salinity-stressed estuary. *Journal of Experimental Marine Biology and Ecology*, 323, 57-69.
- Rowe, G. T. (2001). Seasonal hypoxia in the bottom water off the Mississippi River delta. *Journal of Environmental Quality* 30(2), 281-290.
- SAUV (2009). Solar powered autonomous underwater vehicle, <http://www.physlink.com/news/121304UnderwaterSolar.cfm> , accessed on February 09, 2009.
- Sanders, S.C. (1990). *Vertical transport and dynamic size distribution of New Bedford harbor sediments*. M.S. thesis, Texas A&M University, College Station, TX.
- Sankaranarayanan, S. and McCay, D.F. (2003). Application of a two-dimensional depth-averaged hydrodynamic tidal model. *Ocean Engineering*, 30, 1807-1832.
- Scavia, D., Kelly, E.L.A. and Hagy III, J.D (2006). A simple model for forecasting the effects of nitrogen loads on Chesapeake Bay hypoxia. *Estuaries and Coasts*, 29(4), 674-684.
- Scheffner, N.W., Carson, F.C., Rhee, J.P. and Mark, D.J. (2003). Coastal erosion study for the open coast from Sabine Pass to San Luis Pass, Texas: Tropical storm surge frequency analysis. US Army Corps of Engineers, Waterways Experiment Station, Vicksburg, MS.
- Schmidt, S., Chou, L. and Hall, I.R. (2002). Particle residence times in surface waters over the north-western Iberian Margin: comparison of pre-upwelling and winter periods. *Journal of Marine Systems*, 32, 3-11.
- Sharma, V.K., Rhudy, K.B., Koenig, R. and Vazquez, F.G. (1999). Metals in sediments of the Upper Laguna Madre. *Marine Pollution Bulletin* 38(12), 1221-1226.

- Shenoi, S. S. C., Saji, P. K. and Almeida, A. M. (1999). Near-surface circulation and kinetic energy in the tropical Indian Ocean derived from Lagrangian drifters. *Journal of Marine Research* 57(6), 885-907.
- Smoluchowski, M. (1917). Versuch einer mathematischen theorie der koagulationkinetik kolloider losungen. *Z. Phys. Chem.*, 92, 129-168.
- Spicer, P.T. and Pratsinis, S.E. (1996). Coagulation and fragmentation: universal steady-state particle-size distribution. *AIChE J.* 42, 1612-1620.
- Stanley, D.W and Nixon, S.W.(1992). Stratification and bottom-water hypoxia in the Pamlico River estuary. *Estuaries*, 15, 270-281.
- Steele, JH (1995). Can ecological concepts span the land and ocean domains? *In Ecological Time Series*, Powell TM, Steele JH(eds). New York: Chapman & Hall.
- Sterling, M.C. (2003). *Aggregation and transport kinetics of crude oil and sediment in estuarine waters*. Ph.D. dissertation, Texas A & M University, College Station, TX.
- Sterling, M.C., Bonner, J.S., Page, C.A., Fuller, C.B, Ernest, A.N.S. and Autenrieth, R.L. (2004). Modeling crude-oil droplet-sediment aggregation in nearshore waters. *Environmental Science & Technology*, 38(17), 4627-4634.
- Sterling, M.C., Bonner, J.S., Ernest, A.N.S., Page, C.A. and Autenrieth, R.L. (2005). Application of fractal flocculation and vertical transport model to aquatic sol-sediment systems. *Water Research*, 39, 1818-1830.
- Tedesco, M., Bohlen, W. F., Howard-Strobel, M. M., Cohen, D. R. and Tebeau, P. A. (2003). The MYSound project: Building an estuary-wide monitoring network for Long Island Sound, USA. *Environmental Monitoring and Assessment*, 81(1-3), 35-42.
- Texas Department of Water Resources (1983). Laguna Madre estuary: A study of the influence and freshwater inflow. *Texas Department of Water Resources, Report LP-182*, Austin, TX.
- Thomann, R.V. (1972). *Systems analysis and water quality management*. New York: Environmental Research and Applications Inc.
- Thomann, R.V. (1973). Development of hydrodynamic and time variable water quality models of Boston Harbor [Report]. Westwood, NJ: Hydrosience Inc.

- Thomann, R.V. and Mueller, J.A. (1987). *Principles of surface water quality modeling and control*. New York: Harper International Edition, HarperCollinsPublishers Inc.
- Thomas, D. N., Judd, S. J. and Fawcett, N. (1999). Flocculation modelling: A review. *Water Research* 33(7), 1579-1592.
- Thompson, S.K., and Seber, G.A.F. (1996). *Adaptive sampling*. New York: Wiley.
- Thorne, P. D. and Hanes, D. M. (2002). A review of acoustic measurement of small-scale sediment processes. *Continental Shelf Research*, 22(4), 603-632.
- Tilak, S., Hubbard, P., Miller, M. and Fountain, T. (2007). The Ring Buffer Network Bus (RBNB) data turbine streaming data middleware for environmental observing systems. *Third IEEE International Conference on E-science and Grid Computing*, Bangalore, India.
- Trujillo, D. A., Kelly, F.J., Perez, J.C., Riddles, H.R. and Bonner, J.S. (2004). Accuracy of surface current velocity measurements obtained from HF radar in Corpus Christi Bay, Texas. *IEEE International Geoscience and Remote Sensing Symposium II*, 1179 - 1182.
- Turner, R. E., Schroeder, W. W., and Wiseman, W., J. Jr. (1987). The role of stratification in the deoxygenation of Mobile Bay and adjacent shelf bottom waters. *Estuaries*, 10(1), 13-19.
- Turner, J. S. (1979). *Buoyancy effects in fluids*. New York: Cambridge Univ. Press.
- U.S. CENSUS BUREAU (2002). United States Census 2000. <http://www.census.gov/prod/2002pubs/c2kprof00-us.pdf>, accessed February 01, 2009.
- USEPA (2000). U.S. Environmental Protection Agency, Office of Water. National Water Quality Inventory: 2000 Report. <http://www.epa.gov/305b/2000report/chp2.pdf>, accessed September, 2006.
- Van de Ven T.G.M. and Mason, S.G. (1977). The microrheology of colloidal dispersions. VII. Orthokinetic doublet formation of spheres. *Colloid and Polymer Science*, 255, 468-479.
- Verwey, E. J. W. and Oberbeek, J.Th.G. (1948). *Theory of the stability of lyophobic colloids*. Amsterdam: Elsevier.
- Visbeck, M. and Fischer, J. (1995). Sea surface conditions remotely sensed by upward-

- looking ADCPs. *Journal of Atmospheric and Oceanic Technology*, 12, 141-149.
- Volpe, A.M. and Esser, B.K. (2002). Real-time ocean chemistry for improved biogeochemical observation in dynamic coastal environments. *Journal of Marine Systems*, 36, 51–74.
- Ward, G. H. (1997). *Processes and trends of circulation within the Corpus Christi Bay national estuary program study area*. CCBNEP-21, Corpus Christi Bay National Estuary Program.
- Westerink, J. J., Feyen, J.C., Atkinson, J.H., Roberts, H.J., Kubatko, E.J., Luettich, R. A., Dawson, C., Powell, M.D., Dunion, J.P. and Pourtacheri, H. (2008). A basin- to channel-scale unstructured grid hurricane storm surge model applied to southern Louisiana. *Monthly Weather Review*, 136(3), 833-864.
- Westerink, J. J., Luettich, R.A. and Muccino, J.C (1994). Modeling tides in the western North Atlantic using unstructured graded grids. *Tellus*, 46(A), 178-199.
- Westerink, J.J., Luettich, R.A. and Scheffner, N.W. (1993). ADCIRC : An advanced three-dimensional circulation model for shelves, coasts, and estuaries report 3: Development of a tidal constituent database for the western North Atlantic and Gulf of Mexico. *Technical Report DRP-93-2*, US Army Corps of Engineers, Waterways Experiment Station, Vicksburg, MS.
- Wiebe, P.H., Stanton, T.K., Greene, C.H., Benfield, M.C., Sosik, H.M., Austin, T.C., Warren, J.D. and Hammar, T. (2002). BIOMAPPER-II: An integrated instrument platform for coupled biological and physical measurements in coastal and oceanic regimes. *IEEE J. Oceanic Eng.*, 27, 700-716.
- Wiesner, M.R.(1992). Kinetics of aggregate formation in rapid mix. *Water Research*, 26(3), 379-387.
- YSI (2009). Vertical profiling system.
https://www.yei.com/portal/page/portal/YSI_Environmental/Applications/Application?applicationID=YSI_APP2_OCEANS_COASTAL, accessed February 08, 2009.
- Zhang, Y., Baptista, A.M. and Myers, E.P.(2004). A cross-scale model for 3D baroclinic circulation in estuary-plume-shelf systems: I. formulation and skill assessment. *Continental Shelf Research*, 24, 2187-2214.

VITA

Name: Mohammad Shahidul Islam

Address: c/o The Department of Civil Engineering
Environmental and Water Resources Division
128 A, Wisenbaker Engineering Research Centre
Texas A&M University
College Station, TX 77843-3136

Email Address: rusl001@yahoo.com

Education: Bachelor of Science, 2000
Civil Engineering
Bangladesh University of Engineering and Technology
Dhaka, Bangladesh

Master of Science, 2003
Institute of Environmental Studies
The University of Tokyo, Japan

Doctor of Philosophy, 2009
Civil Engineering
Texas A&M University
College Station, TX